NIRS-M-225

Proceedings of

NIRS - IMP
Joint Symposium on Carbon Ion Therapy

August 14 & 15, 2009

Institute of Modern Physics Lanzhou,China

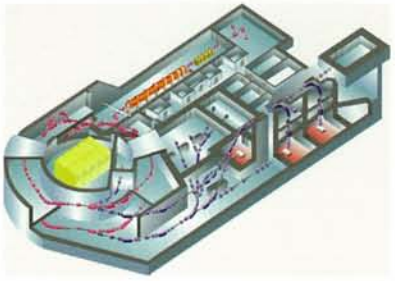

Organized by

NIRS

National Institute

of Radiological Sciences,Japan

and

IMP

Institute of Modern Physics,China

NIRS-IMP Joint Symposium on Carbon Ion Therapy

August 14 - 15, 2009

Institute of Modern Physics Lanzhou,China

Organized by

National Institute of Radiological Sciences,Japan
and
Institute of Modern Physics,China

NIRS-IMP Joint Symposium on Carbon Ion Therapy

14-15 August 2009, Lanzhou
Institute of Modern Physics (IMP), China

8:30-8:40	Registration	
	Opening Ceremony	
8:40-8:45	Opening Remarks	Guoqing Xiao, IMP
8:45-8:50	Opening Remarks	Hirohiko Tsujii, NIRS
8:50-9:00	Group Photo	
	Present Status of IMP Project and Other plans	**Chair : G. Xiao and H. Tsujii**
9:00-9:20	Present Status of IMP Therapy Project and Particle Therapy in China	G. Xiao, IMP
9:20-9:40	Brief Introduction of Plans in Japan	H. Tsujii, NIRS
	Clinical Experiences at NIRS and IMP	**Chair: H. Zhang and T. Kamada**
9:40-9:50	NIRS Introduction	A. Kitagawa, NIRS
9:50-10:20	Overview of the Carbon Ion Therapy at NIRS	H.Tsujii, NIRS
10:20-10:30	Discussion	
10:30-10:45	*Coffee Break*	
10:45-11:00	Skull Base Tumor	A. Hasegawa, NIRS
11:00-11:15	Head & Neck Tumor	K. Jingu/ J.Mizoe, NIRS
11:15-11:30	Lung Cancer	N. Yamamoto/ M.Baba, NIRS
11:30-11:45	Bone & Soft Tissue Sarcoma	S. Sugahara, NIRS
11:45-11:55	Discussion	
11:55-13:55	*Lunch*	
13:55-14:10	Hepatoma	H. Imada/ S. Yasuda, NIRS
14:10-14:25	P/O rec Rectal Cancer	S.Yamada, NIRS
14:25-14:40	Uterine Cancer	S.Kato, NIRS
14:40-14:55	Prostate Cancer	H.Tsuji, NIRS
14:55-15:05	Discussion	
15:05-15:20	*Coffee Break*	
15:20-15:45	Results of Carbon Ion Radiotherapy for Skin Carcinomas in 45 Patients	H. Zhang, IMP
15:45-16:10	About Particle Clinical Study	T. Kamada, NIRS
16:10-16:20	Discussion	
	Ion Beam Biology	**Chair: G. Zhou and R.Okayasu**
16:30-16:45	Repair of DNA Double Strand Breaks Induced by Heavy Ion Irradiation	R. Okayasu, NIRS
16:45-17:00	Biological Effectiveness of Mammalian Cells Exposed to Heavy Ion Beams	Y. Furusawa, NIRS

17:00-17:15	Effects of Heavy Ion Radiation on Cancer Stem Cells of Xenograft Tumor in Nude Mice	S. Sai, NIRS
17:15-17:30	Effect of Hypofractionation on RBE and Estimation of Therapeutic Dose	Y. Matsumoto, NIRS
17:30-17:45	Discussion	

15 August (Saturday)

	Ion Beam Biology	**Chair: G. Zhou and R. Okayasu**
8:30-8:45	Radiosensitivity in Mesothelioma Cell Lines for X Rays and Carbon-ion Beams	C. Liu, NIRS
8:45-9:00	A Novel Mechanism of Cellular Radiosensitivity	G. Zhou, IMP
9:00-9:15	Cytometric Assessment of Histone H2AX Phosphorylation in Tumor Cells Irradiated with Carbon Ions	L. Zhou, IMP
9:15-9:25	Discussion	
	Ion Beam Physics	**Chair: Q. Li and K. Noda**
9:30-9:45	15 Years Experience of the Carbon Ion Production; Stability and Reliability of HIMAC	A. Kitagawa, NIRS
9:45-10:00	New Treatment Facility Project at HIMAC	K. Noda, NIRS
10:00-10:15	Treatment Planning for Scanned Carbon Ion Beams	N. Kanematsu, NIRS
10:15-10:30	Status of New Carbon Therapy Facility at Gunma University	S. Yamada, Gunma University
10:30-10:45	Evaluation of Absolute Doses for Therapeutic Carbon Ion Beams	M. Sakama, Gunma University
10:45-11:00	Research for the RI Beam Medical Application at HIMAC and RI Production Techniques	M. Kanazawa, NIRS
11:00-11:15	*Coffee Break*	
11:15-11:30	Therapeutic Techniques Used in the Heavy Ion Therapy Project at IMP	Q. Li, IMP
11:30-11:45	The Beam Monitoring Detectors for the Heavy-Ion Therapy at IMP	Z. Hu, IMP
11:45-12:00	Accelerator Aspects of the Proposed Tumor Therapy System	M. Song, IMP
12:00-12:15	Injection and Slow Extraction for Carbon Ion Therapy at IMP	Y. Yuan, IMP
12:15-12:30	Injector Linac for Heavy Ion Therapy System in Japan	S. Tatsumi, Sumitomo Heavy Industries
12:30-12:40	Discussion	
	Closing Ceremony	
12:40-12:55	Closing Remarks	H. Tsujii, NIRS
12:55-13:10	Closing Remarks	G. Xiao, IMP

INDEX

INDEX

Ion Beam Physics

Preface

In recent years, there has been a significant increase of interest worldwide in charged particle therapy with protons and carbon ions, which allows a unique precision in delivering a sufficient dose to the target volume while sparing the surrounding normal tissues. Thereby, a significant improvement of local control and survival has been achieved in various types of tumors.

The use of charged particles for radiotherapy was first proposed by R. Wilson in 1946. Since then, more than 70,000 patients have been treated with charged particles in the world, while most of them were delivered with proton beams. Currently, there are about 26 operating facilities for proton therapy, and carbon ion radiotherapy is provided at 4 facilities including the NIRS and IMP. Still more are under construction or planning and over a dozen new facilities will be built within a next decade; most of them are based on university hospitals or cancer centers that have long-standing experiences in modern photon radiotherapy.

Carbon ion radiotherapy has been pioneered at the Institute of Modern Physics (IMP), which is affiliated with the Chinese Academy of Sciences (CAS) and located in Lanzhou. They have high-energy accelerator complex, which is being used for nuclear physics, heavy-ion accelerator, and heavy-ion application.
A large part of the machine time is devoted to, nuclear physics, application and cancer therapy with heavy-ion beams like ^{12}C. In the new Heavy-Ion Cancer Therapy Center, which is run in collaboration with local hospitals more than hundred patients with shallow-seated tumours and a small number of patients with deep-seated tumours have been treated, as well as hypofractionated radiotherapy has been extensively carried out.

At the National Institute of Radiological Sciences (NIRS) of Chiba, Japan, clinical study on carbon ion radiotherapy was begun in 1994 using the Heavy Ion Medical Accelerator in Chiba (HIMAC). The HIMAC is the world's first heavy ion accelerator complex dedicated to cancer therapy. Since then it has been the leading center for clinical and research activities of carbon ion radiotherapy and more than 4,500 patients with a variety of tumors have been treated to date. It has been feasible to treat non-squamous cell type of tumors, and to complete the treatment in a short time with small number of fractions.

This NIRS-IMP joint meeting has been organized with the goal of contributing to the wide distribution of advanced medical, physical and radiobiological knowledges and experiences on carbon ion radiotherapy. We believe that a large number of radiation oncologists, medical physicists and cancer specialists could benefit from this meeting in terms of education, exchange of ideas, and debates on the indications and applications of charged particle radiotherapy. A major goal of this Symposium is also directed to the consolidation of Japan-China collaboration in teaching, research and clinical activities, in the framework of further joint initiatives in development of charged particle radiotherapy.

We are greatly looking forward to having a mutual discussion with you all.

H. Tsujii, Chiba
G. Xiao, Lanzhou

Current Status and Future Plan of Particle Radiotherapy in Japan

Hirohiko Tsujii, M.D.

National Institute of Radiological Sciences, Chiba, JAPAN
e-mail address: Tsujii@nirs.go.jp

Charged particle beams denoted here as protons and carbon ions share the beneficial property of superior physical dose distribution (Bragg peak curve). In addition, carbon ions have a higher RBE compared with protons or photons. At present, there are a total of 7 facilities in operation for charged particle therapy in Japan (Fig.1). These include the National Institute of Radiological Sciences (NIRS: carbon ions), Tsukuba University (PMRC: protons), National Cancer Center East (NCCE: protons), Hyogo Ion Beam Medical Center (HIBMC: protons and carbon ions), Wakasa-Wan Energy Research Center (protons), and Shizuoka Cancer Center (protons), and Minami-Tohoku Proton Center (protons). Specifications of these facilities are described in Table 1.

There are three more facilities under construction. Two facilities for proton RT are being built at Fukui Prefecture and Ibusuki in Kagoshima, where commercially available accelerators will be installed. At Gunma University, a new carbon facility is almost completed. It was originally developed by the physics group of NIRS and is about one-third of the HIMAC in terms of the total cost and size.

Charged particle therapy had been long performed as a clinical research. However, the Japanese government has recently approved it as an Advanced Medical Technology, which has enabled us to charge the fee to the patient. More recently we have established the Japan Clinical Study Group of Particle Therapy (JCPT) for the purpose of advancing the practice of particle therapy by individuals who are interested in charged particle therapy. As an activity for comparing clinical efficacy of different modalities, we have designed protocols to be shared by facilities for both proton and carbon beam treatment.

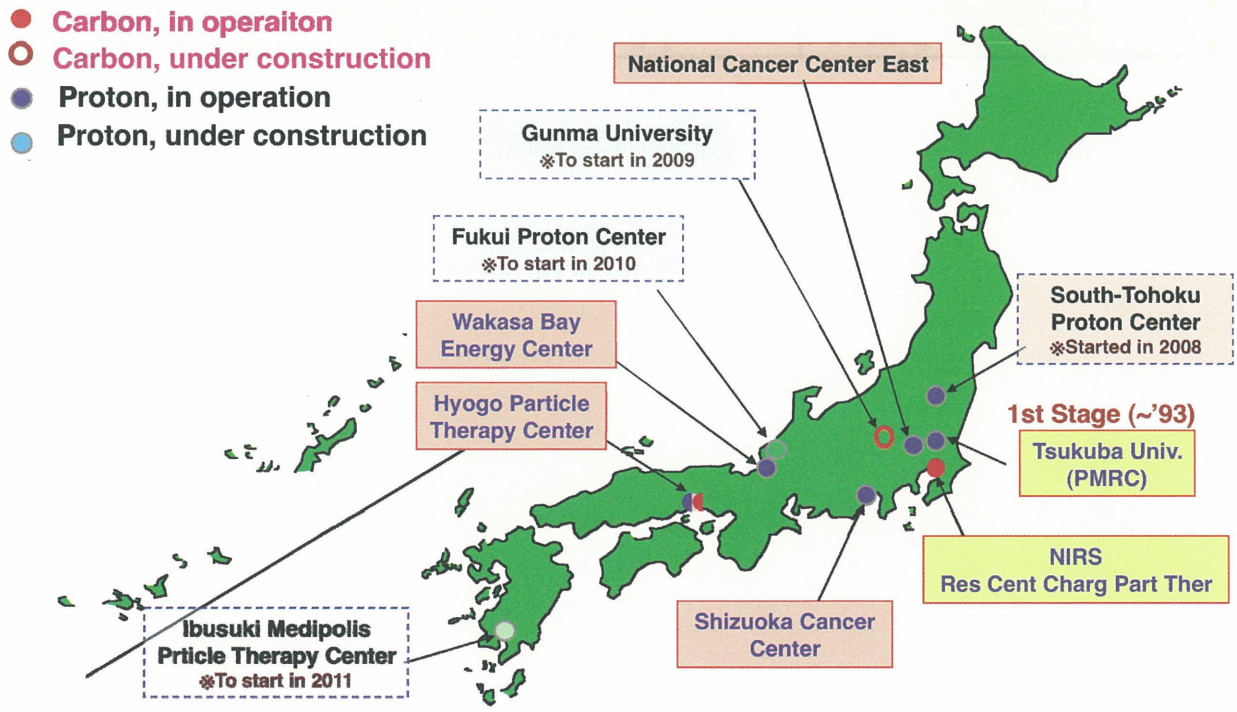

Fig.1 Charged particle therapy facilities in Japan.

There are 7 facilities in operation and 3 facilities under construction

Table 1

Specifications of particle therapy facilities in operation in Japan

		NIRS Chiba	NCCHE Kashiwa	HIBMC Hyogo	PMRC Tsukuba	SCC Shizuoka	WWERC Tsuruga	Minami Touhoku
Particle		C (p~Xe)	P	C P	P	P	P	P
Rx Start		1994	1998	2001	2001	2003	2002	2008
Main Accelerator		Synchro D~40mx2	Cyclo D~4m	Synchro D~30m	Synchro D~7m	Synchro D~6m	Synchro D~10m	Synchro D~6m
Max Energy (MeV/u)		800 (q/m=1/2)	235	P: 230 C: 320	250	235	200	235
Beam Delivery System	Hori-zontal	C : 2 port	p : 1 port	C : 1 port	-	p : 1 port	-	p : 1 port
	Vertical	C : 2 port	-	C : 1 port	-	-	p : 1 port	-
	45°	-	-	C : 1 port	-	-	-	-
	Rot. Gatry	-	p : 2 port	p : 2 port	p : 2port	p : 2 port	-	p : 2 port
	Research	p~Xe : 5	-	p : 1 port	p : 2port	-	p : 1 port	-

Overview of Carbon Ion Radiotherapy at NIRS

Hirohiko Tsujii

National Institute of Radiological Sciences, Chiba, Japan
e-mail: tsujii@nirs.go.jp

Abstract

In June 1994, the world-first clinical center offering carbon ion radiotherapy (C-ion RT) was set to open in at NIRS, Japan. Among several types of ion species, carbon ions were chosen for cancer therapy because they were judged to have the most optimal properties in terms of superior physical and biological characteristics. As of March 2009, a total of 4,504 patients have been registered for C-ion RT. Clinical results have shown that C-ion RT has the potential ability to provide a sufficient dose to the tumor, together with acceptable morbidity in the surrounding normal tissues. Tumors that appear to respond favorably to carbon ions include locally advanced tumors as well as those with histologically non-squamous cell types of tumors such as adenocarcinoma, adenoid cystic carcinoma, malignant melanoma, hepatoma, and bone/soft tissue sarcoma. By taking advantage of the unique properties of carbon ions, treatment with small fractions within a short treatment period has been successfully carried out for a variety of tumors. This means that the facility can be operated more efficiently in carbon ion therapy, offering treatment for a larger number of patients than is possible with other modalities over the same period of time.

Introduction

The structural survey of JASTRO has demonstrated that the number of cancer patients undergoing radiotherapy (RT) has increased to a total of 150,000, an equivalent to roughly 28% of all cancer patients in Japan, with forecasts that this number will continue to rise in the future (1). In recent years, the scope of diseases that can be treated with RT has significantly widened in the wake of the diffusion of high precision RT such as stereotactic RT (SRT), intensity-modulated RT (IMRT) and particle beam RT. These approaches permit administration of a curative dose to the tumor with sparing normal tissues. In this regard, charged particles like protons and carbon ions have come to be clinically effective since R. Wilson first proposed their clinical application in 1946 (2). In the early 1950s, the clinical use of proton beams was initiated at the Lawrence Berkeley National Laboratory (LBNL), paving the way for heavy ion RT starting at the same facility in the 1970s (3, 4). At present, particle beam RT is provided at over 30 facilities worldwide, and still many more are under construction or in the planning stage.

In Japan, the decision was made in 1984 to build the Heavy Ion Medical Accelerator in Chiba (HIMAC) at the National Institute of Radiological Sciences (NIRS) as an integral part of the nation's "Overall Ten-year Anti-Cancer Strategy". The accelerator complex took almost a decade to build, being completed by the end of 1993 (Fig. 1). A year later, clinical study with carbon ions for cancer therapy was initiated. Similar to the proton accelerator built at the Loma Linda University in 1990 as the first proton beam accelerator put primarily into therapeutic service, HIMAC can claim to be the world's first facility dedicated to cancer therapy using carbon ion beams. HIMAC has also been operated as a multipurpose facility available for joint use for both cancer treatment and biological, physical research.

This article reviews the clinical aspects of C-ion RT over the last decade at NIRS.

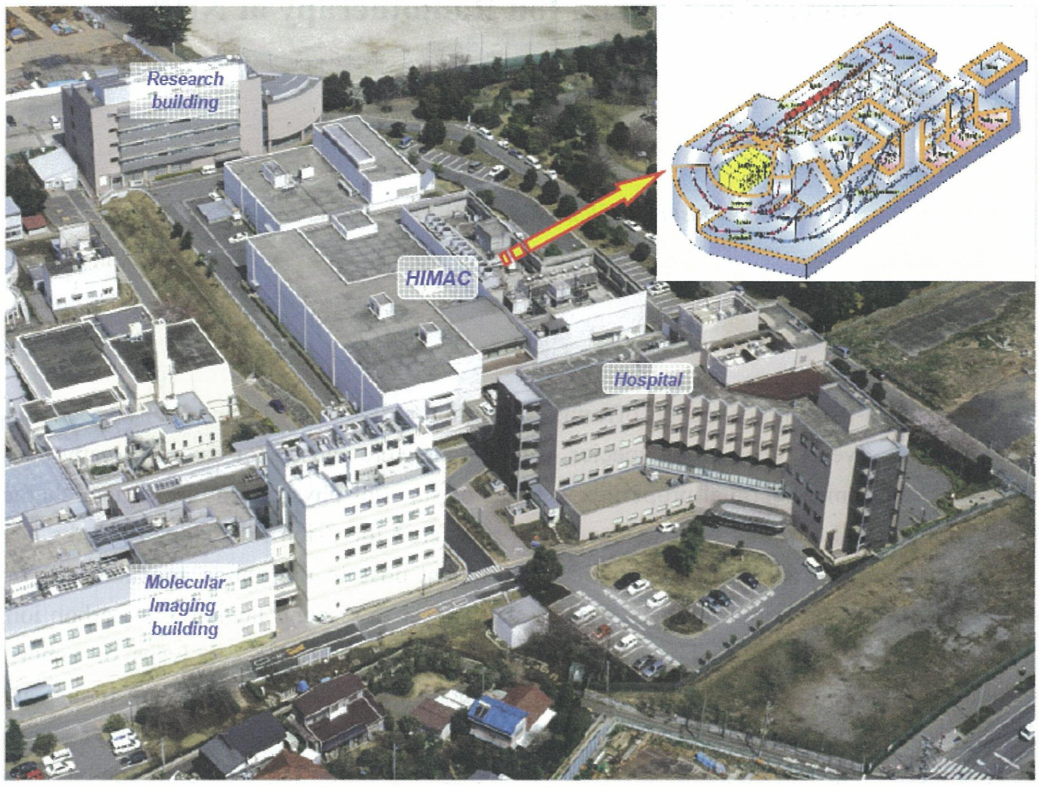

Fig. 1. The HIMAC facility at NIRS.

Characteristics of Carbon Ion Beams

Unlike X-rays, which deposit most of their energy near the skin surface, carbon ion beams are more effective in deeper tissues. The particles release the bulk of their energy as they slow down in the last few millimeters of their track, a point called the Bragg peak. The beams also scatter very little, allowing the maximum radiation dose to be precisely targeted to the tumor, thus minimizing damage to surrounding healthy tissues.

Carbon ions also cause a different type of cellular damage from protons and photons, delivering a larger mean energy per unit length (Linear Energy Transfer: LET) of their trajectory in the body (5-7). Carbon ions directly cleave double-stranded DNA at multiple sites even at the low oxygen content, so they can tackle hypoxic parts of tumors that are resistant to RT. As a result, carbon ion beams are described as a high-LET radiation similarly to neutron beams. However, in contrast to neutron beams, whose LET remains uniform at any depth in the body, the LET of carbon ion beams increases steadily from the point of incidence in the body with increasing depth to reach a maximum in the peak region (Fig.2). This property is extremely advantageous from a therapeutic viewpoint in terms of increased biological effect on the tumor. The reason is that carbon ion beams form a large peak in the body, as the physical dose and consequently their biological effectiveness increase as they advance to the more deep-lying parts of the body. This has opened up the promising potential of their highly effective use in the treatment of intractable cancers that are resistant to photon beams.

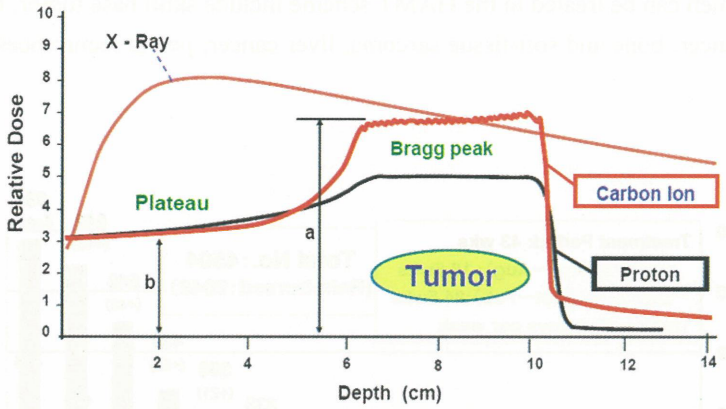

Fig. 2
Charged particles have well-localized energy deposition at the end of the beam path, called the Bragg peak, resulting in excellent dose distribution. The ratio of peak to plateau (a/b) of RBE for carbon ion beams is greater than for proton beams, which is one of the reasons why carbon ion beams have more excellent dose distribution than proton beams.

Carbon Ion Radiotherapy at NIRS

1. Organization for performance of C-ion RT

Consistent efforts have been made from the start to provide C-ion RT on an ethically and scientifically sound basis under the investigative control of Committees headed by the Carbon Ion Radiotherapy Network Committee as the supreme organ. All clinical protocols have been prepared by the Disease-specific Committees, checked by the Ethical Committee, and finally approved by the Network Committee. The Review Committee is appointed to deliberate on the validity of whether individual clinical trials should be continued, and the results of all clinical trials are submitted to the Network Committee whose sessions are invariably held in public.

In November 2003, the Ministry of Health, Labour and Welfare in Japan approved C-ion RT as "Highly Advanced Medical Technology (HAMT)" under the title of "C-ion RT for Solid Cancer". HAMT is designed to respond to the development of new medical technologies and to meet the diversifying needs for advanced treatment. It permits Specific Medical Institutions under the National Health Insurance System to offer advanced medical treatment, thereby enabling them to practice both general and advanced medical treatment within the National Health Insurance System. Under this scheme, care providers are able to charge their patients a special fee for advanced treatment in addition to the ordinary personal share of the medical fee payable by the patient himself under the National Health Insurance System. The treatment fees for HAMT were calculated on the basis of the incidental cost factors, including the construction costs of HIMAC, personnel costs, costs for the materials used for treatment, accelerator operating costs (water, electricity, lighting, etc.) and the expenditures for maintenance and management of running the facility.

2. Patients and treatment techniques

1) Patient characteristics

C-ion RT at NIRS was initiated in June 1994. Up to the present, more than 50 protocols have been established, and phase I/II and II trials have been conducted in an attempt to determine the optimal dose-fractionations and irradiation techniques for each specific tumor (8-11). The number of patients has increased year-by-year, and the facility has meanwhile reached a capacity permitting more than 700 cases to be treated each year (Fig. 3). The registration of patients has reached a total of 4,504 as of March 2009 (Fig. 4). The

categories of disease which can be treated in the HAMT scheme include skull base tumor, head and neck cancer, lung cancer, prostate cancer, bone and soft-tissue sarcoma, liver cancer, pelvic recurrences of rectal cancer, and uveal melanoma.

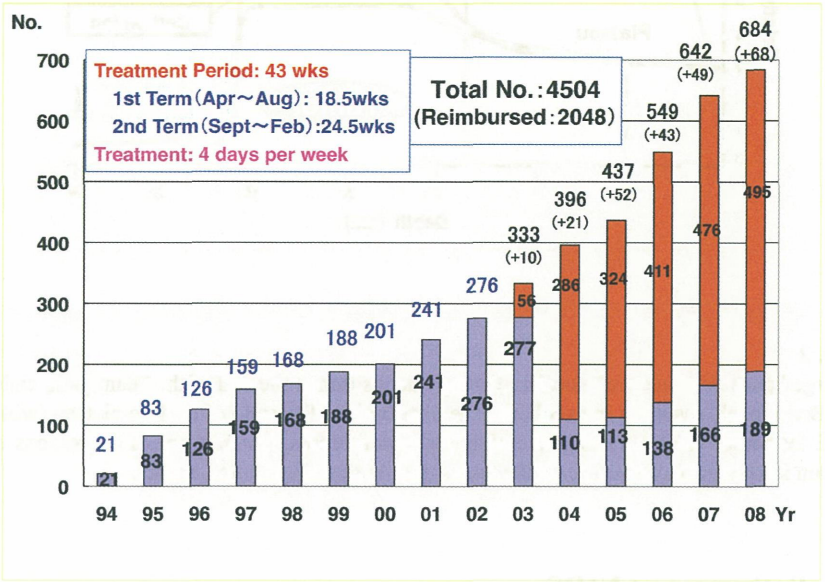

Fig.3
Annual number of patients treated with carbon ion radiotherapy at NIRS (0994.6.21 – 2009.3.1).
Dark bars indicate the patients treated under HAMT, and the light bars the patients treated in clinical trials.

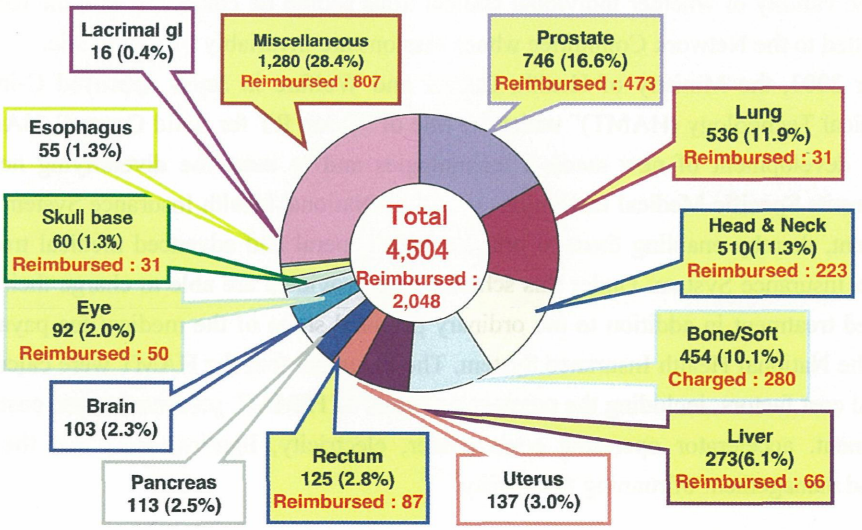

Fig. 4
Distribution of tumor sites treated with carbon ion RT from June 21, 1994 to March 1, 2009.

2) Irradiation techniques

When the patient is referred to our institute, a preliminary screening process takes place to determine whether or not the particular patient is eligible for C-ion RT under any of the disease-specific protocols. This requires

close coordination and consultation with the referring physician. When the decision has been reached that the criteria for patient eligibility are met, the patient is provided with detailed explanations about the possible side effects of treatment and the prospect of the therapeutic outcome in order to obtain the patient's informed consent. The signed consent form is then submitted to the Ethics Committee together with all other necessary documentation. The Committee thereupon deliberates on patient eligibility, and the preparatory steps for treatment will not be initiated until the Committee's approval has been granted.

The first preparatory step to ensure the proper administration of C-ion RT is the fabrication of an immobilizing device for each individual patient. A CT scan for treatment planning is then taken with the patient wearing the immobilizing device (Fig. 5). If the patient requires respiration-synchronized irradiation, the respiration synchronizing system must also be applied at the time of this CT scan (12). The CT image data obtained in this manner are then transferred to the treatment planning system known as HIPLAN (13). At this stage, the irradiation parameters in terms of the number of irradiation portals and irradiation direction are determined in conjunction with the localization of the target volume. Based on this, dose distribution is calculated using HIPLAN. Once the patient-specific irradiation parameters have been determined, the next step is to design the bolus and collimator for the selective irradiation of the tumor strictly in accordance with these parameters.

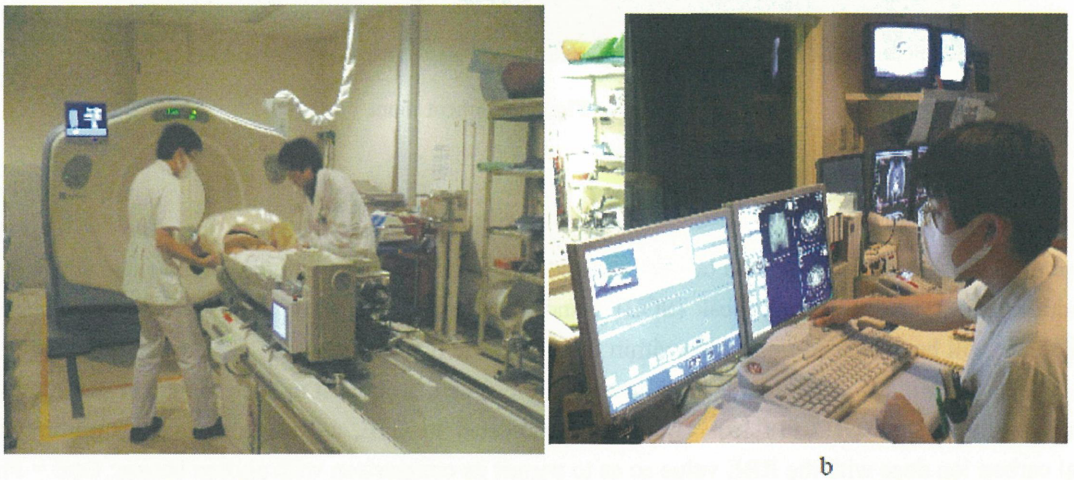

a b

Fig. 5
CT scans for treatment planning are performed with the patient wearing immobilization devices (a). Control console (b).

Based on these preparations, the patient-specific irradiation parameters and dose distribution have now been determined and the calculation results are presented to the Review Board for Treatment Planning, which examines their appropriateness. In many instances, the outcome of these deliberations will be a review request, and on many occasions, a complete redoing of the treatment planning may also be required. Clearly, if such review or redo requests are made very frequently, the entire work schedule may be affected, and it is therefore essential to examine the treatment parameters with the most meticulous care beforehand. After the irradiation parameters applicable to a particular patient have been determined and the bolus and collimator have been fabricated, the final preparations for therapy can now take place by measuring the radiation dose under the same conditions as for the actual RT session and carrying out a mockup rehearsal, followed by delivery of irradiation (Fig. 6).

Fig. 6 Treatment room

3) Dose prescription

In C-ion RT it is necessary to spread out the narrow peak to fit the target volume. Metal ridge filters are used for producing the spread-out Bragg peak (SOBP), and the shape of the SOBP has to be designed so that the target volume will be irradiated uniformly within the peak. The practice is to use HSG cells, which are parotid cancer cells, as substitutes of the tumor cells, to design the dose distribution in such a manner that they will be killed uniformly in the SOBP (14-15). The dose is indicated in GyE, a unit calculated by multiplying the physical carbon ion dose with the RBE value so as to permit its comparison with photon beams: GyE = Physical dose x RBE. It should be pointed out here that the RBE of the carbon ion beams used for RT is 3.0 at the distal part of the SOBP. This value is identical to the RBE determined for the neutron beam RT previously provided at NIRS (15).

As biological dose distribution is flat within SOBP, once the RBE values have been determined at a given position, they are easily calculated at any position by dividing the biological dose by the physical dose. RBE of carbon ions was estimated to be 2.0∽3.0 along SOBP for acute skin reactions. As seen in Fig. 7, a clinical dose of 2.7 Gy (E) would be given at any position within SOBP; for example, a physical dose of 0.9 Gy carbon ions at the 8-mm upstream position would give an RBE value of 2.7/0.9 = 3.0, whereas 1.13 Gy at the middle of SOBP should bring an RBE value of 2.7/1.13 = 2.4.

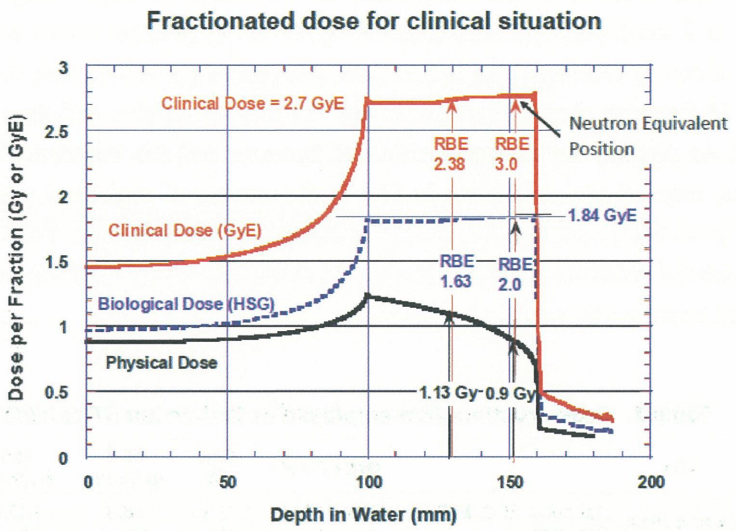

Fig. 7

.Experimental and clinical RBE of 290 MeV/u carbon-ion beams with a 6-cm SOBP.

4) Dose fractionation

C-ion RT at NIRS is available four days a week (Tuesday through Friday). In recent years, Monday has become available on a once-a-month basis for tumors treatable in a single fraction, and this also facilitated an increase in the annual patient number load. HIMAC is in principle closed for therapy on weekends as well as on Mondays, when the accelerator is subjected to maintenance or is used for physical and biological experiments.

The radiotherapeutic approach of our treatment has been to fix both the total number of fractions and the overall treatment time for each tumor. In dose escalation studies, we escalated the dose in incremental steps of 5 or 10% at a time. After the recommended dose thus became established in phase I/II trials, the transition to phase II trials was made. Supposing that a fractionation regimen of 16 fractions spread over four weeks had been selected and that a total dose of 57.6 GyE had been increased by 5% to 60.5 GyE, this would have meant that the dose per fraction would have been stepped up from 3.6 GyE to 3.8 GyE, in light of the fact that the irradiation time and fraction number had been fixed. Once the recommended dose resulting from the dose escalation trial has been decided, phase II trials or Advanced Therapy can then be initiated with this recommended dose.

In view of the unique physical and biological properties of carbon ions, it is theoretically possible to perform hypofractionated RT consisting of only a few irradiation sessions. In contrast, experiments with neutron beams that have the same high-LET components as carbon beams have demonstrated that increasing their fraction dose tended to lower the RBE for both the tumor and normal tissues. In these experiments, however, RBE for normal tissues does not decrease as rapidly as that for the tumor (16). This experimental result substantiates the previous observation that the therapeutic ratio increases rather than decreases even though the fraction dose is increased.

Similar results have also been obtained in experiments conducted with carbon ion beams at NIRS (17,18). They have provided biological evidence for the validity of the short-course hypofractionated regimen with C-ion RT.

5) Results of treatment by tumor type

As stated above, carbon ion beams have a therapeutically favorable biological dose distribution. Utilizing these properties makes it possible to complete the therapy in a short time. As is seen in Table 1, progress in dose escalation has already been made on a scale that permits the RT course for stage I lung cancer and liver cancer to be completed in 1 or 2 irradiation sessions, respectively. Even for prostate cancer and bone and soft tissue tumors that require a relatively prolonged irradiation time, it is possible to accomplish the treatment course with carbon ion beams in 16 fractions over 4 weeks, only half the fraction number and time required for x-ray and proton beam therapy. At present, the average number of fractions and the treatment time per patient is 12.5 fractions and 3 weeks, respectively. As shown in Fig. 3, the number of registered patients has been steadily increasing year after year. Apart from the fact that the irradiation methods have been firmly established and therapy can be administered without difficulty, this may be ascribed to the significant shortening in the number of fractions and overall treatment time per patient.

Table 1. Dose-Fractionation employed in Carbon ion RT at NIRS

Site		GyE / Fr. / Wk	GyE / fr	BED (α/β=10)	BED (α/β=2.5)
Head & Neck	Adenoca, ACC, MMM Sarcoma	57.6 / 16 / 4 70.4 / 16 / 4	3.6 4.4	78.3 101.4	140.5 194.3
Skull base	Chordoma & Chondrosarcoma	57.6 / 16 / 4	3.6	78.3	140.5
Lung	Peripheral	60.0 / 4 / 1 46.0 / 1 / 1dy	15.0 -	150.0 -	420.0 -
Lung	: Mediastinum Hilar : Superficial : Bulky	48.0 / 12 / 3 54.0 / 9 / 3 68.4 / 12 / 3	4.0 6.0 5.7	67.2 86.4 107.4	124.8 183.6 224.4
Liver	Hepatocellular ca Metastasis of Rectal ca	42.8 / 2 / 2dys 46.0 / 1 / 1dy	21.4 -	134.4 -	409.2 -
Bone & soft tissue	sarcoma	70.4/ 16 / 4	4.4	101.4	193.4
Prostate	Low/Medium/High risk	57.6 /16/ 4	3.6	78.3	140.5
Pancreas	Pre-operative RT C-ion+ CDDP 1000mg/m²	35.2 / 8 / 2 45.6 / 12 / 3	4.4 3.8	50.7 62.9	97.2 114.9
Rectum	Post-ope pelvic rec.	73.6 / 16 / 4	4.6	107.5	209.0

Our experience to-date can be summed up by characterizing C-ion RT as follows: 1) By location, it is effective in tumors of the head and neck (including the eye), the base of the skull, lung, liver, prostate, bone and soft tissue, and pelvic recurrence of rectal cancer. 2) By pathological type, it is effective against pathologically non-squamous cell types of tumors for which photon beams are little effective, including adenocarcinoma, adenoid cystic carcinoma, hepatocellular carcinoma, and sarcomas (malignant melanoma, bone and soft-tissue sarcoma, etc.). For certain cancers such as malignant melanoma of the head and neck, it was important to develop methods for preventing distant metastasis so as to improve the survival rate still further. In this context, C-ion RT combined with chemotherapy has been initiated. For intractable cancers such as malignant glioma, cancer of the pancreas, uterine cancer and esophageal cancer, it is necessary to further improve therapeutic outcomes. To this end, clinical trials are being continued.

In terms of toxic reactions (side effects), significant progress has been made, as the toxicities initially associated with dose escalation such as ulceration and perforation of the gastrointestinal tract requiring surgery are no longer encountered in the wake of improvements in irradiation techniques.

The details of the treatment for each tumor are described in the subsequent pages in this volume of the Proceedings.

Summary

The promising aspect of C-ion RT for the treatment of cancer lies in its superior biological dose distribution that makes the carbon ion beam the best-balanced particle beam available. Thus, comparison of the ratio of RBE in the peak region against RBE in the plateau region shows that, of all heavy ion beams, carbon ion beams have the most favorable value.

In the middle of 2009, C-ion RT will reach its 15th anniversary at NIRS. So far, with the support of the many members concerned both inside and outside the Institute, a substantial amount of evidence has been accumulated in terms of the safety and efficacy of C-ion RT for various types of malignant tumors. One of the most important objectives in these endeavors has been to determine, in particular, the validity and limits of hypofractionated, accelerated RT. Furthermore, at the end of 2003, the Institute was successful in obtaining approval for the Highly Advanced Medical Technology (HAMT) from the government. This was an important landmark for widening the scope of diseases corresponding to C-ion RT. In this manner, C-ion RT has meanwhile won for itself a solid place in general medical practice, with the next target being that of obtaining approval for this therapy to be included in general practice under the National Health Insurance scheme.

References

[1] Shibuya H, Tsujii H: The structural characteristics of radiation oncology in Japan in 2003, 27 April 2005. Int J Radiat Oncol Biol Phys. 62: 1472-1476, 2005.

[2] Wilson RR: Radiological use of fast protons. Radiology. 47:487-491, 1946.

[3] Linstadt DE, Castro JR, Phillips TL: Neon ion radiotherapy: results of the phase I/II clinical trial. Int J Radiat Oncol Biol Phys. 20:761-769,1991.

[4] Castro JR: Future research strategy for heavy ion radiotherapy. Progress in Radio-Oncology. (ed. Kogelnik HD), Monduzzi Editore, Italy, pp643-648, 1995.

[5] Raju MR: Heavy particle radiotherapy. Academic Press, New York, 1980.

[6] Chen GTY, Castro JR, Quivey JM: Heavy charged particle radiotherapy. Ann Rev Biophys Bioeng. 10: 499-529, 1981.

[7] Kraft G: Tumor therapy with heavy charged particles. Prog Part Nucl Phys. 45: S473-S544, 2000.

[8] Tsujii H, Morita S, Miyamoto T, et al: Preliminary results of phase I/II carbon-ion therapy at the NIRS. J Brachytherapy Int. 13: 1-8, 1997.

[9] Tsujii H, Mizoe J, Kamada T, et al: Overview of clinical experiences on carbon ion radiotherapy at NIRS. Radiother Oncol. 73(Suppl 2): S41-S49, 2004.

[10] Tsujii H, Mizoe J, Kamada T, et al: Clinical results of carbon ion radiotherapy at NIRS. J Radiat Res. 48 (Suppl A): A1–13, 2007

[11] Tsujii H, Kamada T, Baba M, et al: Clinical advantages of carbon-ion radiotherapy. New J Phys. 10: 1367-2630, 2008.

[12] Minohara S, Kanai T, Endo M, et al: Respiratory gated irradiation system for heavy-ion radiotherapy. Int J Radiat Oncol Biol Phys. 47: 1097-1103, 2000.

[13] Endo M, Koyama-Ito H, Minohara S, et al: HIPLAN - a heavy ion treatment planning system at HIMAC. J Jpn Soc Ther Radiol Oncol. 8: 231-238, 1996.

[14] Kanai T, Furusawa Y, Fukutsu K, et al: Irradiation of mixed beam and design of spread-out bragg peak

for heavy-ion radiotherapy. Rad Res. 147: 78-85, 1997.

[15] Kanai T, Endo M, Minohara S, et al: Biophysical characteristics of HIMAC clinical irradiation system for heavy-ion radiation therapy. Int J Radiat Oncol Biol Phys. 44: 201-210, 1999.

[16] Denekamp J, Waites T, Fowler JF: Predicting realistic RBE values for clinically relevant radiotherapy schedules. Int J Radiat Biol. 71: 681-694, 1997.

[17] Koike S, Ando K, Uzawa A, et al: Significance of fractionated irradiation for the biological therapeutic gain of carbon ions. Radiat Prot Dos. 99: 405-408, 2002.

[18] Ando K, Koike S, Uzawa A, et al: Biological gain of carbon-ion radiotherapy for the early response of tumor growth delay and against early response of skin reaction in mice. J Radiat Res. 46:51-57, 2005.

Carbon Ion Radiotherapy for Skull Base and Paracervical Tumors

Azusa Hasegawa, Jun-etsu Mizoe, Keiichi Jingu, Hiroki Bessho,
Tadashi Kamada, and Hirohiko Tsujii

Research Center for Charged Particle Therapy, National Institute of Radiological Sciences, Chiba, Japan.
E-mail: azusa@nirs.go.jp, j_mizoe@nirs.go.jp

Abstract

To estimate the toxicity and efficacy of the clinical trials for patients with skull base and paracervical tumors treated with carbon ion radiotherapy.

A phase I/II dose escalation study for skull base and paracervical tumor was initiated in April 1997. The phase I/II dose escalation trial was performed up to the fourth-stage dose level. From April 2004, a phase II clinical trial was initiated under the Highly Advanced Medical Technology scheme with an irradiation schedule of 60.8 GyE in 16 fractions over four weeks.

At the time of analysis, there was no evidence of any serious acute or late reactions in skull base and paracervical tumors. For skull base and paracervical tumor, the carbon ion dose in excess of 57.6 GyE improves local control.

Introduction

The limiting factor for photon radiotherapy conventionally applied to the skull base and paracervical tumors is the adjacent normal tissue, seeing that photon radiotherapy has poor local control. On the other hand, proton radiotherapy with its superior physical-spatial distribution has provided a major improvement in local control in view of the possibility of dose escalation. It has been pointed out, however, that in certain patient groups it is difficult to achieve local control with proton radiotherapy even at elevated doses. It has thus been recognized that 1) chordoma patients offer a worse prognosis than chondrosarcoma patients, 2) among chordoma patients, the prognosis for paracervical chordoma patients is worse than for skull base chordoma, it is worse for non-chondroid patients than for chondroid ones, and it is worse for females than for males, and 3) for meningeal tumors, the prognosis for the atypical or malignant types is worse than for the benign type, and the prognosis for the age group of 60 and above is poorer than for those under 60. Therefore, the high RBE of carbon ion radiotherapy has a promising potential for these intractable skull base and paracervical tumors.

Patients and Methods

Prior to this protocol, a pilot study using 48 GyE in 16 fractions over 4 weeks with 8 patients was carried out starting in May 1995. Then, a phase I/II clinical trial (Protocol 9601) was initiated in April 1997. Chordoma, meningioma, chondrosaracoma and other tumors originating from the skull base or paracervical spine located superior to the C2 vertebra were targeted. Only patients with residual tumors after surgery or with inoperable tumors were permitted to partake in the carbon ion radiotherapy. The eligibility criteria for enrollment in this clinical trail were the presence of histologically proven tumor, patient age ranging from 15 to 80 years, KPS of 60% or more, neurological function of grade I or II, absence of anti-cancer chemotherapy within the previous four weeks, survival expectancy of six months or more, and no distant metastasis to other parts. In the meantime, the carbon ion dose was escalated in successive stages: 48.0 GyE (4 patients), 52.8 GyE (6 patients), 57.6 GyE (10 patients) and 60.8 GyE (9 patients). The phase I/II clinical trial was concluded in February 2004, and in April 2004 a phase II clinical trial was initiated under the Highly Advanced Medical Technology scheme with an irradiation schedule of 60.8 GyE in 16 fractions over 4 weeks. Twenty-five patients had been enrolled into this trial up to August 2008.

Acute toxicity was assessed based on the Radiation Therapy Oncology Group (RTOG) score, late toxicity was determined based on the RTOG / European Organisation for Research and Treatment of Cancer (EORTC) score. Local control and overall survival rates were calculated according to the Kaplan-Meier method.

Treatment planning and Dose volume histogram analysis

The patients were positioned in customized cradles (Moldcare; Alcare, Tokyo Japan) and immobilized with a low-temperature thermoplastic (Shellfitter; Kuraray Co, Ltd, Osaka, Japan). A set of 3 mm-thick CT images was taken for treatment planning. Three-dimensional treatment planning was performed by the Heavy Ion Plan software (HIPLAN). The clinical target volume (CTV) and normal structures were delineated on CT images to permit DVHs analysis. In addition, T2 weighted and gadolinium-enhanced T1 weighted images were routinely taken for treatment planning using the fusion technique in conjunction with a treatment planning CT. The initial CTV (CTV1) included the gross tumor volume (GTV) and suspected subclinical lesions. A margin of 3-5mm was usually added to the GTV to create to a small CTV (CTV2) in order to boost treatment. When the tumor was located close to critical organs, such as the brainstem, the spinal cord, the eyeballs or optic nerve, the margin was reduced accordingly. In treatment planning, cumulative dose volume histograms (DVHs) of the critical normal structures and dose-surface histograms (DSHs) of the skin were calculated. DVHs and DSHs for the following structures must be provided: cerebrums, brainstem, medullary, pons, spinal cord, optic nerves and chiasma, eyeballs and skin. For normal tissues, the maximum dose was set as 60 GyE for the surface of the brainstem and spinal cord, 50 GyE for the center of the brainstem and spinal cord and 55 GyE for the chiasma and contralateral optic nerve in accordance with the protocol for the base of skull and paracervical tumors of the Proton Radiation Oncology Group (PROG). In particular, when the both optic nerves were involved in a high dose area, treatment planning was performed to spare the contralateral optic nerve and chiasm using our previously criteria. These outcomes of the visual function for the patients are analyzed in progress as a prospective study.

Results

The 54 patients included in the analysis between May 1995 and August 2008 consisted of 25 males and 29 females. One female patient with chondrosarcoma had to be excluded because she was treated with surgery for metastasis and her diagnosis was changed to malignant melanoma. She was treated with 57.6 GyE. The age range of the 53 patients was from 16 to 78, with a median of 49 years. Histologically, 31 patients had chordoma, 10 chondrosarcoma, 6 malignant meningioma, 5 olfactory neuroblastoma and 1 giant cell carcinoma.

Acute reactions were of a minor nature, as 1 patient of the 48 GyE group showed a grade 3 skin reaction and 1 patient of the 57.6 GyE group showed a grade 3 mucosal reaction. A late grade 2 brain reaction was detected in 2 patients, but no other adverse reactions were discovered. At the time of analysis, there was no evidence of any serious acute or late reactions.

The tumor effect remains mostly as stable disease (SD) within six months after carbon ion radiotherapy, and there were in most cases no changes in tumor size during the follow-up periods. Local control was defined as showing no evidence of tumor regrowth by MRI, CT, physical examination, or biopsy. The five-year local control rates according to prescribed tumor dose were 75% at 48 GyE (n=4), 67% at 52.8 GyE (n=6), 78% at 57.6 GyE (n=9) and 95% at 60.8 GE (n=34) (Fig. 1). The five-year OS rates were 50% at 48 GyE, 100% at 52.8 GyE, 100% at 57.6 GyE and 79% at 60.8 GyE (Fig. 2). Four of 34 patients irradiated with a dose of 60.8 GyE died of interrupted pneumonia, distant metastasis, hepatic failure, and marginal failure. Local tumor control was achieved in these cases. The five-year local control (LC) rates according to histological types were 80% for chordomas (n=31), 100% for chondrosarcomas (n=10), 80% for malignant meningiomas (n=6), and 100% for olfactory neuroblastomas (n=5). The five-year overall survival (OS) rate was 87% for chordomas, 64% for chondrosarcomas, 83% for malignant meningiomas, and 100% for olfactory neuroblastomas. Two of the six malignant meningioma patients died because of distant metastasis 23 months, and local recurrence 85 months, respectively, after carbon ion radiotherapy. This local recurrence patient had had a postoperative recurrence and received low-dose carbon ion radiotherapy of 52.8 GyE.

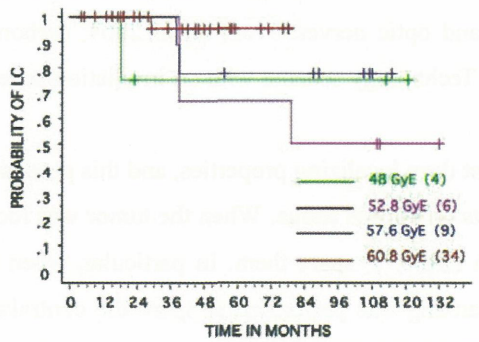

Figure 1. Local Control Curve for Skull Base Tumor (Apr 97~Aug 08)

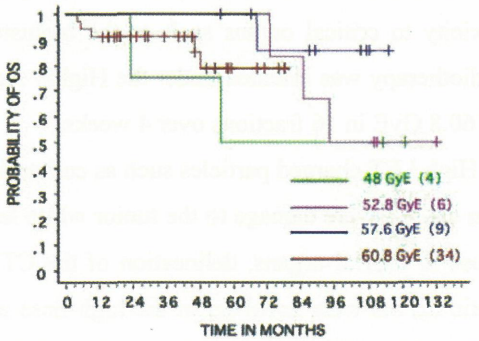

Figure 2. Overall Survival Curve for Skull Base Tumor (Apr 97~Aug 08)

The 31 chordoma patients were divided into two groups, a low-dose group (n=10) irradiated with doses ranging from 48 to 57.8 GyE and a high-dose group (n=21) irradiated with 60.8 GyE. The five-year LC rates were 60% for the low-dose group and 94% for the high-dose group. One patient of the high-dose group developed marginal failure 29 months later. The five-year OS rates were 90% for the low-dose group and 87% for the high-dose group. Two patients from the high-dose group died due to hepatic failure and marginal failure.

Figure 3 shows LC and OS curves for 21 chordomas irradiated with 60.8 GyE.

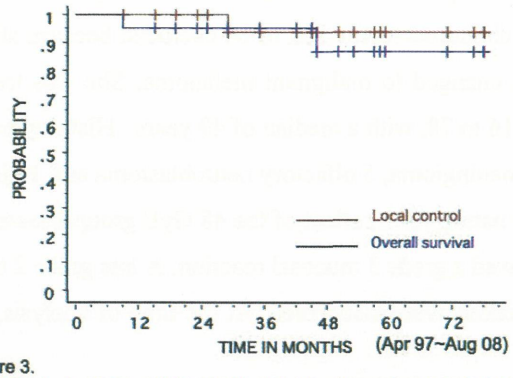

Figure 3.
Local Control and Overall Survival for 21 Chordomas irradiated with 60.8 GyE

Discussion

In this phase I/II clinical study for skull base and paracervical tumors, dose escalation trials were performed up to the fourth-stage dose level. Because dose escalation is implemented after checking the reactions of the important adjacent organs – the brain and spinal chord – the scheduled enrollment period was exceeded and therapy was commenced under the Highly Advanced Medical Technology scheme for these patients in April 2004 with a dose fractionation regimen of 60.8 GyE in 16 fractions over 4 weeks. No tumor regression was seen in most cases regardless of carbon ion dose. The lower dose groups (48.0 and 52.7 GyE) showed local recurrence in two chordoma and one malignant meningioma. The third-stage dose escalation group (57.6 GyE) showed local recurrence in two chordoma and one chondrosarcoma. The fourth-stage dose escalation group (60.8 GyE) showed local recurrence in one chordoma.

Conclusion

The carbon ion dose in excess of 57.6 GyE improves local control. Additionally, we did not observe severe toxicity to critical organs such as the brainstem, spinal cord and optic nerves. From April 2004, carbon ion radiotherapy was initiated under the Highly Advanced Medical Technology scheme with an irradiation schedule of 60.8 GyE in 16 fractions over 4 weeks.

High LET charged particles such as carbon ions have excellent dose localizing properties, and this potentiality can cause severe damage to the tumor while lessening the effects on normal tissue. When the tumor was located close to critical organs, delineation of the CTV was done with efforts to spare them. In particular, when both optic nerves were involved in the high-dose area, treatment planning was performed to spare the contralateral optic nerve and chiasm according to our previous dose criteria. For tumors close to the brainstem and spinal cord, we recommend surgical resection to create a space between the tumor and brainstem or spinal cord before carbon ion radiotherapy. This allows the prevention of severe toxicity to the brainstem and spinal cord. Tumors such as chordoma can thus only be judged on the results of long-term prognosis. Consequently, it will take more time to reach a definitive conclusion. It is clear that carbon ion radiotherapy compared with photon or other charged particle radiotherapy will deliver a high local control rates with low toxicity to the surrounding normal tissues.

Case Description

Postoperative recurrence of chordoma in the left parapharyngeal space (Fig. 4): Female, 63 year. Sixty-six months have elapsed since carbon ion radiotherapy by a regimen of 52.8 GyE in 16 fractions over 4 weeks. The tumor has virtually disappeared and the post-treatment course remains favorable, with no evidence of tumor recurrence.

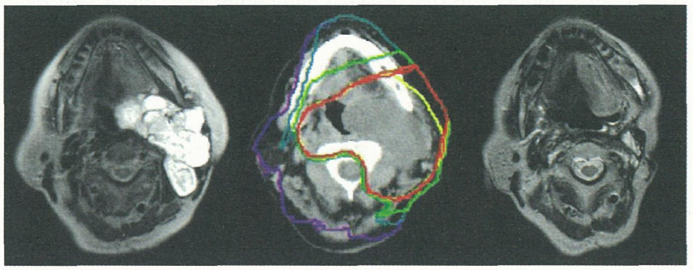

Figure 4. Postoperative Recurrence of Chordoma in the Left Parapharyngeal Space treated with Carbon Ion Radiotherapy
Images of T2-weighted MRI before carbon ion radiotherapy, isodose distribution, and 66 months later. The dose delivered to the clinical target volume was 52.8 GyE in 16 fractions over 4 weeks.
Isodose level: red = 96%; orange = 90%; green = 50%; cyan = 30%; purple = 10%.
Contour: yellow = clinical target volume.

References

[1] Tsujii H, Mizoe J, Kamada T, *et al*. Overview of clinical experiences on carbon ion radiotherapy at NIRS. *Radiother Oncol* 2004;73:41–49.

[2] Tsujii H, Mizoe J, Kamada T, *et al*. Clinical results of carbon ion radiotherapy at NIRS. *Radiat Res* 2007;48:A1–13.

[3] Endo M, Koyama-Ito H, Minohara S, et al: HIPLAN-A heavy ion treatment planning system at HIMAC. *J Jpn Soc Ther Radiol Oncol* 1996; 8: 231-238.

[4] Hasegawa A, Mizoe J, Mizota A, Tsujii H. Outcomes of visual acuity in carbon ion radiotherapy: analysis of dose–volume histograms and prognostic factors. *Int J Radiat Oncol Biol Phys*, 2006; 64 (2): 396-401.

[5] Mizoe J, Hasegawa A, Takagi R, Bessho H, Onda T, Tsujii H: Carbon ion radiotherapy for skull base chordoma. *Skull Base,* 2009; 19 (3): 219-224.

Head and Neck Tumors

Kenichi Jingu, Jun-etsu Mizoe, Azusa Hasegawa, and Hiroki Bessho

Research Center for Charged Particle Therapy, National Institute of Radiological Sciences, Chiba, Japan
Corresponding Author: Jun-etsu Mizoe, e-mail address: j_mizoe@nirs.go.jp

Introduction

Clinical trial with carbon ion radiotherapy for the head and neck tumors was conducted under "the Phase I/II Clinical Trial (Protocol 9301) on Heavy Particle Radiotherapy for Malignant Head and Neck Tumors", that was initiated in June 1994 by way of a dose escalation study on a fractionation method of 18 fractions over 6 weeks. This trial was followed by a next dose fractionation and dose escalation study commenced in June 1996 under "the Phase I/II Clinical Trial (Protocol 9504) on Heavy Particle Radiotherapy for Malignant Head and Neck Tumors" using a fractionation method of 16 fractions over 4 weeks. The results of these two trials were published in 1994 [1]. Following the outcome of these two studies, the "Phase II Clinical Trial on Heavy Particle Radiotherapy for Malignant Head and Neck Tumors (Protocol 9602)" was initiated on a 64.0GyE/16 fractions/4 weeks fractionation method (or 57.6 GyE/16 fractions/4 weeks when the wide-range of the skin was included in the target volume) in April 1997.

Based on the results of preliminary analysis of the 9602 protocol, two protocol were derived with effect from April 2001 into 1) the "Phase I/II Clinical Trial of Carbon Ion Radiotherapy for Bone and Soft Tissue Sarocomas in Head and Neck (Protocol 0006)" designed as a dose escalation study for bone and soft-tissue tumors, and 2) the "Phase II Clinical Trial of Carbon Ion Radiotherapy Combined with Chemotherapy for Mucosal Malignant Melanoma in Head and Neck (Protocol 0007)" for the treatment of malignant melanoma with concomitant chemotherapy.

1. Phase II Clinical Trial on Heavy Particle Radiotherapy for Malignant Tumors in Head and Neck (Protocol 9602)

The eligibility criteria for enrollment in this Clinical Study were the presence of histologically proven malignancy, measurable tumor in the head and neck region including N0M0 in principle, with no co-existent malignant active tumor, no distant metastasis to other parts, an age range from 15 to 80 years and a prospective prognosis of at least 6 months or longer. The candidates were also required to have a Karnofsky performance status index (K.I.) of 60% or more and to give their written informed consent for inclusion in this Clinical Study. A further requirement was the absence of prior radiotherapy for the carbon treated area, the absence of intractable inflammatory lesion and no interval time less than four weeks from the completion of last chemotherapy.

The clinical trial was commenced in April 1997, and by February 2009 a total of 351 patients corresponding to 354 lesions was registered (for three patients, a second lesion was treated in the same patient). Five of the 351 patients were excluded from the analysis because of 1) that carbon ion radiotherapy had to be cancelled for two patient with malignant melanoma due to a deterioration of the symptoms, 2) that another patient with lacrimal gland tumor was diagnosed as a metastasis from the thyroid gland before carbon ion radiotherapy, 3) that the ameloblastoma of a further patient was diagnosed as a benign tumor after histological re-examination and 4) that the histological confirmation was done by cytology only. The data for 349 lesions of 346 patients

treated until February 2009 are recorded as follows: Patient age ranged from 16 to 80, averaging 57 years of age, with 176 male and 173 female. Their K.I. ranged from 60% to 100%, with the median value being 90%. The sites of disease are consisted of 91 lesions with paranasal sinus, 71 with nasal cavity, 43 with salivary gland, 43 with oral cavity, 38 with orbita, 36 with pharynx, 11 with thyroid gland, 9 with auricula and 7 with tumors in other sites. Histologically, the tumors are classified as follows: 120 with adenoid cystic carcinoma, 102 with malignant melanoma, 40 with adenocarcinoma, 19 with squamous cell carcinoma, 13 with papillary adenocarcinoma, 11 with mucoepidermoid carcinoma, 6 with osteosarcoma, 6 with acinic cell carcinoma, 5 with unfifferentiated carcinoma and 27 with other histological types of tumor. There were five cases of T1, 27 of T2, 52 of T3, 151 of T4, 77 of post operative, 27 of post chemotherapy, 9 of post operative and post chemotherapy and one of post carbon ion radiotherapy. Carbon ion radiotherapy was given on a fractionation method of 16 fractions/4 weeks. The 349 lesions were irradiated with a dose of 57.6GyE in 243 cases and with one of 64.0GyE in 106 cases.

Acute reactions of the normal tissues of the 349 lesions which were treated until February 2009 included grade 3 skin reactions in 15 patients (5%) and in the mucosa in 49 patients (14%), and no reactions worse than grade 3 were observed. Late toxic reactions comprised grade 2 skin reaction in 7 patients (2%) and mucosa reactions in 8 patients (3%), with no evidence of radiation-induced toxicities worse than these.

The tumor reaction at six months after treating the 328 lesions was CR for 40 lesions, PR for 148 lesions, NC for 135 lesions and PD for 5 lesions, with the response rate (CR+PR) being 57%. The five-year local control rate was 70% and five-year overall survival was 48% (Fig. 1). Five-year local control rate by histological type was 81% for the 38 adenocarcinoma, 74% for the 107 adenoid cystic carcinoma, 74% for the 100 malignant melanoma and 70% for the 19 squamous cell carcinoma (Fig. 2). The five-year survival rate was 68% for adenoid cystic carcinoma and 56% for adenocarcinoma (Fig. 3).

Although the reactions in normal tissues included acute grade 3 skin and mucosal reactions in approximately 10% of the subjects, the late reactions were grade 2 or less. This therapy can therefore be described as presenting no clinical problems. The overall local control rate was 70% at 5 years. The therapeutic effectiveness of the therapy was particularly outstanding for non-squamous cell carcinoma, a tumor intractable to photon radiotherapy. Treatment results of combined surgery and radiotherapy ranged from 49% to 98% of five-year local control and from 40~80% of five year over all survival. Recommended treatment is surgery with or without radiotherapy [2]. When they were treated by radiotherapy alone, the local control was 20~25% [3, 4]. In the present study, the local control rate was 70%, in spite of including 141 cases (43%) of T4 and 110 cases (34%) of recurrence of post operative and/or post chemotherapy. Therefore the local control of carbon ion radiotherapy is promising for locally advanced head and neck cancer.

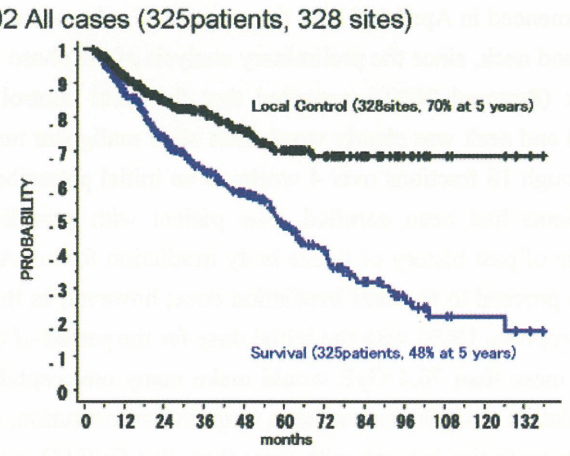

Fig.1: Local control and survival curves of the H&N cancer (9602).

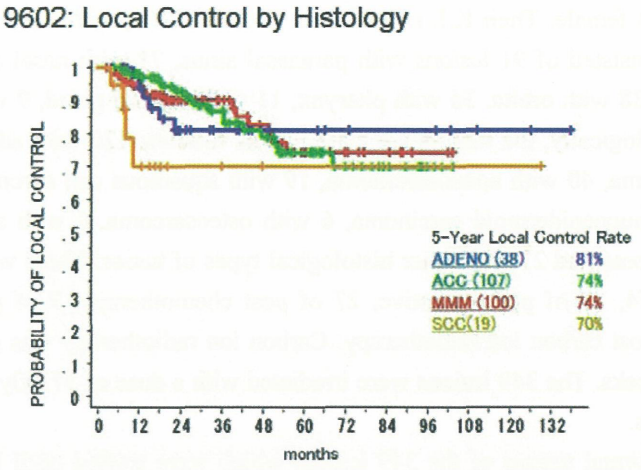

Fig. 2: Local control curves by histology (9602).

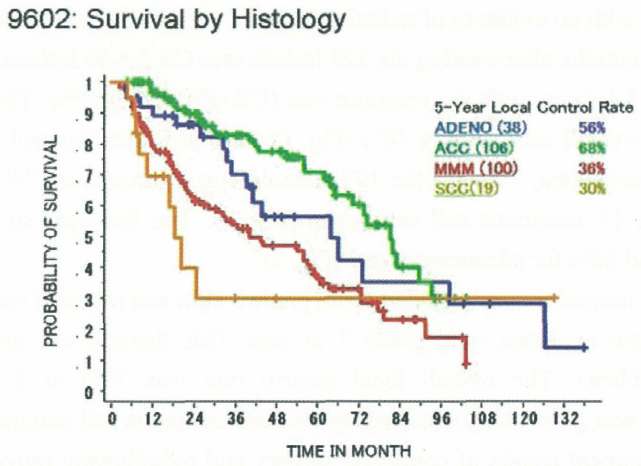

Fig. 3: Survival curves by histology (9602).

2. Phase I/II and II Clinical Trials of Carbon Ion Radiotherapy for Bone and Soft Tissue Sarcomas in Adult Head and Neck (Protocol 0006)

Phase I/II protocol was commenced in April 2001 for the purpose of a dose escalation study against bone and soft-tissue tumors in the head and neck, since the preliminary analysis of the phase II clinical trial for malignant tumors in the head and neck (Protocol 9602) suggested that the local control and survival of bone and soft-tissue sarcoma in the head and neck was clearly worth than other malignant tumor. We adopted 70.4 GyE (fraction dose of 4.4 GyE) through 16 fractions over 4 weeks as an initial prescribed dose in the present study. Until February 2008, 28 patients had been enrolled. One patient with parapharyngeal osteosarcoma was excluded from analysis because of past history of whole body irradiation for her ALL. According to following toxicities, we might be able to proceed to the next irradiation dose; however, in the present study, because the local control rate had been appropriate 100% with the initial dose for the period of the present phase I study and because it was definitive that more than 70.4 GyE would make many unacceptable adverse effects from the results of carbon ion dose escalation study for sarcomas in trunk in our institution, Kamada et al. described that 4 of 17 patients had Grade3 late toxicities in trunk with more than 70.4 GyE [5], we determined that 70.4 GyE / 16fr. is a recommend irradiation-dose for unresectable bone and soft tissue sarcomas in adult head and neck.

This phase I/II study was completed on February 2008. From April 2008, phase II clinical study was started with same dose fractionation of 70.4 GyE/16 fractions/4 weeks.

Till the February of 2009, three patients were enrolled into this phase II study. A total of 30 patients of phase I/II and II study were analyzed. They consisted of 10 patients with osteosarcoma, 6 patients with MFH, 2 patients with chondrosarcoma, 2 patients with hemangiopericytoma, 2 patients with myxofibrosarcoma, 2 patients with leimyosarcoma, and each one patient with fibrosarcoma, angiosarcoma, small round cell sarcoma, spindle cell sarcoma, PNET and rhabdomyosarcoma.

In preliminary analysis of the 29 patients who had follow-up period for more than six months, almost of all patients presented less than grade 2 acute reactions; however, only one patient presented an early grade 3 mucosal reaction. All late skin and mucosal reactions were grade 1 or less. The tumor reactions consisted of CR (4), PR (5) and SD (20). The response rate was 31%. The median observation period was 29 months. The three-year local control rate was 91.8% and their three-year overall survival rate was 72.8% (Fig. 4).

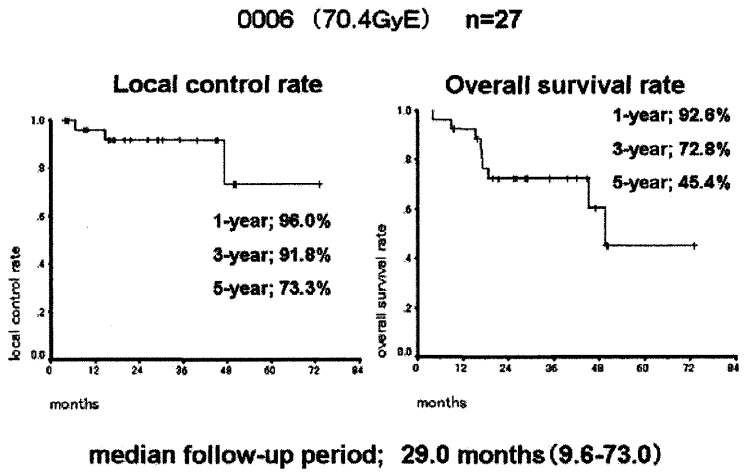

Fig. 4: Local control curve and survival curve of bone and soft tissue sarcoma in H&N (0006).

Bone and soft tissue sarcomas in head and neck are rare mesenchymal malignant neoplasms accounting for less than 10% of all bone and soft tissue sarcomas and approximately 1% of all head and neck neoplasms. Willers et al. said that wide resection margins are anatomically difficult to achieve, and the delivery of high radiation dose can be limited by the vicinity of critical normal tissue structures (spinal cord, brain stem, optic chiasm, eyes). Accordingly, local control rates for head and neck sarcomas are lower compared to the extremities [6]. Five years local control rate of combined surgery and radiotherapy is 60-70% with five years overall survival. Local control of surgery alone is around 54% and that of radiotherapy alone is 43- 50% [7]. However, in cases with unresectable sarcoma, the local control and survival prognosis were miserable. Conventional radiotherapy with a total dose less than 65 Gy showed no local control [8, 9, 10]. Results of carbon ion radiotherapy in our previous study (9602) for bone and soft tissue sarcomas in head and neck, in which study patients were treated by 64.0 or 57.6 GyE/16 fraction, showed 24% of five years local control and 36% of overall survival. On the other hand, the three-year local control rate of this study (0006) was 91.8% and their three-year overall survival rate was 72.8%. The results showed improved tendency of 0006 study in both local control and overall survival, especially, local control significantly was improved.

Now we perform a phase II clinical study with the dose of 70.4 GyE for unresectable bone and soft tissue sarcomas in head and neck.

3. Phase II Clinical Trial for Mucosal Malignant Melanoma in Head and Neck Combined with Chemotherapy (Protocol 0007)

Although the phase II Clinical Study for the Head and Neck tumors (Protocol 9602) had achieved a satisfactory local control rate for the malignant melanoma, the survival rate was not commensurate with the favorable local control rate of the malignant melanoma. In view of this, this protocol was started in April 2001 for the purpose of prophylactic therapy against distant metastasis, the major cause of death in malignant melanoma of the head and neck region.

Carbon ion radiotherapy was administered on a fractionation method of 57.6 GyE/16 fractions/4 weeks. Concomitant chemotherapy (DAV: Day 1: DTIC 120mg/m2 + ACU 70mg/m2 + VCR 0.7mg/m2; Days 2~5: DTIC 120mg/m2, 4 weeks' interval, a total of 5 courses) was administered at a rate of two courses before, and three courses after carbon ion radiotherapy. The results for the seven patients treated until February 2002 show that at the time of completion of the two courses of DAV chemotherapy prior to carbon ion radiotherapy, there were 2 PR, 2 NC and 3 PD patients, necessitating the early commencement of carbon ion radiotherapy. From April 2002 onwards, carbon ion radiotherapy and DAV chemotherapy were carried out concurrently.

Until February 2009, a total of 89 patients who were performed concurrent chemotherapy were enrolled Analysis of the 89 patients shows that their age ranged from 26 to 74 years, with the average age being 59.9 years. Their K.I. ranged from 70% to 100%, with a median of 90%. By site of disease, they consisted of 73 patients in the nasal cavity and paranasal sinus, 10 patients in the oral cavity, 4 patients in the pharynx and 3 patients in the orbit.

The acute reactions of 82 patients who have a follow-up time more than 6 months were consisted of one patient with grade 3 skin reaction and 11 patients with grade 3 mucosal reaction while the other toxicities that were observed were grade 2 or less. All late reactions in both the skin and mucosa were grade 1 or less.

The local tumor reactions show CR for 20, PR for 33, SD for 30, and PD for no patients. The effective rate was 63.9%. The 5-year local control and survival rates of 75 concomitant patients were 85.9% and 58.3% (Fig.5). Of these 75 concomitant patients, the 5 years survival rate of 60 patients whose GTV is less than 60cc was 67.6% and one of 15 patients with GTV larger than 60cc was 24.1 % ($p<0.005$) (Fig. 6).

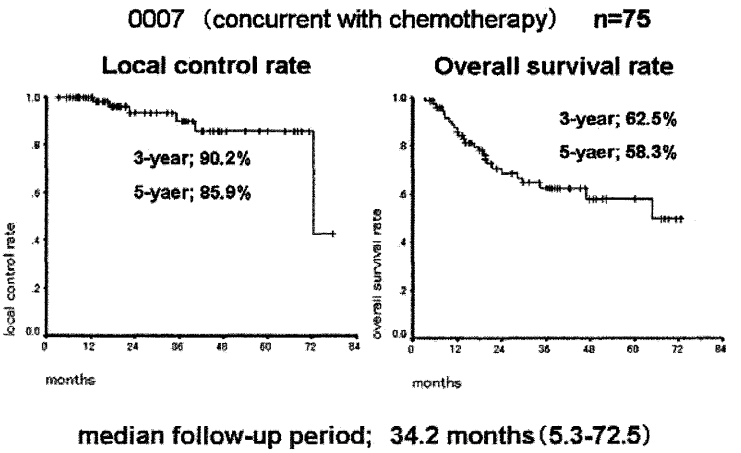

Fig. 5: Local control curve and survival curve of mucosal malignant melanoma (0007).

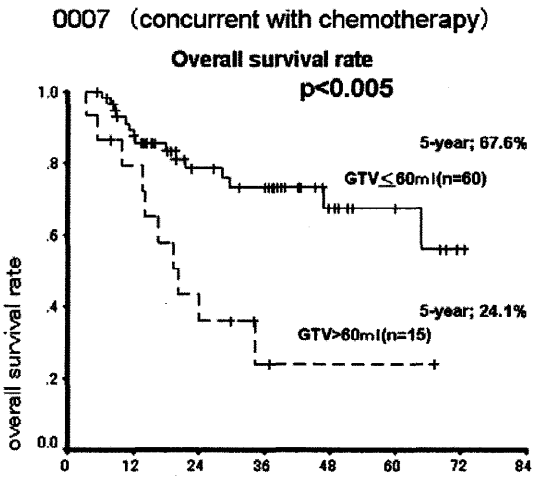

Fig. 6: Survival curves of mucosal malignant melanoma subdivided by GTV at 60 cm^3 (0007).

The reported local failure of systemic therapy including surgery, operation and chemotherapy is very high (45-54%) [10, 11]. Five years local control of carbon ion radiotherapy showed 77% in 9602 protocol and 85.9% in 0007 protocol. These results will show an effectiveness of carbon ion radiotherapy for the local control of mucosal malignant melanoma in head and neck. The review article by Lengyel E et al. reported 5 years survival rates of 17-48%, which is attributed mainly to a haematogenous dissemination [12]. Overall 5 years survival rate of carbon ion radiotherapy showed 37% in 9602 and 57.9% in 0007 protocol. There will be some tendency of improving result in concurrent and adjuvant chemotherapy (0007).

Conclusion

Malignant tumors in head and neck are therapeutically very diverse because of the many important organs present in this region and the great variety of tissue types. Carbon ion radiotherapy also requires considerable versatility in terms of the use of a specific radiation dose suited for the particular histological type and the application of concurrent chemotherapy. At present, efforts are being made to increase the patient numbers in order to produce results that can provide cogent clinical evidence.

References

[1] Mizoe JE, Tsujii H, Kamada T, et al. Dose escalation study of carbon ion radiotherapy for locally advanced head-and-neck cancer. Int J Radiat Oncol Biol Phys. 2004;60:358-64.

[2] Terhaard CH, Lubsen H, Rasch CR, et al. The role of radiotherapy in the treatment of malignant salivary gland tumors. Int. J. Radiation Oncology Biol. Phys. 2005;61:103–111.

[3] Mendenhall WM, Morris CG, Amdur RJ, et al. Radiotherapy alone or combined with surgery for salivary gland carcinoma. Cancer. 2005;103:2544-50.

[4] Schulz-Ertner D, Nikoghosyan A, Didinger B, et al. Therapy strategies for locally advanced adenoid cystic carcinomas using modern radiation therapy techniques. Cancer. 2005;104:338-44.

[5] Kamada T, Tsujii H, Tsuji H, et al. Efficacy and safety of carbon ion radiotherapy in bone and soft tissue sarcomas. J Clin Oncol. 2002;20:4466-71.

[6] Willers H, Hug EB, Spiro IJ, et al. Adult soft tissue sarcomas of the head and neck treated by radiation and surgery or radiation alone: patterns of failure and prognostic factors. Int J Radiat Oncol Biol Phys. 1995;33:585-93.

[7] Mendenhall WM, Mendenhall CM, Werning JW, et al. Adult head and neck soft tissue sarcomas. Head Neck. 2005:27:916-22.

[8] Le QT, Fu KK, Kroll S, et al. Prognostic factors in adult soft-tissue sarcomas of the head and neck. Int J Radiat Oncol Biol Phys. 1997;37:975-84.

[9] Barker JL Jr, Paulino AC, Feeney S, et al. Locoregional treatment for adult soft tissue sarcomas of the head and neck: an institutional review. Cancer J. 2003;9:49-57.

[10] Chen SA, Morris CG, Amdur RJ, et al. Adult head and neck soft tissue sarcomas. Am J Clin Oncol. 2005;28:259-63.

[11] Mendenhall WM, Amdur RJ, Hinerman RW, et al. Head and neck mucosal melanoma. Am J Clin Oncol. 2005;28:626-30.

[12] Lengyel E, Gilde K, Remenár E, et al. Malignant Mucosal Melanoma of the Head and Neck -a Review-. Pathology Oncology Research. 2003;9:7-12.

Carbon Ion Radiotherapy in Hypofraction Regimen for Stage I Non-Small Cell Lung Cancer

Masayuki Baba, Naoyoshi Yamamoto, Mio Nakajima, Kyosan Yoshikawa, Reiko Imai, Naruhiro Matsufuji, Shinichi Minohara, Tada-aki Miyamoto, Hiroshi Tsuji, Tadashi Kamada, Jun-etsu Mizoe, and Hirohiko Tsujii

Hospital, Research Center for Charged Particle Therapy, National Institute of Radiological Sciences, Chiba, Japan
e-mail address: baba@nirs.go.jp

Abstract

From 1994 to 1999, we conducted a phase I/II clinical trial for stage I non-small cell lung cancer (NSCLC) by using carbon ion beams alone, demonstrating optimal doses of 90.0GyE in 18 fractions over 6 weeks (Protocol #9303) and 72.0GyE in 9 fractions over 3 weeks (Protocol #9701) for achieving more than 95% local control with minimal pulmonary damage. In the present study, the total dose was fixed at 72.0GyE in 9 fractions over 3 weeks (Protocol #9802), and at 52.8GyE for stage IA and 60.0GyE for stage 1B in 4 fractions in 1 week (Protocol #0001). Following this schedule, we conducted a phase II clinical trial for stage I NSCLC from 1999 to 2003. We also conducted a phase I/II single fractionation clinical trial (Protocol #0201), a dose escalation study. The total dose was initially 28.0GyE in 2003, and it was raised to 44.0GyE in 2007. This article describes the intermediate steps. Most targets were irradiated from four oblique directions. A respiratory-gated irradiation system was used for all sessions. Local control and survival were assessed by Kaplan-Meier method. For statistical testing, the Log-rank test was used.

The local control rate for all patients (#9802 and #0001) was 91.5%, and those for T1 and T2 tumors were 96.3% and 84.7%, respectively. While there was a significant difference (p=0.0156) in tumor control rate between T1 and T2, there was no significant difference (P=0.1516) between squamous cell carcinomas and non-squamous cell carcinomas. The 5-year cause-specific survival rate was 67.0% (IA: 84.4, IB: 43.7), and overall survival was 45.3% (IA: 53.9, 1B: 34.2). No adverse effects greater than grade 2 occurred in the lung.

In a single fractionation trial, the local control rate for all 72 patients was 89.3%, and the control rates for T1 and T2 tumors were 94.6% and 78.7%, respectively. No adverse effects greater than grade 2 occurred in the lung.

Carbon beam radiotherapy, an excellent new modality in terms of high QOL and ADL, was proven to be a valid alternative to surgery for stage I cancer, especially for elderly and inoperable patients.

Introduction

In 1998, lung cancer became the leading cause of cancer-related death in Japan, as it had done in Western countries. Surgery plays a pivotal role in the curative treatment for non-small cell lung cancer (NSCLC), but it is not necessarily the best treatment for elderly persons and/or patients with cardiovascular and pulmonary complications. Conventional radiotherapy as an alternative, however, produces a five-year survival rate in merely 10-30% of the patients due to poor control of the primary tumor. Dose escalation is essential to improve the effectiveness of radiotherapy, but this involves increasing risk of pulmonary toxicity. Carbon ion radiotherapy (CIRT) is a promising modality because of its excellent dose localization and high biological effect

on the tumor. Our clinical trials led us to conclude that irradiation with heavy particle beams, notably carbon ion beams, offers a significant potential for improving tumor control without increasing toxicity risks.
Between 1994 and 1999, a phase I/II study of the treatment of stage I NSCLC by CIRT was first conducted using a dose escalation method to determine the optimal dose. An additional purpose was to develop correct, reliable and safe irradiation techniques for CIRT. As reported in our phase I/II study [1], the following results (Table 1) were obtained: 1) The local control rate was dose-dependent, reaching more than 90% at 90.0GyE with a regimen of 18 fractions over 6 weeks and at 72.0GyE with 9 fractions over 3 weeks. Both doses were determined to be optimal. It was found that setting the provisional target by allowing for the difference with the CT value can prevent marginal recurrence [2]. 2) Damage to the lung was minimal, with grade 3 radiation pneumonitis occurring in 2.7% of the cases. Respiratory-gated and 4-portal oblique irradiation directions excluding opposed ports proved successful in reducing the incidence of radiation pneumonitis. 3) Survival was strongly influenced by local control and tumor size of the primary lesion. The early detection of nodal and intralobar metastasis followed by irradiation with carbon beams can prevent the survival rate from decreasing further. Local failure, distant metastasis and malignant pleurisy were responsible for decreases in survival.

Adverse reactions in lung
1) minimum damage to lung (grade 3 radiation pneumonitis was 2.7%)
2) influenced by dose, respiration movement, and port direction and number
Local control
1) dose-dependent, but less dependent on tumor size and histological type
2) more than 90% by optimal dose and demonstrated by pathological CR
Survival
1) influenced by local control state and tumor size
2) less decreased by nodal and intralobar metastasis but more by local failure, malignant pleurisy and distant metastasis

Table 1 Results of phase I/II study on carbon beam radiotherapy for stage I non-small cell lung cancer

In the present study, a phase II clinical trial and a phase I/II dose escalation clinical trial are reported. In the phase II clinical trial, the total dose was fixed at 72.0GyE in 9 fractions over 3 weeks [3], and at 52.8GyE for stage IA NSCLC and 60.0GyE for stage IB NSCLC in 4 fractions in one week [4]. Using this optimal schedule, the phase II clinical trial was initiated in April in 1999 and closed in December in 2003, accruing a total number of 127 patients.

The phase I/II dose escalation clinical trial was initiated in April 2003. The initial total dose was 28.0GyE administered in a single fraction using respiratory-gated and 4-portal oblique irradiation directions, with the total irradiation dose being escalated in increments of 2.0GyE each, up to 44.0GyE. This clinical trial is still in progress. This article describes the intermediate steps of the phase I/II clinical trial and the preliminary results of the phase II clinical trial in terms of local control and survival after CIRT.

Materials and Methods

[Phase II clinical trial]

One hundred and twenty-nine patients with 131 primary lesions were treated with CIRT. Fifty-one primary tumors of 50 patients were treated by carbon ion beam irradiation alone using a fixed total dose of 72GyE in 9 fractions over 3 weeks (#9802 protocol [3]). The remaining 79 patients had 80 stage I tumors (#0001 protocol [4]) For survival, 127 patients were evaluated, as 2 patients had been treated twice, one in the first protocol

#9802, and one in the second protocol #0001. The IA and IB stage tumors were treated with fixed doses of 52.8GyE and 60.0GyE in 4 fractions in one week, respectively. Mean age was 74.5 years, and gender breakdown was 92 males and 37 females. The tumors were 72 T1 and 59 T2. Mean tumor size was 31.5 mm in diameter. By type, there were 85 adenocarcinomas, 43 squamous cell carcinomas, 2 large cell carcinomas and 1 adenosquamous cell carcinoma. Medical inoperability stood at 76%.

[Phase I/II clinical trial (single fractionation)]

Seventy-two patients were treated in this clinical trial between April 2003 and August 2007. As mentioned above, the intermediate steps of this still ongoing phase I/II clinical trial included a total dose of 36.0GyE or more, the follow-up time was 6 months or more after CIRT, and the local control ratio of T1 tumors (≦30mm in diameter) was as high as 90% at the total dose of 36.0GyE. The 72 primary tumors of the 72 patients were treated by carbon ion beam irradiation alone using a total dose of 36.0GyE (n=18), 38.0GyE (n=14), 40.0GyE (n=15), 42.0GyE (n=15), or 44.0GyE (n=10) per single fractionation. Mean age was 75 years, and gender breakdown was 23 females and 49 males. The tumors were 47 T1 and 25 T2. Mean tumor size was 27.7 mm in diameter. By type (cancer type was determined by biopsy), there were 45 adenocarcinomas, 26 squamous cell carcinomas, and one large cell carcinoma. Medical inoperability was 65% (Table 2).

Age (mean)		46-87 (75)
Gender	Female	23
	Male	49
PS	0	45
	1	26
	2	1
Tumor size (mean)		10-62 (27.7)*
Stage	IA	47
	IB	25
Histology	Adenoca.	45
	Sq cell ca.	26
	Large cell ca.	1
Reason of poor candidate for surgery		
	Refusal	25 (35)**
	Medically inope.	47 (65)**
Total dose (GyE)		
	36.0	18
	38.0	14
	40.0	15
	42.0	15
	44.0	10
*mm, **percent		Aug. 31, 2007

Table 2 Treatment & characteristics of 72 patients with stage I NSCLC

[Carbon ion beam irradiation]

The same system of carbon ion beam irradiation was used in both phase II and phase I/II clinical trials. The targets were usually irradiated from four oblique directions without prophylactic elective nodal irradiation (ENI). A greater than 10-mm margin was set outside the gross target volume (GTV) to determine the clinical target volume (CTV). The planning target volume (PTV) was established by adding an internal margin (IM) to the CTV. The IM was determined by extending the target margin in the head and tail direction by a width of 5 mm, leading to a successful prevention of marginal recurrence possibly resulting from respiration movement [2]. Fig. 1 shows the dose distribution maps for a representative case. A respiratory-gated irradiation system was used in

all irradiation sessions. Fig. 2 shows the CIRT room. We used vertical or horizontal beams in 2 oblique positions including 4 directions-irradiation totally.

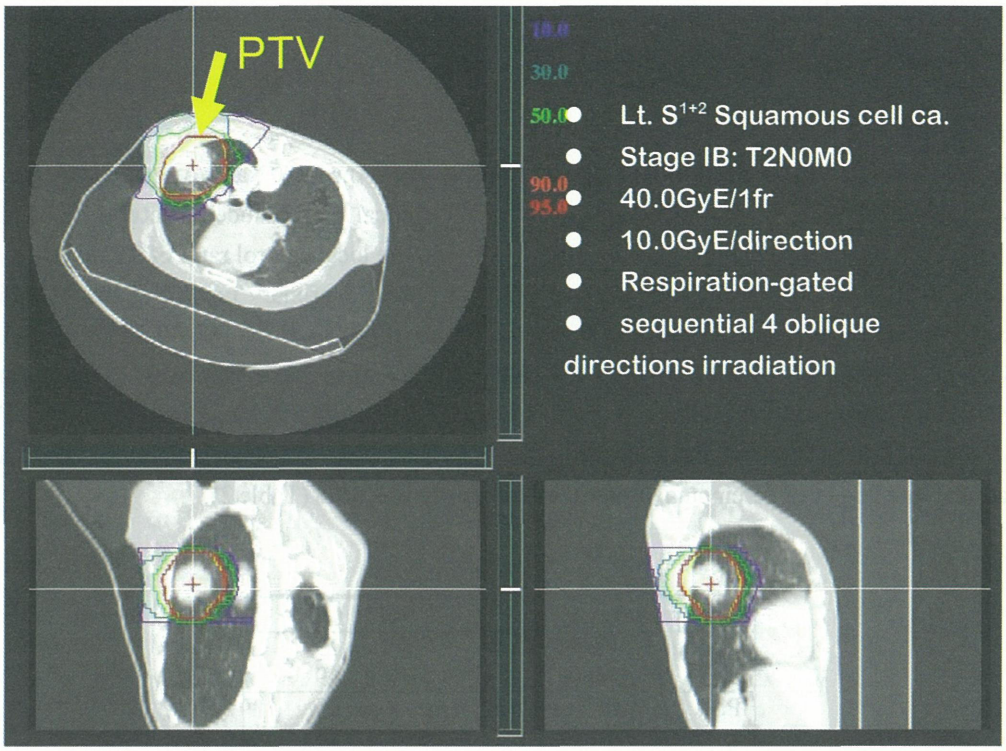

Fig. 1 Dose distribution maps of a 71-yr-old female)

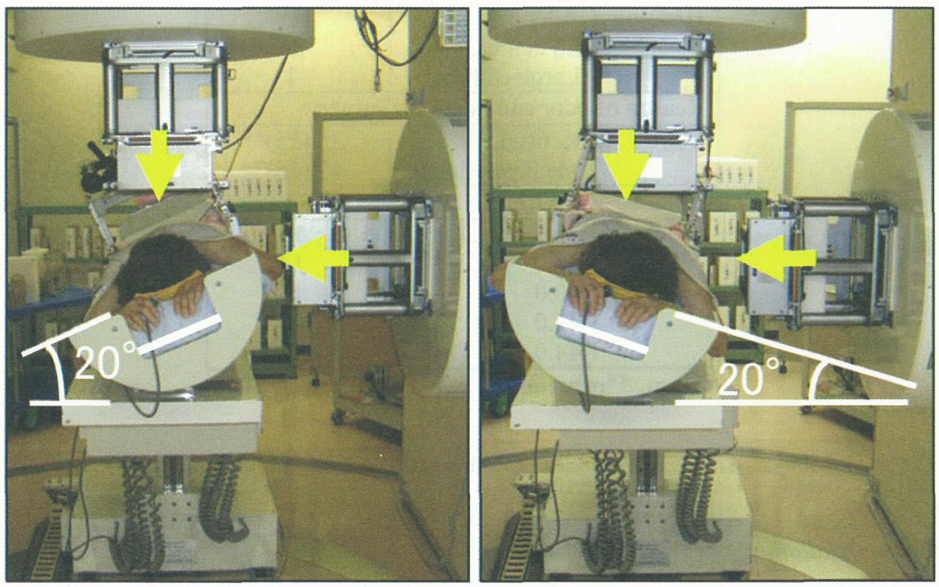

Fig. 2 Treatment room

[Statistical analysis]

Local control and survival were assessed by Kaplan-Meier method. For statistical testing, the Log-rank test was used.

Results

[Phase II clinical trial (#9802, #0001)]

All patients were followed up until death, with a median follow-up time of 50.8 months, ranging from 2.5 months to 70.0 months. The local control rate for the 131 primary lesions was 91.5% (Fig. 3), those for T1 (n=72) and T2 (n=59) tumors were 96.3% and 84.7% and for squamous cell type (Sq) (n=43) and non-squamous cell type (Non-Sq) (n=88) were 87.1% and 93.8%, respectively. While there was significant difference (p=0.0156) in tumor control rate between T1 and T2, there was no significant difference (P=0.1516) between squamous and non-squamous in T1+T1, nor between T1 and T2. However, with respect to squamous cell type cancer, local control was 100% for T1 (n=17) and 78.0% for T2 (n=26), with a near-significant difference (p=0.0518). The local control of non-squamous tumors was 95.3% for T1 (n=55) and 91.0% for T2 (n=33), with no significant difference (p=0.3364).

The 5-year cause-specific survival rate of the 127 patients was 67% (Fig. 3), breaking down into 84.8% for stage IA and 43.7% for stage IB tumors (Fig. 4A). The 5-year overall survival rate was 45.3% (Fig. 3), breaking down into 53.9% for stage IA and 34.2% for stage IB tumors (Fig. 4B).

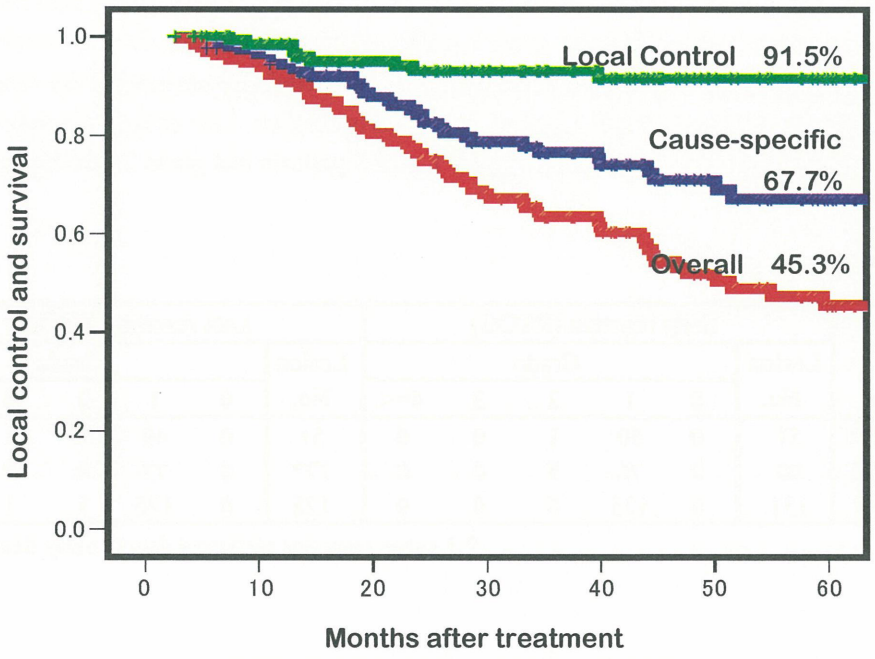

Fig. 3 Local control (n=131) and survivals (n=127) by CIRT

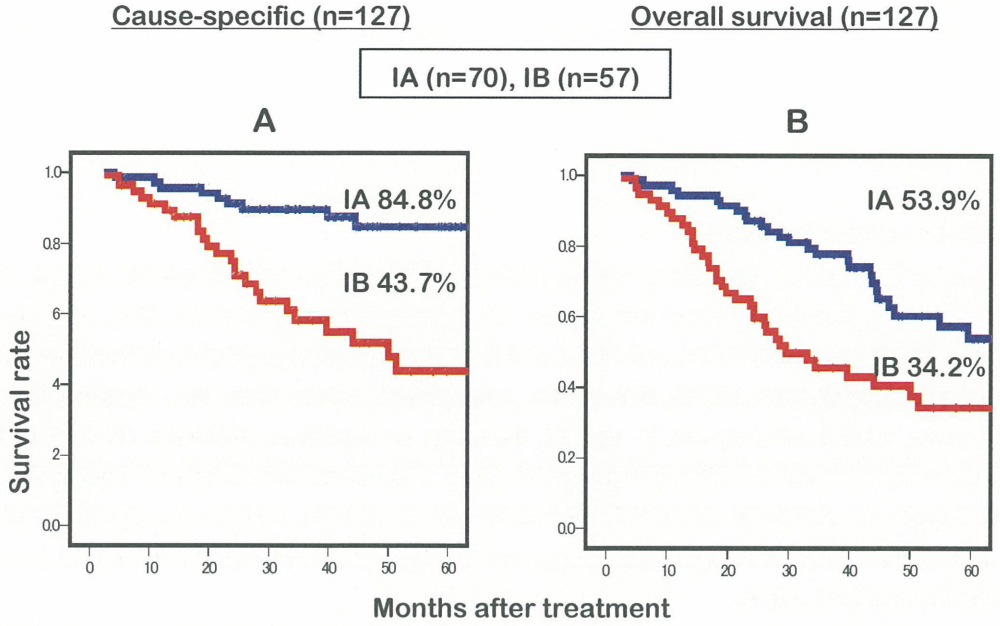

Fig. 4 Survivals of patients by stage IA and stage IB

Toxicities to the skin and lung caused by CIRT were assessed according to RTOG (early) and RTOG/EOTRC (late) as shown in Tables 3, 4. Early skin reactions were assessed for 131 lesions and late skin reactions for 128 lesions. Of the early reaction lesions, 125 were grade 1 and 6 were grade 2. Among the late reaction lesions, 126 were grade 1, 1 was grade 2, and 1 was grade 3. Lung reaction was clinically assessed in the total 129 patients. One hundred twenty-seven had grade 0 and 2 had grade 2 in early reaction. Late effects werefollowed up in 126 patients: 7 patients had grade 0, 116 patients had grade 1, and 3 patients had grade 2. No higher than a single grade 2 reaction was observed.

Skin		Early reaction (RTOG)					Late reaction (RTOG)					
		Lesion No.	Grade				Lesion No.	Grade				
			0	1	2	3	4=<		0	1	2	3	4=<
	#9802	51	0	50	1	0	0	51	0	49	1	1	0
	#0001	80	0	75	5	0	0	77*	0	77	0	0	0
	Total	131	0	125	6	0	0	128	0	126	1	1	0

* 3 cases were not observed due to early death

Table 3 Adverse skin reactions by CIRT

Fifty-three of the 127 patients (41.7%) had recurrence, all occurring between 1 and 54 months (median, 10.5 months) after the commencement of therapy. No occurrence was observed in the other 74 patients (58.3%). The 9 primary recurrences (7.1%) and 11 regional metastases (8.7%) consisting of 7 regional nodes (5.5%), one

intrabronchial (0.8%), and 3 intralobar metastases (PM1) (2.4%) occurred in the loco-regional site. In one patient primary recurrence was seen at the margin, while in another it occurred in-field.

Lung		Early reaction (RTOG)						Late reaction (RTOG)					
		Lesion	Grade					Lesion	Grade				
		No.	0	1	2	3	4=<	No.	0	1	2	3	4=<
	#9802	50	49	0	1	0	0	50	0	48	2	0	0
	#0001	79	78	0	1	0	0	76*	7	68	1	0	0
	Total	129	127	0	2	0	0	126	0	116	3	0	0

* 3 cases were not observed due to early death

Table 4 Adverse lung reactions by CIRT

By sub-stage classification, the incidence of loco-regional recurrence, pleural dissemination, and distant metastasis for stage IB (63%) was much higher than for IA (24%). The total incidence of first recurrence for stage IB (63%) tended to be higher than for stage IA (24%). Verification by χ^2 test showed no significant difference (χ^2=1.63).

The cause of death was as follows: 62 out of the 127 patients (48.8%) died, half of disease progression. Among the patients with recurrence, 5 of 9 with primary recurrence (55%) died from disease progression. Ten of the 11 patients with regional metastases were re-treated, 9 with CIRT and 1 with photons. Seven of these patients, although they had no further recurrence, died due to intercurrent disease, and 1 with node metastasis but no re-treatment died of disease progression. Eight of the 11 patients with regional metastases (72%) died, and 9 of the 10 patients (90%) with malignant pleurisy and 17 of the 23 patients (74%) with distant metastases died of disease progression. Five of them died due to primary recurrence, and 26 due to metastasis and dissemination. For the remaining 31 patients, intercurrent diseases were the cause of death [3, 4].

[Phase I/II clinical trial (single fractionation)]

All patients were followed up until death, with a median follow-up time of 16.1 months, ranging from 1.6 months to 21.6 months. The overall local control rate for the 72 primary lesions was 89.3%, and those for the T1 (n=47) and T2 (n=25) tumors were 94.6% and 78.7%, respectively (Fig. 5). The 28-month overall survival rate was 85.4% and the cause-specific survival rate was 98.0%.

Toxicities of CIRT to the skin and lung were assessed according to NCI-CTC (early) and RTOG/EOTRC (late) as shown in Tables 5 and 6. Early skin reactions were assessed for 72 lesions and late skin reactions for 69 lesions. Of the early reaction lesions, 69 were grade 1 and one was grade 2. Among the late reaction lesions, 65 were grade 1 and one was grade 2. Lung reactions were clinically assessed in the 72 patients. Forty-five had grade 0, and 27 had grade 1 among early reactions. Late reactions were followed up in 69 patients, with 12 showing grade 0 and 57 grade 1. The clinical course of a 71-year-old female is shown in Fig. 6 and Fig. 7. Tumor shrinkage and slight lung fibrosis is apparent, and grade 1 skin reaction was observed.

Discussion

In the present study, local control, cause-specific, and overall survival rates for the 127 patients in the phase II clinical trial were 91.5%, 67.0%, and 45.3%, respectively. Also, overall local control, local control in T1 tumor, and local control in T2 tumor were 89.3%, 94.6%, and 78.7%, respectively, by single fractionation. Local control

in T1 tumor has successfully been raised more than 94% using single fractionation. Toxicities to skin, lung and bone were minimal.

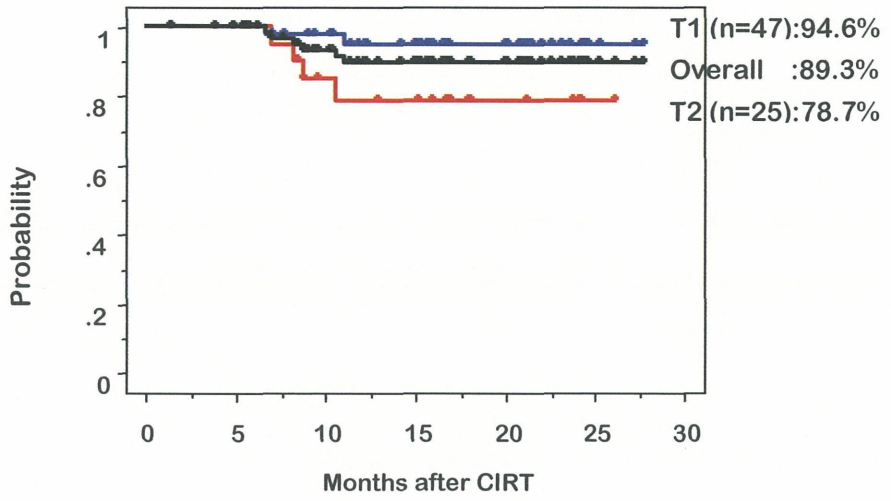

Fig. 5 Tumor control rates after ICRT using single fractionation

Skin	Total dose (GyE)	Early reaction (NCI-CTC)						Late reaction (RTOG/EORTC)					
		No. of Case	Grade					No. of Case	Grade				
			0	1	2	3	4=<		0	1	2	3	4=<
	36.0	18	0	18	0	0	0	17*	0	17	0	0	0
	38.0	14	0	14	0	0	0	13*	0	13	0	0	0
	40.0	15	1	13	1	0	0	15	2	12	1	0	0
	42.0	15	0	15	0	0	0	14*	0	14	0	0	0
	44.0	10	1	9	0	0	0	10	1	9	0	0	0
	Total	7	2	69	1	0	0	69	3	65	1	0	0

*One case was not observed in each group

Table 5 Adverse skin reaction after CIRT using single fractionation

Lung	Total dose (GyE)	Early reaction (NCI-CTC)						Late reaction (RTOG/EORTC)					
		No. of Case	Grade					No. of Case	Grade				
			0	1	2	3	4=<		0	1	2	3	4=<
	36.0	18	12	6	0	0	0	17*	3	14	0	0	0
	38.0	14	9	5	0	0	0	13*	2	11	0	0	0
	40.0	15	11	4	0	0	0	15	4	11	0	0	0
	42.0	15	9	6	0	0	0	14*	1	13	0	0	0
	44.0	10	4	6	0	0	0	10	2	8	0	0	0
	Total	72	45	27	0	0	0	69	12	57	0	0	0

*One case was not observed in each group

Table 6 Adverse lung reaction after CIRT using single fractionation

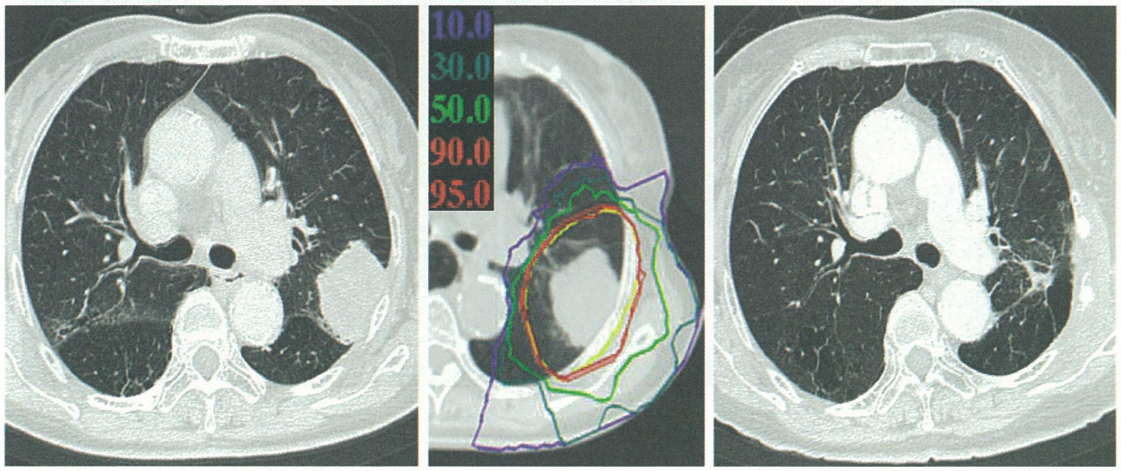

Fig. 6 Clinical course of 71-year-old female (T2N0M0 squamous cell carcinoma) after CIRT (40GyE/ single fractionation). CT (A), dose distribution map (B), and CT (C) at18 months after CIRT are shown. Apparent tumor shrinkage was observed without severe lung fibrosis.

Out of the 131 primary cancers of 127 patients, local occurrence occurred in 9 patients (6.8%). The average recurrence time was 17.2 months, ranging from 7 to 39 months. According to our previous study, the observation period required to determine local control of the irradiated lesions was at least 3 years post therapy [1]. However, the present study suggested the need for a longer observation period. It is self-evident that prolonged survival guarantees more reliable observation of local control results.

For the correct assessment of local control of patients who could not be observed for such a long duration because of death resulting from metastasis/dissemination or intercurrent disease, a histological approach based on repeated bronchoscopy was used, providing evidence of the absence of viable tumor cells in the collected specimens [3].

Furthermore, definite tumor control was also confirmed by the autopsies of CIRT-treated patients and in cases treated by surgery [5]. Such high and definite tumor control appears to be an outstanding feature of CIRT. Presumably, this is primarily due to the radiobiological nature of the high LET beams, which may account for the higher survival rate of stage I NSCLC. On the other hand, the failure of local control for primary tumors directly affects the poor survival of stage I NSCLC patients [1, 3]. Among our cases, 5 of 9 patients with primary recurrence (55%) died due to disease progression.

Eleven regional recurrences occurred. This incidence was close to that of surgery (7.5% [6], 11% [7]). Eight of them (72%) died. Only one patient, with no retreatment, died due to disease progression. The other 7 retreated patients died due to intercurrent death. Martini et al. [6] reported that any resection less than lobectomy and no lymph node dissection had adverse effects on recurrence and survival. In contrast, our treatment strategy for regional recurrence is thought to have gained validity as the standard surgical procedure for stage I NSCLC.

Nine of the 10 patients (90%) with malignant pleurisy and 17 of the 23 patients (74%) with distant metastasis died of disease progression. The poor prognosis of stage IB cases was based on the high incidence of pleural and distant metastasis.

Fig. 7 Skin reaction after CIRT (40.0GyE/1fr). Grade 1 reactions were observed.

With clinical stage I NSCLC, our 5-year overall survival results were somewhat inferior to the surgical ones [3, 5]. This difference may be due to the significant age gap between the two groups. The incidence of death due to recurrence in the surgical groups was 29% or 36%, whereas that due to intercurrent diseases was 19% or a few % [6, 7]. In contrast, our patients showed a higher incidence of death due to intercurrent diseases (60%) than death due to recurrence (40%). Comparison of stage IA with stage IB revealed a large difference in stage IA between overall (53.9%) and cause-specific (84.8%) survival, while there was a smaller difference in stage IB between overall (34.2%) and cause-specific (43.7%) survival. Such large and small survival differences in the two stage I subgroups might well be explained by the low incidence of recurrence death in stage IA (24%) and its high incidence in stage IB (63%). Generally, such a high frequency of intercurrrent death might be related to the advanced age of our patients, as they were on average 10 years older than the surgical patients [6, 7]. As we have reported, elderly patients 80 years and older can be treated safely by CIRT [8].

Compared with pulmonary damage reported in stereotactic radiotherapy for stage I NSCLC [9-11], the incidence and severity in our patients seem to be remarkably low. These lesser adverse effects on the lung were achieved as a result of the small volume irradiated. This advantage is a result of the excellent dose distribution property unique to carbon ion beams and lies in the formation of a Bragg peak in contrast to X-ray as a permeating beam.

Conclusions

One hundred twenty-seven stage I NSCLC patients with 131 primary tumors were treated with CIRT using a total dose of 72GyE in a regimen of 9 fractions over 3 weeks, and 52.8GyE for stage IA and 60GyE for stage IB at 4 fractions in one week. In addition, 54 stage I NSCLC patients with 54 primary tumors were treated with single-fraction CIRT using total doses ranging from 38.0GyE to 44.4GyE.

1. The local control rate of 131 primary lesions was 91.5%. There was statistical difference between the local control rates for T1 and T2, and near significance between squamous cell carcinoma and non-squamous cell carcinoma of T2.
2. Five-year overall and cause-specific survival rates of 127 patients were 45.3% and 67.0%, respectively.
3. Five-year overall survival rates of the patients with stage IA and stage IB were 53.9% and 34.2%, while five-year cause-specific survival rates with stage IA and stage IB were 84.8% and 43.7%, respectively.
4. There was high incidence of intercurrent death due to advanced age and related complications.
5. Adverse effects on skin and lung were minimal, indicating the safety of the modality. Carbon beam radiotherapy, which is an excellent new modality in terms of a high QOL and ADL, is a valid alternative to surgery for stage I cancer, especially for elderly and inoperable patients.
6. In CIRT using single fractionation with a total dose range from 36.0GyE to 44.0GyE, the local control rate for the 72 primary lesions was 89.3%, and those for the T1 (n=47) and T2 (n=25) tumors were 94.6% and 78.7%, respectively.
7. CIRT using single fractionation is very effective, viewed at an intermediate step, and is a safe modality for stage I NSCLC.

References

[1] Miyamoto T, Yamamoto N, Nishimura H, et al. Carbon ion radiotherapy for stage I non-small cell lung cancer. Radiother Oncol 2003;66:127-140.

[2] Koto M, Miyamoto T, Yamamoto N, et al. Local control and recurrence of stage I non-small cell lung cancer after carbon ion radiotherapy. Radiother Oncol 2004;71:147-156.

[3] Miyamoto T, Baba M, Yamamoto N, et al. Curative treatment of stage I non-small cell lung cancer with carbon ion beams using a hypo-fractionated regimen. Int J Radiat Oncol Biol Phys 2007;67:750-8.

[4] Miyamoto T, Baba M, Sugane T, et al. Carbon ion radiotherapy for stage I non-small cell lung cancer using a regimen of four fractions during 1 week. J Thorac Oncol 2007;2:916-26.

[5] Yamamoto N, Miyamoto T, Nishimura H, et al. Preoperative carbon ion radiotherapy for non-small cell lung cancer with chest wall invasion - pathological findings concerning tumor response and radiation induced lung injury in the resected organs. Lung Cancer 2003;42:87-95.

[6] Harpole DH, Herndon JE, Yung WG, et al. Stage I nonsmall cell lung cancer. A multivariate analysis of treatment methods and patterns of recurrence. Cancer 1995;76:787-796.

[7] Martini N, Bains MS, Burt ME, et al. Incidence of local recurrence and second primary tumors in resected stage I lung cancer. J Thorac Cardiovasc Surg 1995;109:120-129.

[8] Sugane T, Baba M, Imai R, et al. Carbon ion radiotherapy for elderly patients 80 years and older with stage I non-small cell lung cancer. Lung Cancer (2008), doi:10.1016/j.lungcan.2008.07.007.

[9] Nagata Y, Takayama K, Matsuo Y, et al. Clinical outcomes of a phase I/II study of 48Gy of stereotactic body radiotherapy in 4 fractions for primary lung cancer using a stereotactic body frame. Int J Radiat Oncol Biol Phys 2005;63:1427-1431.

[10] Onishi H, Shirato H, Nagata Y, et al. Hypofractionated stereotactic radiotherapy (HypoFXSRT) for stage I non-small cell lung cancer: updated results of 257 patients in a Japanese multi-institutional study. J Thorac Oncol 2007;2 (7 Suppl 3):S94-100

[11] Timmerman R, McGarry R, Yiannoutsos C, et al. Excessive toxicity when treating central tumors in a phase II study of stereotactic body radiation therapy for medically inoperable early-stage lung cancer. J Clin Oncol 2006;24:4833-4839

Carbon Ion Radiotherapy in Bone and Soft Tissue Sarcomas

Tadashi Kamada, Shinji Sugahara, Hiroshi Tsuji, Itsuko Serizawa, Reiko Imai, Tohru Okada, and Hirohiko Tsujii

Research Center for Charged Particle Therapy, National Institute of Radiological Sciences, Chiba, Japan
e-mail address: t_kamada@nirs.go.jp

Abstract

The Heavy Ion Medical Accelerator in Chiba (HIMAC) is the world's first heavy ion accelerator complex dedicated to medical use in a hospital environment. Heavy ions have superior depth-dose distribution and greater cell-killing capability. In June 1996, clinical research for the treatment of bone and soft tissue sarcomas was begun using carbon ions generated by the HIMAC. As of August 2008, a total of 421 patients with bone and soft tissue sarcoma were enrolled into the clinical trials. Most of the patients had locally advanced and/or medically inoperable sarcomas. The clinical trial revealed that carbon ion radiotherapy provided definite local control and offered a survival advantage without unacceptable morbidity in bone and soft tissue sarcomas that were hard to cure with other modalities.

1. Introduction

Tumors arising from bones, muscles, and vessels are referred to as bone and soft tissue sarcomas. While the incidence of these tumors is extremely low, they are capable of occurring ubiquitously throughout the body. For this reason, they are occasionally detected too late or their accurate diagnosis presents difficulty and incomplete treatment is administered on the false recognition of their being benign.

While tumor resection is the most common treatment modality for such bone and soft tissue sarcomas, major progress has been made in their management, thanks to the development of combined therapy modalities in recent years, in the wake of surgical advancements. These methods combine chemotherapy and radiotherapy with new imaging diagnostics such as MR, CT, and PET. Among these tumors, osteosarcoma originating in the limbs accounts for the majority of malignant bone tumors, and limb-sparing surgery not requiring arm or leg amputation has become possible through a combination of surgical resection with chemotherapy. The therapeutic results have also recorded a dramatic improvement in recent years: Whereas the five-year survival rate was only 10-20% in the 1970s, the latest data are up to as high as 50 - 80%. Similarly, soft tissue sarcomas developing in muscle or other soft tissues have meanwhile come to be treated by combined chemo-radiotherapy modalities and functional preservation operations achieving a five-year survival rate in excess of 70%. In the case of tumors that have developed in or near the spinal cord or in the pelvis, as well as advanced limb tumors and postoperative recurrent tumors, however, chemotherapy may often not be very effective and curative surgery may be difficult to perform. Moreover, most bone and soft tissue sarcomas are known to be resistant to conventional radiation. Thus, despite the significant progress seen in the treatment of bone and soft tissue sarcomas in recent years, patients judged intractable to surgery still face the harsh reality of being less likely to find an effective treatment option. In this regard, carbon ion radiation with its superior dose conformity and its potent biological effect holds out much promise for also achieving outstanding results with radio-resistant bone and soft tissue sarcomas. This

article presents our experiences with carbon ion radiotherapy using the Heavy Ion Medical Accelerator in Chiba (HIMAC) at NIRS.

2. Patients and Methods

A dose escalation trial (phase I/II trial) using carbon ion beams was carried out on 64 lesions of 57 bone or soft tissue sarcoma patients during the period from June 1996 until February 2000 [1]. A fixed-dose phase II trial was then initiated in April 2000, and records as of August 2008 show that 377 lesions of 358 patients have been treated. Both of these trials included bone or soft tissue sarcoma patients for whom surgical resection was contra-indicated. The main eligibility criteria are listed in Table 1. While the phase II trial included patients with radiation-associated sarcoma, it did exclude patients with intravascular tumor embolus. Three hundred and eighty-eight patients (414 lesions) in these 2 trials have been followed for 6 months or longer after carbon ion treatment as of August 2008. Their clinical characteristics are summarized in Table 2. There were 230 males and 158 females, and their age ranged from 12 to 85 years, with a median of 52 years. Tumor locations were as follows: 89 lesions in the spine or paraspinal region; 298 in the pelvis, and 27 in the extremities and other sites. The tumors were categorized as 304 primary bone and 84 primary soft tissue sarcomas. Histological classification showed that chordoma was the most frequent tumor, accounting for 126 patients, followed by osteosarcoma in 66 patients, chondrosarcoma in 63 patients, MFH (including 14 bone primaries) in 30 patients and Ewing/PNET in 28 patients (including 5 soft tissue primaries). For pathological confirmation, central pathological review of surgical or biopsy specimen was carried out. All patients enrolled in the trials gave their written informed consent.

Table 1. Eligibility

• Histologically confirmed bone or soft tissue sarcomas
• Unresectable or declines surgery
• Gross measurable lesion
• Lesion size <15cm in maximum diameter
• KPS 60~100%
• No prior radiotherapy to the lesion
• Signs informed consent statement

Abbreviations: KPS, Karnofsky performance status

Table 2. Patient characteristics

Characteristic		No. (N = 388)
Age, years		
Median (range)		52 (12~85)
Sex		
Female/ Male		158/230
Tumor sites (414 lesions)		
Pelvis		298
Spine/para-spine		89
Extremities etc		27
Histology		
	Bone	304
	Chordoma	126
	Osteosarcoma	66
	Chondrosarcoma	63
	PNET	23
	MFH	14
	Others	12
	Soft tissue	84
	MFH	16
	MPNST	15
	Synovial sarcoma	8
	Liposarcoma	8
	PNET	5
	Leiomyosarcoma	5
	Rhabdomyosarcoma	4
	Others	23
Clinical target volume, cm^3		
Mean (range)		489 (16~2900)

Abbreviations: PNET, primitive neuroectodermal tumor; MFH, malignant fibrous histiocytoma; MPNST, malignant peripheral nerve sheath tumor

The features of the Heavy Ion Medical Accelerator in Chiba (HIMAC) and the carbon ion beam have been previously described. In brief, the accelerated carbon ion beam energies were 290, 350, and 400 MeV. The range of the beams was a depth of 15– 25 cm in water. An appropriately sized ridge filter corresponding to the tumor size was selected to form the spread-out Bragg peak (SOBP). A compensation bolus was fabricated for each patient to make the distal configuration of the SOBP similar to the shape of the target volume. A multi-leaf collimator defined the margins of the target volume. Patients were placed in customized cradles and immobilized with a low-temperature thermoplastic sheet. A set of 5-mm-thick CT images was taken for the treatment planning. Three-dimensional treatment planning was performed with HIPLAN software (National Institute of Radiologic Sciences, Chiba, Japan) for the planning of carbon ion therapy. A margin of 5 mm was usually added to the clinical target volume to create the planning target volume. When the tumor was located close to critical organs such as the spinal cord, skin or bowel, the margin was reduced accordingly. The clinical target volume was covered by at least 90% of the prescribed dose. Dose was calculated for the target volume and any nearby critical structures and expressed in Gray-Equivalent (GyE = carbon physical dose (Gy) x Relative Biological Effectiveness {RBE}). Carbon ion radiotherapy was given once daily, 4 days a week (Tuesday to Friday), for a fixed 16 fractions in 4 weeks. Patients were treated with two to eight irregularly shaped ports (median, 3 ports).

One port was used in each session. At every treatment session, the patient's position was verified with a computer-aided on-line positioning system. The patient was positioned on the treatment couch with the immobilization devices, and digital orthogonal X-ray TV images in that position were taken and transferred to the positioning computer. They were compared with the reference image on the computer screen and the differences were measured. The treatment couch was then moved to the matching position until the largest deviation from the field edge and the isocenter position was less than 2 mm. For all of these patients, a total dose ranging from 52.8 GyE to 73.6 GyE was administered by a fractionation regimen of 16 fractions over four weeks (with single radiation doses of 3.3 - 4.6 GyE).

3. Results

A dose escalation trial (phase I/II trial) with a total dose ranging from 52.8 GyE to 73.6 GyE administered in 16 fractions over four weeks (single radiation doses of 3.3 - 4.6 GyE) was carried out on 64 lesions of 57 bone and soft tissue sarcoma patients between June 1996 and February 2000. As 7 of the 17 patients treated with 73.6 GyE were found to have grade 3 RTOG acute reactions (skin), dose escalation was halted at this dose level. No other grade 3 or worse acute reactions were detected. These findings made it clear that with a fractionation regimen of 16 fractions over four weeks, a total dose of 70.4 GyE was the maximum applicable dose in cases in which skin presented a problem, and a total dose of 73.6 GyE was possible in other cases. The overall local control rate was 89% at 1 year, 63% at 3 years, and 63% at 5 years. A significant difference was found between the local control rates achieved with a total dose of 57.6 GyE or less and those with 64.0 GyE or more. The median survival period was 31 months (2-96 months), and the 1-, 3- and 5-year survival rates were 82%, 47%, and 37%, respectively. A fixed-dose phase II trial was then initiated in April 2000, and as of August 2008, 362 patients have been enrolled for treatment. The number of lesions and patients analyzed six months or longer after therapy stands at 350 lesions of 331 patients, with 10 of these lesions having been treated with a dose of 73.6 GyE (4.6 GyE per fraction), 19 with 64 GyE (4.0 GyE per fraction) and 21 with 67.2 GyE (4.2 GyE per fraction). The remaining 299 lesions were treated with a dose of 70.4 GyE (4.4 GyE per fraction). As of the present, the 2- and 5-year local control rates are 88% and 79%, and similarly, the overall survival rates are 79% and 57%, respectively (Figure 1).

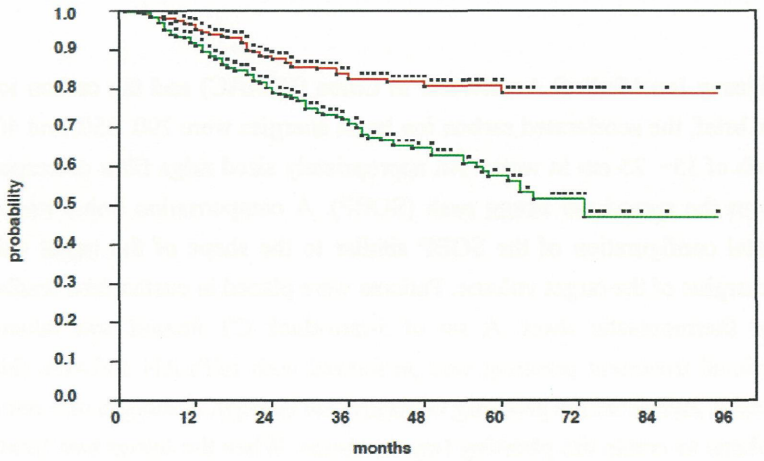

Figure 1. Actuarial local control and overall survival in the 331 phase II study patients with bone or soft tissue sarcomas. Local control rate at 5 years was 79%, and overall survival rate at 5 years was 57%.

Radiation morbidities are summarized in Table 3. Grade 3 or worse toxic reactions included 2 patients with acute skin toxicities (grade 3) and 7 patients with late skin toxicities (grade 3: 6 patients; grade 4: 1 patient).

These late skin reactions suggest that the following may be risk factors in addition to the total dose: 1) subcutaneous tumor invasion, 2) tumor volume, 3) sacrum, 4) previous surgery, 5) additional chemotherapy, and 6) irradiation from two portals. It was possible, however, to prevent these reactions by aiming for a standard dose of 70.4 GyE and by modifying the irradiation method that may include irradiation from three portals, in order to reduce the dose delivered to the skin.

The entire evaluable population for both the above clinical trials amounted to 414 lesions of 388 patients, and their aggregate 5-year local control rate presently stands at 76% and their 5-year overall survival rate at 54% (Figure 2). The 126 chordoma patients (excluding patients with the base of the skull primaries) of this total have a 5-year local control rate of 89% and a 5-year overall survival rate of 85% (Figure 3) (A report on the 30 sacral chordoma patients who were observed for a period of two years or longer was published in the Clinical Cancer Research [2]).

The 5-year local control rate and 5-year overall survival rate for the 65 patients with osteosarcoma of the trunk were 62% and 28% (Figure 4) and for the 63 chondrosarcoma patients 65% and 59%, respectively. (Figure5)

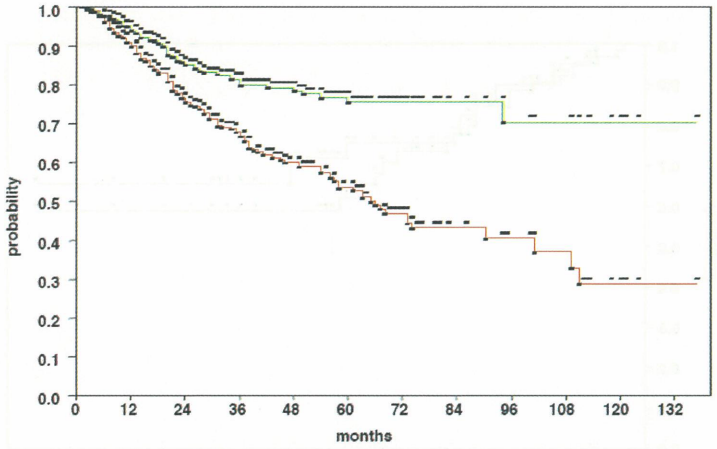

Figure 2. Actuarial local control and overall survival in the 388 patients with bone or soft tissue sarcomas. Local control rate at 5 years was 76%, and overall survival rate at 5 years was 54%.

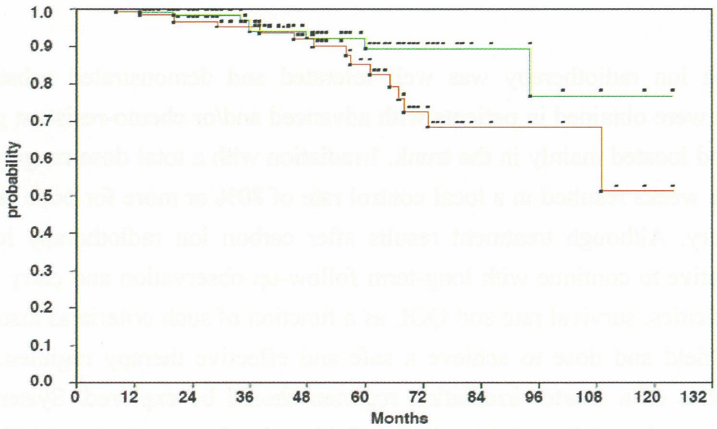

Figure 3. Actuarial local control and overall survival in the 126 patients with chordoma. Local control rate at 5-years was 89 %, and overall survival rate at 5-years was 85%.

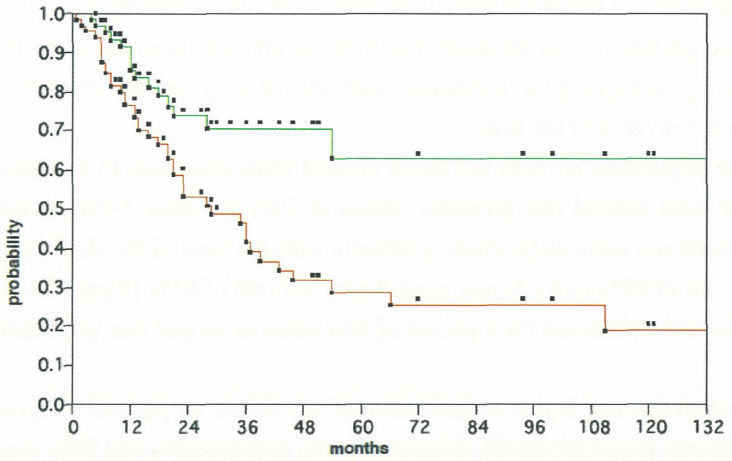

Figure 4. Actuarial local control and overall survival in the 65 patients with osteosarcoma of the trunk. Local control rate at 5 years was 62%, and overall survival rate at 5 years was 28%.

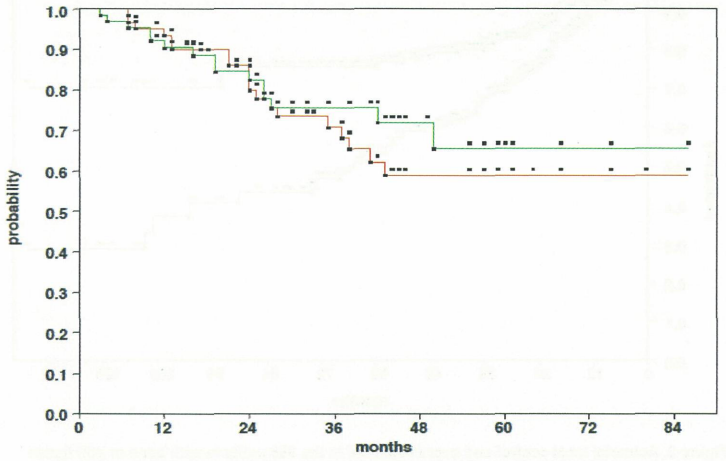

Figure 5. Actuarial local control and overall survival in the 63 patients with chondrosarcoma. Local control rate at 5 years was 65%, and overall survival rate at 5 years was 59%.

4. Discussion

In this study, carbon ion radiotherapy was well tolerated and demonstrated substantial activity against sarcomas. These results were obtained in patients with advanced and/or chemo-resistant gross lesions not suited for surgical resection and located mainly in the trunk. Irradiation with a total dose ranging from 64 to 73.4 GyE in 16 fractions over four weeks resulted in a local control rate of 80% or more for bone and soft tissue sarcomas disqualified from surgery. Although treatment results after carbon ion radiotherapy have so far been quite satisfactory, it is imperative to continue with long-term follow-up observation and carry out further analyses to assess local control, toxicities, survival rate and QOL as a function of such criteria as histological type, location, tumor size, irradiation field and dose to achieve a safe and effective therapy regimen. For small lesions, in particular, the possibilities of a shorter irradiation regimen should be explored. Systematic analyses will be essential to determine the optimum dose and irradiation field setting in accordance with the patient's histological type and tumor location and to shed light on the problems involved. Research will also be needed to clarify the role of heavy particle radiotherapy in the context of combined therapy modalities for bone and soft tissue sarcomas. Not only for patients disqualified from surgery but also for elderly patients and patients with major functional loss consequent to surgical resection, carbon ion radiotherapy is seen as a valid alternative to surgery.

While previous experience with carbon ion radiotherapy to the extremities has so far been rather limited, the combination of carbon ion radiation and surgery could offer a promising potential for patients intractable to limb-sparing surgery as a modality for widening the scope of limb-retaining therapy.

5. Conclusion

Carbon ion radiotherapy is an effective local treatment for patients with bone and soft tissue sarcomas for whom surgical resection is not a viable option, and it shows great promise as an alternative to surgery. The morbidity rate of carbon ion radiotherapy has so far been quite acceptable, although the long-term safety of this approach for patients with sarcomas will need to be monitored.

References

[1] Kamada T, Tsujii H, Tsuji H, et al. Efficacy and Safety of Carbon Ion Radiotherapy in Bone and Soft Tissue Sarcomas. Journal of Clinical Oncology. 2002;20:4466-4471.

[2] Imai R, Kamada T, Tsuji H, et al. Carbon Ion Radiotherapy for Unresectable Sacral Chordomas. Clinical Cancer Research. 2004;10:5741-5746.

[3] Serizawa I, Kagei K, Kamada T, et al.

Carbon Ion Radiotherapy for Hepatocellular Carcinoma

Hiroshi Imada, Hirotoshi Kato, Shigeo Yasuda, Shigeru Yamada, Jun-etsu Mizoe,
Tadashi Kamada, and Hirohiko Tsujii

Hospital, Research Center for Charged Particle Therapy, National Institute of Radiation Sciences, Chiba, Japan
e-mail address: h_imada@nirs.go.jp

Abstract

The objective of this paper is to present a summary explanation of the clinical study on carbon ion radiotherapy for hepatocellular carcinoma (HCC) conducted from April 1995 to August 2005 at the Research Center for Charged Particle Therapy, National Institute of Radiation Sciences, Japan. A total of 193 patients with HCC were enrolled in the clinical trials with carbon ion beams. In the first and second phase I/II clinical trials, dose escalation experiments were carried out in incremental steps of 10%, resulting in the confirmation of both the safety and the effectiveness in short-course regimens of 12, 8 and 4 fractions. Based on the results, a phase II clinical study with fixed fractionation, that is, 52.8 GyE/4 fractions, was performed, where 47 patients were treated with low toxicity, attaining a high local control rate of 95% at 5 years. The last clinical study was conducted from April 2003 to August 2005 with an even more hypofractionated regime of 2 fractions/2 days, in which 36 patients were safely treated within a dose escalation range from 32.0 GyE to 38.8 GyE. The 2-fraction therapy protocol is continuing under the license of Highly Advanced Medical Technology. There have been no therapy-related deaths and no severe adverse events until now.We can conclude that because of the low toxicity and high local control rate, carbon ion radiotherapy has a promising potential as a new, radical, and minimally invasive therapeutic option for HCC.

Introduction

Hepatocellular carcinoma (HCC) is one of the most common malignant tumors with the third highest annual mortality of 598,000 throughout the world (2002), especially in Asia, Africa, as well as a number of countries in Europe, including Spain, Italy, Greece, and France. Worldwide, some 626,000 new cases were reported in 2002. In recent years, the incidence of HCC has shown an increasing trend in Australia, India, Israel, Canada, Italy, Spain, Finland and USA. HCC is associated with liver cirrhosis in 80% of the total HCC patients. This disease is thus a very advanced form of hepatic disorder resulting from hepatitis C or B viral infection. The overall 5-year survival rate for all patients with HCC has remained steady at 3 to 5%. HCC patients often require repeated therapies owing to the multicentric nature of carcinogenesis in the cirrhotic liver. Therefore, both radical effect and minimal invasiveness are essential for the treatment of HCC. A variety of therapies are currently available for the treatment of HCC, but each of them has its specific limitations. None has so far been brought on the market that satisfies the above two essential requirements of radicality and minimal invasiveness in the treatment of tumors of any size encountered in practice.

Methods and Materials

1. Outline of carbon ion radiotherapy for HCC -Clinical Trials to Medical Treatment – (Table 1)

Clinical trials with carbon ion radiotherapy for HCC were initiated in April 1995 (1). A total of 193 patients with HCC were enrolled into the trials. In the first and second phase I/II clinical trials, dose escalation experiments were carried out in incremental steps of 10% each in order to find the optimum dose. In the first of these trials, 24 patients were treated with a 15-fraction regimen at a total dose range of 49.5-79.5 GyE. In the second trial, 86 patients were treated with short-course regimens, at total dose ranges of 54.0-69.6 GyE in 12 fractions, 48.0-52.8 GyE in 8 fractions, and 48.0-52.8 GyE in 4 fractions. Based on the results of these studies, a third protocol was established to implement a phase II clinical trial using a fixed total dose of 52.8 GyE spread over 4 fractions of 13.2 GyE each (2). The fourth protocol, a phase I/II clinical study, was performed using an even more hypofractionated regime of 2 fractions/2 days at total dose levels ranging from 32.0 GyE to 38.8 GyE (3). Most of the subjects enrolled under these four protocols had been judged as not amenable to, or as having had recurrence after, other treatments, or as having no prospect of an adequate treatment effect with any of the existing therapies. This 2-fraction therapy is currently ongoing according to guidelines allowing careful step-wise dose escalations at a 5% increase rate under the license of Highly Advanced Medical Technology.

2. Carbon ion radiotherapy

2-1. Preparation for treatment

One or two metal markers (0.5 × 3 mm) made of iridium wire were inserted near the tumor under ultrasound imaging guidance as landmarks for target volume localization. The irradiation fields were established with a three-dimensional therapy plan based on 5-mm-thick CT images. CT planning was performed using the HIPLAN, which was originally developed for 3D treatment planning (4). The clinical target volume was defined according to the shape of the tumor plus a 1.0-1.5-cm margin. The median target volume was 159 ml (range: 37-1466 ml). Double right-angled field geometry was used for irradiation in most patients (double right-angled field: 77%, double oblique field: 7%, 3-field: 14%, 4-field: 2%). Supine or prone position was selected according to the location of the tumor. Respiration gating was employed in the CT scan planning and irradiation stages (5).

2-2. Verification of patient position and target volume localization

To accurately reproduce the patient position, a low-temperature thermoplastic sheet and a customized cradle were used. Patients were immobilized on a rotating couch to permit either vertical or horizontal beam irradiation from any angle. To assess the accuracy of patient position and target volume localization, orthogonal fluoroscopy and radiography were used immediately prior to each treatment session.

Results

The clinical trial results up to the 4-fraction regimen for which observation has been continued for 5 years or longer are described below. The 2-fraction therapy was not included in this analysis due to its continuation and the as yet short observation time.

1. Toxicities

Not a single therapy-related death occurred. Using the Child-Pugh score, an international standard for assessing the degree of hepatic insufficiency, on a rating scale from 5 to 15 points, with the score increasing with deterioration of hepatic function, post-therapy changes were investigated in order to evaluate the effect of carbon ion radiotherapy on liver function. An increase in score count associated with carbon ion radiotherapy remained within one point or below in many patients in the early (within 3 months of the start of radiotherapy) and late phases (after 3 months) (Fig. 1). This demonstrated that changes in liver function remained minor after carbon ion radiotherapy was initiated. The number of cases reported with a score increase of 2 points or more in

the late phase, which is of particular clinical significance, tended to be smaller with decreasing fraction numbers.

No serious adverse effects were noted either in the skin or digestive organs. All toxicities were judged to be tolerable.

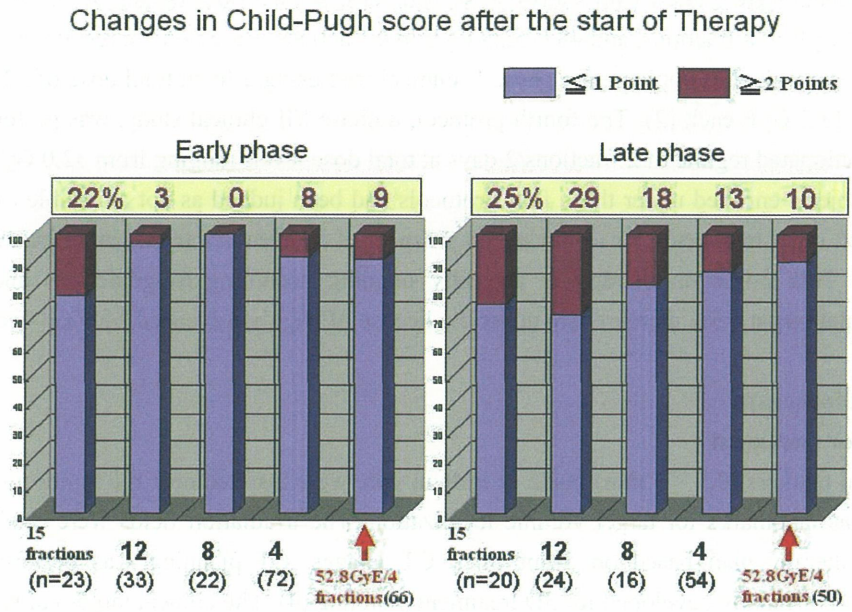

Fig. 1: Changes in Child-Pugh score before and after carbon ion radiotherapy

Variations in Child-Pugh score, an international standard to assess the degree of hepatic insufficiency changes before and after irradiation, were studied. Degrees of hepatic insufficiency can be evaluated with the Child-Pugh score on a scale from 5 to 15 points. The score point increases as the degree of hepatic insufficiency deteriorates.

The increase in score associated with carbon ion radiotherapy remained within one point or below in many patients in the early (within 3 months of start of radiotherapy) and late phases (after 3 months).

2. Anti-tumor effect

HCC develops in a successive manner, fostered by the underlying cirrhosis of the liver. Patient survival is therefore determined by the overall results, including the treatment of recurrent lesions and also the treatment of hepatic insufficiency in case of a decline in liver function. As a result, the survival rate does not reflect the effectiveness of any particular treatment alone. In comparing the effectiveness of the different therapies for HCC, it is therefore easier to make a judgment on the basis of the local control rate rather than the survival rate. In the present clinical trials, other treatments proved ineffective or led to recurrence in 57% of the patients, and as the phase I/II trials were conducted as dose escalation studies to determine the recommendable dose, there is a possibility that some of the patients may have been treated with a smaller than optimum dose. It is therefore not possible to make a simple comparison of the survival rates achieved in these clinical trials with other treatments.

In this study, only patients with an observation period of 3 years or more after the commencement of carbon ion radiotherapy were eligible for analysis and the local control rates for the analyzed lesions are shown separately according to protocol and fractionation regimen (Table 2). There were no significant differences in control rate among the different fractionation schedules.

Table 1. Outline of carbon ion radiotherapy for HCC

Carbon Ion Radiotherapy for HCC

April, 1995～March, 2009 **Total n=259**

Protocol	Disease	Category	Fractionation	Period	Number
1. 9401	HCC	Phase I/II study	15f/5w	1995.4～1997.3	24
			12f/3w		34
2. 9603	HCC	Phase I/II study	8f/2w	1997.4～2001.3	24
			4f/1w		28
3. 0004	HCC	Phase II study	4f/1w	2001.3～2003.3	47
4. 0202	HCC	Phase I/II study	2f/2days	2003.4～2005.8	36
Guideline	HCC	Highly Advanced Medical Technology	4f/1w	2005.9～	10
			2f/2days	2006.4～	56

Table 2. Results of clinical trials for HCC with carbon ion beams

Trial		Phase I/II	Phase I/II			Phase II	52.8GyE/4f
Number of fractions		15	12	8	4	4	4
Total dose (GyE)		49.5-79.5	54.0-69.6	48.0-58.0	48.0-52.8	52.8	52.8
Number of lesions		24	34	24	28	47	69
Maximum tumor diameter (cm)	Median	5.0	3.7	3.1	4.6	3.7	4.0
	Range	2.1-8.5	1.5-7.2	1.2-12.0	2.2-12.0	1.2-7.5	1.2-12.0
Recurrent Tumor	yes	18 (75%)	18 (53%)	16 (67%)	18 (64%)	20 (43%)	35 (51%)
	no	6 (25%)	16 (47%)	8 (33%)	10 (36%)	27 (57%)	34 (49%)
1-year local control (%)		92	97	91	89	96	94
3-year local control (%)		81	86	86	89	96	94
5-year local control (%)		81	86	86	89	96	94

Discussion

1. Standard therapies for HCC

The standard therapies for HCC are hepatectomy, transcatheter arterial embolization (TAE), percutaneous ethanol injection (PEI), and radio-frequency ablation (RFA). According to the Survey and Follow-up Study of Primary Liver Cancer in Japan, the relative shares of these therapies in the total treatment records for the two-year period from January 1, 2002 through December 31, 2003 were: hepatectomy 34%, TAE 30%, and percutaneous local therapy involving PEI, percutaneous microwave coagulation therapy (PMCT), and RFA 31%. The respective merits and demerits of each of these procedures can be summed up by saying that, while they

remove the cancer cells with the greatest degree of certainty by hepatectomy, they are also stressful on the liver and the body as a whole. TAE is clinically useful and has a relatively low degree of invasiveness but is of limited radicality. PEI and RFA, on the other hand, are simple procedures offering a high degree of radicality but their effect is limited to comparatively small tumors (3 cm or smaller in diameter). The use of radiotherapy for HCC has been considered difficult in view of the problems of radiation-induced hepatic insufficiency (6,7). Progress in the development of irradiation devices in recent years, however, has made it possible to achieve highly localized irradiation. This has spurred advances in radiotherapy research for liver cancer (8-15).

2. Optimal candidates for carbon ion radiotherapy

For patients with extensive infiltration and those with multiple lesions it is difficult to achieve radicality with carbon ion radiotherapy alone. Carbon ion radiotherapy is indicated, however, for patients with few restrictions concerning liver function, a level of liver function corresponding to medium or better (Child-Pugh grade A or B). For small lesions 3 cm or less, however, minimal invasiveness, high local control rate, and low-cost therapies such as PEI and RFA are available. In contrast, large lesions 3 cm or above are difficult to treat with PEI or RFA alone, making them ideal targets for carbon ion radiotherapy. Especially for patients with locally concentrated lesions over 3 cm and up to 5 cm, the local control rate was 90% at one to five years, and the cumulative survival rate was 95% at one year, 71% at three years, and 67% at five years. In addition, with relatively good liver function of Child-Pugh grade A, the cumulative survival rate was 94% at one year, 81% at three years and 75% at five years (Fig. 2). These outcomes seem superior to those achieved with other therapies, for example, hepatectomy, for which cumulative survival rates of 91% at one year, 74% at three years, and 59% at five years for a single lesion, and those of 91% at one year, 73% at three years, and 56% at five years for tumors 2 to 5 cm in diameter, have been reported (16). This evidence suggests that patients with locally concentrated lesions over 3 cm, up to 5 cm, are most eligible for carbon ion radiotherapy.

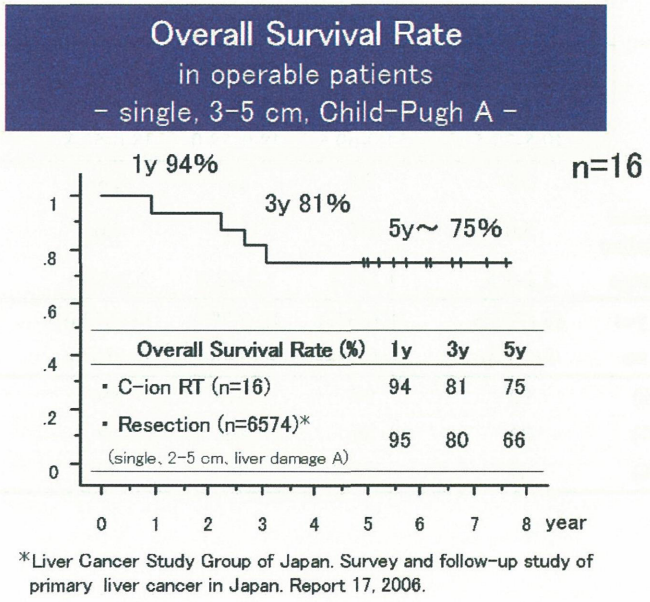

Fig. 2: Overall survival rate in operable patients

3. Future prospects

Hospitalization for HCC carbon ion radiotherapy now totals only 5 days, 3 days for preparation and 2 days for irradiation. The future goal will be to further reduce the number of days of hospitalization and to perform almost all processes on an outpatient basis. In fact, several cases have already received outpatient therapy with carbon ion beams.

Conclusion

Although carbon ion radiotherapy is safe and effective, and it seems to have promising potential as a new, radical, and minimally invasive therapeutic option for HCC, further careful follow-up is still needed to confirm its clinical efficacy in practical medicine. A future goal will be to minimize the number of days of hospitalization and to perform almost all processes on an outpatient basis.

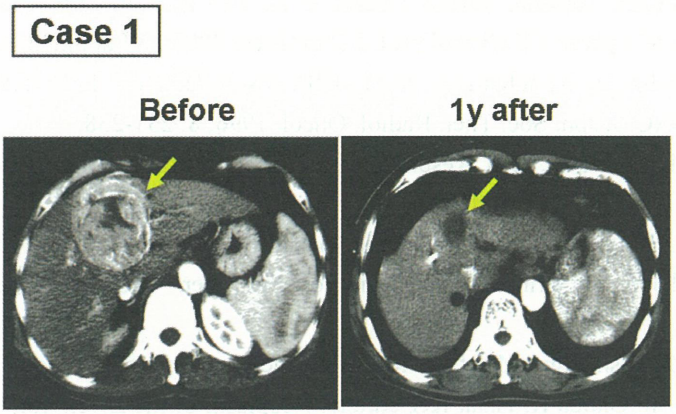

Fig. 3: Case 1
67-year-old male. He had HCC of 7 cm in diameter in segment IV. He survived for 5 years after carbon ion radiotherapy of 72.0 GyE/15 fractions.

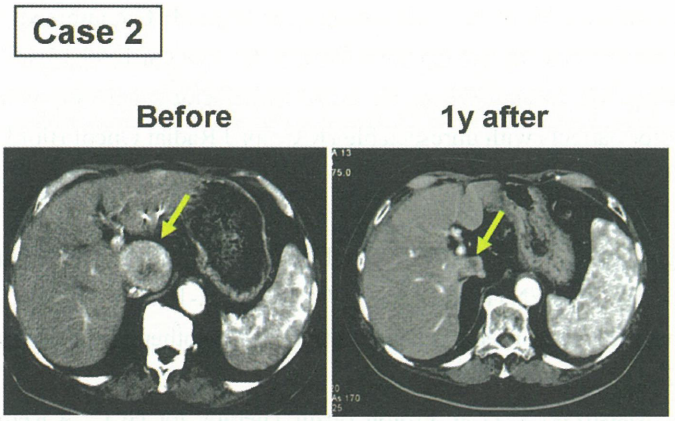

Fig. 4: Case 2
72-year-old male. He had HCC of 4.6 cm in diameter in segment I. He remained alive for 8.0 years after carbon ion radiotherapy of 52.8 GyE/4 fractions.

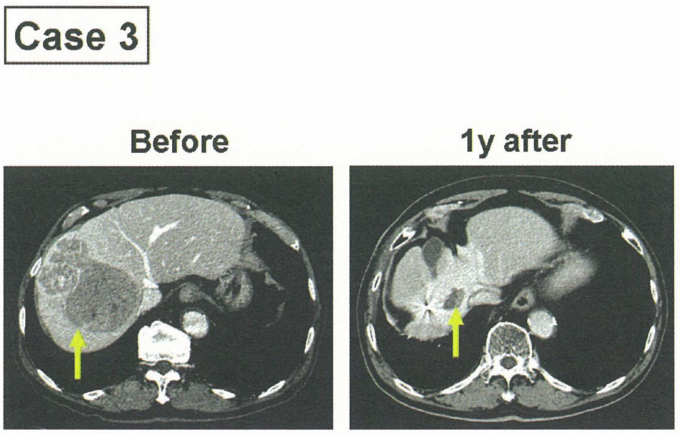

Fig. 5: Case 3
77-year-old man. He had HCC of 10.5×7.7 cm in the right hepatic lobe. He remained alive for 2.0 years after carbon ion radiotherapy of 38.8 GyE/2 fractions.

References

[1] Hirotoshi Kato, Hirohiko Tsujii, Tadaaki Miyamoto, et al. Results of the first prospective study of carbon ion radiotherapy for HCC with liver cirrhosis. Int J Radiat Oncol Biol Phys 2004; 59: 1468-1476.

[2] Hirotoshi Kato, Shigeru Yamada, Shigeo Yasuda, et al. Phase II study of short-course carbon ion radiotherapy (52.8GyE/4-fraction/1-week) for HCC. HEPATOLOGY 2005;42,Suppl.1:381A.

[3] Hirotoshi Kato, Shigeru Yamada, Shigeo Yasuda, et al. Two-fraction carbon ion radiotherapy for HCC: Preliminary results of a phase I/II clinical trial. J Clin Oncol 2005;23,Suppl.:338s.

[4] Endo M, Koyama-Ito H, Minohara S, et al. HIPLAN-A HEAVY ION TREATMENT PLANNING SYSTEM AT HIMAC. J. Jpn. Soc. Ther. Radiol. Oncol. 1996; 8: 231-238.

[5] Minohara S, Kanai T, Endo M, et al. Respiratory gated irradiation system for heavy-ion radiotherapy. Int J Radiat Oncol Biol Phys 2000;47: 1097-1103.

[6] Ingold DK, Reed GB, Kaplan HS, et al. Radiation hepatitis. Am J Roentgenol 1965;93:200-208.

[7] Phillips R, Murikami K. Primary neoplasms of the liver. Results of radiation therapy. Cancer 1960;13:714-720.

[8] Ohto M, Ebara M, Yoshikawa M, et al. Radiation therapy and percutaneous ethanol injection for the treatment of HCC. In: Okuda K, Ishak KG, editors. Neoplasm of the Liver. Tokyo: Springer-Verlag; 1987. p. 335-341.

[9] Robertson JM, Lawrence TS, Dworzanin LM, et al. Treatment of primary hepatobiliary cancers with conformal radiation therapy and regional chemotherapy. J Clin Oncol 1993;11:1286-1293.

[10] Yasuda S, Ito H, Yoshikawa M, et al. Radiotherapy for large HCC combined with transcatheter arterial embolization and percutaneous ethanol injection therapy. Int J Oncol 1999;15:467-473.

[11] Cheng J C-H, Chuang VP, Cheng SH, et al. Local radiotherapy with or without transcatheter arterial chemoembolization for patients with unresectable HCC. Int J Radiat Oncol Biol Phys 2000;47:435-442.

[12] Guo W-J, Yu E-X. Evaluation of combined therapy with chemoembolization and irradiation for large HCC. Br J Radiol 2000;73:1091-1097.

[13] Matsuzaki Y, Osuga T, Saito Y, et al. A New, Effective, and Safe Therapeutic Option Using Proton Irradiation for HCC. GASTROENTEROLOGY 1994;106:1032-1041.

[14] Kawashima M, Furuse J, Nishio T, et al. Phase II Study of Radiotherapy Employing Proton Beam for HCC. J Clin Oncol 2005;23: 1839-1846.

[15] Chiba T, Tokuue K, Matsuzaki Y, et al. Proton Beam Therapy for HCC: A Retrospective Review of 162 Patients. CCR 2005;11:3799-3805.

[16] Liver Cancer Study Group of Japan. Survey and follow-up study of primary liver cancer in Japan. Report 17. Kyoto: Shinko-Insatsu; 2006

Carbon Ion Therapy for Patients with Locally Recurrent Rectal Cancer

Shigeru Yamada, Makoto Shinoto, Shigeo Yasuda, Kouji Imada, Hirotoshi Kato, Tadashi Kamada, Hirohiko Tsujii, Hiroshi Tsuji, Masayuki Baba, Jun-etsu Mizoe, Kyousan Yoshikawa, Susumu Kandatsu, and Takenori Ochiai for the Working Group for Locally Recurrent Rectal Cancer

Hospital, Research Center for Charged Particle Therapy, National Institute of Radiological Sciences, Chiba, Japan, Chiba University Graduate School of Medicine, Chiba, Japan.

e-mail:s_yamada@nirs.go.jp

Abstract

Purpose: To evaluate the tolerance for and effectiveness of carbon ion radiotherapy in patients with locally recurrent rectal cancer.

Patients and Methods: We conducted a phase I/II dose escalation study of carbon ion radiotherapy. One hundred twelvw patients with 117 sites of locally recurrent cancer receiving carbon ion radiotherapy were analyzed. Fifty relapses originated in the presacral region, 38 in the pelvic sidewalls, 16 in the perineal region and 8 in the colorectal anastomosis. The total dose ranged from 67.2 to 73.6 gray equivalent (GyE) and was administered in 16 fixed fractions over 4 weeks (4.2 to 4.6 GyE/fraction).

Results: None of 90 patients treated with the highest total dose of 73.6 GyE experienced National Cancer Institute - Common Toxicity Criteria grade 3 to 5 acute reactions. The local control rate in patients treated with 73.6 GyE in the present study was 94% at three years and 94% at 5 years. Dose escalation was then halted at this level. The median survival time in patients treated with 73.6 GyE was 54 months (range, 7 to 65 months), and the 3- and 5-year overall survival rates were 72% at 3 years and 40% at 5 years, respectively.

Conclusion: Carbon ion radiotherapy seems to be a safe and effective modality in the management of locally recurrent rectal cancer, providing good local control and offering a survival advantage without unacceptable morbidity.

Introduction

The major recurrence patterns after surgery for rectal cancer include liver metastasis and local recurrence, with the rate of local recurrence (LR) for rectal cancer ranging from 10 to 40% [1-3]. Although the use of pre- or postoperative radiation therapy has reduced the incidence of LR, 10-15% of patients still develop recurrence. Patients with locally recurrent rectal cancer have low rates of subsequent local control and overall survival. Surgical resection remains the only potentially curative treatment. Curative surgery of LR is technically difficult and the rates of complications and operative mortality are relatively high. In fact, surgery of LR is seldom feasible, and most patients are referred for radiotherapy. External-beam radiation therapy is generally considered a palliative treatment. LR is resistant to conventional radiotherapy and is located close to critical organs.

The carbon ion beam possesses unique physical and biologic properties [4,5]. It has a well-defined range and insignificant scatter in tissues, and the energy release is enormous at the end of its range. This well-localized energy deposition (high-dose peak) at the end of the beam path, called the Bragg peak, is a unique physical characteristic of charged particle beams, as is the induction of more cell cycle- and oxygenation-independent, irreversible cell damage than that observed with low-LET radiation. To improve long-term local control and survival of locally recurrent rectal cancer, we have initiated a radiation dose-escalation trial using carbon ion beams.

Patients and Methods

1. Patient Eligibility

Patients were included in the study if they were confirmed with locally recurrent rectal cancer without distant metastasis by computed tomography (CT), magnetic resonance imaging (MRI), and carbon-11-methionine positron emission tomography (PET) findings, had adenocarcinoma of the rectum and had a potentially curative resection of the primary tumor and regional lymph nodes performed with neither gross nor microscopic residual disease. Patients who had undergone chemotherapy within 4 weeks before carbon ion radiotherapy or those who had prior radiation therapy at the same site were excluded from the study. The tumor had to be grossly measurable, but the size could not exceed 15 cm. Eligibility criteria included a Karnofsky performance status score higher than 60 and estimated life expectancy of at least 6 months. Exclusion criteria were having another primary tumor, and infection at the tumor site and digestive tract in contact with the clinical target volume. A complete history was obtained and a physical examination was performed before registration, including CT, MRI and PET to determine the extent and size of the tumor. Chest and upper abdominal CT scans were mandatory at the time of entry into the trial. All patients signed an informed consent form approved by the local institutional review board.

2. Carbon Ion Radiotherapy

The Heavy Ion Medical Accelerator in Chiba is the world's first heavy ion accelerator complex dedicated to medical use in a hospital environment. The features of the accelerator and carbon ion beam have previously been described [6,7]. In brief, carbon ion radiotherapy was given once daily, 4 days a week (Tuesday to Friday), for fixed 16 fractions in 4 weeks. Patients were treated with two to five irregularly shaped ports (median, three ports). The clinical target volume (CTV) was determined by setting the margin 5mm outside the gross tumor volume (GTV) and included the regional lymph nodes (LN). The LN areas that should be considered part of the target volume include the internal iliac, external iliac and presacral nodes. Dose constraints of the maximum dose for the intestine and bladder were 30 GyE in 9 fractions and 60 GyE in 16 fractions, respectively. Prophylactic nodal areas of risk are usually treated with 37.8-41.4 GyE in 9 fractions of 4.2-4.6 GyE before irradiation field are reduced in size.

3. Dose Escalation and Toxicity Criteria

At least three patients were treated at the same dose level, and then a 10% escalation of the total dose was carried out after careful observation of normal tissue responses using to NCI-CTC (National Cancer Institute - Common Toxicity Criteria Version 2.0). Dose adjustment was planned if there was any acute RTOG grade 3 or higher toxicity. We followed the standard phase I dose escalation methods. If no dose-limiting toxicity (DLT) was observed in any of the three patients at a given dose level, the dose level was escalated for the next cohort. If DLT was observed in no more than one in three patients, then three more patients were treated at the same dose level. If no further cases of DLT were seen in the additional patients, then the dose level was escalated for the next cohort. Otherwise, dose escalation was stopped. Three patients at any dose level of each site had to be followed up for at least 3 months before a subsequent dose escalation. We used 67.2 GyE in 16 fractions, 4.2 GyE/fraction as the starting dose. For late reactions, the Late Effects of Normal Tissues/Subjective, Objective, Management, and Analytic scoring system was used in addition to the RTOG/European Organization for Research and Treatment of Cancer late scoring system. Scores for late reactions were the highest observed 3 months or later after carbon ion radiotherapy.

4. Toxicity

Toxicity on organs such as the skin, bladder and digestive tract was assessed according to NCI-CTC Version 2.0 (April 30, 1999) and RTOG/EOTRC (late) classification.

5. Tumor Response and Local Control Criteria

Tumor response was defined as the maximum tumor response observed by the RECIST scoring system during the first 6 months after the initiation of carbon ion radiotherapy. Complete response (CR) was defined as the disappearance of all measurable tumor in the treatment volume. Partial response (PR) meant a 30% or greater decrease in tumor size (longest diameter). Stable disease was that with a less than 30% decrease or a less than 20% increase in tumor size. Progressive disease was defined as a 20% or greater increase in tumor size. The absence of local failure in the treatment volume based on CT, MRI, and PET scans was described as local control. Local recurrence was defined in terms of lesions occurring in the tumor bed.

6. Follow-Up

All patients were seen on a regular basis during follow-up. Initial evaluation of tumors using CT, MRI, and PET scans was performed within 1 month after the completion of carbon ion radiotherapy. Thereafter, the patients were followed up by CT or MRI every 1 or 2 months for the next 6 months, and then the intervals between imaging and follow-up were extended to 3 to 6 months. PET was not performed regularly after the initial evaluation.

7. Statistics

Survival time and local control time were defined as the interval between the initiation of carbon ion radiotherapy and the date of death or the date of diagnosis of local failure, respectively. The survival and local control curves were generated by Kaplan-Meier method and the log-rank test was used for comparisons.14,15 Results were considered significant at $P < 0.05$.

Results

1. Patient Characteristics

Between April 2001 and August 2008, 115 patients (121 lesions) were enrolled into this study. One patient was excluded because of subarachnoid hemorrhage before treatment. Thus, 114 patients of 115 eligible patients were treated with carbon ion radiotherapy. Two more patients were excluded because of peritoneal dissemination or lymph node metastasis of the mediastinum. Thus, 117 lesions in 112 patients (74 men and 38 women) were treated with carbon ion radiotherapy. Patient characteristics are summarized in Table 1. Median age was 62.5 years (range 27 to 83 years). All patients presented with adenocarcinoma at initial surgery. Abdominoperineal resection had been performed in 61 patients, anterior resection in 49, and Hartmann's resection in two. Fifty relapses originated in the presacral region, 38 in the pelvic sidewalls, 16 in the perineal region, and 8 in the colorectal anastomosis. Carbon beams of 290, 350 and 400 MeV/nucleon energy were generated by the HIMAC synchrotron. Carbon ion therapy was given once daily, 4 days a week, for fixed 16 fractions in 4 weeks. The dose was set at 67.2 GyE (4.2 GyE per fraction) and escalated to 73.6 GyE (4.6 GyE) at 5% increments.

2. Toxicity

Toxicities in the 114 patients (120 lesions) receiving carbon ion therapy are listed in Table 2. They were relatively few and mild in these patients. All patients completed the scheduled treatment course. No grade 3 to 5 acute toxicity was observed. Two grade 3 late skin and one gastrointestinal reactions were observed among the ute120 lesions.

Table 1. Patient Characteristic

Characteristics	No. of Pts. (N=112)
Age, years	
Median	62.5
Range	27-83
Female/Male	74/38
Primary tumor operation	
abdominoperineal excision	61
low anterior resection	49
Hartmann's resection	2
Tumor sites (n=59)	
presacral	50 (+1)
lymph nodes	38 (+2)
perineal	16 (+1)
anastomotic	8 (+1)

Table 2. Acute and Late Toxicities by NCI-CTC and RTOG/EORTC Scoring System

	Acute (NCI-CTC)						Late (RTOG/EORTC)					
	No. of patients	Gr0	Gr1	Gr2	Gr3	Gr4	No. of patients	Gr0	Gr1	Gr2	Gr3	Gr4
Skin	120	24	89	7	0	0	120	54	63	1	2	0
Gastrointestinal	120	118	1	1	0	0	120	118	0	1	1	0
Urinary	120	119	1	0	0	0	120	118	0	2	0	0

MTD of 73.6 GyE had been indicated for patients with bone and soft-tissue sarcomas in the pelvis by a phase I/II dose escalation study of carbon ion radiotherapy. The local control rate in patients treated with 73.6 GyE in the present study was 97% at one year and 92% at 3 years, significantly better than the hitherto reported local control rates. The patients in our series had been considered mostly to have tumors for which there were no other effective local treatments. Despite such dire conditions, patients experienced good tumor control and a relatively low incidence of complications with carbon ion radiotherapy. To confirm these findings, a phase II clinical trial using 73.6 GyE is warranted.

Despite the fact that various types of chemotherapies were applied before or after carbon ion radiotherapy, there were no obvious effects of chemotherapy on the incidence of toxicities in this series.

3. Tumor Response

Evaluation of tumor response was not considered the primary endpoint of this study. Tumor response was evaluated in 117 lesions. One patient was excluded from tumor response analysis because of difficulty in imaging evaluation. CR was observed in 15 lesions and PR in 314(Table 3). Sixty lesions remained stable. The overall tumor response rate (CR+PR) was 47%. Remarkable anti-tumor effects were observed.

Table 3. Tumor Response of 117 Lesions

Total dose (GyE)	No. of lesions	CR	PR	SD	PD
67.2	10	4	1	5	0
70.4	20	0	8	12	0
63.5	87	11	25	51	0

The overall actuarial local control rates at five years were 35%, 89% and 94% at 67.2 GyE, 70.4 GyE and 73.6 GyE, respectively. Ten in-field recurrences were observed among the recurrent patients (Fig.1).

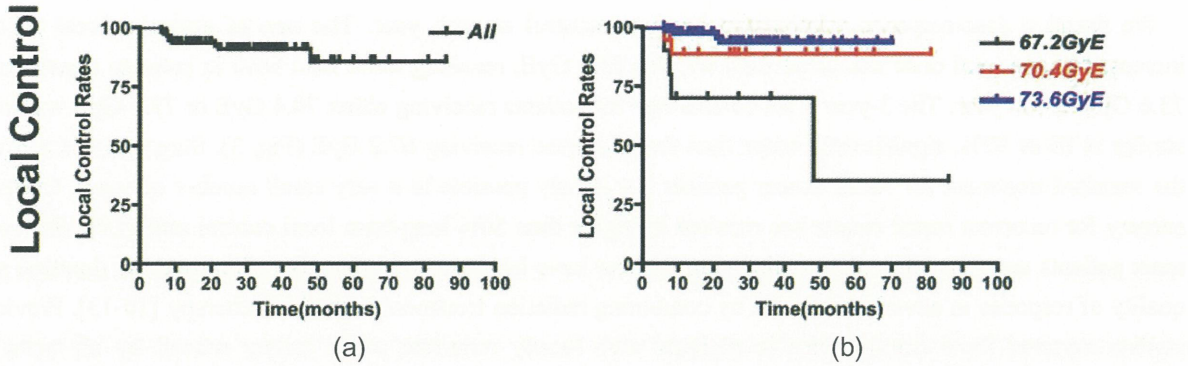

Fig. 1. Local control rates a) in all 116 analyzed lesions, b) by total dose

In terms of symptomatic response within 3 months after treatment, pain improved in 97% of the symptomatic cases. Pain relief was maintained at one year in 67%, 91% and 100% of the patients treated with 67.2GyE, 70.4GyE and 73.6GyE, respectively. In general, symptoms tended to improve during the course of radiation rather than worsen. While most authors agree that irradiation is frequently an effective therapy for symptomatic pelvic tumors, it has also been established that the response usually persists for only about 3-6 months. Symptomatic response rates range from 50% to 94%.

The overall survival estimates for the 112 analyzed patients are shown in Fig 2. The three-year and five-year overall survival rates were 65% and 38%, respectively. The overall survival rates at three years were 36% at 67.2 GyE, 56% at 70.4 GyE, and 72% at 73.6 GyE. There was a clear correlation between overall survival rates and total dose.

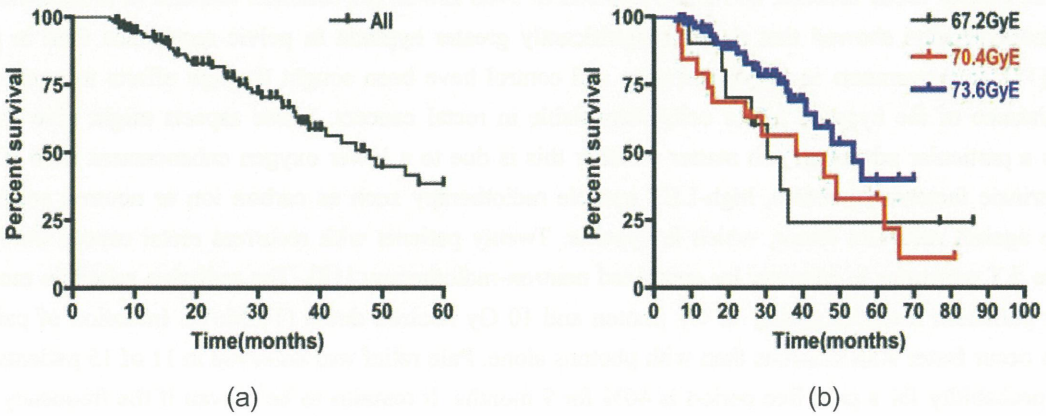

Fig. 2. Overall survival rates a) in all 112 analyzed patients, b) by total dose

Our survival rate data are nearly the same as those associated with surgical resection.

The above results substantiate the superior usefulness of heavy ion radiotherapy in the treatment of recurrent rectal cancer to conventional photon radiotherapy or combinations with chemotherapy.

Discussion

In this study, carbon ion radiotherapy was well tolerated and demonstrated substantial activity against locally recurrent rectal cancer. These results were obtained in patients with advanced and/or chemoresistant gross lesions not suited for surgical resection.

We found a dose-response relationship for local control at each year. The rate of actuarial local control increased as the total dose increased from 67.2 to 73.6 GyE, reaching more than 90% in patients treated with 73.6 GyE at one year. The 3-year local control rate for patients receiving either 70.4 GyE or 73.6 GyE was very similar at 89 or 92%, significantly better than that for those receiving 67.2 GyE (Fig. 3). Surgery is considered the standard treatment for rectal cancer patients but is only possible in a very small number of cases. Curative surgery for recurrent rectal cancer has resulted in higher than 50% long-term local control rate [8,9]. However, most patients must be referred to radiotherapy. There have been several attempts to improve the duration and quality of response in advanced cancers by combining radiation treatment with chemotherapy [10-13]. Previous studies reported local control rates in patients with locally recurrent rectal cancer treated by all types of radiotherapy including other particle beams of less than 50% [14,15]. The local control rate of our 73.6 GyE group could be among the best achieved without surgical resection.

Although the focus of this study was not directed at survival duration, nonetheless, it is noteworthy that improved local control resulted in better survival. We found a dose-response relationship for the survival rate. The 2-year overall survival rate increased as the total dose increased from 67.2 to 73.6 GyE, reaching 93% in patients treated with 73.6 GyE. The 2- and 5-year overall actuarial survival rates were 84% and 40% respectively; in the literature, the reported 2-year survival rate for patients with locally recurrent rectal cancer treated by external-beam radiation was 45% or less [15]. External-beam radiation therapy alone or in combination with chemotherapy provides palliation and modest prolongation of life but has only a minimal curative potential in patients with locally recurrent rectal cancer. The reported 2- year and 5-year overall survival rate in patients with locally recurrent rectal cancer treated by curative surgery were 62-82% and 31-46% respectively. This level of survival rate achieved with carbon ion RT can be considered as equivalent to or better than surgical resection.

Wendling has clearly shown that the oxygenation of differential rectal adenocarcinoma is distinctly lower than that of the normal rectal mucosa, and tissue hypoxia or even anoxia are common features of these tumors [16]. Furthermore, Hockel showed that there is significantly greater hypoxia in pelvic recurrence than in primary tumors [17]. Improvements in tumor response and control have been sought through efforts to overcome the radioresistance of the hypoxic tumor cells identifiable in rectal cancers. These aspects might give high-LET particles a particular advantage, no matter whether this is due to a lower oxygen enhancement ratio (OER) or other intrinsic factors. Therefore, high-LET particle radiotherapy such as carbon ion or neutron seems to be effective against recurrent tumor, which is hypoxic. Twenty patients with recurrent rectal cancer were treated using the d,T generator in Munster by combined neutron-radiotherapy [18]. The radiation schedule most often used for palliation involves giving 40 Gy photon and 10 Gy neutron doses (14 MeV). Initiation of pain relief seems to occur faster with neutrons than with photons alone. Pain relief was achieved in 11 of 15 patients (73%), and the probability for a pain-free period is 46% for 9 months. It remains to be proven if the frequency of pain relief is higher and the pain-free period as well as the progression-free period last longer than with photons. The incidence of acute toxicity was 30% and late toxicity 10%. All toxicity was seen at the skin. A higher neutron dose will give better results, but may cause local radiation side-effects.

Carbon ion therapy offers the potential advantages of improved dose localization and enhanced biological effect [19]. Our results have shown that carbon ion therapy has the promising potential of delivering a sufficient dose to the tumor with acceptable morbidity in the surrounding normal tissues. Tumors that appear to respond favorably to carbon ions include locally advanced tumors with a non-squamous histology such as

adenocarcinoma [20,21]. Carbon ion therapy may very well improve tumor control of recurrent rectal cancer.

In conclusion, carbon ion radiotherapy is an effective local treatment for patients with locally recurrent rectal cancer, and it seems to represent a promising alternative to surgery. The morbidity rate of carbon ion radiotherapy has so far been quite acceptable, although the long-term safety of this approach for patients with sarcomas will still need to be monitored.

References

[1] Kapiteijin E, Marijnen CAM, Colenbrander AC et al. Local recurrence in patients with rectal cancer diagnosed between 1988 and 1992. Eur J Surg Oncol 24:528-535, 1998

[2] Galandiuk S, Wieand HS, Moertel CG, et al. Patterns of recurrence after curative resection of carcinoma of the colon and rectum. Surg Gynecol Obstet 174: 27-32, 1992

[3] Bozzetti F, Mariani L, Micel R, et al. Cancer of the low and middle rectum: local and distant recurrence and survival in 350 radically resected patients. J Surg Oncol 62: 207-213, 1992

[4] Blakely EA, Ngo FQH, Curtis SB, et al. Heavy ion radiobiology: Cellular studies. Adv Radiat Biol 11:295-378, 1984

[5] Hall EJ. Radiobiology for the Radiologist. Philadelphia, PA, JB Lippincott, 1988, pp 281-291

[6] Sato K, Yamada H, Ogawa K, et al. Performance of HIMAC. Nuclear Physics A 588:229-234, 1995

[7] Kanai T, Endo M, Minohara S, et al. Biophysical characteristics of HIMAC clinical irradiation system for heavy-ion radiation therapy. Int J Radiat Oncol Biol Phys 44:201-210, 1999

[8] Lopez-Kostner F, Fazio VW, Rybicki LA et al. Locally recurrent rectal cancer: Predictors and success of salvage surgery. Dis Colon Rectum 44: 173-178, 2001

[9] Wanebo HJ, Antoniuk P, Koness RJ et al. Pelvic resection of recurrent rectal cancer. Dis Colon Rectum 42: 1438-1448, 1999

[10] Ciatt S, Pacini P. Radiation therapy of recurrences of carcinoma of the rectum and sigmoid after surgery. Acta Radiol Oncolo 21: 105-109, 1082

[11] O'Connel MJ, Child DS, Moertel CG. A prospective controlled evaluation of combined pelvic radiotherapy and methanol extraction residue of BCG for locally unresectable or recurrent rectal cancer. Int J Radiat Oncol Biol Phys 8: 1115-1119, 1982

[12] Wong CS, Cummings BJ, Keane TJ. Combined radiation therapy, mitomycin C, and 5-Fluorouracil for locally recurrent rectal carcinoma. Int J Radiat Oncol Biol Phys 21: 1291-1296, 1991

[13] Lybeert MLM, Martijin H, DE NEVE W. Radiotherapy for locoregional relapses of rectal carcinoma after initial radical surgery. Int J Radiat Oncol Biol Phys 24:241-246,1992

[14] Knol HP, Hanssens J, Rutten HJT. Effect of radiation therapy alone or in combination with surgery and/or chemotherapy on tumor and symptom control of recurrent rectal cancer. Strahlenther Onkol 173: 43-49, 1997

[15] Murata T, Fujii I, Yoshino M. Radiation therapy with or without chemotherapy and hyperthermia for recurrent rectal cancer. J Jpn Soc Ther Radiol Oncol 9: 63-71, 1997

[16] Wendling P, Manz R, Thews G, et al. Heterogeneous oxygenation of rectal carcinomas in humans. Advances in Experimental Medicine & Biology 180: 293-300, 1984

[17] Hockel M, Schlenger K, Hockel S. Tumor hypoxia in pelvic recurrences of cervical cancer. Int J Cancer 79, 365-369, 1998

[18] Eising E, Potter R, Haverkamp U. Neutron therapy for recurrence of rectal cancer Strahlenther. Onkol 166: 90-94, 1990

[19] Ando K, Koike S, Ohira C, et al. Accelerated reoxygenation of a murine fibrosarcoma after carbon-ion radiation. Int J Radiat Biol 75: 505-512, 1999

[20] Kamada T, Tsujii H, Tsuji H, et al. Efficacy and safety of carbon ion radiotherapy in bone and soft tissue sarcomas. J Clin Oncol 20: 4466-4471, 2002

[21] Miyamoto T, Yamamoto N, Nishimura H, et al. Carbon ion radiotherapy for stage I non-small cell lung cancer. Radiother Oncol 66: 127-140, 2003

Pancreas Cancer

Shigeru Yamada, Makoto Shinoto, Hirotoshi Kato, Shigeo Yasuda, Tadashi Kamada,
Hirohiko Tsujii, Hiroshi Tsuji, Masayuki Baba, Jun-etsu Mizoe, Tadaaki Miyamoto, Kyousan Yoshikawa,
Susumu Kandatsu, and Hiromitsu Saisho for the Working Group for Pancreas Cancer

Hospital, Research Center for Charged Particle Therapy, National Institute of Radiological Sciences, Chiba, Japan,
Chiba University Graduate School of Medicine, Chiba, Japan.
e-mail: s_yamada@nirs.go.jp

Abstract

Adenocarcinoma of the pancreas continues to be a significant source of cancer mortality in Japan, resulting in approximately 19,000 deaths a year. It is the fifth leading cause of cancer-related deaths in Japan, with a less than 5% 5-year expected survival rate[1]. About 70-75% of patients with pancreas cancer present with locally advanced disease or distant metastases and have a median survival time of only 6 months. For unresectable pancreas cancer, the median survival time with external beam radiation (EBRT) was better than with surgical bypass[2] or stents alone[3]. The median survival OF EBRT alone was 4 to 7 months[4]. The median survival with combined EBRT and chemotherapy for locally unresectable tumor was 8 to 10 months[5], better than with EBRT alone.

Local failure of these combined therapies was still 26 to 48%. On the other hand, surgery with curative intent is undertaken in 15-20% of patients. Even after resection, the predicted 5-year survival rates are still less than 20%[1]. Local recurrence in the pancreatic bed is seen in 50% of the patients undergoing presumed curative resection[6].

We examined the effect of carbon ion therapy in terms of reducing the rate of local recurrence in patients with locally advanced adenocarcinoma of the pancreas or undergoing resection for adenocarcinoma of the pancreas.

Carbon ion therapy

A Phase I/II Clinical Trial of Carbon-ion Therapy for patients with preoperative pancreas cancer (9906) was carried out on surgically resectable patients from June 2000 through February 2003. This was followed by a Phase I/II Clinical Trial of Short-course Carbon-ion Therapy for patients with preoperative pancreas cancer (0203), commencing in April 2003 for similarly surgically resectable patients, with a fractionation regimen from 16 (4 weeks) to 8 (2 weeks) fractions. Concurrently, a Phase I/II Clinical Trial of Carbon-ion Therapy for patients with locally advanced pancreas cancer (0204) was conducted for surgically non-resectable patients with local progressive disease without distant metastasis from April 2003 through February 2007. This was followed by a Phase I/II Clinical Trial of Gemcitabine Combined with Carbon-ion Therapy for patients with locally advanced pancreas cancer.

A. Preoperative pancreas cancer (Protocol 9906, 16 fractions/4 weeks)

Purpose: We examined the effect of preoperative carbon ion therapy in terms of reducing the rate of local recurrence in patients undergoing resection for adenocarcinoma of the pancreas.

Patients and Methods: Twenty-two patients were enrolled into this trial. Median age was 63 years. Carbon ion therapy was given once daily, 4 days a week, for a fixed 16 fractions in 4 weeks. The dose was set at 44.8 GyE and escalated to 48.0 GyE at 5% increments.

Results: All patients completed the scheduled treatment course. Three grade 3 acute reactions and two grade 3 late reactions occurred among 16 of the patients treated with a total dose of 48.0 GyE. The two grade 3 late reactions

were estimated to be caused by carbon ion therapy. Of the 22 patients, 15 (68%) had resection. All tumor specimens pathologically revealed evidence of grade 2 treatment effects with significant fibrosis, hyalinization, and necrosis (pathological grade 2 is defined as less than 33% active cancer cells). Remarkable antitumor effects were observed. The overall local control rates were 100% and 87% at 1 year and 2 years of follow-up, respectively. No local failure was observed in any of the 22 enrolled patients.

Conclusion: Carbon ion radiotherapy seems to be a safe and effective modality in the management of resectable pancreatic carcinoma, providing good local control and offering a survival advantage without unacceptable morbidity.

Patients and Methods

1. Patient Eligibility

Between April 2000 and February 2003, 22 patients judged according to the staging criteria of the Japanese Committee on Cancer as being at clinical stages I, II, III or IVa, equivalent stages I, II or III by the TNM staging criteria, were enrolled into this trial. Criteria for trial eligibility were pathologic confirmation of ductal adenocarcinoma, age of 18 years or more, ECOG performance score 0, 1, or 2, and adequate hematologic, hepatic, renal, and cardiopulmonary function to allow pancreatectomy. Exclusion criteria were having another primary tumor and infection at the tumor site. Patients who had undergone chemotherapy before carbon ion radiotherapy or those who had prior radiation therapy at the same site were excluded from the study. The tumor had to be grossly measurable, but its size could not exceed 15 cm, and the patients were evaluated by surgical consultation with three surgical investigators as to the resectability of the lesion. Chest and upper abdominal CT scans were mandatory at the time of entry into the trial. All patients signed an informed consent form approved by the local institutional review board.

2. Carbon Ion Radiotherapy

The features of the accelerator and the carbon ion beam have previously been described[7,8].

Carbon ion therapy was given once daily, 4 days a week, for a fixed 16 fractions over 4 weeks. The dose was set at 44.8 GyE and escalated to 48.0 GyE at 5% increments. The protocol specifications for carbon ion radiotherapy were as follows. The target volumes were established by CT scan. Field arrangements were generally designed using a 3-field or 4-field plan. The clinical target volume (CTV) included the gross tumor volume (GTV) and regional lymph nodes, which included the celiac, superior mesenteric, peri-pancreatic, portal and para-aortic (celiac-IMA) nodes for pancreatic head cancer and splenic nodes for pancreatic body and tail cancer. The CTV was defined as the gross volume plus 1.0 cm or 0.5 cm (in contact with the gut). At least 50% of the functioning renal parenchyma was limited to 15 GyE or less. The spinal cord dose was limited to 30 GyE or less.

3. Surgery

Surgical resection was to be performed 2 to 4 weeks after the completion of carbon ion radiotherapy if there was no disease progression to an unresectable status as determined by repeated abdominal CT scans, a prohibitive decline in performance status, or other evidence of metastatic disease. Median time from the last day of carbon ion radiotherapy to surgical resection was 21 days (range, 20 - 26 days).

4. Tumor Response and Local Control Criteria

Tumor response was defined as the maximum tumor response observed by the RECIST scoring system during the first 6 months after the initiation of carbon ion radiotherapy. Complete response (CR) was defined as the disappearance of all measurable tumor in the treatment volume. Partial response (PR) meant a 30% or greater decrease in tumor size (longest diameter). Stable disease was that with a less than 30% decrease or a less than 20%

increase in tumor size. Progressive disease was defined as a 20% or greater increase in tumor size. Local recurrence was defined in terms of lesions occurring in the treatment volume based on CT, MRI, and PET scans. The development of a new, low-density mass in the region of the pancreatic bed was considered evidence of local recurrence even in the absence of symptoms, and cytologic or histologic confirmation of recurrent disease was not required. The absence of local recurrence was described as local control.

Histologic evaluation of the effects of carbon ion therapy included assessment of cytologic changes in conjunction with quantification of the amount of viable residual carcinoma cells (Table 1). Upon completion of specimen analysis, all cases were reviewed by the same histopathologist.

Table1. Grading system for radiation treatment effects

Grading system for radiation treatment effects

Grade	Histological appearance
0	No tumor cell destruction evident
1	Less than two-thirds of tumor cells are destroyed
2	More than two-thirds of tumor cells are destroyed
3	No viable tumor cells present

5. Statistics

Survival time and local control time were defined as the interval between the initiation of carbon ion radiotherapy and the date of death or the date of diagnosis of local failure, respectively.

Results

1. Patient Characteristics

None of the 22 patients initially registered into this trial was excluded from the analysis. The patients consisted of 14 males and 8 females. Median age was 63 years (range, 42 - 77 years). Thirty cancers originated in the head of the pancreas, 8 were in the body of the pancreas, and one was in both the head and body (Table 2).

Table2. Patient Characteristics

Characteristics		Number of patients(%)
Age (years)	median (range)	22 (42-77)
Gender	male	14
	female	8
ECOG performance score	0	18
	1	4
Tumor location	head	13
	body-tail	8
	head and body	1
Tumor size by CT (mm)		
Stage (preoperative, TNM))		
T3N0		4
T3N1		18

2. Toxicity

The toxicities in the 22 patients receiving carbon ion therapy are listed in Table 3. The toxicities were relatively few and mild. All patients completed the scheduled treatment course. Three grade 3 acute reactions and two grade 3 late reactions occurred among 12 of the patients treated with a dose of 48.0 GyE. One patient had cholangitis, easily resolved by radiologic stent change and antimicrobials. Two were postoperative complications: one patient had leakage at the choledochojejunostomy, requiring percutaneous drainage, and the other had gastrojejunostomy leakage, requiring percutaneous drainage. Both leakages occurred outside of the treatment fields and were considered to likely not be related to the carbon ion therapy. There was no grade 3 to 5 blood or bone marrow reaction. Both two grade 3 late reactions were post-surgery portal vein stenoses, and both underwent portal vein resections.

Table3. Acute and Late toxicities by NCI-CTC and RTOG/EORTC Scoring System

	Acute (NCI-CTC)						Late (RTOG/EORTC)					
	No. of patients	Gr0	Gr1	Gr2	Gr3	Gr4	No. of patients	Gr0	Gr1	Gr2	Gr3	Gr4
Skin	22	22	0	0	0	0	20	20	0	0	0	0
Gastrointestinal	22	18	3	1	0	0	20	20	0	0	0	0
Bile duct	22	20	0	1	1	0	20	20	0	0	0	0
Portal vein	22	20	0	2	0	0	20	18	0	0	2	0
Leakage	22	20	0	0	2	0	20	20	0	0	0	0

3. Tumor Response

Evaluation of tumor response was not considered the primary endpoint of this study.

All 22 patients had CT scans before registration and 2-4 weeks after completion of the carbon ion radiotherapy. On the basis of the CT scans, only one patient showed complete response, and one also showed partial response. Twenty patients (91%) had stable disease, but none had local tumor progression.

4. Surgical Results

Of 22 patients, 15 (68%) had resection. One of the 22 eligible patients did not undergo surgery. CT scan restaging after carbon ion radiotherapy revealed new liver metastases in this patient. Of the 21 patients undergoing exploratory celiotomy, 5 had no resection. Two had metastases to the liver and three to the peritoneum. Fifteen eligible patients had pancreatic resection; 10 modified Child procedures, two total pancreatectomies, and three distal pancreatectomies were performed. In addition, one patient also underwent solitary liver resection for a small isolated liver metastasis discovered intraoperatively after pancreaticoduodenectomy. This patient, who had pancreatectomy that was not considered potentially curative resection, was included in this analysis. The median time from completion of carbon ion radiotherapy to surgery was 22 days (range, 13 - 29).

5. Pathological Results of Resected Specimens

The pathological characteristics of the 15 resected specimens are listed in Table 3. All tumor specimens revealed evidence of grade 2 treatment effects with significant fibrosis, hyalinization and necrosis, meaning more than two-thirds of the tumor cells were destroyed. The resection margins were examined in all specimens. No patient had a grossly or microscopically positive resection margin.

Table4. Pathologic results of the 15 resected specimens

Total dose (GyE)	No. of patients	Grade0	Grade1	Grade2	Grade3
44.8	5	0	0	5	0
48.0	10	0	0	10	0

6. Patient Outcome

The overall local control rates were 100% at 1 year and 87% at 2 years of follow-up, respectively (Fig.1). One local failure was observed in the residual pancreas at 18 months after pancreaticoduodenectomy. There was no local and regional recurrence within the treatment fields. The 1-year overall survival rates were 62% for all patients and 90% in the resected patients, and median survivals were 13.4 months and 21 months, respectively, with a median follow-up of 13 months (range, 3.3 - 51 months) (Fig.2). Two patients are currently alive without evidence of disease. Twenty patients are dead and 19 patients had metastatic relapse or carcinomatosis. In the nonresected patients, the 1-year overall survival rate and median survival were 30% and 6.3 months.

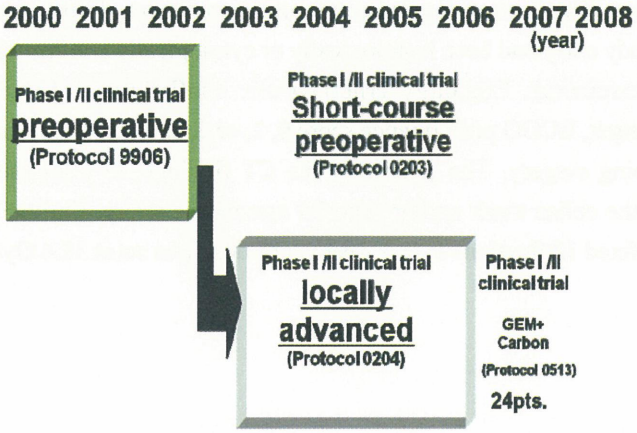

Fig.1 NIRS Sequencing Trial: Schema

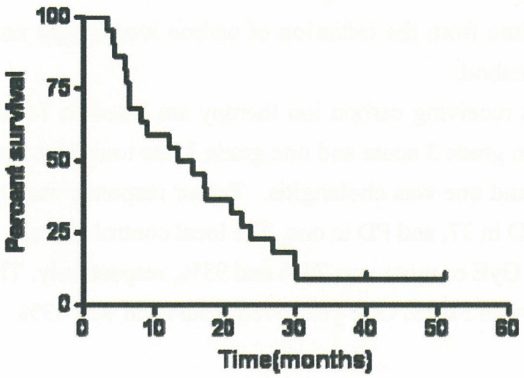

Fig.2. Overall survival for all 22patients

B. Short-course (8 fractions/2 weeks) preoperative pancreas cancer (Protocol 0203)

The phase I/II trial of preoperative carbon ion radiotherapy (8 fractions/2 weeks) for pancreas cancer prior to surgery was performed with the purpose of establishing the safety of carbon ion radiotherapy, determining the recommended dose, and substantiating its preoperative effectiveness.

At present, patient enrollment in the trial is in progress, and the outcomes are pending. The early data indicate the same high level of local control as the 9906 protocol. However, the histological effect is showing a tendency of being somewhat inferior to the 9906 protocol, suggesting that the dose is not adequate. In view of the reports in the literature on drugs with a sensitizing effect in conjunction with heavy particle beams, further studies are scheduled in search for an even more effective treatment modality.

C. Locally advanced pancreas cancer (Protocol 0204, 12 fractions/3 weeks)

The phase I/II trial of carbon ion radiotherapy (12 fractions/3 weeks) for locally advanced pancreas cancer was performed so as to establish the safety of carbon ion radiotherapy, determine the recommended dose, and confirm its efficacy.

Patients and Methods

Between April 2003 and February 2007, 47 patients judged according to the staging criteria of the Japanese Committee on Cancer as being clinical stages IVa or IVb without distant metastasis were enrolled into thi trial. As one patient was excluded because of receiving chemotherapy before treatment, 46 patients were eligible for this analysis. Patients eligible for study entry had been histologically or cytologically confirmed with locally advanced unresectable pancreas ductal carcinoma. Eligibility criteria were: confirmation of ductal carcinoma by CT findings, age of 80 years or younger, ECOG performance score 0, 1, or 2, and hepatic, renal and cardiopulmonary function sufficient for undergoing surgery. The criteria of the CT findings for non-resectability of the tumor included tumor encasement of the celiac trunk and/or superior mesenteric artery. Carbon ion therapy was given once daily, 4 days a week, for a fixed 12 fractions over 3 weeks. The dose was set at 38.4 GyE and escalated to 52.8 GyE at 5% increments.

Results

Toxicity on organs such as skin, bladder and digestive tract was assessed according to the NCI-CTC (acute) and RTOG/EOTRC (late) classifications. Tumor response was defined by the RECIST scoring system as the maximum tumor response observed during the first 6 months after the initiation of carbon ion radiotherapy. Local recurrence was defined in terms of lesions occurring in the tumor bed.

Survival was calculated as the time from the initiation of carbon ion therapy until death. Survival curves were estimated by the Kaplan-Meier method.

All toxicities in the 46 patients receiving carbon ion therapy are listed in Table 8. All patients completed the scheduled treatment course. Seven grade 3 acute and one grade 3 late toxicities were observed. Six of the 7 grade 3 acute toxicities were anorexia and one was cholangitis. Tumor response was evaluated in 46 lesions. CR was observed in one lesion, PR in 7, SD in 37, and PD in one. The local control rate at 1 year in the 46 analyzed patients and in the patients receiving 45.6 GyE or more was 76% and 95%, respectively. The overall survival estimates for the 46 analyzed patients are shown in Fig. 3. One-year overall survival was 43%.

Table5: Acute and Late toxicities by NCI-CTC and RTOG/EORTC Scoring System

	Acute (NCI-CTC)						Late (RTOG/EORTC)					
	No. of patients	Gr0	Gr1	Gr2	Gr3	Gr4	No. of patients	Gr0	Gr1	Gr2	Gr3	Gr4
Skin	22	22	0	0	0	0	20	20	0	0	0	0
Gastrointestinal	22	18	3	1	0	0	20	20	0	0	0	0
Bile duct	22	20	0	1	1	0	20	20	0	0	0	0
Portal vein	22	20	0	2	0	0	20	18	0	0	2	0
Leakage	22	20	0	0	2	0	20	20	0	0	0	0

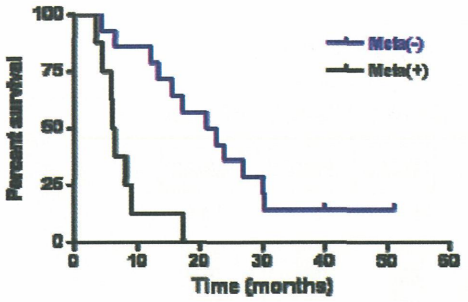

Fig.3 Overall survival for patients with or without distant metastases

The maximum acute reaction of grade 3 was observed in two-thirds of the patients (67%) at 52.8 GyE. From these results, we concluded that the maximum tolerance dose of carbon ions is 52.8 GyE/12 fractions/3 weeks.

On the basis of the literature on drugs with a sensitizing effect in conjunction with heavy particle beams, further studies were scheduled in an effort to find even more effective treatment modalities based on a combination of chemo- and radiotherapy. We started a Phase I/II Clinical Trial of Gemcitabine Combined with Carbon-ion Therapy for patients with local advanced pancreas cancer from April 2007.

D Gemcitabine Combined with Carbon-ion Therapy (Protocol 0513, 12 fractions/3 weeks)

From the results of the 0204 clinical study, carbon ion radiotherapy considerably improved tumor control of locally advanced pancreas cancer with acceptable morbidity in the surrounding normal tissues, but sufficient survival benefit could not be achieved. On the basis of the literature on drugs with a sensitizing effect in conjunction with heavy particle beams, further studies were scheduled in an effort to find even more effective treatment modalities based on a combination of chemo- and radiotherapy. We started a Phase I/II Clinical Trial of Gemcitabine Combined with Carbon-ion Therapy for patients with locally advanced pancreas cancer from April 2007.

The dose escalation schedule of Gemcitabine combined with carbon ion radiotherapy is shown in Fig.3. First the dose of carbon ion radiation was fixed at 43.2 GyE and the dose of gemcitabine was escalated from 400 mg to 1000 mg; then the dose of gemcitabine was fixed at 1000 mg and the dose of carbon ion radiation was escalated from 45.6 Gye to 50.4 GyE. Carbon ion therapy was given once daily, 4 days a week, for a fixed 12 fractions over 3 weeks. Gemcitabine was given once weekly (Fig.5,6).

At present we are trying to give 1000 mg/m^2 combined with 45.6 GyE of carbon ions. All patients completed the scheduled treatment course. This trial is still ongoing. Gemcitabine combined with carbon ion radiotherapy may be well tolerated by patients with pancreas cancer.

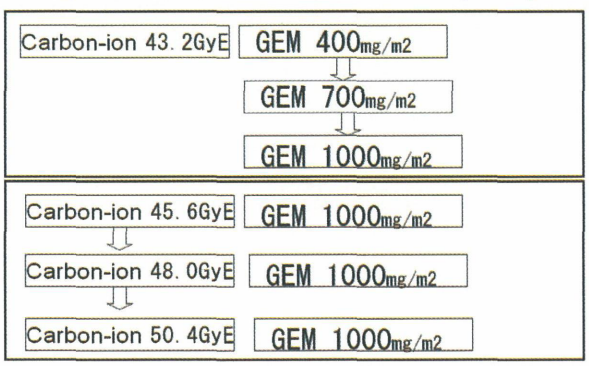

Fig.4 Dose Escalation Schedule (0513)

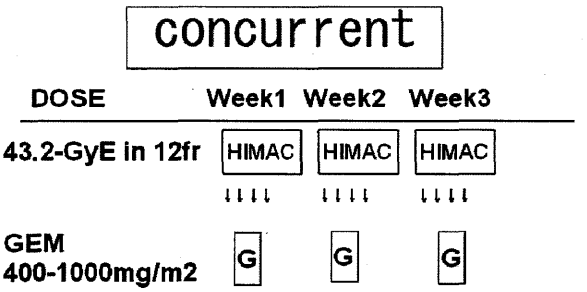

Fig.5 Treatment schema for combination of Gemcitabine and Carbon-ion Therapy

Reference

[1] Registration committee of pancreatic cancer. Annual Report of Nationwide Survey of Pancreatic Cancer. J of Jpn Panc Surg. 18: 101-169, 2003

[2] Lillemoe KD, Cameron JL, Hardacre JM et al. Is prophylactic gastrojejunostomy indicated for unresectable periampullary cancer? Ann Surg. 230: 322-330, 1999

[3] Prat F, Chapat O, Ducot B et al. A randomized trial of endoscopic drainage methods for inoperable malignant stricture of the common bile duct. Gastrointest Endosc. 47: 1-7, 1998

[4] Roldan GE, Gunderson LL, Nagorney DM et al. External beam versus intraoperative and extrabeam irradiation for locally advanced pancreatic cancer: Cancer. 61:1110-1116, 1988

[5] Moertel CG, Gundeson LL, Mailliard JA et al. Early evaluation of combined fluorouracil and leucovorin as a radiation enhancer for locally unresectable, residual, or recurrent gastrointestinal carcinoma. J Clin Oncol. 12:21-27, 1994

[6] Griffin JF, Smalley SR, Jewell W et al. Patterns of failure after curative resection of pancreatic carcinoma. Cancer. 66: 56-61, 1990

[7] Sato K, Yamada H, Ogawa K, et al. Performance of HIMAC. Nuclear Physics A. 588:229-234, 1995

[8] Kanai T, Endo M, Minohara S, et al. Biophysical characteristics of HIMAC clinical irradiation system for heavy-ion radiation therapy. Int J Radiat Oncol Biol Phys. 44:201-210, 1999

Carbon Ion Radiotherapy for Locally Advanced Adenocarcinoma of the Uterine Cervix

Shingo Kato, Hiroki Kiyohara, Hirohiko Tsujii, and Michiya Suzuki, for the Working Group of the Gynecological Tumor

Hospital, Research Center for Charged Particle Therapy, National Institute of Radiological Sciences, Chiba, Japan
e-mail address: s_kato@nirs.go.jp

Abstract

Purpose: To evaluate the toxicity and efficacy of carbon ion radiotherapy (CIRT) for locally advanced cervical adenocarcinoma by phase I/II dose-escalation study.

Methods and Materials: Between April 1998 and August 2008, 45 patients with cervical adenocarcinoma were treated with CIRT. Histologically, 36 patients had adenocarcinomas and 9 had adenosquamous carcinomas. Fifteen patients had stage IIB, 28 had stage IIIB, and 2 had stage IVA disease. The dose of the whole pelvic irradiation was fixed at 36.0 gray equivalent (GyE) in 12 fractions, and an additional dose of 26.4-38.4 GyE in 8 fractions was delivered to the cervical tumor (total dose: 62.4-74.4 GyE). The dose to the GI tracts was limited to less than 60 GyE. The median follow-up duration for all patients was 23 months (range, 6-93 months).

Results: No patient developed severe acute toxicity. No patient developed major late complications except for one patient with a rectovaginal fistula. Local control was obtained in 4 of the 7 patients receiving a total of 62.4-64.8 GyE, in 6 of the 9 patients receiving 68.0 GyE, in 13 of the 19 patients receiving 71.2GyE, and in all of 7 patients receiving 74.4 GyE. The 5-year local control and overall survival rates for stage IIIB or IVA patients who received $\geq$ 68.0 GyE were 64% and 46%, respectively.

Conclusions: Although the number of patients was small, the results have suggested that CIRT provided favorable local tumor control and overall survival with acceptable rates of late complications in the treatment of locally advanced cervical adenocarcinoma.

Introduction

The incidence of adenocarcinoma of the uterine cervix has been increasing over the past few decades (1). Currently, cervical adenocarcinoma accounts for 10-24% of all cervical carcinomas (1, 2).

There have been only a few reports that described the treatment outcomes of patients with cervical adenocarcinoma (3-8). According to these reports, locally advanced adenocarcinomas have a poorer prognosis than squamous cell carcinomas because of a poorer local control rate and higher rate of distant metastasis.

Several randomized phase III clinical trials in the 1990s and meta-analyses demonstrated that the combination of cisplatin-based chemotherapy and radiotherapy improved local control and overall survival in patients with locally advanced cervical cancer compared to radiotherapy alone (9-12). Based on the results, concurrent chemoradiotherapy has become the standard treatment for this disease. However, the majority of the patients included in these studies had squamous cell histology; adenocarcinomas represented approximately 10% of the registered patients. Therefore, the efficacy of concurrent chemoradiotherapy for locally advanced cervical adenocarcinoma has not been thoroughly evaluated clinically.

Carbon ion beams have improved dose localization properties, and this potentiality can produce great effects on tumors while minimizing normal tissue damage. Moreover, carbon ion radiotherapy (CIRT) has various biological advantages in terms of high linear energy transfer (LET) radiation, including a decreased oxygen enhancement ratio, a diminished capacity for sublethal and potentially lethal damage repairs, and diminished cell cycle-dependent radiosensitivity compared to those observed with low LET radiation. Several reports have demonstrated favorable results of CIRT in the treatment of malignant tumors, including head and neck cancer (13), non-small cell lung cancer (14), hepatocellular carcinoma (15), prostate cancer (16), and bone and soft tissue sarcomas (17).

In order to evaluate the efficacy and toxicity of CIRT for locally advanced cervical adenocarcinoma, a phase I/II dose-escalation study has been conducted.

Methods and Materials

1. Patient eligibility

Patients were enrolled into the study if they had medically inoperable adenocarcinoma or adenosquamous carcinoma of the uterine cervix with International Federation of Gynecology and Obstetrics (FIGO) stage IIB, III, or IVA disease (except for rectal invasion). The tumor had to be grossly measurable. Other eligibility criteria included World Health Organization performance status ≤ 3, and estimated life expectancy of ≥ 6 months. Patients who had histories of prior chemotherapy, and surgery or radiotherapy to the pelvis, were excluded from the study. Patients were also excluded if they had severe pelvic infection, severe psychological illness, or active double cancer.

Pretreatment evaluation consisted of an assessment of the patient's history, physical and pelvic examinations by gynecologists and radiation oncologists, cervical biopsy, routine blood cell counts, chemistry profile, chest X-ray, intravenous urography, cystoscopy, and rectoscopy. Computed tomography (CT) scans of the abdomen and pelvis, magnetic resonance imaging (MRI) of the pelvis, and ^{11}C methionine positron emission tomography (PET) scans were also performed for all patients. Patients were staged according to the FIGO staging system, but patients with para-aortic lymph nodes > 1 cm in minimum diameter on CT images were excluded from the study (18). Patients with enlarged pelvic lymph nodes only were included in the study. Tumor size was assessed by both pelvic examination and MRI, and dimensions of the cervical tumor were measured based on T2-weighted MRI images (18). ^{11}C methionine PET scans were supplementally used for detecting distant metastasis. Tumor specimens were reviewed by pathologists of the working group. All patients gave written informed consent according to the institutional regulations.

2. Carbon ion radiotherapy

The treatment consisted of whole pelvic irradiation and local boost, with the target volume being shrunk in three steps so that the highly concentrated dose could be delivered to the tumor without increasing the dose to normal structures. The clinical target volume (CTV) for whole pelvic irradiation (CTV-1) included all areas of gross and potentially microscopic disease, consisting of the primary tumor, uterus, parametrium, at least the upper half of the vagina, and pelvic lymph nodes. Because non-enlarged lymph nodes are poorly visualized on CT, nodal regions were defined by encompassing the pelvic vessels with a 5-10-mm margin. After completing whole pelvic irradiation, local boost irradiation was performed. First, CTV included the gross tumor volume (GTV) and surrounding tissues, such as the parametrium, uterine body, upper vagina, and adjacent lymph nodes (CTV-2). Next, CTV was further shrunk to GTV only, and the intestines and bladder were completely excluded from the target volume (CTV-3). A margin of 5 mm was usually added to the CTV to create the planning target volume (PTV). When the tumor was located close to critical organs such as the bowel or bladder, the margin was reduced accordingly. CTV was covered by at least 90% of the prescribed dose. The dose to the bowel was

limited to < 60 GyE. A spacer was inserted into the vaginal canal to provide a safe distance between the tumor and the rectum (Fig. 1).

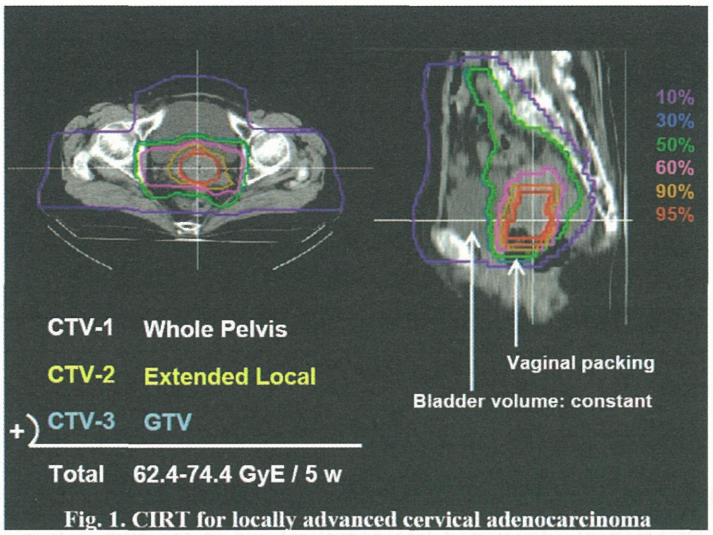

Fig. 1. Carbon ion radiotherapy (CIRT) for locally advanced cervical adenocarcinoma.
Isodose curves of CIRT are superimposed on axial and sagittal CT images.

Carbon ion radiotherapy was given once daily, 4 days per week, for a fixed 20 fractions in 5 weeks. The dose to PTV was fixed at 36 GyE/12 fractions. A dose escalation study was planned in the local boost session with an initial dose of 26.4 GyE for 8 fractions (3.3 GyE/fraction) up to 38.4 GyE (4.8 GyE/fraction) by 10% increments. At every treatment session, the patient was positioned on a treatment couch with immobilization devices, and the patient's position was verified using a computer-aided, on-line positioning system. In order to minimize internal target positional uncertainty, 100 ml of normal saline was infused into the bladder. Patients were also encouraged to use laxatives, if necessary, to prevent constipation throughout the treatment period.

3. Assessment of toxicity and efficacy

Acute toxicity was graded according to the Radiation Therapy Oncology Group (RTOG) acute radiation morbidity scoring system, with the highest toxicity within 3 months from the initiation of CIRT. Late toxicity was graded according to the RTOG/European Organization for Research and Treatment of Cancer (EORTC) late radiation morbidity scoring scheme (19). The effect of the treatment was evaluated in terms of local control and overall survival. Local control was defined as showing no evidence of tumor regrowth or recurrence in the treatment volume based on physical examinations, CT, MRI, PET, and/or biopsy. Local control and overall survival rates were calculated by the Kaplan-Meier method.

Results

Between April 1998 and August 2008, a total of 45 patients with cervical adenocarcinoma or adenosquamous carcinoma were treated with CIRT. Patient characteristics are summarized in Table 1. Mean age was 60 years. Histologically, 36 had adenocarcinomas and 9 had adenosquamous carcinomas. Fifteen patients had stage IIb, 28 had IIIb, and 2 had stage IVA disease. Eighteen patients had enlarged lymph nodes in the pelvis. All patients had bulky tumors measuring 3.0-11.0 cm in maximum diameter and a median diameter of 5.5 cm. All patients were subjected to periodic follow-up. The median follow-up duration for all patients was 23 months. In the dose-escalation study, 3 patients received a total dose of 62.4 GyE, 4 received 64.8 GyE, 10 received 68.0 GyE, 21 received 71.2 GyE, and 7 received 74.4GyE (Table 2).

Table 1. Patient characteristics

No. of patients	45
Follow-up, range (median) (mo)	6-93 (23)
Age, range (mean) (yrs)	37-85 (60)
Histology	
Adenocarcinoma	36
Adenosquamous carcinoma	9
FIGO Stage	
IIb	15
IIIb	28
IVa	2
Lymph node status	
Negative	27
Positive	18
Tumor size	
3-6 cm	23
6-8 cm	18
8 cm-	3

Table 2. Dose escalation study of CIRT

(n=45)

Whole pelvis (fixed)	Local boost (dose escalation)	Total dose	No. of patients
3.0 GyE x 12 (36.0 GyE)	3.3 GyE x 8	62.4 GyE	3
	3.6 GyE x 8	64.8 GyE	4
	4.0 GyE x 8	68.0 GyE	10
	4.4 GyE x 8	71.2 GyE	21
	4.8 GyE x 8	74.4 GyE	7

1. Toxicity

No patient developed severe acute toxicities in the skin, gastrointestinal (GI), or genitourinary (GU) tract (Table 3). Seven (16%) patients developed late complications in the skin, GI or GU tract. Almost all of the complications were classified as grade 1, but one patient developed Grade 4 late GI toxicity (Table 4). She had a stage IIb cervical adenocarcinoma, measuring 7 cm in maximum diameter. She received a total of 68.0 GyE to her primary tumor. Fourteen months after CIRT, she developed a rectovaginal fistula. She has been alive without disease and intestinal problems for 73 months after receiving a colostomy. She had uncontrolled diabetes mellitus, which may have contributed to her complication. No other patients receiving 68.0-74.4 GyE developed major late GI toxicity (Table 5).

Table 3. Acute toxicities by RTOG scoring system

Site	No. of Patients	RTOG Grade			
		Gr. 0	Gr. 1	Gr. 2	Gr. 3
Skin	45	38	7	0	0
GI tract	45	29	15	1	0
GU tract	45	38	7	0	0

Table 4. Late toxicities by RTOG/EORTC scoring scheme

Site	No. of Patients	RTOG/EORTC Grade				
		Gr. 0	Gr. 1	Gr. 2	Gr. 3	Gr. 4
Skin	45	44	1	0	0	0
GI tract	45	41	3	0	0	1
GU tract	45	40	2	3	0	0

Table 5. Late GI toxicities by carbon ion dose

Total dose (GyE)	No. of Patients	Follow-up (median) (mo)	RTOG/EORTC Grade				
			G0	G1	G2	G3	G4
62.4	3	8-20 (15)	3	0	0	0	0
64.8	4	10-93 (65)	2	2	0	0	0
68.0	10	13-80 (66)	8	1	0	0	1*
71.2	21	9-53 (23)	21	0	0	0	0
74.4	7	6-15 (11)	7	0	0	0	0

* recto-vaginal fistula

2. Local control and survival

The relationship between carbon ion dose and local control is shown in Fig. 2. Three patients with marginal recurrences were excluded from this analysis. Local control was obtained in 4 of the 7 patients (57%) receiving 62.4-64.8 GyE, in 6 of the 9 patients (67%) receiving 68.0 GyE, in 13 of the 19 patients (68%) receiving 71.2GyE, and in all of the 7 patients receiving 74.4GyE.

The actuarial local control and overall survival curves for all patients are shown in Fig. 3. The 3- and 5-year local control rates were 63% and 57%, respectively. Three patients who had developed local recurrences were surgically salvaged, bringing the 5-year local control rate, including the salvage surgery, to 70%. Twenty-four of the 45 patients (53%) developed distant metastases, including 11 patients to the paraaortic lymph nodes, and they subsequently received photon radiotherapy and/or chemotherapy. The 3- and 5-year overall survival rates were 57% and 42%, respectively. With regard to the stage III or IVA patients who received 68.0-74.4 GyE of CIRT, the 5-year local control and overall survival rates were 64% and 46%, respectively (Fig. 4).

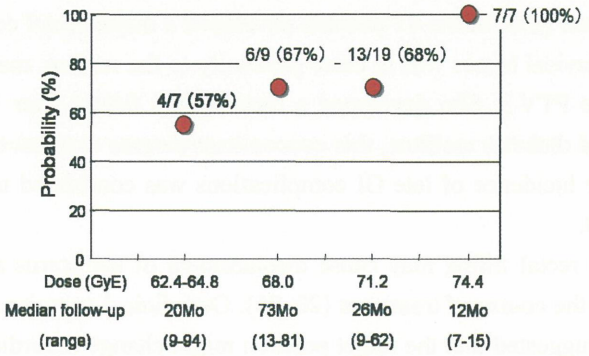

Fig. 2. Dose-response relationship between the dose of CIRT and local control rate (1998.4-2008.8).

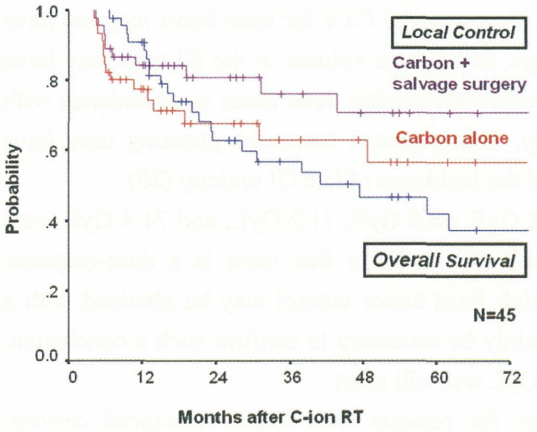

Fig. 3. Overall survival and local control curves in patients with cervical adenocarcinoma treated with CIRT (1998.4-2008.8).

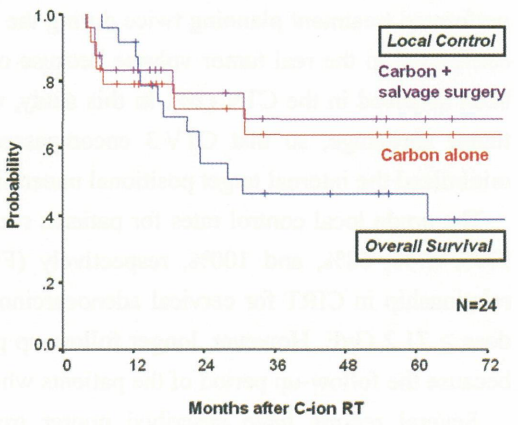

Fig. 4. Overall survival and local control curves in stage IIIb-I patients with cervical adenocarcinoma treated with a dose of 68.0-7 GyE of CIRT (1998.4-2008.8).

Discussion

Two phase I/II clinical studies of CIRT for locally advanced cervical cancer were carried out before this study (20). The following results were obtained from those studies: 1) doses of 35.2-48.0 GyE in 16 fractions (2.2-3.0 GyE/fraction) over 4 weeks could be delivered safely to the whole pelvis, 2) a dose $\geq$ 60 GyE to the GI tract may have caused severe late complications. Based on the results, the dose to the whole pelvis was fixed at 36.0 GyE for 12 fractions (3.0 GyE/fraction) over 3 weeks in the present protocol, which was assumed to be equivalent to 40 Gy of conventional photon radiotherapy. An additional dose of 13.2-19.2 GyE for 4 fractions (3.3-4.8 GyE/fraction) was delivered to the cervical tumor and surrounding tissues including the parametrium, uterine body, upper vagina, and adjacent lymph nodes, where tumor infiltration was highly suspected. Consequently, these lesions were given a total of 49.2-55.2 GyE. Following this, the PTV was shrunk to the GTV only, and the GI tracts were completely excluded from the PTV. The GTV received a total of 62.4-74.4 GyE, whereas the dose to the GI tracts was limited to < 60 GyE (Fig. 1).

The incidence and severity of late complications in this study were significantly lower than those in the previous studies (20). Only one (2%) of the 45 patients developed a major rectal complication (Table 4, 5). The anatomical location of her cervical tumor was in close proximity to the rectum, making it somewhat difficult to exclude the rectum from the PTV-3. She developed a rectovaginal fistula after 3 months of local infection. Because she had uncontrolled diabetes mellitus, this concomitant disease may have had some involvement with this complication. The lower incidence of late GI complications was considered to be attributable to the strict dose constraint to the GI tract.

Variations in bladder and rectal filling may cause displacement of the uterus and upper vagina, leading to systematic errors throughout the course of treatment (20, 21). Our clinical experience using repeated MRI or CT scans during treatment also suggested that the target position might change according to the bladder volume. To decrease such positional uncertainties, we infused a fixed volume (usually 100 ml) of normal saline into the bladder throughout the treatment. Patients were also encouraged to use laxatives, if considered necessary, to prevent constipation during treatment.

If a treatment plan is generated based on the single time-point assessment of the target position, tumor volume shrinkage may also result in systematic errors throughout the treatment course (20, 22). In our past studies, we performed treatment planning twice during the course of CIRT. However, the CTV for local boost may not have conformed to the real tumor volume because of tumor shrinkage, and a large volume of the GI tract may have been involved in the CTV (20). In this study, we performed treatment planning three times in accordance with tumor shrinkage, so that CTV-3 encompassed the GTV only. This repeated treatment planning may have minimized the internal target positional uncertainty and lessened the incidence of late GI toxicity (20).

The crude local control rates for patients receiving 62.4-64.8 GyE, 68.0 GyE, 71.2 GyE, and 74.4 GyE were 57%, 67%, 68%, and 100%, respectively (Fig. 2). This result may indicate that there is a dose-response relationship in CIRT for cervical adenocarcinoma and that a high local tumor control may be obtained with a dose $\geq$ 71.2 GyE. However, longer follow-up periods will certainly be necessary to confirm such a conclusion, because the follow-up period of the patients who received 74.4 GyE was still short.

Several reports have described poorer treatment outcomes for patients with locally advanced cervical adenocarcinomas compared with those for patients with squamous carcinomas. Lea et al. treated 83 patients with stage IIb-IVb cervical adenocarcinoma by radiotherapy or chemoradiotherapy and reported 5-year survival rates of 30% for stage IIb and 0% for stage III-IV (6). Eifel et al. in their large series of radiotherapy reported 5-year survival rates of 28% for stage IIb and 26% for stage III (4). In contrast, Grigsby et al. analyzed prognostic factors by multivariate analysis and found that adenocarcinoma was not a significant prognostic factor. However, when comparing the treatment outcomes among patients with stage III disease, the 5-year survival rate of 25% for adenocarcinoma was lower than that of 36.7% for squamous carcinoma (7).

When comparing our treatment results with those of the previous reports, our 5-year overall survival rate of

46% for stage IIIB-IVA patients receiving 68.0 GyE or more seemed favorable (Table 6). Only a few studies have described failure patterns in patients with stage III cervical adenocarcinoma treated by radiotherapy (4, 7). According to those reports, local failure was observed in 39-67%. In contrast, 5-year local control of our stage III-IVA patients was 64% (Fig. 4). Therefore, the favorable survival rate achieved in our study may have been attributable to the high local tumor control achieved by CIRT. Nonetheless, further study will be needed to confirm the efficacy of CIRT in local management, as our patient number was rather small.

Table 6. Outcomes of RT/CRT and C-ion RT for patients with locally advanced cervical adenocarcinoma.

No.	Author	Year	No.	Stage	Therapy	5y OS	Follow-up
1)	Baalbergen A	2004	22	III	RT (+HT)	-	61Mo. (mean)
2)	Lea JS	2002	24	III	RT/CRT	0%	33Mo. (median)
3)	Hopkins MP	1991	25	III	RT	8%	80Mo. (median)
4)	Eifel PJ	1990	46	III	RT	26%	87Mo. (median)
5)	Quin MA	2006	135	IIIB	RT/CRT	24%	NA
6)	NIRS	2008	29	IIIB-IVA	RT/CRT	19%	38Mo. (median)
7)	NIRS	2009	24	IIIB-IVA	C-ion RT (68GyE-)	46%	26Mo. (median)

All published studies included patients with adenosquamous cell carcinoma.

1) Gynecol Oncol 92:262-267.2004. 2) Gynecol Oncol 84:115-119.2002.
3) Obstet Gynecol 72: 789-795.1991. 4) Cancer 65:2507-2514.1990.
5) Int J Gynecol Obstetr 95, suppl 1: 43-103, 2006. (26th FIGO annual report)

In spite of the higher local tumor control, distant metastasis frequently occurred, and the survival rate was still unsatisfactory (Fig. 3, 4). Several studies also described a high rate of distant metastasis, resulting in poor survival (3-7). To improve the survival rate, the use of chemotherapy in combination with CIRT should be explored.

Conclusions

Although the number of patients was small, our results have strongly suggested that CIRT provided favorable local tumor control and overall survival with acceptable rates of late complications in the treatment of locally advanced cervical adenocarcinoma. Further study is needed to confirm the efficacy of CIRT in the local management of locally advanced cervical adenocarcinoma. The use of chemotherapy in combination with CIRT should also be considered to improve the survival rate.

References

[1] Smith HO, Tiffany MF, Qualls CR, Keys CR. The rising incidence of adenocarcinomas relative to squamous cell carcinomas of the uterine cervix - a 24-year population based study. Gynecol Oncol 2000; 78:97-105.

[2] Benedet JL, Odicino F, Maisonneuve P, et al. Carcinoma of the cervix uteri. (In) Journal of Epidemiology and Biostatistics, FIGO Annual Report on the Results of Treatment in Gynaecological Cancer. 6: P7-43, 2001.

[3] Baalbergen A, Ewing-Graham PC, Hop WC, Struijk P, Helmerhorst TJ. Prognostic factors in

adenocarcinoma of the uterine cervix. Gynecol Oncol 2004; 92:262-267.
[4] Eifel PJ, Morris M, Oswald MJ, Wharton JT, Delcos L. Adenocarcinoma of the uterine cervix. Prognosis and patterns of failure in 367 cases. Cancer 1990; 65:2507-2514.
[5] Hopkins MP, Morley GW. A comparison of adenocarcinoma and squamous cell carcinoma of the cervix. Obstet Gynecol 1991; 77:912-918.
[6] Lea JS, Sheets EE, Wenham RM, et al. Stage IIB-IVB cervical adenocarcinoma: Prognostic factors and survival. Gynecol Oncol 2002; 84:115-119.
[7] Grigsby PW, Perez CA, Kuske RR, et al. Adenocarcinoma of the uterine cervix: Lack of evidence for a poor prognosis. Radiother Oncol 1988; 12:289-296.
[8] Kilgore LC, Soong SJ, Gore H, Shingleton HM, Hatch KD, Partridge EE. Analysis of prognostic factors in adenocarcinoma of the cervix. Gynecol Oncol 1988; 31:137-148.
[9] Eifel PJ, Winter K, Morris M, et al. Pelvic irradiation with concurrent chemotherapy versus pelvic and para-aortic irradiation for high-risk cervical cancer: An update of Radiation Therapy Oncology Group Trial (RTOG) 90-01. J Clin Oncol 2004; 22: 872-880.
[10] Rose PG, Bundy BN, Watkins EB, et al. Concurrent cisplatin-based radiotherapy and chemotherapy for locally advanced cervical cancer. N Engl J Med 1999; 340: 1144-1153.
[11] Whitney CW, Sause W, Brundy BN, et al. A randomized comparison of fluorouracil plus cisplatin versus hydroxyurea as an adjuvant to radiation therapy in stages IIB-IVA carcinoma of the cervix with negative para-aortic lymph nodes: A Gynecologic Oncology Group and Southwest Oncology Group study. J Clin Oncol 1999; 17: 1339-1348.
[12] Green JA, Kirwan JM, Tierney JF, et al. Survival and recurrence after concomitant chemotherapy and radiotherapy for cancer of the uterine cervix: a systematic review and meta-analysis. Lancet 2001; 358: 781-786.
[13] Mizoe J, Tsujii H, Kamada T, et al. Dose escalation study of CIRT for locally advanced head and neck cancer. Int J Radiat Oncol Biol Phys 2004; 60: 358-364.
[14] Miyamoto T, Yamamoto N, Nishimura H, et al. CIRT for stage I non-small cell lung cancer. Radiother Oncol 2003; 66: 127-140.
[15] Kato H, Tsujii H, Miyamoto T, et al. Results of the first prospective study of CIRT for hepatocellular carcinoma with liver cirrhosis. Int J Radiat Oncol Biol Phys 2004; 59: 1468-1476.
[16] Tsuji H, Yanagi T, Ishikawa H, et al. Hypofractionated radiotherapy with carbon ion beams for prostate cancer. Int J Radiat Oncol Biol Phys 2005; 63: 1153-1160.
[17] Kamada T, Tsujii H, Tsuji H, et al. Efficacy and safety of CIRT in bone and soft tissue sarcomas. J Clin Oncol 2002; 20: 4466-4471.
[18] Ascher SM, Imaoka I, Hricak H. Diagnostic imaging techniques in gynecologic oncology. In Hoskins WJ, Perez CA, Young RC ed: Principles and practice of gynecologic oncology, 3rd ed. P629-668, Lippincott Williams and Wilkins, Philadelphia, 2000.
[19] Cox JD, Stetz J, Pajak TF. Toxicity criteria of the Radiation Therapy Oncology Group (RTOG) and the European Organization for Research and Treatment of Cancer (EORTC). Int J Radiat Oncol Biol Phys 1995; 31: 1341-1346.
[20] Kato S, Ohno T, Tsujii H, et al. Dose escalation study of carbon ion radiotherapy for locally advanced carcinoma of the uterine cervix. Int J Radiat Oncol Biol Phys 2006; 31: 1341-1346.
[21] Ahmad A, D'Souza W, Salehpour M, et al. Intensity-modulated radiation therapy after hysterectomy: Comparison with conventional treatment and sensitivity of the normal-tissue-sparing effect to margin size. Int J Radiat Oncol Biol Phys 2005; 62: 1117-1124.
[22] Kavanagh BD, Schefter TE, Wu Q, et al. Clinical application of intensity-modulated radiotherapy for locally advanced cervical cancer. Semin Rad Oncol 2002; 12: 260

Carbon Ion Radiotherapy for Prostate Cancer

Hiroshi Tsuji, Tohru Okada, Shinji Sugahara, Hiroyuki Kato, Hitoshi Ishikawa,
Tadashi Kamada, Jun-etsu Mizoe, Tatsuaki Kanai, Hirohiko Tsujii,
and the Working Group for Genitourinary Tumors

Research Center Hospital of Charged Particle Therapy, National Institute of Radiological Sciences, Chiba, Japan
e-mail address:h_tsuji@nirs.go.jp

Abstract

Purpose: Analysis on the results of hypofractionated conformal carbon ion radiotherapy (C-ion RT) for localized prostate cancer was performed, with regard to normal tissue morbidity, biochemical relapse-free rate (bNED), and patient survival.Methods and Materials: Seven hundreds and forty prostate cancer patients who received C-ion RT established through two preceding dose-escalation studies were analyzed in regard to toxicity, survival, and bNED. Results: Concerning radiation morbidity, no grade 3 or higher toxicities were observed either in the rectum or genitourinary system (GU), and the incidences of grade 2 rectum and GU morbidity were only 1.9% and 4.8%, respectively. Incidence of late GU toxicity in the patients treated with C-ion RT of 16 fractions was lower than that of 20 fractions. Overall bNED at 5 years was 90.2%, with only four local recurrences. The bNED of the C-ion RT of 16 fractions was comparable to that of 20 fractions. Gleason's score, T-stage, and initial PSA were significant prognostic factors for bNED, and T-stage and initial PSA were also significant prognostic factors for overall survival rate. The duration of hormonal therapy also had an impact on biochemical control in high-risk patients, but it appeared possible to apply C-ion RT with short-course hormonal therapy to intermediate-risk patients.Conclusion: C-ion RT with the established dose fractionation regimen yielded satisfactory bNED with very few local recurrences, and with minimal morbidity. C-ion RT of 16 fractions could offer even lower incidence of GU toxicity than that of 20 fractions.

Introduction

Prostate cancer is a slow-growing tumor occurring in advanced-age male patients, but the incidence and mortality rate are both rapidly increasing in Asian as well as in Western countries. Radiotherapy is one of the treatments of choice for localized or locally advanced tumor of the prostate. In order to obtain satisfactory results, sufficient radiation effect with desirable dose concentration is required. This tumor is relatively radio-resistant, and severe damage to adjacent normal tissues will have deleterious effects on the quality of life after the treatment.

Carbon ion radiotherapy (C-ion RT) may be the ideal radiation treatment for prostate cancer because of the unique physical and biological advantages of carbon ion beams (1). The successful results obtained with novel conformal radiotherapy techniques, such as three-dimensional conformal radiotherapy (3DCRT) and intensity modulated radiotherapy (IMRT) (2-4), are evidence that dose conformity confers clear advantages to the radiotherapy of prostate cancer. Carbon ion beams offer superior dose conformity in the treatment of deep-seated tumors compared to the state-of the-art techniques of X-ray therapy, and therefore C-ion RT possesses a greater potential of further improving the treatment outcome of prostate cancer (1).

In this respect, high-linear energy transfer (LET) radiation therapy with fast neutrons was found to yield an excellent tumor control rate. Its unacceptably high toxicity (5,6), however, has stood in the way of this therapy coming into wider use. The high incidence of morbidity associated with fast neutron therapy was mainly due to an inferior dose concentration of neutron beams. This problem, however, can be solved by the use of heavy

charged particle beams, such as carbon ions, without foregoing the radiobiological advantages of high LET radiation.

To establish an appropriate dose fractionation regimen for C-ion RT, two phase I/II clinical studies have been performed (7-9) at the National Institute of Radiological Sciences, Chiba, Japan (NIRS) since 1994, using carbon ion beams generated by the Heavy Ion Medical Accelerator in Chiba (HIMAC). A phase II clinical study was then started in April 2000, using the established treatment method of hypofractionated C-ion RT with the recommended dose of 66.0GyE in 20 fractions over 5 weeks that had been proved effective in the phase I/II studies (10,11). The safety and efficacy of this treatment strategy of C-ion RT was further confirmed with this phase II study, and approval for its use as a highly advanced medical technology was obtained in November 2003 (9-11). This article presents the methods and updated outcomes of this established C-ion RT, and also describes its future prospects at NIRS.

Materials and Methods

1. Protocols

So far, a total of 919 patients have been enrolled, 97 patients in the first two phase I/II studies, 176 in the phase II study, and 646 after official approval for the application of the procedure as a highly advanced medical technology (Table 1). Of this total, 740 patients received the established treatment of C-ion RT, and were followed up for at least 6 months and analyzed.

Table1. Clinical studies of C-ion RT for prostate cancer at NIRS

Protocol	Study Design	T-stage	Period	Total Dose (GyE/f)	Hormone therapy	Number of patients
9402	Phase I / II Dose escalation	T2b~T3	95.6~97.12	54.0~72.0/20	(+)	35
9703	Phase I / II Dose escalation	T1~T2a	98.1~00.2	60.0~66.0/20	(-)	20
	Fixed dose	T2b~T3		66.0/20	(+)	42
9904	Phase II Fixed dose	T1~T3	00.4~03.11	66.0/20	High*(+) Low*(-)	176
		T1~T3	03.12~09.2	66.0, 63.0/20 57.6/16	High*>24m Interm*=6m Low*(-)	646
Total			95.6 ~ 09.2			919

*Stratified by risk factors; Clinical stage, initial PSA, and Gleason score

Patients were eligible if they had histologically proven prostatic adenocarcinoma, that is, stage T1, T2 or T3 primary tumors (12) without radiologically detectable distant metastasis (M0), involvement of regional lymph nodes (N0, pN0), or solitary, non-fixed involvement of regional lymph nodes diagnosed by staging pelvic lymphadenectomy (pN1). Eligible patients were required not to have undergone previous treatment for prostate cancer except for hormone therapy. All patients signed an informed consent form approved by the local institutional review board. Pathological specimens were reviewed centrally before registration, and those of the phase I/II studies were reviewed retrospectively.

Until September 2005, patients were stratified into two subgroups, high-risk and low-risk groups according to T-staging, Gleason's score (GS), and initial serum PSA. Thereafter, the high-risk group was further divided into two groups — an intermediate-risk group and a true high-risk group. For the true high-risk group patients, namely, patients with T3 primary tumor, GS $\geq$ 8 or a serum PSA value $\geq$ 20 ng/ml, long-term ($\geq$ 24 months) hormonal therapy was applied in combination with C-ion RT. Patients in the low-risk group, that is, T1/T2a patients with GS < 7 and serum PSA < 20 ng/ml, received only C-ion RT. For the intermediate-risk group

patients, consisting of those with a serum PSA value < 20 ng/ml and T2b primary tumor or GS of 7, combined treatment of C-ion RT and short-course (6 months) hormonal therapy was performed (Fig.1).

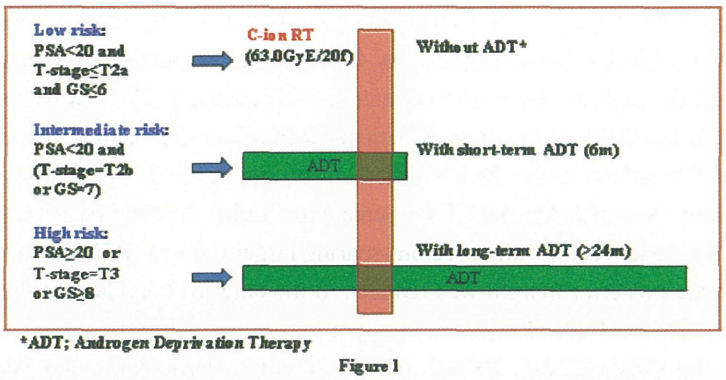

Fig. 1 Current treatment strategy for prostate cancer at NIRS

Patients were divided into three risk groups of high, intermediate, and low, according to their T-stage, initial PSA, and Gleason score.

2. Carbon Ion Radiotherapy

1) Treatment techniques

In order to make good use of excellent dose concentration of carbon ion beam, it is extremely important to keep high precision and sufficient reproducibility in the patient positioning and field. Techniques we applied were;

a) Rigid immobilization
b) Volume control of the rectum and the bladder
c) Precise field-localization with bony structure

a) Rigid immobilization

The feet and head of patients were positioned in the customized cradles (Moldcare; Alcare, Tokyo, Japan) and the pelvis was immobilized with a low-temperature thermoplastic of 3 mm thickness (Shellfitter; Keraray Co, Ltd, Osaka, Japan). A relatively thick body-shell can give mild pressure on the lower abdominal wall and reduce organ motion in the pelvis. With this method of immobilization, intra-fractional motion of the prostate was evaluated less than 2 mm and, therefore, respiratory gating was not used.

b) Volume control of the rectum and the bladder

Bladder was filled with 100ml of sterilized water both at the time of CT acquisition and at each treatment session in the case of beam irradiation in the vertical direction. The patient was instructed to empty the rectum as much as possible just before the treatment and a laxative or enema was used, if necessary. Amount of gas in the rectum was carefully observed by positioning images and the set-up was repeated unless the rectum was empty enough.

c) Precise field-localization with bony structure

At every treatment session, the patient's position was verified with a computer-aided, on-line positioning system. The patient was positioned on the treatment couch with the immobilization devices, and digital orthogonal x-ray television images were taken in that position and transferred to the positioning computer. The positioning images were compared with reference images, which were checked to confirm their match with the digitally reconstructed radiograph (DRR). Any differences, if found to exist, were measured. The treatment couch was then moved to the matching position until the largest deviation of all measured points was less than 2mm.

2) Treatment Planning

A set of 2.5-mm-thick CT images was taken for treatment planning, with the patient placed in immobilization devices. Three-dimensional treatment planning was performed using HIPLAN software (National Institute of Radiological Sciences, Chiba, Japan) (13). Clinical target volume (CTV) was defined as consisting of the prostate and the seminal vesicle (SV) demonstrated by CT images, irrespective of T-stage or other risk factors. MRI was also taken in all the patients and used as a reference for defining CTV. However, the whole SV should not always be included in the CTV, in the case of patients with a low risk. Thus, for example, the CTV of the patients staged as T1 or T2a did not cover the SV tips. Further, anterior and lateral safety margins of 10mm and a posterior margin of 5mm were added to the CTV to create the initial planning target volume (PTV-1). In order to reduce the dose to the anterior rectal wall, a rectum-sparing target volume (PTV-2) was used for the latter half of the C-ion RT, where the posterior margin was reduced to the anterior boundary of the rectum. Evaluation of the plan was routinely performed at the case conferences before the actual treatment, using the dose-volume histograms (DVH) for the CTV, PTV-1, PTV-2, and the rectum. Particularly, the DVH of the rectum was evaluated with comparing the reference DVH that was obtained from the analysis using actual DVH data of preceded dose-escalation studies. If the rectal DVH of the new patient was beyond the reference DVH at the high dose area, the treatment planning was revised.

C-ion RT was given once a day, 4 days a week (Tuesday to Friday). One port was used in each session. Patients were treated from 5 irregularly shaped ports, one anterior-posterior port and a pair of lateral ports for the PTV-1 and another pair of lateral ports for the PTV-2. A hundred % of the prescribed dose was given at the maximum dose point of each portal. The PTV-2 was covered by at least 90% of the prescribed dose and the minimum dose of the PTV-1 was more than 50% of the maximum dose and depended on the volume spared by PTV-2.

Dose was expressed in Gray-Equivalent (GyE = physical carbon ion dose (Gy) x Relative Biological Effectiveness {RBE}). Irrespective of the size of the Spread-Out Bragg Peak (SOBP), the RBE value for carbon ions was estimated to be =3.0 at the distal part of the SOBP. The compensation bolus was fabricated for each patient to make the distal configuration of the SOBP similar to the PTV. The multi-leaf collimator or the customized brass collimator defined the margins of the PTV. Fig. 2 shows the representative dose distribution.

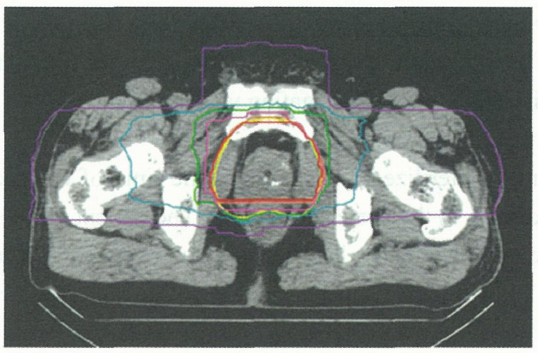

Figure 2

Fig. 2 Typical dose distribution of carbon ion radiotherapy

The irradiated dose was fixed at 63.0GyE or 66.0GyE/20fractions as the recommended dose fractionation schedule established in the two previous phase I/II studies involving dose escalation from the initial dose of 54.0GyE/20fractions to 72.0GyE/20f in 10% increments (11). In addition, more hypofractionated schedule of 57.6GyE/16fractionas was applied since September 2007. This newly applied fractionation had been tested in the other patients group who could not enrolled to the clinical studies because of the prolonged neoadjuvant hormonal therapy since April 2003.

3. Androgen Deprivation Therapy (ADT)

Before C-ion RT, neoadjuvant androgen deprivation therapy (ADT) such as medical or surgical castration with or without antiandrogen was applied for 2 to 6 months to the patients of the high-risk and intermediate-risk groups. Adjuvant ADT was continued for a duration of 6 months for the intermediate-risk patients and for more than 24 months for the high-risk patients. The median duration of ADT of 622 patients receiving combined treatment was 24.1 months. The remaining 118 patients received C-ion RT only.

Results

Of the 740 analyzed patients, 427 (57.7%) were categorized as high-risk, 179 (24.2%) as intermediate-risk, and 134 (18.1%) as low-risk according to our definition of risk grouping. The average pretreatment PSA value was 26.1 ng/ml, with a median of 13.5 ng/ml and a range of 3.4 - 810.0 ng/ml. Two hundreds and sixty eight (36.2%) patients had an initial PSA value of more than or equal to 20 ng/ml. Two hundreds and forty three (32.8%) patients had T3 primary tumors and the remaining 497 (67.2%) had T1 or T2 tumors. One hundred and eighty eight (25.6%) patients had GS of less than, or equal to 6, 335 (45.6%) had GS of 7, and 212 (28.8%) had GS of more than, or equal to 8. Median follow-up period was 33.8 months at the time of analysis.

1. Toxicity

The cumulative incidence of late rectum and genitourinary morbidities in the 664 patients treated with either of 20 fractions or 16 fractions and followed up more than 12 months are summarized in Table 2. None of the patients had developed grade 3 or higher morbidities up to the latest follow-up. Grade 2 morbidities of the genitourinary system and rectum were observed in 4.8% and 1.9% of the patients, respectively. Regarding the effect of alteration in dose fractionation, both the rectal and GU toxicity in 66.0GyE/20f were a little more frequent than those in 63.0GyE/20f or 57.6Gy/16f. Incidence of rectal toxicity in 63.0GyE/20f and 57.6GyE/16f are comparable, whereas incidence of GU toxicity in 57.6GyE/16f is even lower that that in 63.0GyE/20f.

Table 2. Late gastrointestinal and genitourinary morbidity after C-ion RT in patients followed up more than 12 months

Dose GyE/f.	No.pts.	Rectum				Bladder/urethra			
		Grade0	G1	G2	G3	Grade0	G1	G2	G3
66.0/20	250	199	43	8	0	93	136	21	0
	(%)	(79.6)	(17.2)	(3.2)	(0)	(37.2	(54.4)	(8.4)	(0)
63.0/20	216	191	21	4	0	122	86	8	0
	(%)	(88.4)	(9.7)	(1.9)	(0)	(56.5)	(39.8)	(3.7)	(0)
57.6/16	198	179	17	2	0	133	62	3	0
	(%)	(90.4)	(8.6)	(1.0)	(0)	(67.2)	(31.3)	(1.5)	(0)
Total	664	569	81	14	0	348	284	32	0
	(%)	(86.9)	(11.2)	(1.9)	(0)	(52.4)	(42.8)	(4.8)	(0)

2.Survival and Tumor Control

The Kaplan-Meier estimates of overall and biochemical relapse free (bNED) survivals for the 740 patients at five years were 95.4% and 90.2%, respectively (Fig.3). By the date of analysis, 22 patients had died, 5 of metastasis from the prostate, and 17 of other malignancies or intercurrent diseases. So far, no patient belonging to the low-risk and intermediate-risk groups has died of prostate cancer.

A total of four patients, three presenting with slowly elevated PSA and positive biopsies at 24 months, 38 months, and 48 months after C-ion RT, and one with apparent growth of tumor on the MRI images, were judged as having local recurrence. By the date of analysis, 43 patients met the Phoenix criteria of biochemical failure:

more than 2.0 ng/ml rise of PSA from the nadir. Of these 43 patients, 19 patients were diagnosed as having metastasis – 8 in bone and 11 in paraaortic or pelvic lymph nodes – 2 to 62 months after biochemical relapse, 4 were judged as having local recurrence, and the remaining 20 patients had no clinical evidence of recurrent lesions at the date of analysis.

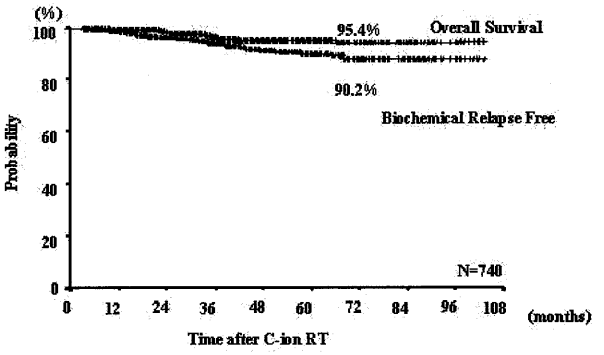

Fig. 3 Overall and biochemical relapse free survival curves of all analyzed patients Figure indicates 5-year rate of each curve.

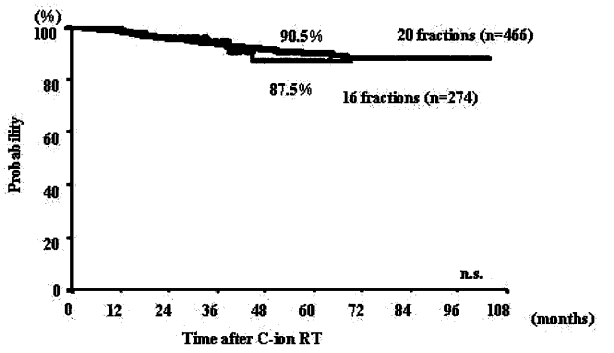

Fig. 4 bNED according to altered fractionation of carbon ion radiotherapy

3.Prognostic factors

Additional analysis was carried out to evaluate the influence of several prognostic factors on bNED and overall survival (OS), such as pretreatment serum PSA, GS, clinical stage, and dose fractionation. As a result, initial PSA of more than or equal to 20.0ng/ml was a significant factor for lower bNED and OS. Five-year bNED and OS in T1/2 patients were significantly better than those in T3 patients. However, the 5-year bNED of 89.6% was remarkably high compared to other radiotherapy series for T3 patients. The centrally reviewed GS also had significant influence on bNED, as 5-year bNED of the patient subgroup with GS ≥ 8 was significantly lower than those of the subgroups with GS ≤ 6 and GS = 7, though OS was not significantly different (Table 3). Regarding the effect of altered fractionation on bNED, there was no difference among the patients treated in 20f and those in 16f (Fig. 4). On the basis of these results on bNED and toxicity, that is relatively low toxicity with comparable bNED in 16 fractions, we started to treat all new patients with a dose fractionation of 57.6GyE/16f in September 2007.

Table 3. Biochemical relapse free rate (bNED) and overall survival rate (OS) according to risk factors

			5-year rates (%)			
		No.pts.	bNED	p-value	OS	p-value
All		590	90.4		94.7	
Stage	T1/2	407	94.1	0.0081	97.6	0.0129
	T3	183	83.2		89.6	
PSA	< 20	385	92.6	0.0531	95.5	0.0432
	20 ≤	205	87.8		91.5	
Gleason score	≤ 6	157	92.7	0.0189	96.1	
	7	260	94.7	0.0006	96.0	n.s.
	8 ≤	173	79.5		90.4	

Discussion

In this article, the patients treated with the carbon ion radiotherapy (C-ion RT) procedure established in our phase I/II clinical studies were analyzed. The results have demonstrated that C-ion RT achieves a very high biochemical control rate with a relatively low morbidity. A high rate of biochemical control was achieved as a result of the excellent dose concentration associated with C-ion RT and the efficient application of hormonal therapy. A number of studies using radiation therapy in combination with hormonal therapy have also indicated a high rate of biochemical control (13-14). Comparing the bNED and survival rates of our series with the studies in the literature, both were even better than those of the combinations of hormone therapy and conventional photon radiotherapy (Table 4). We presume this to be due to the positive impact of carbon ion beams on local control.

Table 4. Comparing bNED and survival rate of C-ion RT with other studies of combined treatment of hormone therapy and radiotherapy

Studies	No. pts.	Stage	Dose (Gy/fr.)	Hormone	bNED (%)	Survival (%)
EORTC* Phase III	208	T2-4	70/35	(-)	43	62
	207			(+)	81	79
RTOG** 8531Phase III	468	T1-3	65-70/35	(-)	20	71
	477			(+)	53	75
Carbon Phase I/II & II	339	High risk	66.63(GyE)/20 57.6(GyE)/16	(+)	88	93

EORTC: European Organization for Research and Treatment of Cancer; N Eng J Med 1997;337: 295-300, Bolla M. et al
RTOG: Radiation Therapy Oncology Group; IJROBP 2008; 47(3): 617-627, MackTeach III et al

In photon radiotherapy, the rate of local recurrence can be affected by the actual volume or pathological differentiation of tumor tissue. However, high LET radiation can be expected to be more effective for large-volume, poorly differentiated tumors compared to photon irradiation, and, in fact, very few local recurrences were actually observed in our series, even in the T3 tumor with a high GS. Although the evaluation of local control after radiotherapy of prostate cancer is a controversial issue, it is clear that high bNED cannot be achieved without sufficient local tumor control. The very high bNED attained in the patients of the intermediate-risk group indicated that biochemical failure occurred only in patients with high risk factors for metastasis, such as high PSA, T3, or poorly differentiated histology. This strongly suggests that eradication of cancer tissues in the prostate was achieved by C-ion RT in most patients.

A very low incidence of rectum morbidity was recorded, and this is ascribable to the physical properties of heavy charged particles in terms of dose conformity. This also substantiates the validity of our methods of patient positioning and target setting, and of our irradiation techniques. In addition, the acceptable incidence of genitourinary morbidity and the very high efficacy against local tumors confirm the accuracy of our dose calculation, the biological advantage of carbon ion beams, and the effect of a relatively high dose by a hypofractionated schedule.

A further move in the direction toward a more hypofractionated regimen of 16 fractions over 4 weeks has already been made. In 274 patients treated with a C-ion dose of 57.6 GyE in 16 fractions, bNED was comparable to that of 66.0GyE/20f or 63.0GyE/20f, and incidence of GU toxicity was even lower. Therefore, this new dose fractionation is applied to all new patients at the NIRS.

Conclusions

In conclusion, carbon ion radiotherapy administered by hypofractionated schedule is an effective and safe option in the treatment of locally confined prostate cancer. With an appropriate use of hormonal therapy, satisfactory biochemical control can be achieved even in high-risk patients. Trials with greater hypofractions have started at NIRS with the aim of establishing even more sophisticated methods of C-ion RT.

References

[1] Nikoghosyan A, Schulz-Ertner D, Didinger B, et al: Evaluation of therapeutic potential of heavy ion therapy for patients with locally advanced prostate cancer. Int J Radiat Oncol Biol Phys 58(1): 89-97, 2004

[2] Perez CA, Michalski J: Outcome of external-beam radiation therapy for localized carcinoma of the prostate (stages T1b, T2, and T3). In: Greco C, Zelefsky MJ, editors. Radiotherapy of prostate cancer. Amsterdam: Harwood Academic Publishers; p.155-184, 2000

[3] Hanks GE, Hanlon AL, Pinover WH, et al: Dose escalation for prostate cancer patients based on dose comparison and dose response studies. Int J Radiat Oncol Biol Phys 2000; 46: 823-832.

[4] Zelefsky MJ, Fuks Z, Hunt M, et al: High-dose intensity modulated radiation therapy for prostate cancer: Early toxicity and biochemical outcome in 772 patients. Int J Radiat Oncol Biol Phys 2002; 53: 1111-1116.

[5] Laramore GE, Krall JM, Thomas FJ, et al: Fast neutron radiotherapy for locally advanced prostate cancer: final report of a Radiation Therapy Oncology Group randomized clinical trial. Am J Clin Oncol 1993; 16: 164-167.

[6] Haraf DJ, Rubin SJ, Sweeney P, et al: Photon neutron mixed-beam radiotherapy of locally advanced prostate cancer. Int J Radiat Oncol Biol Phys 1995; 33: 3-14.

[7] Tsujii H, Morita S, Miyamoto T, et al: Preliminary results of phase I/II carbon-ion therapy at the National Institute of Radiological Sciences. J Brachytherapy Int 1997; 13: 1-8.

[8] Akakura K, Tsujii H, Morita S, et al: Phase I/II clinical trials of carbon ion therapy for prostate cancer. Prostate 2004; 58: 252-258.

[9] Tsuji H, Yanagi T, Ishikawa H, et al: Hypofractionated radiotherapy with carbon ion beams for prostate cancer. Int J Radiat Oncol Biol Phys 2005; 63(4): 1153-1160.

[10] Ishikawa H, Tsuji H, Kamada T, et al; A phase II trial using carbon ion radiotherapy (C-ion RT) for prostate cancer. JCO 23(16) part 1 Supple. 2005; 410S-410S.

[11] Ishikawa H, Tsuji H, Kamada T, et al: Carbon Ion Radiation Therapy for Prostate Cancer: Results of a Prospective Phase II Study. Radiother Oncol in press.

[12] International Union Against Cancer (UICC). TNM Classification of Malignant Tumours, 5th ed. New York: Wiley-Liss, Inc. 1997; p 170-173.

[13] Bolla M, Gonzalez D, Warde P, et al: Improved survival in patients with locally advanced prostate cancer treated with radiotherapy and goserelin. N Engl J Med 1997; 337: 295-300.

[14] Roach MIII, Lu J, Pilepich MV, et al: Predicting long-term survival, and the need for hormonal therapy: a meta-analysis of RTOG prostate cancer trials. Int J Radiat Oncol Biol Phys 2000; 47: 617-627.

Results of Carbon Ion Radiotherapy for Skin Carcinomas in 45 Patients

H. Zhang[1,2], S. Li[3], X.H. Wang [4], Q. Li1,[2], S.H. Wei[3], L.Y. Gao[4], W.P. Zhao[1,2], Z.G. Hu1, R.S. Mao[1], H.S. Xu[1], H.Y.Cai [4], Y.Y. Yue[3], G.Q. Xiao[1]

[1]*Institute of Modern Physics, CAS, Lanzhou 730000, China, zhangh@impcas.ac.cn*

[2] *Key Laboratory of Heavy Ion Radiation Medicine of Gansu Province, Lanzhou 730000, China*

[3] *The General Hospital of Lanzhou Command, Lanzhou 730050, China*

[4] *Tumor Hospital of Gansu Province, Lanzhou 730050, China*

Purpose:

To evaluate outcome and toxicity after carbon ion radiotherapy (RT) in skin carcinomas.

Patients and Methods:

Between November 2006 to March 2009, forty-five patients with squamous cell carcinoma of the skin (n=16), basal cell carcinoma of the skin (n=12), malignant skin melanoma (n=7), Bowen's disease (n=8) and Paget's disease (n=2) were treated with carbon ion RT at Heavy Ion Research Facility in Lanzhou (HIRFL) within a Phase I trial. Two and three-dimensional conformal irradiation methods realized by the passive beam delivery system and the average RBE of 2.5-3 within the target volume were used in the trial. In 45 patients, there were 12 with failures or recurrences of conventional RT and 17 with recurrences of surgeries. They received total doses and fractionations (fr) of 42-70.4GyE/4-10fr for squamous cell carcinomas, 54.8-70GyE/6-11fr for basal cell carcinomas, 61-75GyE/6-7fr for malignant skin melanomas, 40-60GyE/6-7fr for Bowen's diseases and 36-42.5/6-8fr for Paget's diseases, with a weekly fractionation of 7×3-15 GyE/fraction. Local control rates were estimated according to WHO criteria and acute and late side effects were scored according to the Common Toxicity Criteria (CTC). Results: Forty-four patients were followed-up and one was lost to follow-up. The mean follow-up was 15 months with ranging from 3-24 months. All of the tumors responded well to the treatment. Two-year local control rates were 90%, 96.7%, 100%, 94% and 100% for squamous cell carcinomas, basal cell carcinomas, malignant skin melanomas, Bowen's diseases and Paget's diseases, respectively. Progression-free survival was 100% at one year and 92.3% at two year for 26 patients (who were followed-up longer than two year). No severe side-effects > CTC grade III have been observed.

Conclusions:

The preliminary results demonstrated that heavy ion radiotherapy offers high local tumor control rates without significant toxicity to the surrounding normal tissues for patients with skin carcinomas, although the follow-up was short.

Carbon Ion Radiotherapy: Clinical Study

Tadashi Kamada, Hirohiko Tsujii

Research Center for Charged Particle Therapy, National Institute of Radiological Sciences, Chiba, Japan
e-mail address: t_kamada@nirs.go.jp

1. Introduction

The pioneering work in carbon ion radiotherapy by Japanese and European investigators has generated great enthusiasm. However, as a particle therapy center is certain to be an extremely complex and expensive medical facility, it may become a source of disagreement in the radiation oncology community.
The paradigm of drug development in medical oncology from phase I to phase II to phase III trials remains unaltered, but this is not the case in radiation oncology.
According to the presentations at the NCI "Workshop on Advanced Technologies in Radiation Oncology" in December 2006, there were only a few level-I trials of implemented new technologies in radiation oncology. [1]
For protons, the physical proof of better depth dose characteristics, virtually identical biological effects compared with X-rays, and the fact that decreased doses to normal tissues always result in decreased toxicity, argue against conducting phase III trials comparing protons with X-rays. [2]
Radiation oncology has not, until this decade, seen such dramatic changes in technological innovations, and they give rise to new and complicated issues. What kind of studies should be carried out to sort out the indications, advantages, and disadvantages? In this presentation, the issue of the evaluation of the clinical results of carbon ion radiotherapy and their comparison with other modalities will be discussed.

2. Carbon Ion Radiotherapy Clinical Trial at HIMAC

The carbon ion radiotherapy program was initiated based on the rationale of exploiting the high physical selectivity of carbon ions, as well as their high LET, with the attendant potential radiobiological advantage for selected tumor types. From the beginning all carbon ion radiotherapies were carried out as prospective phase I/II and II clinical trials in an attempt to identify tumor sites suitable for this treatment, including radio-resistant tumors, and to determine optimal dose-fractionation, and especially for hypo-fractionation, in common cancers. Our ultimate goal is to prove the efficacy and safety of carbon ion radiotherapy in cancer treatment.
Conducted carbon ion radiotherapy protocols and their time lines are summarized in Table 1. A total of 46 protocols have been conducted. The number of patients receiving carbon ion radiotherapy has already reached more than 4,000, and in the year 2008 more than 700 patients were treated in such protocols at NIRS.

Clinical studies revealed that intractable cancers such as advanced head and neck cancer, large skull base tumors, pelvic recurrence of operated rectal cancer, and inoperable sarcomas can be cured, and cancers in the lung, liver, and prostate can be cured safely with a shorter treatment period. [3]

3. Should Carbon Ion Radiotherapy be Subjected to Randomized Clinical Trials?

When comparing various therapies, the results of randomized controlled studies provide the strongest evidence. Dr. Lawrence, the chief editor of the Journal of Clinical Oncology, has made the following statement about the need for phase III (randomized controlled studies) when comparing different therapies, or different types of therapeutic equipment, in the field of radiation oncology: "*In medical oncology, there is a need to compare drug treatment A to drug treatment B. It is not possible to determine which is better without carrying out a randomized trial. In radiation oncology, one can know, based on physics, that protons deliver a better dose distribution than photons or that IMRT is superior to three-dimensional conformal therapy. If treatment planning and delivery are carried out using consistent methodology, there is no debate; this is a matter of physics. The big question is: is any observed difference clinically meaningful enough to justify the added expense? What kind of trial needs to be designed to answer this question? Would it be difficult to run a randomized trial in the United States asking whether a treatment that is superior based on physics translates into superior patient survival and/or quality of life? Would patients permit themselves to be randomly assigned to the standard but less expensive therapy?*" [4]

Progress in radiation oncology is inextricably linked to the development of treatment facilities, however almost no randomized controlled study has been conducted for the purpose of the introduction of any new modality. In fact, no randomized controlled study was conducted in the shift from cobalt to LINAC, but if there had been there would have been little difference between cobalt and LINAC in the treatment results in patients with early glottic cancer. Cobalt irradiation has advantages in terms of both cost and equipment maintenance, and the results of LINAC may be poor unless a suitable energy is selected. Cobalt is sufficient to treat laryngeal cancer, and it may be unnecessary to introduce LINAC to achieve successful treatment for this cancer. In recent years, however, treatments with cobalt have been significantly reduced in developed countries. The distribution

of the very-high-energy x-rays of LINAC allows safer treatment of deeply situated targets, and the design of a study to determine the difference between cobalt and LINAC in patients with glottic cancer is itself a problem.

In any case, the question remains "Should Carbon Ion Therapy be Subjected to Randomized Clinical Trials?" What must be seen in a phase II study to justify moving to phase III? No matter how exciting the laboratory technique and how great the improvement in animal models, there must be evidence that the method is transferable to humans and that successes in the laboratory can be reproduced in humans. Further, there must be real promise of improvement in phase II studies in human tumors. There is real promise of improvement in our carbon ion radiotherapy results presented at this meeting, and it justifies the move to phase III.

4. From Phase II Clinical Trials to Randomized Clinical Trials (RCT)

However, before moving to a phase III study, several questions are raised. First, are there comparable phase II results in other modalities? If the answer to the first question is yes, do those modalities use the same eligibility criteria? And third, how do we recruit the patients for the phase III trial? Our patients often travel long distances to Chiba seeking carbon therapy. Finally, we charge patients more than $30,000 USD for carbon ion therapy; how do we fund such a trial? Carbon ion radiotherapy is successful in advanced head and neck cancer, large skull base tumors, recurrent rectal cancer and inoperable sarcomas that are not treatable by other means. For these intractable diseases, it is clear that there are no ample data with other modalities. For these diseases, there is no idea how to conduct a phase III study and to obtain consent from patients. Hence, the answer to the question, should carbon ion therapy be subjected to randomized trials, is "No" in these intractable diseases. In lung, liver, and prostate cancer, promising results have been obtained with carbon ion radiotherapy. A randomized controlled study might be possible in these rather common cancers. However, as described above, patients are traveling long distances to Chiba to obtain carbon ion therapy. It will be very hard to obtain consent from these patients for a randomized trial. Thus, our answer to the question is that it is untenable. RCT provides the firmest evidence in various clinical settings, but it is too difficult to conduct RCT for assessment of new radiation therapy technologies.

5. Methodologies for Critical Assessment of New Health Technologies

We radiation oncology researchers need to develop new methodologies for critical assessment of new health technologies as a complement to RCT. Possible future comparative studies of carbon ion radiotherapy may include the following: 1) multi-institutional prospective clinical studies using the same protocols that can be applied to other therapies (non-randomized concurrent clinical trial), 2) matched-pair controlled studies in subjects matched to those receiving other therapies, and 3) RCT between carbon ion and proton or other high-tech radiotherapies.

Comparative studies, feasible at present, to further clarify the usefulness of carbon ion radiotherapy at various indications, include those in which the same protocol applied to other therapies is followed, the backgrounds of the subjects are matched, and the treatment desired by the study participants is performed. In this case, consent from study participants can be easily obtained, the study cost is low, and an agreement among the participating facilities is relatively easily obtained, as the treatment desired by the patients is provided by the co-operating institutions. For realizing this type of comparative study, a project team has been organized to conduct a multi-institutional prospective prostate cancer study in all particle therapy facilities in operation in Japan. This study is expected to start within 1 or 2 years. This could represent a new methodology for the assessment of new radiotherapy technologies. Another method would be to determine the inclusion criteria for patients already treated and then to comparatively analyze the therapeutic results in a matched-pair study. This is feasible if consent is obtained from the institutions that performed the treatments being compared. We conducted a matched-pair study of sacral chordoma with patients treated at the Massachusetts General Hospital in Boston with proton therapy.[5] However, there were only a few matched cases in both institutions and were not able to carry out the comparison. Nonetheless, this can be retried with other institutions or performed with more common cancers.

6. Summary

At present, most of the patients receiving carbon ion radiotherapy at NIRS visit the clinic seeking this specific modality, and it is difficult to obtain consent for a randomized controlled study from these patients and it may be unnecessary to conduct a phase III trial. However, in selected tumors where the high-LET benefit could be appreciated, we can participate in randomized studies. Finally, studies aimed at clarifying the usefulness of carbon ion radiotherapy and elucidating any advantages from hypo-fractionation should be considered. A multi-institutional prospective non-randomized concurrent phase II clinical trial is one such new approach, and it will be proposed not only to the Japanese, but also to the international community of particle therapy and radiation oncology.

References

[1] http://www3.cancer.gov/rrp/workshop/2006AdvancedRadiationTech/presentations.html

[2] Goitein M, Cox JD: Should randomized clinical trial be required for proton radiotherapy? J Clin Oncol 26:175-176(2008)

[3] Tsujii H, Mizoe J, Kamada T et al: Clinical results of carbon ion radiotherapy at NIRS. J Radiat Res 48: Suppl., A1-A13 (2007)

[4] Lawrence TS, Petrelli NJ, Li BD, Galvin JM: Think globally, act locally. J Clin Oncol 25:924-930(2007)

[5] Park L, Delaney TF, Liebsch NJ et al: Sacral chordomas: Impact of high-dose proton/photon-beam radiation therapy combined with or without surgery for primary versus recurrent tumor. Int J Radiat Oncol Biol Phys 65: 1514-1521(2006)

Repair of DNA Double Strand Breaks Induced by Heavy Ion Irradiation

Ryuichi Okayasu, Takamitsu Kato, Akira Fujimori, Miho Noguchi, and Yoshihiro Fujii

Heavy-Ion Radiobiology Research Group, Research Center for Charged Particle Therapy, National Institute of Radiological Sciences, Chiba, Japan

Corresponding Author: Ryuichi Okayasu, e-mail address: rokaysu@nirs.go.jp

Abstract

At the National Institute of Radiological Sciences (NIRS), over 4000 cancer patients have been treated by heavy ions with an impressive success rate. There are clinical, physical and biological factors behind this achievement, and in this presentation a few critical biological issues are discussed. Besides the physical advantage of the dose distribution of heavy ions, two important biological factors exist; one of them the inhibition of DNA double-strand break (DSB) repair by heavy ions and the other the reduced variation of cell survival levels throughout the cell cycle. The repair of DNA DSB was examined using constant field gel electrophoresis as well as gamma-H2AX assay, and both techniques clearly showed a significant inhibition of initial rejoining of DSBs induced by 70 keV/μm carbon ions. The degree of repair inhibition seems to be reflected in the radiation cell survival level. Using synchronized CHO cells, we investigated cell survival levels throughout the cell cycle with carbon ions, and the result was compared with that with X-rays. Our data indicated that much less variation in the cell survival level was observed when carbon ions were used to irradiate cells. Moreover, gene expression studies using a unique method developed at NIRS provided new insight into biological damage induced by heavy ions. These data together provide biological reasons for the successful outcome reported at the heavy ion facility at NIRS.

Introduction

It is generally believed that high linear energy transfer (LET) heavy ion radiation can induce a more complex type of DNA damage to cells, specifically DNA double-strand breaks (DSBs), than traditional X-rays or gamma-rays, and this, in turn, leads to a higher rate of killing of tumor cells when these lesions are not repaired [1-12]. As mentioned elsewhere, the physical dose distribution of heavy charged particles with the Bragg peak gives further advantage to treating tumor tissues more selectively and evade surrounding normal tissues.

Another important biological aspect of high LET heavy ion radiation is its reduced cell cycle dependency of cell survival rate. For mammalian cells in general, late S-phase cells are the most resistant, and cells in the mitotic phase are the most sensitive to low LET radiation sources [13]. In contrast, with high LET heavy ion radiation, the cell cycle responses seem much more modest. In 1975, using an accelerator available in Berkeley, Bird and Burkib [14] showed that the cell survival levels throughout the cell cycle phases are fairly similar, with no distinct dependency on the location of cells in the cell cycle. Although these data are very important and useful for heavy ion radiobiology, there have been almost no similarly repeated experiments using other heavy ion facilities. Recently, we have repeated the experiment with synchronized mammalian cells at the heavy ion medical accelerator (HIMAC) in Chiba, and some of the significant results are presented.

In this manuscript, data on DNA DSBs and their repair are presented first. Then some recent gene expression studies are described, followed by data on radio-sensitivity throughout the cell cycle with high LET irradiation.

Material and Methods

Cell survival and irradiation

Cells were irradiated with a Shimadzu Pantak HF-320 X-ray machine at a dose rate of 0.93 Gy/min. All heavy ion irradiations were performed at the heavy ion medical accelerator in Chiba (HIMAC) at the National Institute of Radiological Sciences (NIRS). We chose the LET value for carbon ions (290MeV/n, original energy) to be 70 keV/μm. Lucite absorbers (146 mm H_2O equivalent thickness) were used to obtain the desired LET value. Under this condition, about 50% of the original carbon beams remained (corresponding beam energy = ~ 40MeV/n). All cell survival experiments were performed using the conventional colony formation assay [15].

Cell synchronization

Synchronized cultures were obtained from exponentially growing cells by the technique of mitotic selection, using mechanical shake-off [14]. Throughout the shake-off procedure, pre-warmed medium was used to maintain the physiological temperature. The decanted suspension of selected cells was counted, and appropriate dilutions were made for plating cells for colony formation.

DNA DSB repair (constant field gel electrophoresis)

The method has been reported previously [16]. Immediately after irradiation (20 Gy) on ice, the medium was replaced with warm medium and cells were incubated in an incubator (37°C) for repair. At each repair point, cells were washed, trypsinized on ice for 20 min, and washed again in cold medium. The resulting cell pellets were embedded in 1% agarose (InCert agarose, FMC) at a density of 1.5 X 10^6 cells/ml, and placed on ice. These agarose samples were cut into plugs, and placed in lysis solution (TREVIGEN) containing proteinase K for 1 h on ice, and incubated for 24 h at 50°C. The plugs were equilibrated in TE buffer (SIGMA, pH 8.0), loaded on 0.6% SeaKem Gold agarose gels (Cambrex), and subjected to electrophoresis at 0.6 V/cm in 0.5 X TBE buffer for 36 h. The gel was stained with ethidium bromide and de-stained. The fluorescence intensities were measured with a UV transilluminator and a digital camera with an orange filter. NIH Image software was used for the analysis of DSB damage, and the fraction of released DSBs was calculated.

DNA DSB repair (H2AX)

The fixation and staining method for immunocytochemistry closely followed that previously described by K.Rothkamm and M.Löbrich [17]. For immunostaining, cells were cultured on flaskettes and synchronized into G1 phase by isoleucine deprivation as described above. After irradiation, cells were fixed in 4% paraformaldehyde for 15 min, washed 3 times in PBS for each 10 min, permeabilized for 5 min on ice in 0.2% Triton X-100, and sites that may have nonspecifically bounded the detecting antibody probe were blocked in PBS with 10% goat serum for 3 washes of 10 min each at room temperature. The flaskettes were then incubated with anti-γ-H2AX antibody (Trevigen) for 1 h, washed 3 times in PBS for 10 min each, and incubated with FITC-conjugated goat anti-rabbit secondary antibody (Sigma) for 1 h at 37°C. Cells were washed 4 times in PBS for 10 min each, and mounted by using Slow Fade (Molecular Probes) to reduce photobleaching during observation. Images of cells were obtained using an Olympus A70 fluorescence microscope equipped with an image analysis system. The processed images were stored and cells from these were later scored.

Gene Expression

Gene expressions were studied with the HiCEP method developed at NIRS, and the details are available from previous publications [18,19].

Results

Repair of DNA DSB is inhibited by 70 keV/μm carbon ion irradiation

We analyzed repair of DNA DSB using a gel-based assay. Fig.1 shows the results of DNA DSB rejoining kinetics in prostate cancer cells (DU145) irradiated with X-rays and 70 keV/μm carbon ions using constant field gel electrophoresis (CFGE) technique. The corresponding radiation cell survival levels are also shown in the figure.

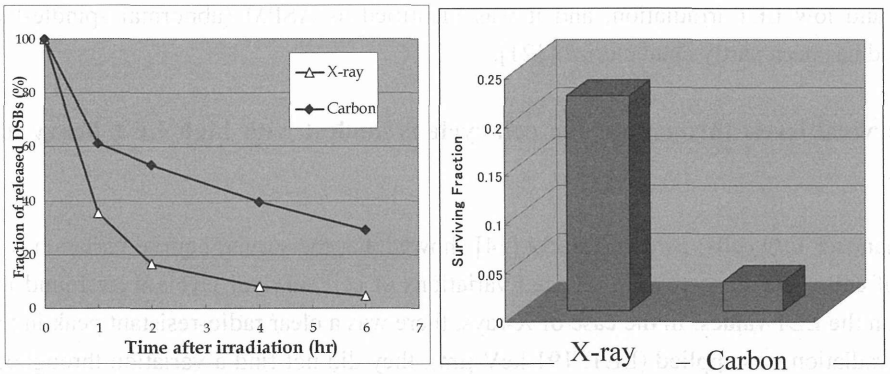

Fig.1. (Left) Comparison of DNA DSB repair kinetics in DU-145 tumor cells irradiated with X-rays and 70 KeV/μm carbon ions. (Right) Cell survival levels (4 Gy) with corresponding irradiation sources are also provided.

The rejoining kinetics of DNA DSB with carbon ions was clearly impaired when compared to X-irradiation. The cell survival data with these two radiation sources seem to reflect the rejoining ability shown in this figure.
The gel assay we used above is useful; however, the radiation dose (e.g., 20 Gy) necessary for this assay is comparatively high and the data from the gel-assay cannot be compared with the cell survival data. Thus, we employed an immuno-staining focus assay to detect DSB repair. Fig. 2 shows the DSB appearance/disappearance kinetics using sensitive gamma-H2AX assay; the dose used here was 1 Gy for all radiation sources. As expected, the foci with X-irradiation disappeared quickly, while the foci with 70 keV/μm carbon ions disappeared much less efficiently. Moreover, the kinetics of foci appearance induced by 13 keV/μm carbon ions (the flat dose distribution part before the Bragg peak) behaved similarly to the kinetics obtained with X-rays.

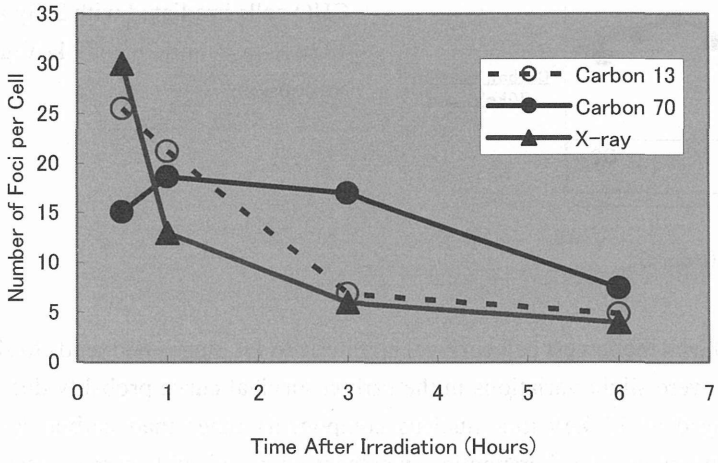

Fig. 2 Kinetics of gamma-H2AX foci appearance/disappearance in human cells irradiated with 1 Gy X-rays, 13 keV/μm and 70keV/μm carbon ions.

These useful data obtained at low doses reaffirmed the more severe biological outcome with high LET heavy ions. The DSB repair data were also shown to reflect the data at the chromosome level [e.g., 20].

Gene expression studies provide different patterns for high LET radiation

At NIRS, we have a unique system to detect gene expressions [18,19]. This sensitive method is called HiCEP (high coverage expression profiling) and was able to give us some new insights with high LET irradiation. Although variations in well-known genes for DNA damage responses were detected with high LET irradiation, we found some genes that are continually over-expressed only with high LET heavy ions, but not with low LET irradiation. ATF3 is

one of these genes, and its significance is under investigation. In addition, we found a gene that was significantly down-regulated with both high and low LET irradiation, and it was identified as ASPM (abnormal spindle-like microcephaly associated gene) and has been partly characterized [21].

Variation in radiation cell survival levels throughout the cell cycle is modest with high LET heavy ion irradiation

Using synchronized Chinese hamster V79 cells, Bird and Burki [14] showed that the survival curve variation was found for X-rays as a function of cell cycle stages, while reduced variations of cell survival levels were found for heavy ion irradiation depending on the LET values. In the case of X-rays, there was a clear radio-resistant peak in the late S-phase. When carbon ion irradiation was applied (LET: 191 keV/μm), they did not find a variation throughout the cell cycle stages. The variation in cell survival seemed to disappear for high LET irradiation after LET reached about 200 keV/μm in their experiment.

We have performed a similar experiment with synchronized CHO cells using the HIMAC accelerator, and the cell survival data as a function of the cell cycle phases are shown in Fig.3. In order to better understand the tendency of the cell cycle effect, it is best to compare the data with 4 Gy X-rays and those with 2 Gy carbon ions due to a similar biological effectiveness. The variation for the carbon ions data appears less distinct throughout the cell

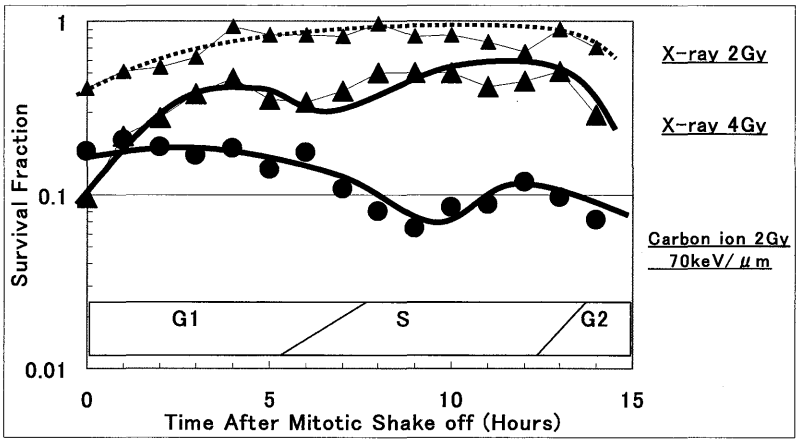

Fig. 3 Comparison of radiation cell survival levels in synchronized CHO cells irradiated with 2 Gy and 4 Gy X-rays, and 2 Gy 70 keV/μm carbon ions.

cycle than that for X-rays. The X-ray curve shows the lowest cell survival at mitotic to G1 stages and tends to show a higher level toward the S-phase stage. There were slight variations in the carbon survival curve probably due to the mixed populations of carbon beams employed at 70 keV/μm; nucleus components other than carbon ions are included in the beam [22]. Despite these situations, the therapeutic advantages obtained with carbon beams are obvious when compared to X-rays.

Discussion

In this report, we have shown some of the critical biological characteristics associated with high LET heavy ion irradiation as compared with low LET irradiation. The repair of DNA DSB indicated clear evidence of inhibition of DSB rejoining in cells irradiated with high LET carbon ions, even at low radiation doses. It is significant that the cells irradiated with lower LET (13 keV/μm) carbon ions showed a tendency similar to X-irradiated cells. This indicates that much less radiation damage can be expected with the flat part of dose distribution curve of carbon ion beams. This seems to give an advantage to carbon ion treatment, as tumor cells are targeted with the Bragg peak part

of the beam.

Our recent data on the variation of cell survival levels throughout the cell cycle can give us further insight into high LET radiobiology. High LET radiation significantly reduces the variation in cell survival levels observed with low LET radiation. This gives another advantage to heavy ion therapy, as the radio-resistant peak at S-phase may not be a significant problem with high LET irradiation treatment. We have also extended our cell cycle related studies with DSB repair-defective mutants, and new understanding has been obtained with these studies (data not shown).

References

[1] Barendsen GW. Impairment of the proliferative capacity of human cells in culture by alpha-particles with differing linear-energy transfer. Int J Radiat Biol Relat Stud. Phys Chem Med 1964;15:453-466.

[2] Cox R, Thacker J, Goodhead DT, Munson RJ. Mutation and inactivation of mammalian cells by various ionizing radiations. Nature 1977; 267:425-427.

[3] Tobias CA, Blakely EA, Alpen EL, et al. Molecular and cellular radiobiology of heavy ions. Int J Radiat. Oncol Biol Phys. 1982; 8:2109-2120.

[4] Goodwin E, Blakely E, Ivery G, Tobias C. Repair and misrepair of heavy-ion-induced chromosomal damage. Adv. Space. Res. 1989; 9:83-89.

[5] Hendry JH. The slower cellular recovery after higher-LET irradiations, including neutrons, focuses on the quality of DNA breaks. Radiat. Res. 1991;128:111-113.

[6] Rydberg B, Lobrich M, Cooper PK. DNA double-strand breaks induced by high-energy neon and iron ions in human fibroblasts. I. Pulsed-field gel electrophoresis method. Radiat. Res. 1994;139:133-141.

[7] Frankenburg-Schwager M, Harbich R, Beckonert S, Frankenburg D. Half-life values for DNA double-strand break rejoining in yeast can vary by more than an order of magnitude depending on the irradiation conditions. Int. J. Radiat. Biol. 1994;66:543-547.

[8] Loucas BD, Geard CR. Kinetics of chromosome rejoining in normal human fibroblasts after exposure to low- and high-LET radiations. Radiat. Res. 1994;138, 352-360.

[9] Taucher-Scholz G, Heilmann J, Kraft G. Induction and rejoining of DNA double-strand breaks in CHO cells after heavy ion irradiation. Adv. Space. Res. 1996;18:83-92.

[10] Suzuki M, Kase Y, Kanai T, Ando K. Correlation between cell killing and residual chromatin breaks measured by PCC in six human cell lines irradiated with different radiation types. Int. J. Radiat. Biol. 2000; 76:1189-1196.

[11] Suzuki M, Piao C, Hall EJ, Hei TK. Cell killing and chromatid damage in primary human bronchial epithelial cells irradiated with accelerated 56Fe ions. Radiat. Res. 2001;155:432-439.

[12] George K, Wu H, Willingham V, Furusawa Y, Kawata T, Cucinotta FA. High- and low-LET induced chromosome damage in human lymphocytes: a time-course of aberrations in metaphase and interphase. Int. J. Radiat. Biol. 2001; 77:175-183.

[13] Hall EJ, Giaccia AJ. Radiobiology for the Radiologist. Lippincott Williams & Wilkins; 2005;6th edition.

[14] Bird RP, Burki HJ. Survival of synchronized Chinese hamster cells exposed to radiation of different linear-energy transfer. Int. J. Radiat. Biol. 1975;27:105-120.

[15] Okayasu R, Okada M, Okabe A, Noguchi M, Takakura K, Takahashi S. Repair of DNA damage induced by accelerated heavy ions in mammalian cells proficient and deficient in the non-homologous end-joining pathway. Radiat. Res. 2006;165:59-67.

[16] Hirayama R, Furusawa Y, Fukawa T, Ando K. Repair kinetics of DNA-DSB induced by X-rays or carbon ions under oxic and hypoxic conditions. J. Radiat. Res. 2005;46:325-332.

[17] Rothkamm K, Löbrich M. Evidence for a lack of DNA double-strand break repair in human cells exposed to

very low x-ray doses. Proc. Natl. Acad. Sci. U S A. 2003;100:5057-5062.
[18] Fukumura R, Takahashi H, Saito T, et al. A sensitive transcriptome analysis method that can detect unknown transcripts. Nucleic Acids Res. 2003; 31, e94.
[19] Fujimori A, Okayasu R, Ishihara H, et al. Extremely low-dose ionizing radiation upregulates CXC chemokines in normal human fibroblasts. Cancer Res. 2005;65: 10159-10163.
[20] Sekine E, Okada M, Matsufuji N, Yu D, Furusawa Y, Okayasu R. High LET heavy ion induces lower numbers of initial chromosome breaks with minimal repair than low LET radiation in normal human cells. Mutat. Res. 2008;652:95-101.
[21] Fujimori A, Bing W, Suetomi K, et al. Ionizing radiation downregulates ASPM, a gene responsible for microcephaly in humans. Biochem. Biophy. Res. Commun. 2008;369:953-957.
[22] Matsufuji N, Fukumura A, Komori M, Kanai T, Kohno T. Influence of fragment reaction of relativistic heavy charged particles on heavy-ion radiotherapy. Phys. Med. Biol. 2003;48:1605-1623.

Biological Effectiveness of Mammalian Cells Exposed to Heavy Ion Beams

Yoshiya Furusawa

Research Center for Charged Particle Therapy, National Institute of Radiological Sciences, Chiba, Japan
e-mail address: furusawa@nirs.go.jp

Abstract

The LET-RBE spectra were investigated using cultured V79 cells by accelerated heavy ions. Cells were exposed to ^{3}He-, ^{12}C-, and ^{20}Ne-ion beams at HIMAC, the Medical Cyclotron at NIRS, and RRC at RIKEN with an LET ranging over approximately 10-500 keV/μm under aerobic conditions. Cell-survival curves were fitted by equations from the linear-quadratic model to obtain survival parameters, and the RBE values were analyzed as a function of LET. The RBE increased with LET, reaching a maximum at around 200 keV/μm, then decreased with a further increase in LET. Clear splits of the LET-RBE spectrum were found among ion-spices. The LET-RBE spectra were fitted by a newly contrived equation that including three parameters: L_p, A, and W. The parameters will indicate a LET that gives a maximum RBE, a related value to maximum RBE, and indicates the width of the peak of RBE, respectively. It is also found that the parameters can be defined as functions of atomic numbers of the accelerated ions. At a given LET, the RBE-value for lighter ions was higher than that for heavier ions at lower-LET region. The LET that gives maximum RBE shifts to higher LET for heavier-ions, and the maximum values of the peak of RBE decreased with the atomic number of the irradiated ions.

Introduction

The Heavy Ion Medical Accelerator in Chiba (HIMAC) was constructed at the National Institute of Radiological Sciences (NIRS), Chiba, Japan, in 1993 to perform advanced radiotherapy treatment of cancer[1], [2]. Clinical trials were also started using carbon-ion beams in June 1994, and over 3100 patients had been treated with HIMAC carbon-ion beams by 2007. For a requirement of pre-clinical radiobiological studies and the cooperative research projects in radiobiological field, a great numbers researchers visit HIMAC and huge number of data were obtained by researchers inside and outside NIRS including overseas. HIMAC is also available for scientific experiments, such as medical sciences, physics, radiation biology, and so on. The main subjects for radiobiological studies at HIMAC are studies concerning radiation therapy using heavy-ion beams. However results from the radiobiological studies are applicable for estimating radiobiological effects in a field of radiation protection study for the space, where the most biologically effective radiation is HZE beams.

The relative biological effectiveness (RBE) is one of the most important parameters in determining the biological effectiveness of heavy-ion beams. An accurate knowledge of the RBE was required at HIMAC when heavy-ion beam for cancer therapy will be started. RBE is roughly a simple function of LET, which is the rate of energy deposition in the linear dimension. However the detail and the suitable RBE for cancer therapy is not known, because there are big differences between low- and high-dose region, alternated by hypoxia, discrepancies among particles and by biological end-points. LET indicates the rate of energy deposition in the linear dimension of the absorbing material. There are differences in the radial energy deposition densities for beams of the same LET among accelerated ion species because of a difference in their electric charge and

velocity. This distribution of different track structures of the ionization density may produce different radiobiological effects on cells. However, there are few systematic biological data on the RBE and the LET of heavy ions, because it is usually difficult to expose many biological materials with the same exposure system under the same biological condition.

When we design a therapeutic ion beam, we must know biological effectiveness of the beam. However the LET and ion spices of the beam at defined depth in the body, the physical characteristics of the beam are very complex, because of the nuclear fragmentation of projectile ion and mixture of beams having different LETs to produce a spread-out Bragg peak. To know the RBE for those all ion spices at all radiation doses (or cell survival levels) and all LETs in the beam through biological experiments.

Only a data show here is cell killing on V79 cells as determined by a loss of colony-forming ability, and please see previous publication [5] for HSG cells that has used at HIMAC beam design. The data covers several ion-species, lighter-ions and heavier-ions than therapeutic carbon-ions. We will discuss the LET dependency of cell killing in an intermediate LET region (approximately 10-500 keV/μm) as well as the difference in the RBE spectra among the accelerated ion species. Also we will introduce a method to estimate biological effectiveness of heavy ions as a function of ion species and LETs. In addition, we will discuss possible method to estimate the biological effectiveness to all fragmented beams that have not measured biological experiments.

Experiments

1. Facility and Ion Beams

We exposed cells to ^{3}He-, ^{12}C-, and ^{20}Ne-ion beams. The exposures were carried out at the HIMAC, the medical cyclotron (NIRS-MC) at NIRS, and the ring cyclotron (RRC) facility at the Institute of Chemical and Physical Research (RIKN). The exposure systems at HIMAC, NIRS-MC and RRC were basically the same, and all the beam performance has confirmed by physics group of NIRS. An X-ray machine (Model Shinai-7, Shimadzu Co., Tokyo; 200 kVp, 20 mA, W-target, 0.5-mm aluminum + 0.5-mm copper filter) was used for obtaining the reference survival curves for RBE.

Dosimetry and LET determination at those facilities has previously reported[3][4][5]. Briefly, the dose rates of the beam were measured with a calibrated parallel-plate ionization chamber and/or a plastic scintillation counter at the sample position. A monitoring ionization chamber was placed upstream of the sample. The ratios between the monitor and the calibrated chamber were measured to determine the beam intensity at the sample position for the same ion. The exposure doses were automatically determined by a computer-aided irradiation system by integrating the output current from the monitor chamber.

The accelerated energies of beams used in our experiments were ranging from 12 MeV/u to 400 MeV/u. The LETs at the sample position were selected by changing the accelerated energy of the ion beam and adjusted by using an adequate thickness of aluminum or plastic (Lucite) absorbers[3]. For the experiment at higher-LET beams, we chose as possible as lower energy beam, however we also used some absorbers to select a LET values. Thus secondary ion beams generated in the absorbers cannot be avoided. The most affective ion in secondary beams at carbon experiments is a helium-ion with a LET of several keV/μm. The contribution of the absorbed dose from secondary ions was less than 2 %, as estimated from data obtained by a carbon 290 MeV/u carbon-ion beam near the end of its penetration[6][7]. For the other beams, there are no measurement of the fluence, dose, and LETs of secondary particles by a certain physical experiments. However we can roughly estimate the contribution of the dose from secondary beam by the dose at down stream of the penetration depth of each Bragg-peak. The values were less than 5% for all experiments. The dose would be smaller for beams having shorter penetration ranges than the estimated range.

TABLE 1. Ion Beams Used and possible LET

Ion	Energy in vacume (MeV/u)	LET_{min}[#] (keV/μm)	LET_{max}[#] (keV/μm)	Institute	Facility
^{3}He	6	28	90	NIRS	Cyclotron
^{4}He	150	2.2	50	NIRS	HIMAC
^{12}C	6	250	500	NIRS	Cyclotron
^{12}C	135	21	250	RIKEN	RRC
^{12}C	135/290/350/400	21/13/12/11	250	NIRS	HIMAC
^{20}Ne	135	58	400	RIKEN	RRC
^{20}Ne	135/230/400	58/41/30	400	NIRS	HIMAC

[#] minimum LET for each beam, and possible maximum LET used for cell experiments.

2. Cell Culture and Survival Curve Fitting

Chinese hamster V79 cells cultured in Ham's F10 medium supplemented with 15% fetal bovine serum, 0.5 mg/ml Heart Infusion Broth (238400, Difco), and 100 U/ml penicillin and 100 μg/ml streptomycin was used. Cells were harvested by trypsinization, and seeded in dishes were cultured for about 1 day at 37°C in a 5% CO_2 incubator prior to exposure. After exposure, the cells were harvested by trypsinization, and re-suspended in a flesh medium. The numbers of cells in the suspension were counted by a particle counter, diluted with the medium, seeded in three 6-cm culture dishes at approximately 100 expected survivors per dish, and then incubated in an incubator for 6 days. The colonies in the dishes were fixed and stained. Colonies consisting of more than 50 cells were counted under a stereomicroscope as the number of viable cells. The plating efficiencies were greater than 80%. The α and β parameters were obtained from survival data plots by curve fitting using the LQ equation; $SF = \exp(-\alpha D - \beta D^2)$, by using computer programs. The D_{10} values were obtained from the α and β parameters from each survival data set.

Examples of survival curves were shown in Fig. 1. The curves for low-LET radiation showed a gentle curve with large shoulders. The curves become steeper and the shoulder was reduced with increasing of the LET. Gentle curves without shoulder were found at high-LET region. The survival curves for a lower-LET beam were well fitted by the LQ equation, and the survival curve parameters for X-rays; D_{10}, α, and β, were 7.07 Gy, 0.184 Gy^{-1}, and 0.0200 Gy^{-2}, respectively. When cells exposed to high-LET beams, data fitted well by the equation without the β term (or $\beta = 0$), because the curves were linear exponential. The curves were steepest and had no shoulder at LET 150 keV/μm or more, and the slope changed gradually with father increasing of the LET. Numerical data of survival parameters including other cell lines than V79 cells are reported previously [5] together with physical parameters of the beams (E, LET, LET_{100} and Z^{*2}/β^2). The RBE values were calculated as the ratio of the D_{10}s to that of X-rays. RBEs for different LET beams compared to X-rays were obtained for all the beams tested.

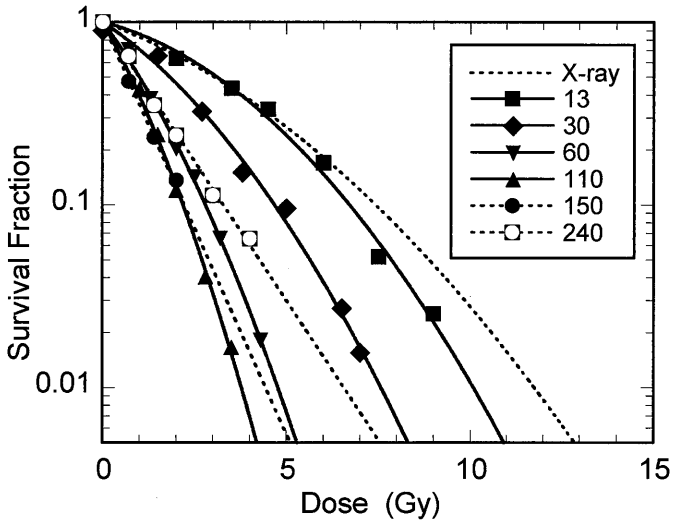

<Fig.1> Survival Curves for V79 Cells Exposed to Carbon Ions and X-rays. LET values of ion beams are indicated in the figure in keV/μm unit.

Analysis

1. Fitting of LET-RBE Curve

An experimental equation of LET-RBE relationships as a function of LET was investigated. The equation can be divided into two parts, and the relationship is expressed by using a composite function of the components. The first part (C1) describes a simple decreasing component of RBE with the LET, and the second part (C2) describes a peak of the RBE at a defined LET. The first part is expressed as;

$$C1_{(L)} = 1 / \mathrm{sqrt}\{(L/L_p)^2+Q/L+1\},$$

where L is the LET value of the ion-beam, L_0 is an LET that shows the inflection point of LET-RBE relationship, and Q is a parameter that defines the shape of the curve at inflection point. The second part is expressed as;

$$C2_{(L)} = A \exp\{ -\ln(L / L_p)^2 / W \},$$

where A is the maximum magnitude of the RBE, L_0 is the LET that gives maximum magnitude of the peak in the part, and the W is the width of the peak of RBE. The L_0 in C1 and C2 must be different parameter, but power of the C2 is major at around L_0. Also, Q can be negligible by the same reason. Here, we made the L_0 of the C1 and C2 to be the same and set Q = 0, to reduce the number of the parameters. Finally, here we used an equation;

$$RBE_{(L)} = 1 / \mathrm{sqrt}\{(L / L_p)^2 + 1\}+A \exp\{-\ln(L / L_p)^2 / W \},$$

to analyze the LET-RBE relationship. Calculations were performed by a fitting method using a computer program to minimize the weighted residuals.

The LET-RBE curves were determined using method described above for ^{3}He-, ^{12}C- and ^{20}Ne-ions with the LET ranging 18.6 - 90.8, 22.5 - 502, and 62.1 - 693 keV/μm, respectively, and the results were shown in Fig. 2. The LET-RBE spectra for all ion beams include ^{3}He-ion could be fitted with the fitting equation, and the values of the fitting parameters could be obtained.

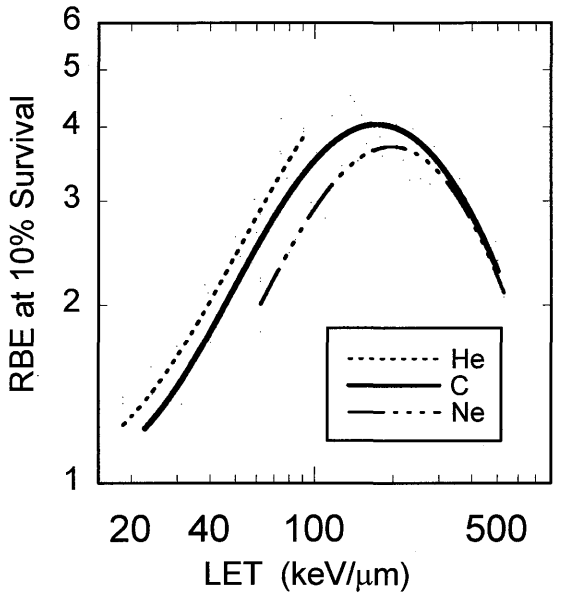

<Fig.2> Fitting of RBE as a Function of LET for V79 Cells Exposed to ^{3}He-, ^{12}C- and ^{20}Ne-Ion Beams (each data point not shown).

The spectra for those ions were different by the ion species especially in the low and middle LET range (<200 keV/μm), the RBEs showed different values for three different beams (^{3}He > ^{12}C > ^{20}Ne) at the same LET. The RBE spectra for ^{3}He-ion beams start to increase in a lower LET region compared to the other ion beams and reached a larger RBE (~ 4.0) at 90 keV/μm, but didn't showed a maxima. A peak RBE (3.56) was found at 88.3 keV/μm for a ^{3}He-ion beam by a similar experiment[8][9]. The depth-width of the Bragg peak for ^{3}He-ion beam is too narrow to expose a whole cell with a traversal having the same LET and the same dose rate. This means that the energy would be deposited at different LET and dose rates in a cell. The RBE may increase further more at higher LET of ^{3}He-ion, and it could be estimated to reach ~6 by the calculation. The maximum RBE values were found at around 200 keV/μm for ^{20}Ne-ion, and at around 150 keV/μm for ^{12}C-ion.

The difference in the RBE due to the ions is clear in lower-LET region up to 200 keV/μm (Fig. 2), where complete data sets for those three ions exist. For instance, the RBEs were, 3.3, 2.8 and 2.2 at 70 keV/μm for ^{3}He-, ^{12}C- and ^{20}Ne-ion, respectively. In the other word, the LET that gives 3.0 for the RBE of ^{3}He ions was 65 keV/μm, and that for ^{12}C- or ^{20}Ne-ion were at around 77 or 105 keV/μm. This means that to give the same radiobiological effectiveness for ^{12}C- and ^{20}Ne-ion beams to ^{3}He-ion beams, 1.2 or 1.6 times higher LET is required, respectively. There are considerable data[10][11][12] demonstrating such differences in the biological effectiveness of different ion species at the same LET. There is also a theoretical analysis[13] that predicts a difference between the LET-RBE spectra for different ions.

2. Fitting Parameters and Atomic Number

The LET-RBE relationships for ion-beams tested were plotted by a fitting method as described above. In general, the RBE increased with LET, showed peaks at around 100-200 keV/μm, and then decreased with LET. The LET-RBE spectra are different for the different ion spices. The LET-RBE curves are clearly different for the different ion beams. We thought that here must be a relationship between the parameters of the LET-RBE curves and atomic number of the accelerated ions, and the parameters Lp, A and W of LET-RBE curves were plotted as a function of atomic number of the ions (Fig. 3). The Lp increased and the A decreased exponentially with the increase of atomic number, and W was a constant. The relationship could be expressed as ;

Lp = 149·exp(0.0271·Z), with r = 0.985,
A = 583·exp(-0.0373·Z), with r = 0.997, and
W = 1.49.

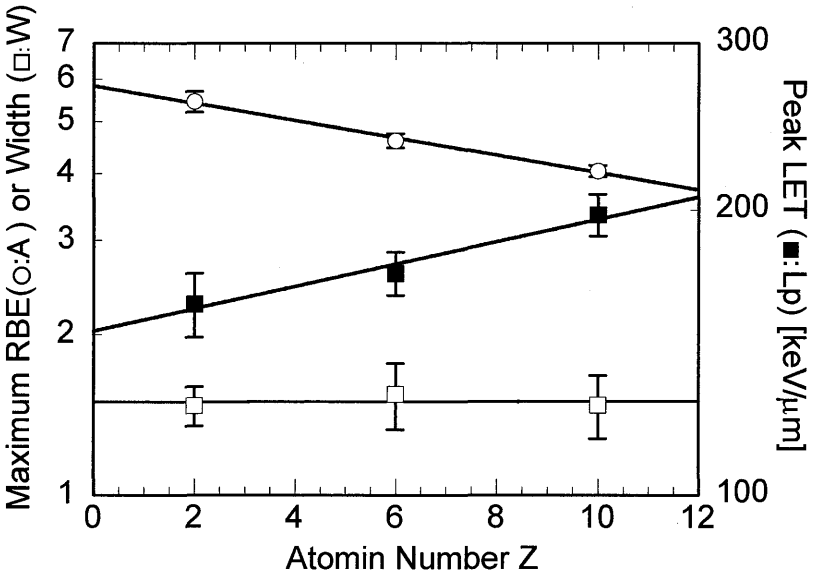

<Fig.3>. Parameters of LET-RBE Fitting Equation as a Function of Atomic Number of the Accelerated Ion (Z). The parameters are LET that gives the maximum RBE (L_p), amplitude (A) of the peak of RBE, and the width of the peak (W) of RBE.

Conclusion

We obtained LET-RBE spectra for killing of V79 cells exposed to different ion beams. At a given LET, the RBE-value for lighter ions was higher than that for heavier ions at lower-LET region. The LET-RBE relationship could fitted by a newly contrived equation that including three parameters; L_p, A, and W. It is also found that those parameters can be defined again as functions of atomic numbers of the accelerated ions. The LET of the maximum RBE (L_p) shifts to higher LET values for heavier-ions, amplitude (A) of the peak of RBE decreased with the atomic number of the irradiated ions, and the width of the peak (W) was a constant.

Using those parameters, we are possible to estimate RBEs to the beams at any LET and any ion spice that has not been measured the survival data biologically. Together with physical measurement of the fragmented beam i.e. components in total beam including atomic numbers and it's LET spectrum, we may possible to estimate total/average RBE of the beam. This means we may possible to estimate biological effectiveness to design further therapeutic beams with high accuracy.

Acknowledgement

We thank all staff members in the Division of Accelerator Physics and Engineering and the Division of Radiobiology and Biodosimetry at NIRS for their kind support during a part of this work. We thank the cyclotron crews at NIRS, and RIKEN for providing steady beams during the experiments. This investigation was partly supported by Special Coordination Funds of the Science Technology Agency, and the cooperative research with heavy-ion at HIMAC.

References

[1] H. Tsujii, J. Mizoe, T. Kamada, M. Baba, H. Tsuji, H. Kato, S. Kato, S. Yamada, S. Yasuda, T. Ohno, T. Yanagi, R. Imai, K. Kagei, H. Kato, R. Hara, A. Hasegawa, M. Nakajima, N. Sugane, N. Tamaki, R. Takagi, S. Kandatsu, K. Yoshikawa, R. Kishimoto and T. Miyamoto Clinical Results of Carbon Ion Radiotherapy at NIRS, J Radiat Res (Tokyo) 48 Suppl A (2007) A1-A13.

[2] M. Torikoshi, S. Minohara, N. Kanematsu, M. Komori, M. Kanazawa, K. Noda, N. Miyahara, H. Itoh, M. Endo and T. Kanai Irradiation System for HIMAC, J Radiat Res (Tokyo) 48 Suppl A (2007) A15-25.

[3] T. Kanai, T. Kohno, S. Minohara, M. Sudou, E. Takada, F. Soga, K. Kawachi and A. Fukumura Dosimetry and measured differential W values of air for heavy ions, Radiat Res 135 (1993) 293-301.

[4] T. Kanai, M. Endo, S. Minohara, N. Miyahara, H. Koyama-ito, H. Tomura, N. Matsufuji, Y. Futami, A. Fukumura, T. Hiraoka, Y. Furusawa, K. Ando, M. Suzuki, F. Soga and K. Kawachi Biophysical characteristics of HIMAC clinical irradiation system for heavy-ion radiation therapy, Int J Radiat Oncol Biol Phys 44 (1999) 201-210.

[5] Y. Furusawa, K. Fukutsu, M. Aoki, H. Itsukaichi, K. Eguchi-Kasai, H. Ohara, F. Yatagai, T. Kanai and K. Ando Inactivation of aerobic and hypoxic cells from three different cell lines by accelerated (3)He-, (12)C- and (20)Ne-ion beams, Radiat Res 154 (2000) 485-496.

[6] N. Matsufuji, A. Fukumura, M. Komori, T. Kanai and T. Kohno Influence of fragment reaction of relativistic heavy charged particles on heavy-ion radiotherapy, Phys Med Biol 48 (2003) 1605-1623.

[7] N. Matsufuji, M. Komori, H. Sasaki, K. Akiu, M. Ogawa, A. Fukumura, E. Urakabe, T. Inaniwa, T. Nishio, T. Kohno and T. Kanai Spatial fragment distribution from a therapeutic pencil-like carbon beam in water, Phys Med Biol 50 (2005) 3393-3403.

[8] M. Folkard, K.M. Prise, B. Vojnovic, H.C. Newman, M.J. Roper and B.D. Michael Inactivation of V79 cells by low-energy protons, deuterons and helium-3 ions, Int J Radiat Biol 69 (1996) 729-738.

[9] M. Belli, D.T. Goodhead, F. Ianzani, G. Simone and M.A. Tabocchini Direct comparison between protons and alpha-particles of the same LET: II. Mutation induction at the HPRT locus in V79 cells., International Journal of Radiation Biology 61 (1992) 625-629.

[10] E.A. Blakely, F.Q.H. Ngo, S.B. Curtis and C.A. Tobias Heavy-ion radiobiology: Cellular studies, in: J.T. Lett (Ed.), Advances in Radiation Biology, Academic Press, New York, 1984, pp. 295-389.

[11] G.W. Barendsen Response of cultured cells, tumors and normal tissues to radiations of different linear energy transfer, in: M. Ebert and A. Howard (Eds.), Current Topics in Radiation Research, North-Holland Publish Co., Amsterdam, 1968, pp. 293-356.

[12] H. Wulf, W. Kraft-Weyrather, H.G. Miltenburger, E.A. Blakely, C.A. Tobias and G. Kraft Heavy-ion effects on mammalian cells: Inactivation measurements with different cell lines, Radiation Research 8 (1985) S122-134.

[13] M. Scholz and G. Kraft Calculation of Heavy Ion Inactivation Probabilities Based on Track Structure, X Ray Sensitivity and Target Size, Radiation Protection Dosimetry 52 (1994) 29-33.

Effects of Heavy Ion Radiation on Cancer Stem Cells of Xenograft Tumor in Nude Mice

*[1]Sei Sai, [1]Yoshitaka Matsumoto, [1]Yoshiya Furusawa, [2] Hirohiko Tsujii, and [1]Ryuichi Okayasu [1]

[1]Heavy ion Radiobiology Research Group, Research Center for Charged Particle Therapy, National Institute of Radiological Sciences, Chiba, Japan.
[2]Research Center Hospital for Charged Particle Therapy, National Institute of Radiological Sciences, Chiba, Japan.
*Corresponding Author: *Sei Sai, e-mail address: saisei@nirs.go.jp*

Abstract

Experiments were design to determine the effects of Carbon ion radiation on cancer stem cells within xenograft tumors, and to assess the impact of high LET radiation on radiocurability. HCT116 human colon cancer cells were inoculated into nude mice and animals were irradiated when tumors reached a certain size. When irradiated with 15 Gy Carbon ions, the xenograft tumors re-grew after 60 days. However, when irradiated with 30 Gy all tumors were eradicated without relapse within the 90 day follow-up period. In comparison, with X-ray radiation, the tumors were suppressed for 31 days with a dose of 30 Gy and eradicated following a 60 Gy dose. The relative biological effectiveness (RBE) value of Carbon ion relative to X-rays was calculated at 3.82. At an isodose of 30 Gy, Carbon ion radiation predominantly induced tumor cell cavitation and fibrosis, whereas X-ray radiation only partially destroyed the tumor cell mass. Tumor-supplying blood vessels were markedly reduced in mice following Carbon ion irradiation compared to mice irradiated with X-rays. The expression of cancer stem cell related markers or proteins, such as CD133, EpCAM, HIF-1α and B-catenin was predominantly suppressed following Carbon ion radiation. In contrast, X-rays actually increased the expression of these factors. In conclusion, heavy ion radiation can disrupt cancer stem cell populations more effectively than conventional X-ray treatment. These findings emphasize the importance of utilising heavy ion radiation as a tool to achieve high tumor radiocurability.

Introduction

Colorectal cancer is a common gastrointestinal malignancy and remains to be the major leading cause of cancer-related deaths in the world [1]. Radiation therapy is an effective nonsurgical intervention for colon cancer, but most of the tumors invariably recur after radiation therapy. Therefore, determination of the mechanisms of recurrence and radioresistance in these tumors and others could lead to advances in the treatment of cancer.

Recently, cancer stem cells, a minority subpopulation of cells that have the capacity to self-renew, have been identified in a growing number of solid tumors, and are typically recognized by virtue of the expression of cell surface markers, such as CD133, CD44, and EpCAM [2]. The correlation between CD133 and cancer stem cells has been documented in multiple solid tumors, including brain [3], pancreatic [4], liver [5, 6], and colon cancers [7]. The cancer stem cells that populated the original tumor may be resistant to the treatments to repopulate the recurrent tumor even after the bulk of the tumor has been removed by resection or chemoradiation therapy [8].

High LET heavy ion radiation have several potential advantages over low LET photon radiation, such as increased relative biological effect, reduced oxygen enhancement ratio, decreased cell cycle-dependent radiosensitivity, and induction of complex DNA damage that not easily repaired [9, 10]. Over the past decades, heavy ion radiotherapy has been successful in treating many kinds of human cancers, including lung, liver, prostate, sarcoma etc. [11]. However, to the best of our knowledge, there are still no definitive reports on the effects of heavy ion radiation on cancer stem cells or the histopathological changes with regards to tumor control. In the present study, we try to explore the influences of carbon ion radiation on expression of cancer stem cell markers and its relationship to radiocurability of xenograft tumors in nude mice.

Materials and Methods

Cell lines

The colon adenocarcinoma cell line HCT-116 was purchased from American Type Culture Collection (ATCC). The cells were cultured in Dulbecco's Modified Eagle's Medium (DMEM) (Invitrogen, Grand Island, NY) supplemented with 10% with heat-inactivated 5% (v/v) fetal calf serum (Beit-Ha'Emek, Israel), 100 unit/mL penicillin and 100 μg/mL streptomycin (Invitrogen) in a 37°C with 5% CO2-in-air. The medium was changed every other day.

Animals and Xenograft transplantation

BALB/cAJcl-nu/nu male mice (5-week-old) were purchased from CLEA Japan, Inc. Tokyo, Japan. Mice were provided with water and food *ad libitum* and were housed at 5 animals per cage. All surgical procedures and care administered to the animals were in accordance with the NIRS Animal Care and Use Committee. Tumors were established by subcutaneous inoculation of 8×10^5 HCT-116 cells into the skin of mice right leg. Tumor growth was monitored every 3 days by measuring two perpendicular diameters. Tumor volume was calculated according to the formula $0.52 \times a \times b^2$, where a and b are the largest and smallest diameters, respectively.

Radiation

Mice were irradiated with carbon ion beams accelerated by the HIMAC at NIRS in Japan. The details concerning the beam characteristics of carbon ion beams, biological radiation procedures, and dosimetry have been described elsewhere (12). Briefly, the initial energy of the carbon ion beams was 290 MeV/n, 50KeV/μm, 6-cm, SOBP. The energy of heavy ion beams at the radiation site was obtained by comparing the calculated and measured depth-dose distribution. As a reference, mice were also irradiated with conventional 200 kV_p X-ray (Pantac HF-320S, Shimadzu Co., Tokyo) at NIRS. Transplanted xenograft tumors were irradiated with various doses of X-ray (15, 30, 60 Gy) or carbon ion (5, 15, and 30 Gy).

Gross Morphology and Histopathology

Gross morphological changes were followed up to 3 months after a single fraction of X-ray or carbon ion radiation. At selected time points, tumors were excised and histopathological examinations were performed. Xenograft tumors from different groups were fixed in 10% neutral formalin and processed in paraffin-embedded followed by sectioning (4 μm) onto slides. Sections were stained with hematoxylin and eosin (HE) and assessed microscopically.

Tumor Growth Delay and Relative Biological Effects

The tumor growth delay (TGD) of xenograft tumors after treatment with X-ray or carbon ion was estimated at the tumor volume of 600 mm3. The relative biological effectiveness (RBE) of carbon ion at the middle of a 6-cm SOBP relative to X-ray was calculated by Kaleidagraph software.

Immunohistochemistry

Immunohistochemical staining was performed with the Elite ABC Kit (Vector Laboratories; Burlingame, CA) according to the manufacturer's protocol. In brief, sections cut from formalin-fixed, paraffin-embedded tissue blocks were deparaffinized and rehydrated, and incubated in 0.3% hydrogen peroxidase to block endogenous peroxidase action. Then the antigen retrieval was performed by autoclave using a 10 mM citrate buffer (pH 6.0). The slides were preincubated with normal horse serum (Vector Laboratories, Burlingame, CA) to diminish nonspecific binding of the secondary antibody and then incubated overnight at 4 C with anti-CD133 (AC133, human monoclonal, Miltenyi Biotec), anti-β-catenin (mouse monoclonal,BD Transduction Labs), anti-HIF-1α (mouse monoclonal, abcam), and anti-EpCAM (mouse monoclonal, Acris Antibodies GmbH). Slides were then rinsed and incubated with universal secondary antibody containing anti-mouse/anti-goat IgG for 30 min, developed with diaminobenzadine for 10 min, and counterstained with hematoxylin for 2 min. Ten fields were selected and expression was evaluated in 1000 tumor cells with high power (x200) microscopy. As a negative control, the sections were stained without primary antibodies to monitor the background staining level. Cytoplasmic and/or nucear staining were considered to indicate specific HIF-1α, β-catenin, EpCAM, and CD133 immunoreactivity. Each slide was assessed for the intensity of immunostaining, background, and percentage of cells expressing the target protein.

Statistical analysis

One-way ANOVA and Bonferroni multiple comparison tests were used when mean differences between the groups were evaluated by StatView software (SAS Institute, Inc., Cary, NC). For all comparisons, p values less than 0.05 were defined as significant.

Results

Tumor Growth Control by Carbon ion vs X-ray Radiation

Transplanted xenograft tumors grow fast without any treatment and the tumor volume became more than 400 mm3 after subcutaneously implanted to the mice for 21 days. At an iso dose of 30 Gy, Treatment with X-ray radiation only suppressed tumor growth for 31 days, whereas carbon ion radiation increased tumor size at the initial 6 days and then gradually decreased. The tumor was finally disappeared after 90 days follow up without relapse (**Fig.1A**).

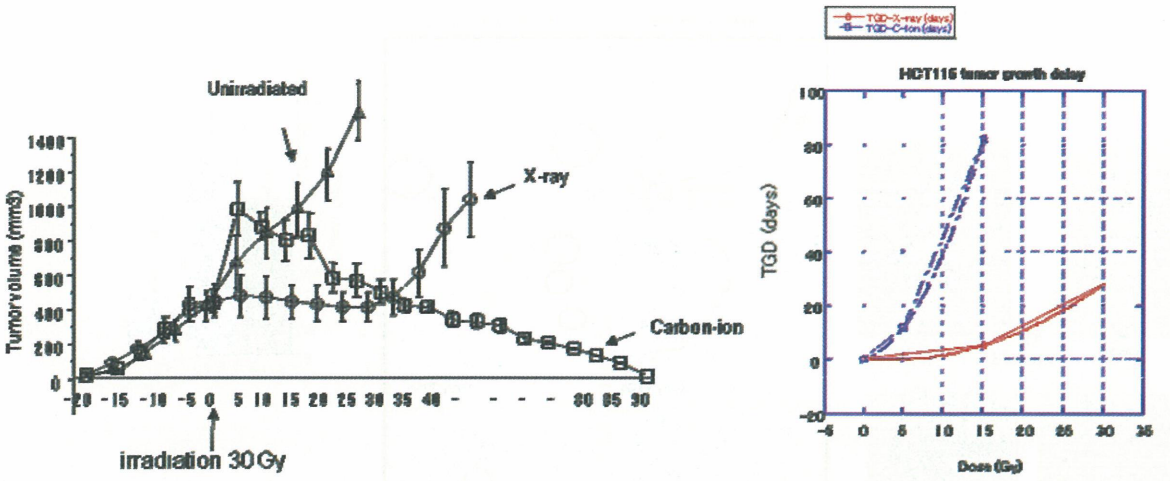

A B

Figure 1. A. HCT116 xenograft tumor growth control by X-ray or carbon ion radiation. **B.** HCT116 xenograft tumor growth delay after irradiated with X-ray or carbon ion.

Tumor Growth Delay and Relative Biological Effects of Carbon ion relative to X-ray Radiation

To determine the tumor growth control possibility by carbon ion radiation, the xenograft tumors were also treated with various doses. The tumor growth delay of xenograft tumors after treatment with 15 Gy and 30 Gy of X-ray was 5 and 28 days, whereas treatment with 5 Gy and 15 Gy by carbon ion was 12 and 82 days, respectively, when estimated at the time of tumor regrew to a volume about 600 mm3 **(Fig.1B)**. To obtain the tumor growth delay for 20 days, the dose of X-ray or carbon ion was estimated as 25.94 Gy and 6.78 Gy. It is therefore the RBE value of carbon ion at the middle of a 6-cm SOBP relative to X-ray was calculated as 3.82 **(Fig.1B)**.

Gross Morphological and Histopathological Changes after Carbon ion vs X-ray Radiation

Fig. 2A illustrates gross tumor morphology before and after treatment with carbon ion (30 Gy) or X-ray (30 Gy) radiation after 31 days. Tumor-supplying vessels were very clearly seen in the unirradiated mice as well as in X-ray irradiated mice, but markedly reduced in carbon ion irradiated mice. Histopathological changes of xenograft tumors after irradiated with X-ray or carbon ion for 31 days were examined by H&E staining. Carbon ion radiation predominantly induced colon cancer cell cavitations, fibrosis and most of the cells were killed and the duct-like architecture was completely disrupted. In contrast, X-ray radiation only partially destroyed colon cancer cells and the duct-like architecture still remained (**Fig.2B**). Histopathological features were similar between xenograft tumors irradiated with 30 Gy carbon ion and 60 Gy X-ray (data not shown).

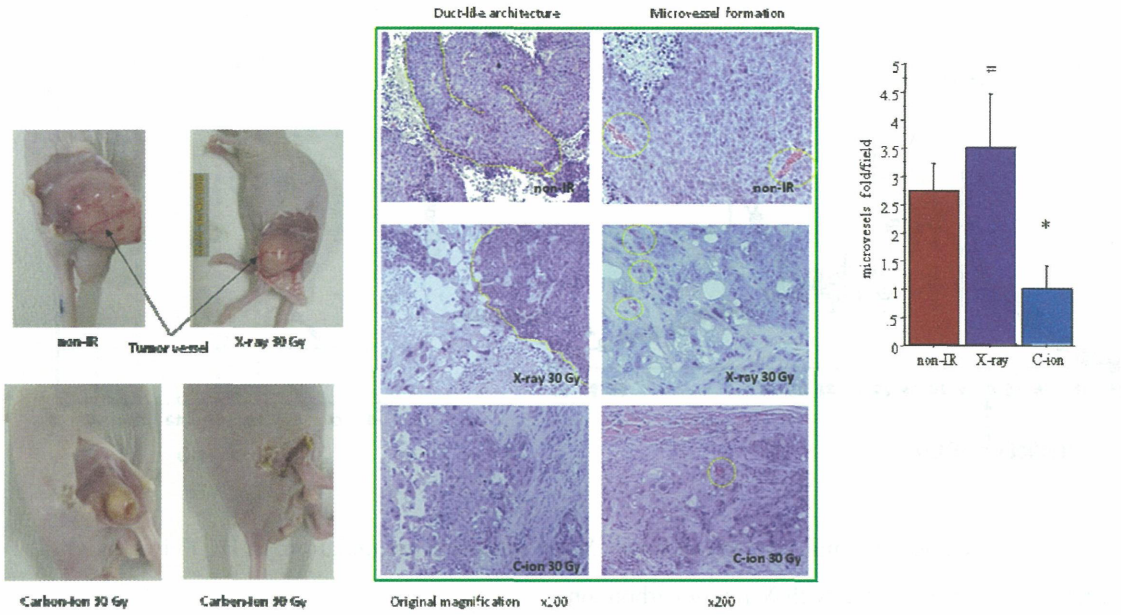

A **B**

Figure 2. Gross morphological changes (A) and histopathological features (B) of HCT116 xenograft tumours after treated with X-ray or carbon ion radiation for 4 weeks. #, $P<0.05$, *, $P<0.01$, compared to non-IR.

Expression of Cancer Stem Cell Markers or Proteins CD133, EpCAM, β-catenin, and HIF-1α after Carbon ion vs X-ray Radiation

The influences on the expression of cancer stem cell markers or proteins CD133, EpCAM, β-catenin, and HIF-1 α in the xenograft tumors after irradiated with carbon ion or X-ray ((30 Gy) for 31 days were examined by immunohistochemilcal staining. As shown in **Fig.3**, carbon ion radiation predominantly suppressed expression of both CD133 EpCAM, and HIF-1 α, but not β-catenin. In comparison, X-ray significantly increased expression of CD133, EpCAM, HIF-1 α, as well as β-catenin compared to those of unirradiated tumors. The expression of CD133, EpCAM was also slightly decreased or unchanged with carbon ion at dose of 15 Gy, but increased with 5 Gy, suggesting that lower dose of carbon ion radiation cannot suppress cancer stem marker expression. In comparison, the expression of CD133, EpCAM, HIF-1α and β-catenin was enhanced by X-ray at dose of 15 Gy, but markedly reduced at dose of 60 Gy (data not shown).

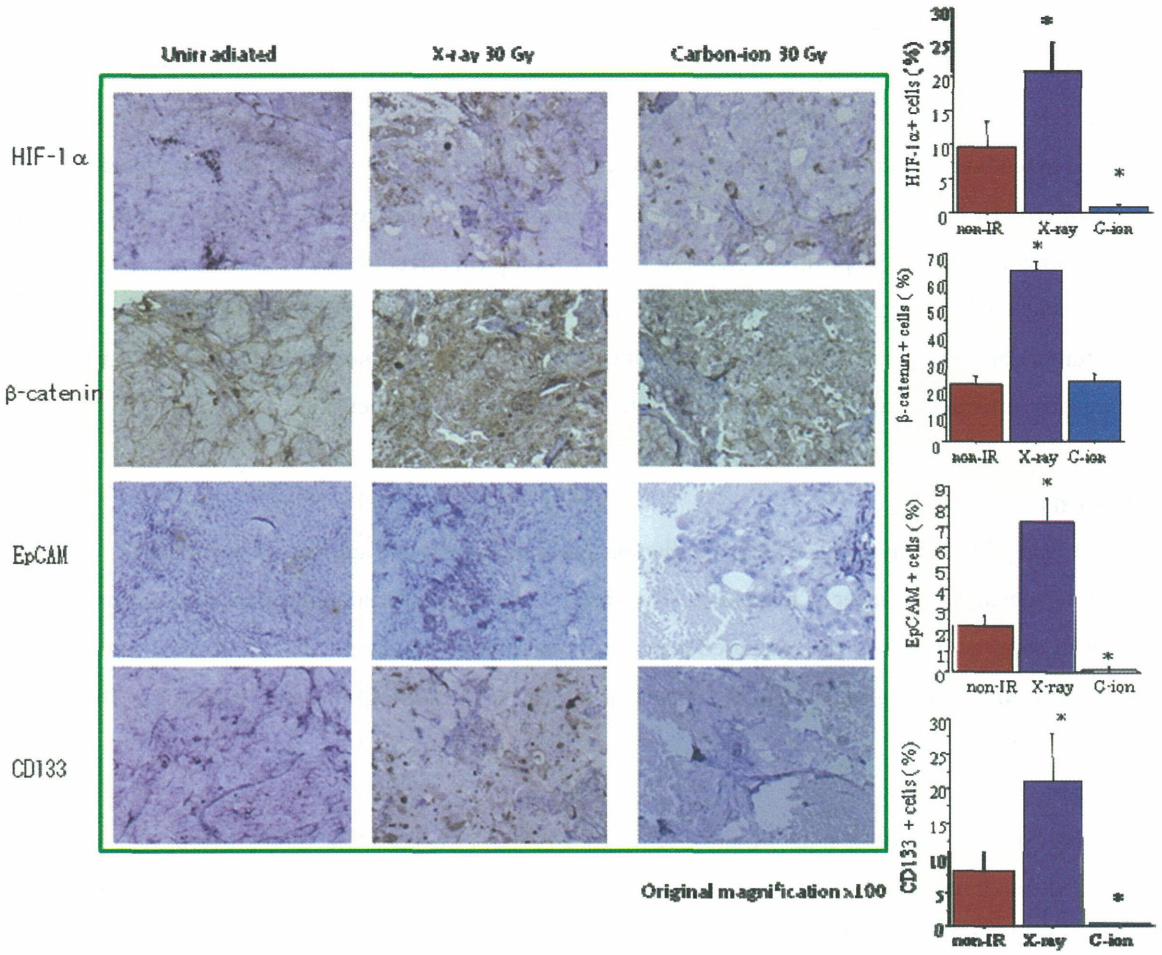

Figure 3. Expression changes of HIF-1α, β-catenin, CD133 and EpCAM in the HCT116 xenograft tumours after treated with carbon ion or X-ray radiation for 31 days. $P<0.01$, compared to non-IR.

Discussion

At an isodose of 30 Gy , we surprisingly found that, carbon ion radiation effectively suppressed expression of cancer stem cell markers CD133, EpCAM as well as HIF-1α, whereas X-ray radiation remarkably increased these protein levels. We also found that carbon ion radiation predominantly induced colon cancer cell cavitations, fibrosis and completely disrupted duct-like structure, whereas X-ray radiation only partially disrupted colon cancer cells and the duct-like structure still remained, when the xenograft tumors histopathologically examined after one month. The relative biological effects (RBE) value of carbon ion relative to X-ray was 3.82, suggesting that heavy ion radiation have more than 3 times of biological effects on the tumor control capability.

It has been shown that anticancer therapies are only effective if the cancer stem cells are effectively eradicated or inactivated [12]. Failure to incapacitate this potent fraction of cells, inevitably leads to repopulation and regrowth of the lesion [12]. In the present study, HCT116 xenograft tumors are particularly resistant to X-ray irradiation, likely due to the observed increase in expression of cancer stem cell markers and proteins. In contrast, heavy ion radiation significantly inhibited the expression of these markers, resulting in effective tumor control. In addition, Carbon ion irradiation also had a more severe impact on tumor morphology. Gross morphological examination of the tumor mass, one month post irradiation with Carbon ions, showed cavitations and fibrosis in

addition to significant disruption of the tumor-supplying blood vessels. In contrast, X-rays only partially disrupted cancerous cell morphology and blood vessels remained intact. These findings are in support of previous reports that heavy ion radiation inhibits angiogenesis *in vitro* [13]. In addition, it has also been reported that cancer stem cells are predominantly located in hypoxic regions, consistent with the increased local expression of HIF-1α expression [14]. Interestingly during analysis we observed CD133 positive cells in a parallel conformation to HIF-1α positive cells. The relative biological effect (RBE) of Carbon ion relative to X-rays was valued at 3.82, suggesting that heavy ion radiation has over three times the biological effect of X-rays on tumor control capacity. The findings presented here highlight the potential benefits of utilising heavy ion treatment for effectively targeting otherwise highly resistant cancer stem cells.

Conclusions

High LET heavy ion radiation can effectively disrupt cancer stem cells and subsequently eradicate transplantable human colon cancer in nude mice. This may be one of the crucial molecular mechanisms of high radiocurability induced by heavy ion compared to conventional low LET X-ray.

Acknowledgment We are grateful to Dr. Angela Noon for her kind help in proof reading of this paper.

References

[1] Jemal A, Siegel R, Ward E, et al. Cancer statistics, 2006. CA Cancer J Clin 2006;56:106-30.

[2] Dylla SJ, Beviglia L, Park IK, et al. Colorectal cancer stem cells are enriched in xenogeneic tumors following chemotherapy. PLoS One. 2008; 18;3:e2428.

[3] Bao S, Wu Q, McLendon RE, et al. Glioma stem cells promote radioresistance by preferential activation of the DNA damage response. Nature 2006 ;444:756-60.

[4] Lee CJ, Dosch J, Simeone DM. Pancreatic cancer stem cells. J Clin Oncol 2008;26:2806-12.

[5] Yin S, Li J, Hu C, et al. CD133 positive hepatocellular carcinoma cells possess high capacity for tumorigenicity. Int J Cancer 2007;120:1444-50.

[6] Ma S, Lee TK, Zheng BJ, et al. CD133+ HCC cancer stem cells confer chemoresistance by preferential expression of the Akt/PKB survival pathway. Oncogene 2008;27:1749-58.

[7] Ricci-Vitiani L, Lombardi DG, Pilozzi E, et al.Identification and expansion of human colon-cancer-initiating cells. Nature 2007;445:111-5Hambardzumyan D, Squatrito M, Holland EC. Radiation resistance and stem-like cells in brain tumors. Cancer Cell 2006;10:454-6.

[8] Griffin TW. Particle-beam radiation therapy. In: Perez CA, Brady LW, editors. Principles and practice of radiation oncology. 2nd ed. Philadelphia (PA): J.B. Lippincott Co.; 1992. p. 368–87.

[9] Okayasu R, Okada M, Okabe A, et al. Repair of DNA damage induced by accelerated heavy ions in mammalian cells proficient and deficient in the non-homologous end-joining pathway. Radiat Res 2006;165:59-67.

[10] Tsujii H, Mizoe J, Kamada T, et al. Clinical Results of Carbon ion Radiotherapy at NIRS. J Radiat Res (Tokyo). 2007;48 Suppl A:A1-A13.

[11] Kanai T, Matsufuji N, Miyamoto T, et al.Examination of GyE system for HIMAC carbon therapy. Int J Radiat Oncol Biol Phys 2006;64:650-6.

[12] Dingli D, Michor F. Successful therapy must eradicate cancer stem cells. Stem Cells 2006;24:2603-10.

[13]Takahashi Y, Teshima T, Kawaguchi N, et al.Heavy ion radiation inhibits in vitro angiogenesis even at sublethal dose. Cancer Res 2003;63:4253-7.

[14] Keith B, Simon MC. Hypoxia-inducible factors, stem cells, and cancer. Cell 2007;129:465-72.

Effect of Hypofractionation on RBE and Estimation of Therapeutic Dose

Yoshitaka Matsumoto, Daisuke Shimao, Mizuho Aoki, Nobuo Kubota, Yuki Kase, Naruhiro Matsufuji, Ryoichi Hirayama, Tatsuaki Kanai, Hirohiko Tsujii, Koichi Ando, and Yoshiya Furusawa

Research Center for Charged Particle Therapy, National Institute of Radiological Sciences, Chiba, Japan
Corresponding Author: Yoshitaka Matsumoto, e-mail address: y_matsu@nirs.go.jp

Introduction

Heavy-ion beams with high linear energy transfer (LET) have the advantage of good dose distribution for tumor and increasing relative biological effectiveness (RBE) with depth [(1)]. The Heavy Ion Medical Accelerator in Chiba (HIMAC) was constructed at the National Institute of Radiological Sciences (NIRS). Clinical trials have been demonstrated using carbon-ion beams for different cancers, lung cancer, bone & soft tissue sarcomas, hepatomas, prostate cancer, choroidal cancer, rectal cancer and head and neck cancer since July 1994 [(2, 3, 4)]. Up to March 2009, over 4500 patients have been treated including over 2000 patients subject to Highly Advanced Medical Technology program.

Recently, carbon-ion beam is a candidate for use in hypofractionated radiotherapy, having small fraction number and large fraction size to some kind of tumors, malignant melanoma of choroid, non-small cell lung cancer or hepatocellular carcinoma. Hypofractionation has a benefit for patients as the abbreviation of the treatment period. In this case, RBE values at high dose region (low survival level) must be considered, however the RBE is calculated physically and is not verified biologically. To estimate the lower survival, the extrapolation of the survival data, HSG cells on HIMAC has been used for the treatment planning. However, general colony formation assay can get only first third decades' data, and it may be far-fetched that the very low survival data will be presumed from the data in 1.0 – 0.001 of surviving fraction. It is important that to obtain the survival data as possible as lower region using various methods. We tried to get the survival data and estimate the RBE values at lower survival region using a multicellular spheroid technique and the multi-process formula fitting analysis in this study.

Methods and Materials

Culture of monolayer cells

One human malignant melanoma cell line, HMV-I was used in this study. Cells were cultured in Eagle's MEM with 10% FBS and antibiotics. Exponentially growing cells were seeded in flasks in CO_2 incubator, and cultured for about 2-2.5 days prior to exposure. After irradiation, cells were harvested, counted and seeded in three dishes, and then incubated for 13 – 14 days. Colonies containing more than 50 cells were counted as survivors.

Culture of muliticellular spheroids

Spheroid plates were used to make multicellular spheroids. Briefly, exponentially growing cells were seeded in the wells at concentration of 800 cells per a well 2 or 2.5 days before irradiation. Each 10-15 spheroids were then transferred to petri dishes and incubated for hours to attach the spheroids on the bottom of the dishes. Immediately before the irradiation, medium was removed from dishes, and then the samples were irradiated with X-rays or heavy-ion beams. After the irradiation, the spheroids' position was marked and cultured CO_2 incubator for 13 - 14 days, and then spheroids colonies were counted. Pictures of spheroids were obtained using microscope with CCD camera, and the diameter of spheroids was measured. The average diameter of a spheroid was 209±30 μm. Additionally, the spheroids were collected in a tube and trypsinized, and the cell number in a spheroid was counted. The average cell number in a spheroid was 1109±128 cells.

Irradiation

X-rays were produced by a generator operated at 200 kVp, and filtered with 0.5 mm Al and Cu. X-rays data was used for the reference survival curves for RBE calculation. Carbon or Argon ions having dose-averaged LET of 13, 35, and 100, or 300 keV/μm were provided by 290 or 500 MeV/nucleon beams at NIRS-HIMAC.

Curve fitting analysis

Three dose-survival formulas were used for the fitting analysis of the data. In addition to the linear-quadratic (LQ) equation, the multi-target single-hit (MT) and the multi-process (MP) equations were used.

$SF = \exp(-\alpha D-\beta D^2)$ ·····(LQ)

$SF = 1-(1-\exp(-D/D_0))^n$·····(MT)

$SF = \exp(-\alpha D)(1-(1-\exp(-D/D_0))^n)$ ·····(MP)

Where, SF is the surviving fraction, D is the dose (Gy), a is, b is, Do is , and n is .

The three formulas were set in a curve sitting analysis software. The experimental data was fitted with formulas and various survival parameters (a, b, D_0) were calculated. At first, the survival data of only monolayer cells (SF = 10^{-3} - 10^{0}) was fitted with three equations, respectively. Secondary, these fitting curves were extrapolated to low survival region (SF = 10^{-3} -10^{-5}), and then the differences of the survival data between the experimental values and the calculation values were compared among these three equations.

Results

Survival curves of monolayer cells and spheroids

Dose-response of HMV-I cells exposed to X-rays or heavy-ion beams as a monolayer cells were fitted by the LQ equation. The curves of high LET, 100 and 300 keV/μm showed linear without shoulder. The survival curves of HMV-I spheroids exposed to X-rays or heavy-ion beams could fits with the MT equation. The surviving fraction of spheroids showed 1.0 until definite dose, for example 9.0 Gy for X-rays, and then the fraction was drastically decreased depend on the dose.

Combination of survival curves of monolayer cells and spheroids

To obtain the clonogenic survival data in wide survival range, we tried to combine them that obtained from monolayer cells and multicellular spheroids. To get the lower survival data, the surviving fraction of spheroids was converted to the fraction of single cell in a spheroid. At the results, the low survival data from 10^{-3} to 10^{-5} of surviving fraction was obtained and plotted in addition to monolayer survival data. The fit with LQ, MT, or MP equations with experimental plots were investigated in wide survival region. For shortness' sake, X-rays data having big shoulder and 100 keV/μm carbon beams data showed linear curve were used to this analysis. In this analysis, the three fitting equations were fitted to the survival data of only first three decades (monolayer cells' data), and extrapolated to 10^{-5} of SF range (Fig. 1). The fitting survival curves of three equations were differed in lower survival region, and the MP equation showed best fit to experimental plots in wide region. Therefore, we used MP equation to fit the survival curves, calculate the survival parameters and estimate the RBE values in wide survival region.

Estimation of relative biological effectiveness

To estimate the RBE values in wide survival range, all the survival plots were fitted with MP equation (Fig. 2). In this analysis, these curves were fitted to all data (10^{0} - 10^{-5}). The survival parameters were calculated by MP equation fitting to survival data merged monolayer cells with spheroids data. The RBE values in wide survival range (10^{0} - 10^{-9}) were estimated using the parameters, and the SF-RBE curves were obtained. RBE values were

decreased with decrease of the SF, and converged to about 1.1 – 1.4 values at the very low survival level, 10^{-9}.

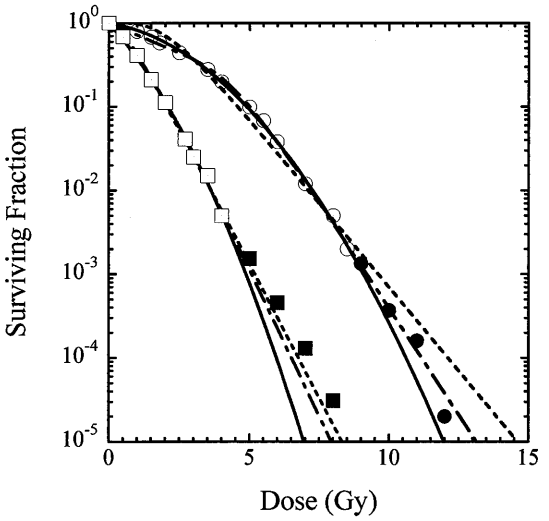

Fig. 1 Clonogenic survival curves of HMV-I cells exposed to X-rays or 100 keV/μm carbon-ion beams. The three equations, LQ, MT and MP were fitted with the survival data only first third decades obtained from monolayer cells. Two beams were used for the analysis, circle symbols showed X-rays data, and square symbols showed 100 keV/μm carbon-ion beams data. Open symbols showed monolayer cells survival data, and closed symbols showed the spheroids survival data. The three fitting lines, —— shows LQ, ------- shows MT, and — - — shows MP fitting, respectively. LQ showed good fit at high survival range, but misfit at lower range. MT showed good fit low survival range for high LET beam (carbon-ion beam) but not low LET beam (X-rays). MP showed good fit in wide survival range, and to both beams (X-rays and carbon-ion beams).

Fig. 2 Surviving fraction-RBE curves of various LET to reference beam, X-rays. In high survival range, RBE was differed depending on the LET values, high LET beams, 100 and 300 keV/mm showed very high RBE values, more than 2.5 to 4.0. But the RBE was decreased with the decrease of surviving fraction, and the RBE was converged to around 1.3 without recourse to LET.

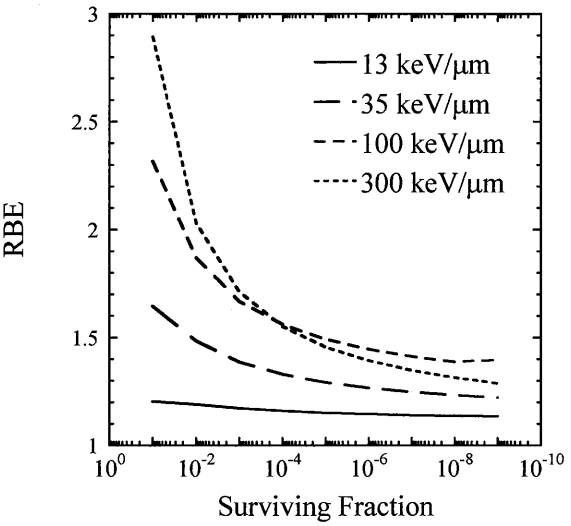

Discussion

Our goal is to estimate the RBE values for heavy-ion beams at high dose (low survival) range. We tried to get the data using the spheroids' technique in this study.

In this study, the MP equation showed bet fitting to the experimental plots in wide dose range compared with LQ and MT equation (Fig. 1) and plots for other LET beams (not shown). Whereas, LQ equation showed a good fit at higher survival range, but fitting curves kept bending in the lower survival range (Fig. 1). The LQ model is currently the most reliable method to fit, but it is known that this model showed good fit in only first three decades of a survival curve but not less than 1% survival region [5]. Additionally, the LQ model predicts a constant increasing slope at high dose region in contrast the constant slope observed in experimental survival curves [6]. On the other hand, MT equation showed good fitting to raw data in middle dose range, whereas especially in low dose range the equation did not fit the data (Fig. 1). The MP model showed good fit to survival data of mammalian cells exposed to X-rays more than MT model [7]. The MP model has a demerit in the analysis because there are three parameters, however as described above, the MP model has a considerable merit as getting the better fit with experimental data. We suggest that it may be necessary we investigate the availability of the MP model in addition to the LQ model analysis to guess the cell survival and RBE values in the high dose (low survival) region as a future plan in HIMAC.

The RBE values were estimated using the survival data in wide range obtained from monolayer cells and spheroids. The values were converged to 1.1 -1.3 in low survival region (10^{-9}). In HIMAC, the clinical RBE, ~3.0 and biological RBE, ~1.7 is used to calculate the start clinical dose for all dose range [8], and then the dose-escalation study has been performed. This method to estimate the RBE too high can be said that it is consequentially safe. However, the estimate dose might be insufficient to control the tumor completely. We suggest that it becomes possible to estimate the dose necessary for treatment more strictly using the multi-process model and the RBE values obtained from the survival data as low as possible.

Conclusion

In this study, we could get the lower survival data to 10^{-6} region after X-rays or heavy-ion irradiation having various LET values using multicellular spheroids technique in addition to monolayer cell survival, and we estimated RBE at wide dose region down to cell survival level, 10^{-9}. The RBE values were converged to around 1.3 in low survival region, so when we use hypofractionated heavy-ion therapy it must be consider that the change of RBE values depending on the fraction size.

Acknowledgement

This work was supported in part by a Grant –in-Aid from the Ministry of Education, Culture Sports, Science and Technology and by the Special Coordination Funds for Research Project with Heavy Ions at the National Institute of Radiological Sciences-Heavy-ion Medical Accelerator in Chiba (NIRS-HIMAC). We acknowledge all staff members in the Heavy-Ion Radiobiological Research Group for their kind help and suggestions and the HIMAC crews for their kind operation at sample irradiation.

References

[1] Tsujii H, Mizoe J, Kamada T, et al. Clinical Results of Carbon Ion Radiotherapy at NIRS. J Radiat. Res. 2007; 48 Suppl. A: A1-13.

[2] Kamada T, Tsujii H, Tsuji H, et al. Efficacy and safety of carbon ion radiotherapy in bone and soft tissue sarcomas. J. Clon. Oncol. 2002; 15: 4466-71.

[3] Miyamoto T, Yamamoto N, Nishimura H, et al. Carbon ion radiotherapy for stage I non-small cell lung cancer. Radiother. Oncol. 2003; 66: 127-40

[4] Kato H, Tsujii H, Miyamoto T, et al. Results of the first prospective study of carbon ion radiotherapy for hepatocellular carcinoma with liver cirrhosis. Int. J. Radiat. Oncol. Biol. Phys. 2004; 59: 1468-76

[5] Malaise EP, Lambin P, Joiner MC. Radiosensitivity of human cell lines to small doses. Are there some clinical implications? Radiat. Res. 1994; 138: S25-7

[6] Garcia LM, Leblanc J, Wilkins D, et al. Fitting the linear-quadratic model to detailed data sets for different dose ranges. Phys. Med. Biol. 2006; 51: 2813-23

[7] BENDER MA, GOOCH PC. Spontaneous and x-ray-induced somatic-chromosome aberrations in the Chinese hamster. Int. J. Radiat. Biol. 1961; 4: 175-84

[8] Tsuji H, Ishikawa H, Yanagi T, et al. Carbon-ion radiotherapy for locally advanced or unfavorably located choroidal melanoma: a Phase I/II dose-escalation study. Int. J. Radiat. Oncol. Biol. Phys. 2006; 67: 857-62

Radiosensitivity in Mesothelioma Cell Lines for X Rays and Carbon-ion Beams

Cuihua Liu[1], Masao Suzuki[1], Chizuru Tsuruoka[1], Kumie Nojima[2], Yoshiya Furusawa[1]

[1] *Heavy-ion Radiobiology Research Group, Research Center for Charged particle therapy, National Institute of Radiological Sciences, Chiba, Japan.*
[2] *Research Center for Radiation Protection, Research Center for Charged particle therapy, National Institute of Radiological Sciences, Chiba, Japan.*
e-mail address: cuihua@nirs.go.jp

Abstract

Malignant pleural mesothelioma (MPM) is an aggressive tumor arising from serous surfaces and often related to asbestos exposure. Taking into account a latency period of 20-40 years, it has been estimated that the number of men dying from MPM increase each year until a peak is reached in about 2020. MPM is resistant to various forms of therapy, such as radiotherapy, surgery or chemotherapy, and only slightly improve prognosis. So far, no effective therapeutics including chemotherapy or radiotherapy has been established for the disease-advanced case. The present study was carried out in order to examine the radiosensitivity of MPM cell lines by X rays and carbon-ion beams. Officially distributed 6 kinds of MPM cell lines were used and irradiated with X rays or carbon-ion beams (13.3keV/μm and approximately 80keV/μm) at the Heavy Ion Medical Accelerator in Chiba (HIMAC). Cell-killing effect was detected using a colony-formation assay. D_{10}, which is one of the parameters for cellular radiosensitivity, of 6 cell lines ranges from 2.74Gy to 5.42Gy for X rays, 2.17Gy to 4.21Gy for 13keV/μm- and 1.08Gy to 2.38Gy for 80keV/μm-carbon ions. The relative biological effectiveness (RBE) values calculated by the D_{10} relative to X rays, ranges from 1.24 to 1.42 for 13keV/μm- and from 2.31 to 3.09 for approximate 80keV/μm-carbon ions on each cell line. The results suggest that the irradiation of high LET carbon ions are also significantly more effective in cell killing for the 6 kinds of MPM cell lines than that of low LET X rays.

Introduction

Malignant pleural mesothelioma (MPM) is an aggressive and lethal cancer arising from mesothelial cells lining of serous membranes, and is considered to be often associated with previous exposure to asbestos fibers. Taking into account a latency period of 20-40 years, since 1970s the wide use of asbestos mineral fibers the incidence of this tumor is ever increasing, it has been estimated that the number of men dying from MPM increase each year until a peak being expected around 2020 in industrialized countries and possibly later in other regions of the world [1, 15, 16, 17]. In Japan, 500 patients with MPM died in 1995, and that number increased to approximately 900 patients in 2003 [8]. MPM is resistant to various forms of therapy, such as radiotherapy, surgery or chemotherapy, and only slightly improve prognosis. Very few patients are suitable for any potentially curative treatment [2, 3]. So far, no effective therapeutics including chemotherapy or radiotherapy has been established for the disease-advanced case. Many studies have showed that high LET radiations are more effective in cell-killing effect than low LET radiations, such as X-ray or gamma rays [9, 10, 11]. Now the HIMAC was performed advanced radiotherapy treatment of cancer and more than 3100 patients has been treated

with the HIMAC carbon-ion beams by 2007 [12,13], heavy charged particle therapy approved is now being performed with greater therapeutic effect to treat the cancer and improve symptoms in many patients than low-LET photon therapy. Some patients that are difficult to cure with other therapies showed remarkable efficacy especially with heavy charge particles, such as adenoma adenoid cystic carcinoma, malignant melanoma, hepatocellular carcinoma and sarcoma. But until now there are no reports for cell-killing effects for mesothelioma cells by heavy charge particles. It is, therefore, necessary and important to investigate the biological data by heavy-ion beams for heavy-ion radiotherapy. The present study was carried out in order to examine the radiosensitivity and determine RBE values of malignant pleural mesothelioma cell lines irradiated with heavy ions.

Materials and methods

Cells

Six human malignant pleural mesothelioma (MPM) cell lines were used for this study. Those cell lines were obtained from the American Type Culture Collection (ATCC), and the Riken Bio Resource Center (BRC) in Japan. Cells were cultured in Roswell Park Memorial Institute (RPMI) 1640 medium (sigma) supplemented with 10% fetal bovine serum and antibiotics, and they were maintained at 37℃ in a humidified atmosphere of a 5% CO_2 incubator. Each cell line was inoculated into 25-cm^2 plastic flasks at various cell concentrations for 3-4days before irradiation, by which time each cell was confluent.

Irradiation

Cells were irradiated with carbon-ion beams accelerated by the HIMAC. Briefly, the initial energy of the carbon-ion beams was 290MeV/n. The LET values used were to be 13keV/μm and 80keV/μm. The details of the HIMAC beam-delivery system, physical characters, biological irradiation procedures and dosimetry have been described elsewhere [17, 18]. For a comparison, we used 200kV X rays (20mA) filtered with 0.5mm Cu and 0.5mm Al by TITAN irradiator (Shimadzu, Japan) at the dose rate of 0.95Gy/min. All irradiations were carried out at room temperature.

Colony formation assay

Confluent cells were irradiated with X rays or heavy ions, and then cells were harvested by trypsinnzation and re-suspended in a fresh medium. The numbers of cells in the suspension were counted by a particle counter, diluted with the medium, plated on to plastic dishes (Falcon 3003) with a diameter of 100mm, aiming for 50~100 colonies per dish for the cell-survival assay. Colonies were fixed and stained with 0.2% violet-Methanol solution after a 14 to 21-day incubation period, the period of which fitted in each cell line for colony formation. Colonies consisting of more than 50 cells were counted as survivors.

Chromosome analysis

For the preparation of chromosome samples, RPMI 1640 medium containing 0.1ug/ml demecolcine (Wako pure chemical industries Ltd.) was added in cultured each cell line, which was in the late log phase, and treated for 3h. The cells were then treated with 75mM KCl solution for 20 minutes at 37°C and fixed in the methanol/acetic acide (3:1) solution. The cell's suspension was dropped onto slides, air dried, and stained with a 2%Giemsa solution. The number of chromosomes in 100 metaphases was scored.

Results

Figure 1 showed the mean numbers and the distribution of chromosome about six kinds of malignant pleural

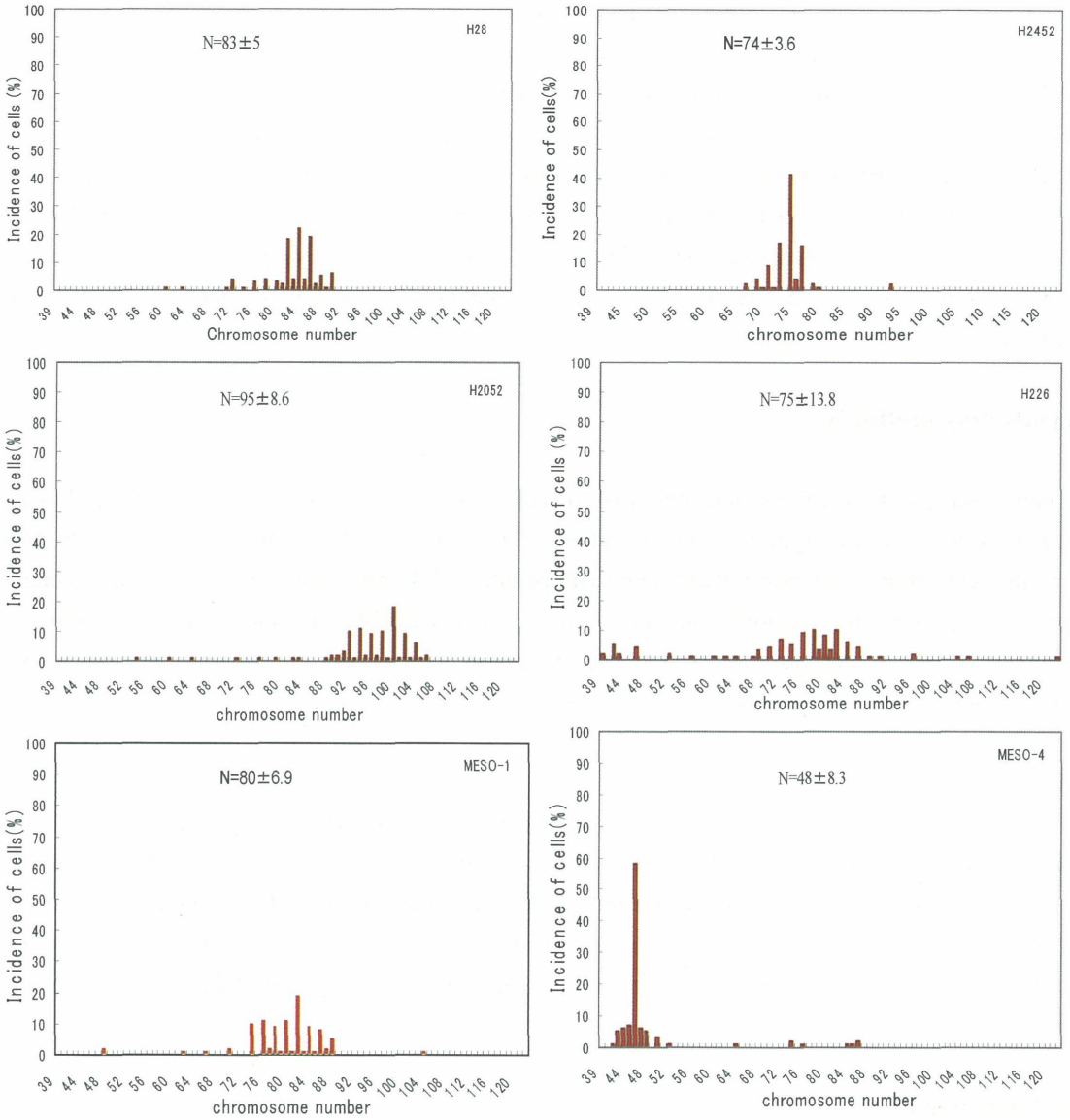

Figure1. The distribution of modal chromosome number with 6 kinds of malignant pleural mesothelioma cells.

mesothelioma cell lines. Different mesothelioma cell lines showed a great variation in numbers of chromosome, and the number of chromosomes in same cell line is also great different. The mean numbers of chromosomes in each cell line are to be 48-95.

Survival data of Figure 2 shows dose-response curves for cell-killing effect on 6 kinds of human malignant pleural mesothelioma cell lines irradiated with X-rays and carbon-ion beams with 2 different LET values (13keV/um and approximate 80keV/um). D_{10}, α and β values were calculated based on the survival curves, fitting by the linear-quadratic model: $SF=\exp^{(-\alpha D-\beta D2)}$ (table 1 and 2). From the D_{10} values which were determined as the dose (Gy) required to reduce the surviving fraction to 10%, we calculated the RBE of carbon-ion beams compared to X rays. The RBE values ranged to be 1.24～1.42 for 13keV/um-beam irradiation and 2.31-3.09 for approximate 80keV/um-beam irradiation on these malignant pleural mesothelioma cell lines.

The survival curves of those mesothelioma cell lines like other kinds of cell lines for X rays or low LET carbon beams showed a gentle curve with large shoulders, and become steeper for the higher LET carbon beams.

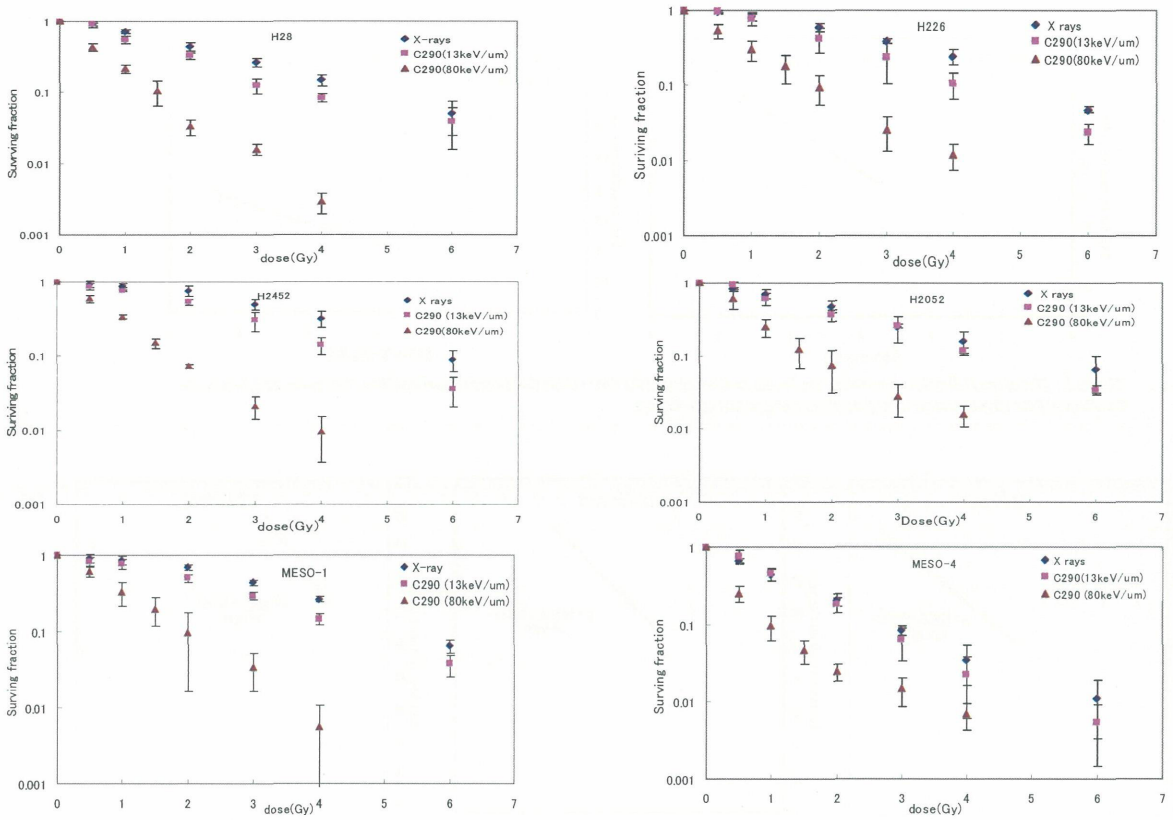

Figure 2. Dose-response curves for survival following irradiation by 200-kV X-rays(◆)and carbon-ion beams(■,13keV/um;▲,approximate 80keV/um). The LET values of approximate 80 keV/um beams in each graph show the mean values ± the standard deviations of at least three independent experiments in each cell line.

Table 1. α and β values for x-rays and carbon-ion beams calculated by survival curves of each cell line

	X-ray(200kV)		carbon-ion 13keV/um		carbon-ion(80keV/um)	
cell	α (Gy^{-1})	β (Gy^{-2})	α (Gy^{-1})	β (Gy^{-2})	α (Gy^{-1})	β (Gy^{-2})
H28	0.3186	0.0376	0.2941	0.0320	1.5447	-0.0581
H226	0.1150	0.0672	0.3246	0.0446	1.1893	-0.0040
H2052	0.4203	0.0100	0.4338	0.0489	1.6083	-0.0911
H2452	0.1179	0.0615	0.2417	0.0913	1.3154	-0.0229
MESO-1	0.0781	0.0654	0.3770	0.0802	0.7345	0.1017
MESO-4	0.8757	-0.0099	1.0611	0.0005	2.4927	-0.3245

Table 2. D10 values for x-ray and carbon-ion beams by based on survival curves of each cell line

	X-ray	carbon-ion(13keV/um)		carbon-ion(80keV/um)	
cell	D10(Gy)	D10(Gy)	RBE	D10(Gy)	RBE
H28	4.76±0.29	3.48±0.35	1.40±0.16	1.67±0.23	3.00±0.34
H226	5.08±0.35	3.63±0.31	1.42±0.12	1.86±0.16	2.79±0.22
H2052	5.09±0.51	3.96±0.5	1.33±0.19	1.7±0.23	3.09±0.38
H2452	5.28±0.33	4.21±0.62	1.32±0.22	1.81±0.04	2.93±0.07
MESO-1	5.42±0.33	4.13±0.33	1.34±0.12	2.38±0.21	2.31±0.20
MESO-4	2.74±0.14	2.17±0.07	1.24±0.02	1.08±0.07	2.43±0.15

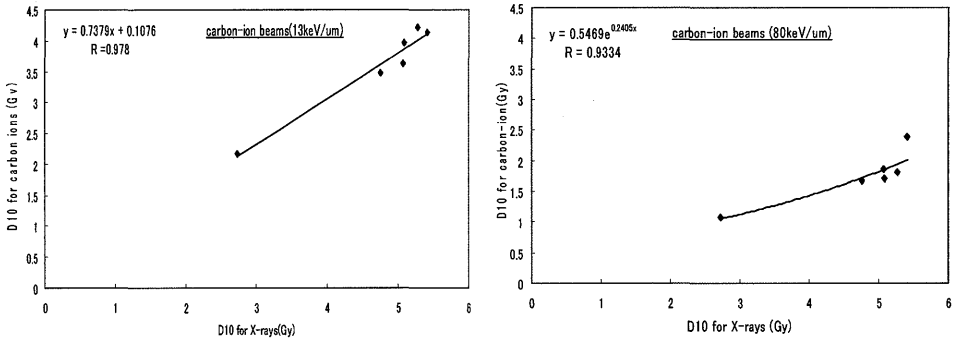

Figure 3 : Plot of the D10 values for carbon-ion beams as a function of the D10 values for X-rays in each cell line. The presented results are the mean and the standard error of at least three independent experiments.

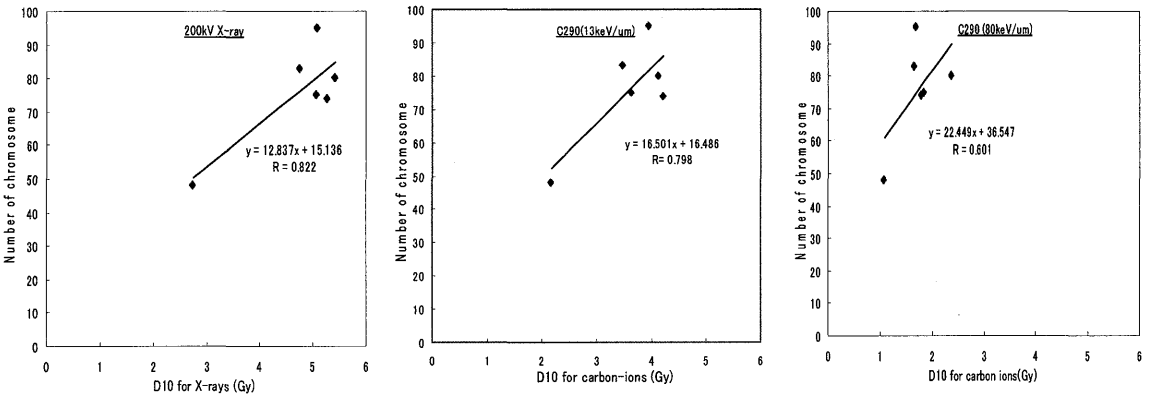

Figure 4: Plot of the numbers of chromosome as a function of the D10 values for X-rays and carbon-ion beams in each cell line

Figure 3 showed the D_{10} values for carbon-ion beams with 2 different LET values plotted as a function of the D_{10} values for X rays on each cell line. The results indicated there was a linear correlation in low LET carbon-ion beams but there was an exponential function correlation between X rays and high LET carbon-ion beams. Unlike low LET carbon-ion beams, the D_{10} values of high LET carbon ions increased slowly according to the increase the D_{10} values of X rays. Otherwise we examined the chromosome number on each cell line to clarify the relationship between the cellular radiosensitivity and chromosome number of a cell. Figure 4 shows the plotted data of the D_{10} values for X rays and carbon-ion beams as a function of the chromosome number. The result showed that the D_{10} values are not clearly correlated to the chromosome number of each cell line except for the MESO-4 cell line.

The resulting values for α and β are given in Table 2. In almost experiments except for MESO-1 negative β values were observed in the data irradiated by 80keV/um carbon-ion beams. In most cases the negative β values were not significantly different from zero.

Discussion

In this report, the radiosensitivity of six malignant pleural mesothelioma cell lines irradiated with X rays or heavy-ion beams were investigated. The D_{10} values, which is one of the parameter for cellular radiosensitivity, of six kinds of cell lines range from 2.74-5.42Gy for X rays, 2.17-3.48Gy for low LET carbon-ion beams (13keV/um), and 1.08-2.38Gy for high LET carbon-ion beams (80keV/um). The RBE values on each cell line used in this study, calculated by the D_{10} relative to X rays, range from 1.24 to 1.42 for 13keV/um- and from 2.3 to 3.09 for approximate 80keV/um-beam irradiation. Häkkinen *et al.* reported that different mesothelioma cell lines showed a great variation in radiosensitivity [4]. Suzuki *et al.* [11] showed in the reports using carbon-ion beams that RBE values for the 16 kinds of different human cells range from 1.06 to 1.33 for 13keV/um beams

and from 2.00 to 3.01 for 77keV/um beams. Blakely *et al.* showed that the RBE values for inactivation of T-1 cells in an aerobic condition were about 1.2 for the 13keV/um beams and 2.3-2.9 for the 85keV/um beams. The RBE values of our result in this report for the HIMAC carbon-ion beams were almost consistent with previous reports. Here we first reported that an increase in RBE with increasing LET was detectable in all of the six kinds of malignant pleural mesothelioma cell lines as well as other human cell lines.

We also have shown in this study some of the critical biological characteristics of mesothelioma cells associated with carbon-ion-beam irradiations as compared with X-ray irradiations. We examined the chromosome number and distribution on each cell line to clarify the relationship between the cellular radiosensitivity and chromosome number of a cell. Our present data was indicated that no strong correlation appears between the cellular radiosensitivity and chromosome numbers in the case of either X ray or carbon-ion beam. Schwartz *et al.* [6] reported that there was no relationship between DNA content and radiation sensitivity as measured by the cell survival assay or the induction of chromosome aberrations, although cells with larger DNA contents tended to have more chromosome damage per cell at equitoxic doses.

Suzuki *et al.* showed that the radiosensitivity (D_{10} values) between X rays and carbon-ion beams was well correlated [7]. Our data indicated that the radiosensitivity (D_{10} values) for X rays was a good linear correlation with those for low LET carbon-ion beams, but there was an exponential function correlation between X rays and high LET carbon-ion beams. The D_{10} values of high LET increased slowly according to the increase in D_{10} values of X rays. The result indicates that much less radiation damage can be expected with low LET carbon-ion beams and high LET carbon-ion beams can have highly cell-killing effect even on radioresistant malignant pleural mesothelioma cell lines. Terato and Nikijoo *et al.* [14, 20] reported that high LET ionizing radiation might induce complex clustered DNA damage which was refractory to repair or associated with error-prone repair and results in severe biological endpoints as compared to sparsely distributed lesions. This seems to give an advantage to carbon-ion treatment, as tumor cells are targeted with the Bragg peak part of the beam.

Although now we know the increase in cell-killing efficiency of six kinds of mesothelioma cell lines with high LET carbon-ion irradiation compared to X rays, the mechanism have not been investigated. Apoptosis induced by high LET heavy-ions also may be as a possible mechanism whereby heavy ions can overcome the radioresistance upon X-ray irradiation [7, 21], and we will study that in future.

Conclusion

To our knowledge, for the first time the radiosensitivity of six kinds of mesothelioma cells have been investigated in response to carbon-ion irradiation. We have shown that the RBE values of those mesothelioma cell lines for carbon-ion beams were also consistent with previous reports using carbon-ion beams with similar LET values. This result suggested the possibility that the radiation therapy by carbon-ion beams was effective for the malignant pleural mesothelioma.

Acknowledgements

The authors wish to thank the staff of the HIMAC for their help with heavy-ion irradiation. This study was supported by the research project with Heavy Ions at NIRS-HIMAC and in part by the grant (18310042) from the Japanese Ministry of Education, Culture, Sports, Science and Technology.

References

[1] Britton, M. The epidemiology of mesothelioma. Semin. Oncol., 2002, 29, 18-25.

[2] Tsiouris A, Walesby RK. Malignant pleural mesothelioma: current concepts in treatment. Nat Clin Pract Oncol. 2007 Jun; 4(6):344-52.

[3] Chapman E, Berenstein EG, Diéguez M et al. Radiotherapy for malignant pleural mesothelioma. Cochrane

Database Syst Rev. 2006 Jul 19; 3: CD003880.

[4] Häkkinen AM, Laasonen A, Linnainmaa K, et al. Radiosensitivity of mesothelioma cell lines. Acta Oncol. 1996;35(4):451-6.

[5] Waite K, Gilligan D. The role of radiotherapy in the treatment of malignant pleural mesothelioma. Clin Oncol (R Coll Radiol). 2007 Apr;19(3):182-7. Epub 2007.

[6] Schwartz JL. The radiosensitivity of the chromosomes of the cells of human squamous cell carcinoma cell lines. Radiat Res. 1992 Jan; 129(1):96-101.

[7] Meijer AE, Jernberg AR, Heiden T, et al. Dose and time dependent apoptotic response in a human melanoma cell line exposed to accelerated boron ions at four different LET. Int J Radiat Biol. 2005 Apr;81(4):261-72.

[8] Statistics and Information Department. Labour and welfare of Japan. Vital statistics of Japan 2003. Tokyo: Health and Welfare Statistics Association, 2003.

[9] Suzuki M, Watanabe M, Suzuki K, et al. Neoplastic cell transformation by heavy ions Radiation Res. 1989;120:468-476.

[10] Borek C, Hall EJ, Rossi HH, malignant transformation in cultured hamster cell produced by X-ray, 430-keV monoenergetic neutrons, and heavy ions. Cancer Res 1978; 38:2997-3005.

[11] Suzuki M, Kase Y, Yamaguchi H, et al. Relative biological effectiveness for cell-killing effect on various human cell lines irradiated with heavy-ion medical accelerator in Chiba (HIMAC) carbon-ion beams. Int J Radiat Oncol Biol Phys. 2000 Aug 1; 48(1):241-50.

[12] Tsujii H, Mizoe JE, Kamada T, et al. Clinical Results of Carbon Ion Radiotherapy at NIRS Journal of Radiation Research, Vol. 48 (2007) No. Suppl.A pp.A1-A13.

[13] Torikoshi M, Minohara S, Kamematsu N, et al. Irradiation System for HIMAC Journal of Radiation Research, Vol. 48 (2007) No. Suppl.A pp.A15-A25.

[14] Terato H, Tanaka R, Nakaarai Y, Nohara T at al. Quantitative analysis of isolated and clustered DNA damage induced by gamma-rays, carbon ion beams, and iron ion beams. J Radiat Res (Tokyo). 2008 Mar; 49(2):133-46. Epub 2008 Jan 24.

[15] Usami N, Fukui T, Kondo M, et al. Establishment and characterization of four malignant pleural mesothelioma cell lines from Japanese patients. Cancer Sci. 2006 May; 97(5):387-94.

[16] Zangemeister-Wittke U, Hopkins-Donaldson S. Apoptosis regulation and drug resistance in malignant pleural mesothelioma. Lung Cancer. 2005 Jul; 49 Suppl 1:S105-8.

[17] Kleinberg L, Lie AK, Flørenes VA, et al. Expression of inhibitor-of-apoptosis protein family members in malignant mesothelioma Hum Pathol. 2007 Jul; 38(7):986-94. Epub 2007 Mar 9.

[18] Tsuruoka C, Suzuki M, Kanai T, et al. LET and ion species dependence for cell killing in normal human skin fibroblasts. *Radiat. Res.*163, 494-500 (2005).

[19] T.Kanai, M.Endo, S.Minohara, et al. Biophysical characteristics of HIMAC clinical irradiation system for heavy-ion radiation therapy. *Int. J. Radiat. Oncol. Biol. Phys.*, 44, 201-210 (1999).

[20] Nikjoo H, Bolton CE, Watanabe R, et al. Modelling of DNA damage induced by energetic electrons (100eV to 100 keV). Radiat Prot Dosimetry. 2002; 99(1-4):77-80.

[21] Yamakawa N, Takahashi A, Mori E, et al. High LET radiation enhances apoptosis in mutated p53 cancer cells through Caspase-9 activation Cancer Sci. 2008 Jul;99(7):1455-60.

A Novel Mechanism of Cellular Radiosensitivity

Guangming Zhou[1], Junhong Li[1,2], Libin Zhou[1], Ryoichi Hirayama[3], Jiayun Zhu[1], Yoshitaka Matsumoto[3], Sheng Zhang[1,2], Atsushi Mizota[4], Yoshiya Furusawa[3]

[1]*Institute of Modern Physics, Chinese Academy of Sciences, Lanzhou, China*
[2]*Graduate School of Chinese Academy of Sciences, Beijing, China*
[3]*Research Center for Charged Particle Therapy, National Institute of Radiological Sciences, Chiba, Japan*
[4]*Department of Ophthalmology, Juntendo University Urayasu Hospital, Chiba, Japan*
Corresponding Author: Guangming Zhou, e-mail address: zhougm@impcas.ac.cn

Abstract

To investigate the correlation between cell cycle arrest induced by ionizing radiation and cellular radiosensitivity, two human melanoma cell lines, 92-1 and OCM-1, were irradiated with 200 kVp X-rays and 100keV/μm carbon ions. The radiosensitivities of both cell lines were assessed by colony forming assay, DNA damage and repair by Comet assay, cell cycle distribution by flow cytometry, and protein expression by Western blot and immunofluorescence. The radiosensitivity of 92-1 cells was significantly higher than that of OCM-1 cells. Evident G2 arrest was induced in both cell types in a dose-dependent manner. The G2 arrest in OCM-1 cells could reach to a higher maximum than that in 92-1 cells exposed to the same dose. Different from OCM-1 cells, part of the G2-blocked 92-1 cells could not reenter cell cycle. Those cells could not reenter cell cycle was proportional to the irradiation dose. Abortion of G2 block with caffeine promoted cell cycle reentering and enhanced cell survival relatively, which implies that the disability to reenter cell cycle is related to cellular radiosensitivity. Revealing the mechanism will provide promising means to sensitize cells to ionizing radiation.

Introduction

It has been generally accepted that DNA is the key target of ionizing radiation and DNA double-strand break (DSB) is initially the most critical damage. The induction and/or repair of DSB are intricately involved in radiosensitivity [1-2]. Cellular processes relating to DNA damage and repair, such as those signaling pathways recognizing DNA damage and activating repair systems, are sure to have substantial influence on radiosensitivity [3] but their correlation with radiosensitivity remains unclear.

Many advances in radiobiological study have been made in the most recent years [4], among which cell cycle regulation mechanism is thought to be extremely important for earning cells sufficient time to facilitate repair, and to minimize replication and subsequent segregation of DNA lesions [5]. DNA damage generally results in G2 arrest of the cell cycle [6-7]. It has been supposed that the longer the time consumed for DNA repair before apoptosis, the more resistant the cell line will be [8]. Radioresistance of some human cancer cells is closely correlated to γ-ray-induced G2 arrest [9]. Abrogation studies also support this hypothesis. Caffeine [10-11], pentoxifylline [12] and protein kinase inhibitor 7-hydroxystaurosporine [13] sensitize cells to ionizing radiation by abrogating G2/M arrest. However, some reverse results have also been reported. Schwartz et al.[14] failed to confirm the correlation between G2 phase duration and radiosensitivity. Xu et al.[15] believed that G2/M checkpoint abnormality was not linked to cellular radiosensitivity. Playle et al.[16] pointed out that abrogation of the ionising radiation-induced G2 checkpoint was not necessarily associated with sensitisation to ionising radiation although some colorectal tumour cell lines can be radiosensitised by G2 checkpoint inhibitor UCN-01.

Mainly because of the various cell types they used, the correlation between cell cycle block and cellular radiosensitivity is still inconclusive.

Well-established human uveal melanoma cell lines 92-1 [17] and OCM-1 [18-19] were used in present study to investigate the cell cycle variations induced by X-rays. Finally, a correlation between G2 arrest and radiosensitivity was confirmed by a detailed comparison of the does response and kinetics of G2/M phase of these two types of cells.

Methods and Materials

Cell culture

Human melanoma cell lines 92-1 and OCM-1 were grown with RPMI-1640 medium (Sigma) complemented with 10% fetal bovine serum (FBS, Hyclone), 100 μg/ml streptomycin and 100 units/ml penicillin in a humidified atmosphere of 95% air and 5% CO_2. 5×10^5 cells were seeded in 25 cm^2 culture flasks 2 days before irradiation, which resulted in less than 70% confluence at the time the cells were irradiated.

Irradiation

X-ray irradiations were performed with a Pantak-320S generator (Shimadzu, Tokyo) operated at 200 kVp and 20 mA with 0.5 mm Al and 0.5 mm Cu filters. The dose rate was 1 Gy/min. 100keV/μm carbon ions were generated by HIMAC and the dose rate was 1 Gy/min. All irradiations were carried out at room temperature.

Colony formation assay

Cell survival was determined by conventional colony-formation assay. Briefly, cells were collected by trypsinization and resuspended in RPMI-1640 medium complemented with 10% FBS. Cell concentration was determined with a cell counter (Coulter, model Z1 with a 100 μm aperture tube). Cells were diluted with medium and seeded in 60 mm Petri dishes (3002 Falcon) to provide 50-100 colonies per dish. Dishes were incubated for 18 and 13 days for 92-1 and OCM-1 cell lines, respectively, then fixed with 10% formalin in PBS and stained with 1% methylene blue. Colonies containing more than 50 cells were identified as survivors under a stereomicroscope. The plating efficiency of 92-1 cell line was 0.53±0.09 and that of OCM-1 cell line was 0.65±0.03 (mean±SD). Both multi-target model and linear-quadratic model were employed to analyze the survival data (KaleidaGraph, Synergy Software).

Cell Cycle Assay

After post-incubation for various periods, cells were harvested and fixed with 70% of pre-chilled ethanol for over 24 h at –20°C. The fixed cells were washed and resuspended in PBS, treated with 100 μg/ml RNase A, and stained with 50 μg/ml propidium iodide (PI) for 30 min at 37°C. Cell cycle distribution was analyzed with Modfit software (Verity Software, Topsham, ME) from the histogram of DNA content measured with a flow cytometer (FACScan, Becton Dickinson).

Immunofluorescence

Exponentially growing cells were plated in four-well slide chambers (Lab-Tek, Naperville, IL, USA) at a density of 8×10^3 cells/well and then irradiated with x-rays or carbon beam, fixed for 10 min in 4% paraformaldehyde, permeabilized for 20 min in methanol at -20°C, blocked for 1 h with 5% skim milk, and stained with primary antobodies (mouse anti-γH2AX antibody was purchased from Upstate Biotechnology, mouse anti-ATM pS1981 from Rockland, CyclinB, 14-3-3, Cdc2, Cdc2 phosphorylated at Thr14 and Tyr15,

Caspase3,and γ-tublin from Santa Cruz, USA) for 2 h. The bound antibody was visualized using Alexa Fluor® 488 anti–mouse antibody or Alexa Fluor® 546 anti–rabbit antibody (Molecular Probes, Eugene, OR, USA), and cell nuclei were counterstained with DAPI solution (Invitrogen, Eugene, OR, USA). Slides were observed under a fluorescence microscope (Keyence, Tokyo, Japan). At least 100 cells were scored for each sample, and the average number of foci per cell was calculated.

Western blot

Western blots were carried out following routine protocol. Briefly, cells were collected by centrifugation at 300 g, 4°C for 5 min, and lysed in appropiate amounts of lysis buffer (Biyuntian, China). Samples were centrifuged at 10000 g, 4°C for 15 min and the concentration of total protein was determined from the supernatants using BCA protein assay kit (Pierce, Rockford, IL, USA). Thereafter, samples were mixed with sample buffer (250 mM Tris HCl, 5% β-mercaptoethanol, 50% glycerol, 10% SDS, 0.5% bromophenol blue), boiled for 5 min, and equal amounts of protein (10 μg) were separated by 10% SDS-PAGE gels (BioRad, Tokyo, Japan). PVDF membranes (GE healthcare, Beijing, China) were rinsed in 100% methanol for 10 seconds and subsequently in transfer buffer (48 mM Tris, 39 mM Glycine, 0.037% SDS, 20% methanol) for 5 min, and blotting was performed at 0.8mA/cm^2 for 1 h in a transblot semidry blot cell (BioRad, USA). Thereafter, membranes were blocked for 1 h in blocking buffer (PBS-T, 5% skim milk) and incubated with primary antibodies for 1 h. After three washes with PBS-T, membranes were incubated with secondary antibody for 1 h. Finally, the membranes were washed three times in PBS-T and protein bands were visualized using the enhanced chemiluminescence (ECL) system (Amersham-Buchler, Braunschweig, Germany) and exposed to X-ray medical film (Kodak, Japan). The primary antibodies to β-actin and α-tubulin were purchased from Santa Cruz, and the others were the same as those used in immunofluorescence.

Statistical analysis

All the experiments were repeated at least three times, and the data were presented as mean ± standard error margin (SEM). Significance levels were assessed by student's *t*-test, and $p<0.05$ was considered as statistical significance.

Results

Cell survival of both cell lines was measured by routine colony-forming assay. The sensitivities of 92-1 and OCM-1 cells were dramatically different (Figure 1). As shown in Table 1, D10 and other survival parameters were obtained by multi-target model. SF2, the survival fraction induced by 2 Gy of irradiation, were 0.87 and 0.13, and the D10 were 7.10 Gy and 2.21 Gy, respectively. Significant differences in their radiosensitivity were revealed between the two cells lines.

Figure 2 shows the cell cycle distribution of 92-1 and OCM-1 cells exposed to 10 Gy of X-rays. Both cell lines were blocked at G2 phase. More than 80% of OCM-1 cells were blocked in G2/M phase while less than 60% of 92-1 cells exposed to the same dose were blocked. More attractive difference was in the ovecoming of G2 block. OCM-1 cells overcame the block and reentered the cell cycle in 48 hours. However, the cell cycle distribution in 92-1 exposed to 10 Gy of X-rays lasted for as long as 6 days after cells were blocked in G2 phase. The flow cytometry profile revealed that the blocked cells did not exit the cell cycle but stay un-changed. Similar results were observed when cells exposed to 100keV/μm carbon ions (data not shown).

Figure 3 presents the percentage of G2/M-phase 92-1 cells exposed to various doses of X-rays. In both cases, those cells cannot reenter cell cycle were proportional to the radiation dose. When the dose was over 3 Gy, cell cycle "ceased" in more and more cells.

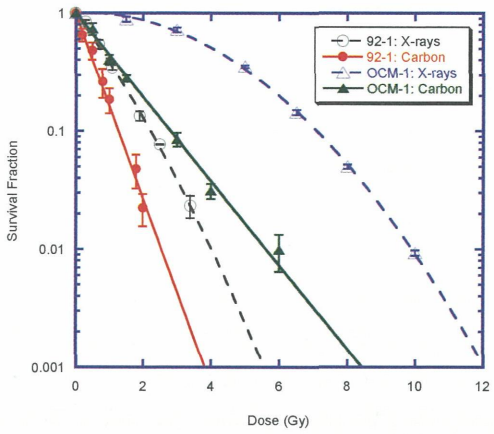

Figure 1. Survival curves of 92-1 cells (circle) and OCM-1 cells (triangle) irradiated by X-rays (open) or 100keV/μm carbon beam (solid).

Table 1 Parameters of survival curves

		D0	D10	Dq	m	SF_2 (%)
X-rays	92-1	1.00±0.11	2.21±0.05	0.11±0.03	1.11±0.02	13.1
	OCM-1	2.16±0.03	7.10±0.03	0.31±0.02	1.94±0.07	87.2
Carbon	92-1	0.51±0.04	1.32±0.14	0.34±0.19	1.22±0.11	2.70
	OCM-1	1.24±0.08	2.70±0.17	-0.03±0.02	0.97±0.02	19.0

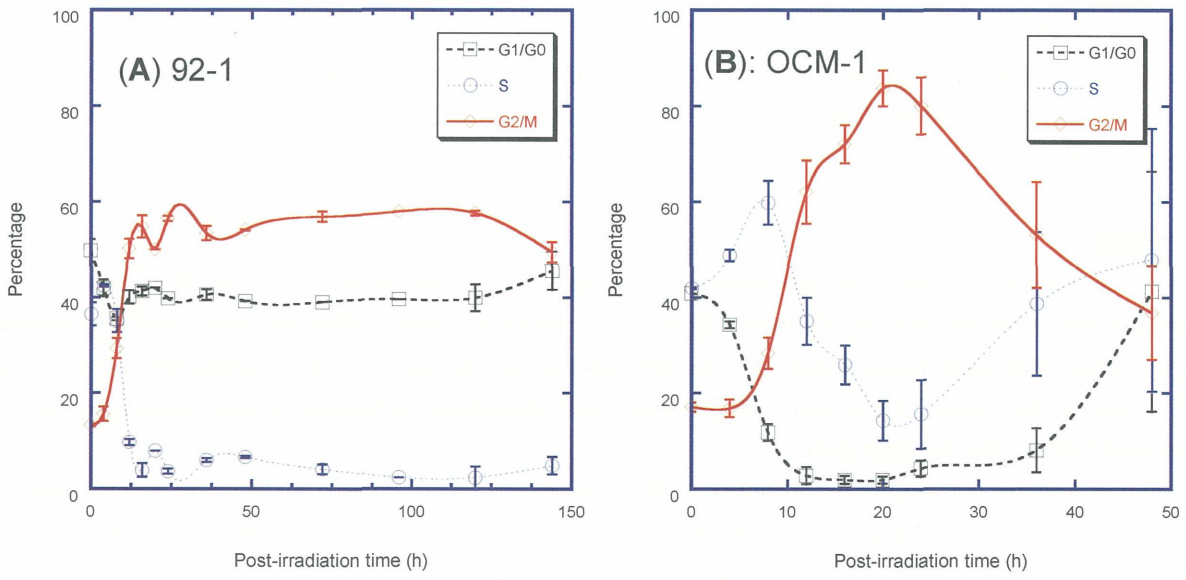

Figure 2. Cell cycle kinetics of 92-I and OCM-1 exposed to Gy of X-rays.

It has been reported that two main factors play important role in G2-M transition, cyclin B1 and Cdc2 (Stewart and Pietenpol, 2002). The activation of CyclinB1/Cdc2 requires enough expression and nuclear-localization of CyclinB1, and phosphorylation of Thr161 and dephosphorylation of Thr14 and Tyr15 of Cdc2. Immunofluorescence revealed that both cell lines met no problem in nuclear-cytoplasm trafficking. However, different from OCM-1 cells, the CyclinB1 and phosphorylated Cdc2 were mainly located in nuclei (Figure 4).

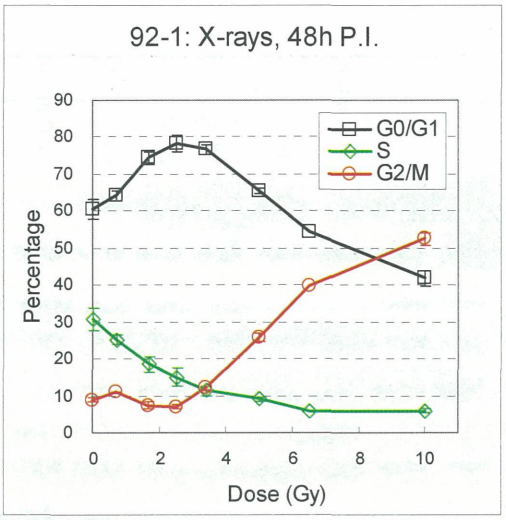

Figure 3. Cell cycle distribution of 92-1 cells exposed to various doses of X-rays.

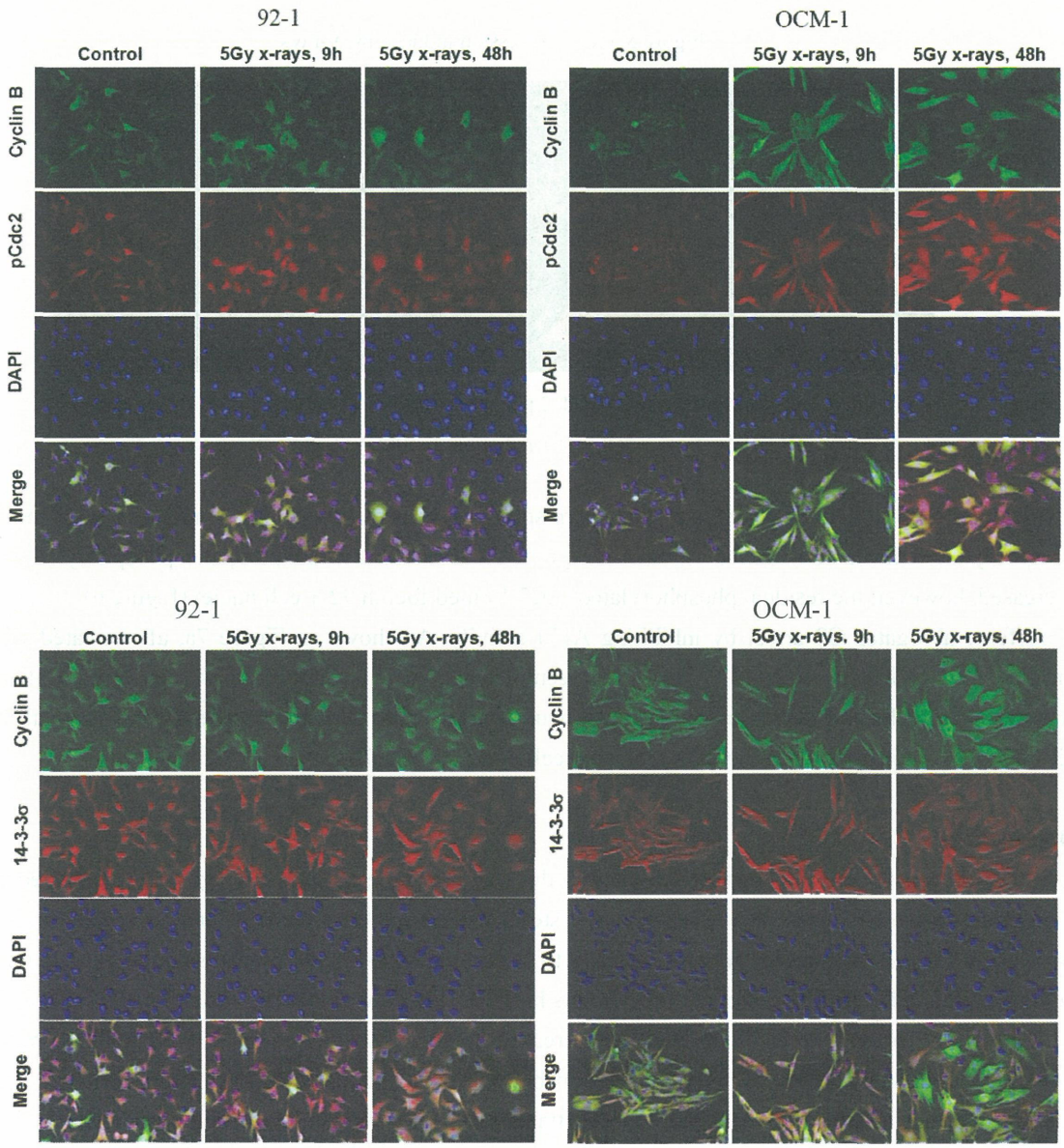

Figure 4. Immunofluorescence.

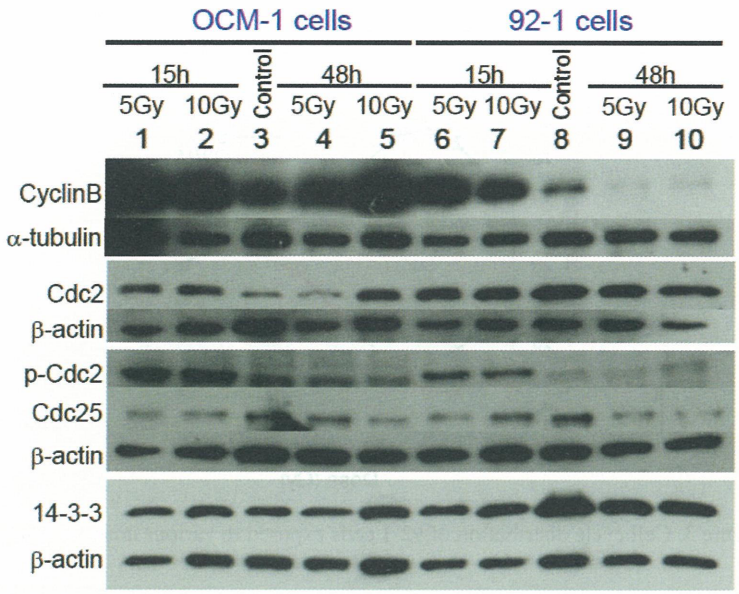

Figure 5. Gene expression induced by X-rays

Figure 6. Immunofluorescence of Cdc2 phosphorylated at Thr14 and Tyr15 in 92-1 cells.
A, control; B, 10 Gy X-rays, 9 h post-irradiation; C, 10 Gy X-rays, 48 h post-irradiation

Cdc25 in both cell lines was lower than corresponding control, which was consistent with the increased phosphorylaiton level of Cdc2 at Thr14 and Tyr15. At 48 h after irradiation, the phosphorylation of Cdc2 decreased, however, the residual phosphorylated Cdc2 formed foci in 92-1 cell nuclei (Figure 6).

Caffeine abrogates G2 arrest by inhibiting ATM activity. As shown in Figure 7a, after treated with 10mM caffeine, 92-1 cells exposed to 10 Gy of X-rays reentered cell cycle and apoptosis was activated. Caffeine *per se* is cytotoxic to cells and decreases cell survival. But despite of the toxicity of caffeine, the survival fraction of 92-1 cells was increased when the cells reentered cell cycle (Figure 7b).

Discussion

Cell cycle checkpoints are supposed to identify the level and type of DNA damage, arrest damaged cells at an appropriate phase and activate various repair systems to remedy their damage. It is a crucial self-protective mechanism for cells to monitor genome integrity to ensure the high-fidelity transmission of genetic information. In mammalian cells, loss of cell cycle checkpoints has been linked with genetic instability and cancer formation [20]. Abrogation of cell cycle block leads to increased apoptosis when combined with ionizing radiation [11]. However, controversy exists over the correlation between cell cycle and cellular radiosensitivity. One of the possible reasons is the cell types. Various cell types used by different research groups make it difficult for comparison, especially because the induction of apoptosis by caffeine [21], the sensitization of cells to ionizing radiation by pentoxifylline [12], and so on, are cell-type specific.

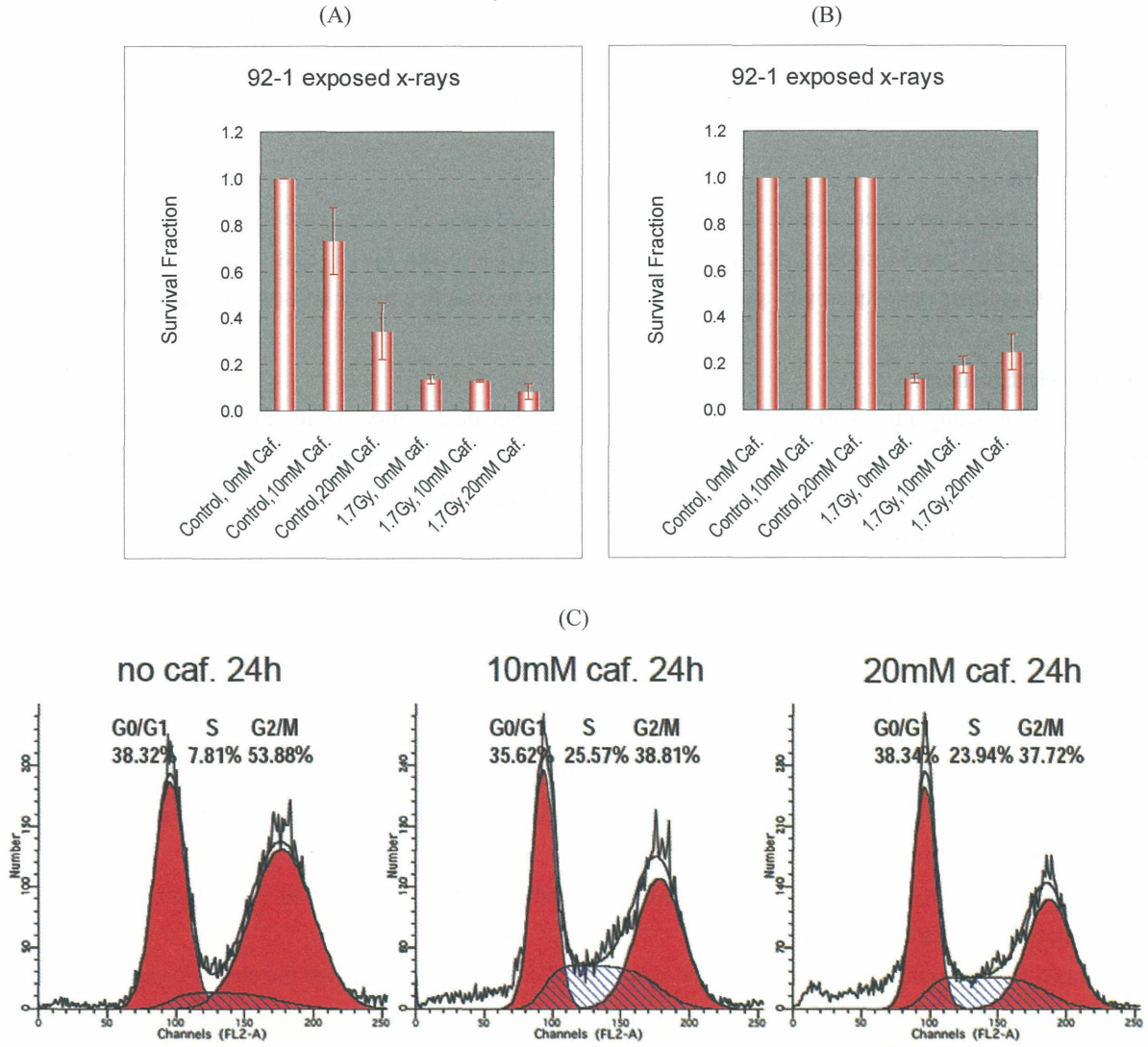

Figure 7. Survival of 92-1 cells exposed to 10 Gy of X-rays. 48 hours later after exposed to X-rays, cells were treated with caffeine for 24 hours, and then cell cycle distribution was examed with flow cytometry and colony-forming assay was performed to detect survival fractions. A, cells without any treatment were used as control; B, survival fractions of X-ray+caffeine treatment were normalized to corresponding samples treated only with caffeine. C, cell cycle distribution of 92-1 cells at 48 h after exposed to 10 Gy of X-rays.

The p53 status of two cell lines we used in present study have been well characterized by previous studies [22-24], which verified that 92-1 cells have wildtype p53 while OCM-1 cells have not. Recent discoveries have shown that the induction and maintenance of G2 arrest employ distinct mechanisms [25-28], with the former being p53-independent and the latter p53-dependent. Our results provided supportive data, which showed that both 92-1 and OCM-1 cells were blocked in G2 phase by ionizing radiation no matter of the p53 status. But, G2 arrest in OCM-1 cells were overcome in 48 hours while that in 92-1 cells last for 6 days.

The cell cycle block happened in 92-1 cells exposed to 10 Gy radiations was not a simple G2 block since the proportion of each phase remained stable and no more G1- or S- phase cells ran into G2 phase. It seemed that the cell cycle process ceased. Those cells with ceased cell cycle induced by 5 Gy of X-rays or 1.7 Gy of carbon beam were also out of cell cycle processing for hours (data no shown). Although Western blot revealed that degradation of CyclinB1 and the foci of phosphorylated Cdc2 might contributed to the cell cycle cease, further studies should be carried out to reveal further mechanisms.

Conventional colony forming assay reflects the proliferative death. Cell cycle cease blocks cell division and consequently reduces colony forming ability and survival fraction. Thus, 92-1 cells apprear radiosensitive to ionizing radiations. Cell cycle cease induced by ionizing radiation is related to cellular radiosensitivity. The mechanism of this novel phenomenon might provide *de novo* means to sensitize tumor cells to radiotherapy.

Conclusion

We report here a new phenomenon that ionizing radiation induces cell cycle cease following G2 arrest by degrading CyclinB1 and forming Cdc2 foci phosphorylated at Thr14 and Tyr15. This cell cycle cease might contribute to cellular radiosensitivity and provide new means to sensitize tumor cells to radiotherapy.

Acknowledgement

We thank Dr. Dong Yu, National Institute of Radiological Sciences, Chiba, Japan, for kind offer of some antibodies and valuable discussion, Dr. Cuihua Liu, Dr. Xing Cui and Dr. Koichi Ando from the same institute for their helpful suggestions. This work was supported by the Century Program of the Chinese Academy of Sciences, No. O760140BRO.

Reference

[1] El-Awady RA, Dikomey E and Dahm-Daphi J. Radiosensitivity of human tumour cells is correlated with the induction but not with the repair of DNA double-strand breaks. British Journal of Cancer. 2003; 89: 593-601.

[2] Barendsen GW. RBE-LET relationships for different types of lethal radiation damage in mammalian cells: comparison with DNA dsb and an interpretation of differences in radiosensitivity. International Journal of Radiation Biology. 1994; 66: 433-436

[3] Benotmane MA. Molecular aspects of individual radiosensitivity. Journal of Biological Regulators and Homeostatic Agents. 2004; 18: 357-62

[4] Khanna KK and Jackson SP. DNA double-strand breaks: signaling, repair and the cancer connection. Nature Genetics. 2001; 27: 247-254.

[5] Piwnica-Worms H. Cell cycle: Fools rush in. Nature. 1999; 401: 535-537.

[6] Bennett CB, Snipe JR, Westmoreland JW, Resnick MA. SIR functions are required for the toleration of an unrepaired double-strand break in a dispensable yeast chromosome. Molecular and Cellular Biology. 2001; 21: 5359-5373.

[7] Sasaki Y, Itoh F, Suzuki H, et al. Identification of genes highly expressed in G2-arrested Chinese hamster ovary cells by differential display analysis. Journal of Clinic Laboratory Analysis. 2000; 14: 314-319.

[8] Aldridge DR and Radford IR. Explaining differences in sensitivity to killing by ionizing radiation between human lymphoid cell lines. Cancer Research. 1998; 58: 2817-2824.

[9] Tamamoto T, Ohnishi K, Takahashi A, et al. Correlation between γ-ray-induced G2 arrest and radioresistance in two human cancer cells. International Journal of Radiation Oncology Biology Physics. 1999; 44: 905-909.

[10] Bache M, Pigorsch S, Dunst J, et al. Loss of G2/M arrest correlates with radiosensitization in two human sarcoma cell lines with mutant p53. International Journal of Cancer. 2001; 96:110-117.

[11] Bernhard EJ, Muschel RJ, Bakanauskas VJ, and McKenna WG. Reducing the radiation-induced G2 delay causes HeLa cells to undergo apoptosis instead of mitotic death. International Journal of Radiation Biology. 1996; 69: 575-584.

[12] Theron T, Binder A, Verheye-dua F and Bonm L. The role of G2-block abrogation, DNA double-strand break repair and apoptosis in the radiosensitization of melanoma and squamous cell carcinoma cell lines by

pentoxifyline. Internation Journal of Radiation Biology. 2000; 76: 1197-1208.

[13] Wang Q, Fan S, Eastman A, Worland PJ, Sausville EA, O'Connor PM. UCN-01: a potent abrogator of G2 checkpoint function in cancer cells with disrupted p53. Journal of the National Cancer Institute. 1996; 88: 956-65.

[14] Schwartz JL, Cowan J, Grdina DJ and Weichselbaum RR. Attenuation of G2-phase cell cycle checkpoint control is associated with increased frequencies of unjoined chromosome breaks in human tumor cells. Radiation Research. 1996; 146: 139-143.

[15] Xu B, Kim ST, Lim DS, Kastan MB. Two molecularly distinct G(2)/M checkpoints are induced by ionizing irradiation. Molecular and Cellular Biology. 2002; 22: 1049-1059.

[16] Playle LC, Hicks DJ, Qualtrough D, Paraskeva C. Abrogation of the radiation-induced G2 checkpoint by the staurosporine derivative UCN-01 is associated with radiosensitisation in a subset of colorectal tumour cell lines. British Journal of Cancer. 2002; 87: 352-358.

[17] Waard-Siebinga ID, Blom DR, Griffioen M, et al. Establishment and characterization of an uveal-melanoma cell line. International Journal of Cancer. 1995; 62: 155-161.

[18] Kan-Mitchell J, Mitchell MS, Rao N, Liggett PE. Characterization of uveal melanoma cell lines that grow as xenografts in rabbit eyes. Investigative Ophthalmol & Visual Science. 1989; 30: 829-34.

[19] Luyten GPM, Naus NC, Mooy CM, et al. Establishment and characterization of primary and metastatic uveal melanoma cell lines. International Journal of Cancer. 1996; 66: 380-387.

[20] Hartwell LH and Kastan MB. Cell cycle control and cancer. Science. 1994; 266: 1821-8.

[21] Blasina A, Price BD, Turenne GA, McGowan CH. Caffeine inhibits the checkpoint kinase ATM. Current Biology. 1999; 9:1135-1138.

[22] Matsumoto Y, Iwakawa M, Fursawa Y, et al. Gene expression analysis in human malignant melanoma cell lines exposed to carbon beams. International Journal of Radiation Biology. 2008; 84: 299-314.

[23] Jia L, Osada M, Ishioka C, et al. Screening the p53 status of human cell lines using a yeast functional assay. Molecular Carcinogenesis. 1997; 19: 243-253.

[24] Ma J, Wei F, Li H, et al. Detection of p53 gene mutations in 14 tumor cell lines. Chineses Journal of cancer Biotherapy. 2008; 15(2): 163-168.

[25] Desimone JN, Bengtsson U, Wang ZQ, Lao XY, Redpath JL and Stanbridge EJ. Complexity of the mechanisms of initiation and maintenance of DNA damage-induced G2-phase arrest and subsequent G1-phase arrest: TP53-dependent and TP53-independent roles. Radiation Research. 2003; 159: 72–85

[26] Melchionna R, Chen XB, Blasina A and McGowan CH. Threonine 68 is required for radiation-induced phosphorylation and activation of Cds1. Nature Cell Biology. 2006; 2: 762-765.

[27] Chan TA, Hermeking H, Lengauer C, Kinzler KW and Vogelstein B. 14-3-3Sigma is required to prevent mitotic catastrophe after DNA damage. Nature. 1999; 401: 616-620.

[28] Ohki R, Nemoto J, Murasawa H, et al. Reprimo, a new candidate mediator of the p53-mediated cell cycle arrest at the G2 phase. Journal of Biology Chemistry. 2000; 275: 22627-22630.

Cytometric Assessment of Histone H2AX Phosphorylation in Human Melanoma Cells Irradiated with Carbon Ions

Libin Zhou [1], Yoshiya Furusawa [2], Ryoichi Hirayama [2], Yoshitaka Matsumoto [2], Wenjian Li [1], Guangming Zhou [1], Qiang Li [1], Ping Li [1]

[1] *Biophysics Department, Institute of Modern Physics, Chinese Academy of Sciences, Lanzhou, China*

[2] *Research Center for Charged Particle Therapy, National Institute of Radiological Sciences, Chiba, Japan*

Corresponding Author: Yoshiya Furusawa, e-mail address: furusawa@nirs.go.jp

Abstract

The aim of this study is to investigate kinetic variation of histone H2AX phosphorylation (γH2AX) in human melanoma cells (OCM-1) after irradiation with carbon ions. We analyzed cell survival, cell cycle distribution and gamma H2AX immunofluorescence change using flow cytometry. Results suggested that γH2AX positive cells increased as a function of radiation dose (0.5-4Gy) followed by dose-dependent decay. In this study, we concluded that there was significant linear correlation between surviving fraction and residual γH2AX level in human melanoma OCM-1 cells 8 hours after carbon ion irradiations.

Introduction

During past 40 years, the incidence of melanoma increased substantially. Although melanoma only accounts for 10% of skin cancer, it is responsible for at least 80% of skin cancer death. It is reported that most melanomas have poor sensitivities in radiotherapy or chemotherapy [1]. Recently, high linear energy transfer (LET) charged particles therapy is an interesting approach for the treatment of melanoma because of its increased potential to kill low-LET radio-resistant cells [2].

DNA double-strand breaks are generally accepted to be the most important potentially lethal lesions produced by ionizing radiation. A method for the sensitive detection of individual double-strand breaks is based on measurement of a specific phosphorylation on histone H2AX, that occurs rapidly at the site of each double-strand break [3]. Antibody labeling of the phosphorylated form of H2AX (γH2AX) together with flow cytometry provides a rapid and objective method of quantifying this molecule after irradiation [4]. In contrast to other DNA damage assays (e.g., pulsed-field gel electrophoresis or comet assay), γH2AX can be used to detect double-strand breaks at therapeutic doses. Some researchers reported that the fraction of tumor cells retaining γH2AX foci 24h after X-irradiation has been correlated with the fraction of cells that survive to form a colony [5, 6]. The aim of this study was to evaluate the response of a melanoma cell line to carbon ion irradiations by determining γH2AX cytometric variation and cell colony survival.

Material and Methods

1. Cells

Human choroidal melanoma cells (OCM-1) were used in this study. OCM-1 cells were cultured in RPMI 1640 medium (Sigma) supplemented with 10% fetal bovine serum (FBS, Hyclone), 100 ug/ml

streptomycin and 100 units/ml penicillin (Gibco, Japan). Cells were incubated at 37℃ in a humidified atmosphere with 5% CO2.

2. Irradiation

Monolayer cell samples were irradiated with carbon ions generated by Heavy Ion Medical Accelerator in Chiba (HIMAC) of National Institute of Radiological Sciences (NIRS). The dose-averaged LET of carbon ion beams was selected to be 50keV/um.

3. Clonogenic assay

Clonogenic assay was measured by the standard colony formation method. Briefly, exponential growing cells were seeded in 60 mm dishes to form approximately 75 surviving colonies after 14 days of incubation. The colonies were fixed with 10% formalin and stained with 1% methylene blue. The surviving fraction was then calculated from the colony count.

4. Flow cytometry for histone H2AX phosphorylation

Cells were fixed in a solution of 1% methanol-free formaldehyde for 15 min on ice followed by suspension in 70% ethanol. Samples could be kept at -20°C for up to 2 weeks before analysis. Fixed samples were rehydrated in 1% BSA solution and incubated for 2 h with anti-gamma H2AX monoclonal antibody (Abcam, 1:200 dilution). Then samples were washed by centrifugation and resuspended for one hour in secondary Alexa fluor 488 conjugated goat anti mouse IgG (Invitrogen, 1:200dilution). After a second rinse, cells were resuspended in 10ug/ml Propidium iodide (PI; Sigma) to stain DNA. Analysis was conducted using BD FACS-Calibur. All samples staining-prepared should be analyzed within 24hr.

Results

In this study, we detected the kinetics of γH2AX in OCM-1 cells from 2hr to 16hr after carbon ion irradiation using flow cytometry. After reaching maximum levels 2 hr after irradiation, average γH2AX intensity decreased in OCM-1 cells over the next 16 h. However, values did not return to control levels after 16 hours after exposure. Figure 1 showed that γH2AX histograms shifted to the right side representing higher γH2AX intensity with the increasing irradiation doses.

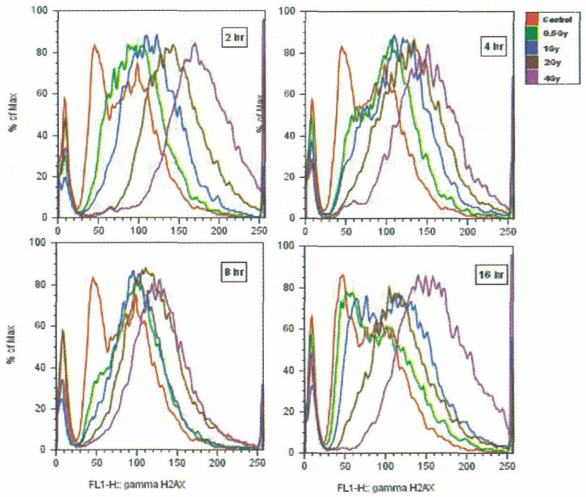

Figure 1. Variation in relative position of histogram representing gamma H2AX immunofluorescence intensities in OCM-1 cells irradiated by carbon ions with different doses.

Figure 2 represented the distribution of γH2AX positive cells after carbon ions irradiation. The maximum value occurred at 2hr after 4Gy irradiation, which was 77.02%, respectively. Then it decreased to 17.30% at 8hr. However, at 16hr the positive cells increased once more, to 32.18%. Possible reason for this tendency might be that most OCM-1 cells were arrested in G2/M phase 16hr after 4Gy irradiation (figure 4).

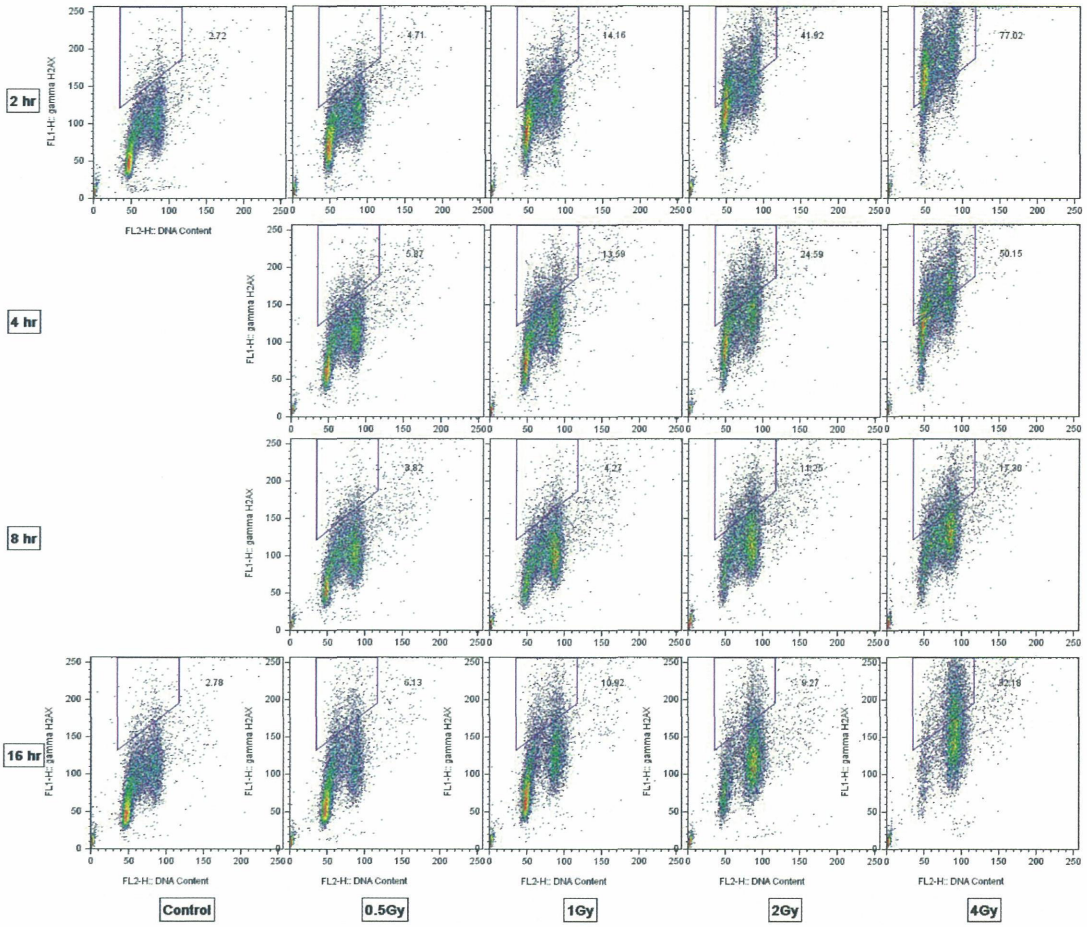

Figure 2. kinetic of histone H2AX phosphorylation in OCM-1 cells irradiated with carbon ions. Controls from 2hr, 4hr and 8hr groups did not have significant difference in this study(data not shown here).

To determine whether the residual level of γH2AX after irradiation might be related to survival assay, γH2AX expression measured in cells fixed at different time points after 0–4Gy were compared each other. The correlation between surviving fraction and the percentage of γH2AX positive cells at 8 h post-irradiation was analyzed (figure 3). Linear regression analysis revealed a significant correlation (R^2= 0.89, $p < 0.05$) between surviving fraction and the percentage of γH2AX positive cells.

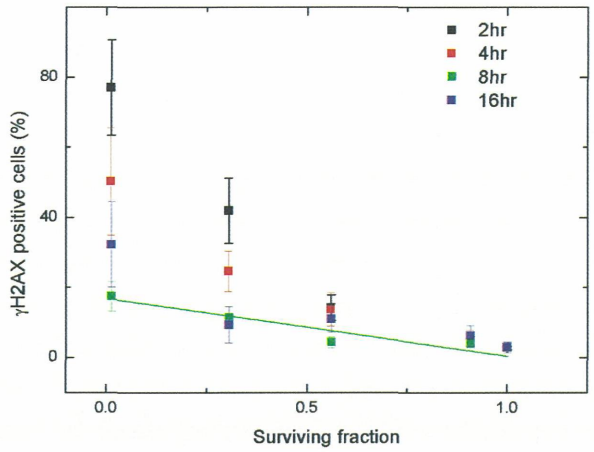

Figure 3. Correlation between surviving fraction and the percentage of γH2AX positive cells at different time points. Linear fitting for data of 8hr after irradiation, R^2=0.89, p< 0.05.

Meanwhile, we could analyze the variation of cell cycle distributions at different time points after irradiation (figure 4, table 1). Thus, to assess the mean extent of DNA damage (frequency of DSBs) for cells at a particular phase of the cycle, the mean values of γH2AX IF could be possible. Since we could calculate separately for G1, S, and G2/M cells by the computer-interactive "gating" analysis (data were not shown here).

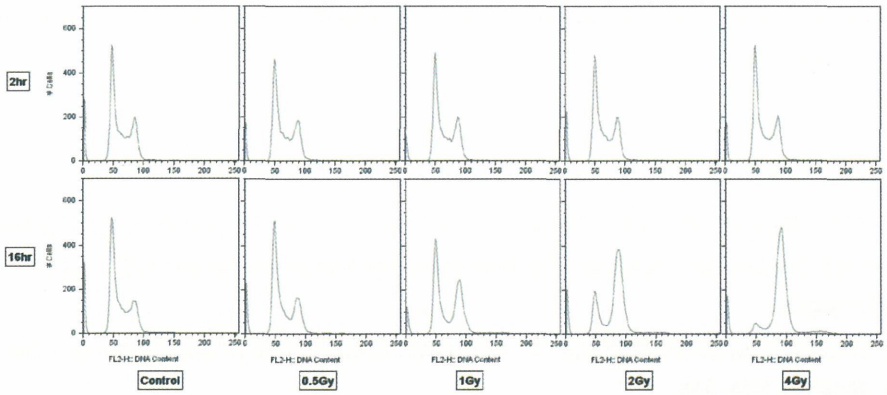

Figure 4. Cell cycle block of OCM-1 cells after carbon ion irradiation.

Table 1. Cell cycle distribution in OCM-1 cells after carbon ion irradiation with different dose.

Dose (Gy)	Time after irradiation (hr)	G0/G1 phase (%)	S phase (%)	G2/M phase (%)
0	2	54.60	2.01	29.91
	16	60.68	1.78	29.18
0.5	2	55.32	2.03	32.48
	16	59.86	1.73	31.02
1	2	56.98	2.14	32.77
	16	49.33	1.13	41.91
2	2	55.59	1.94	30.99
	16	23.75	0.61	62.86
4	2	56.80	1.96	31.46
	16	7.96	0.46	73.52

Discussion

Recently, γH2AX as an ultra-sensitive indicator of the presence of DSBs (sensitive even at the mGy level) has largely supplanted physical methods for the detection of DSBs [6]. Analysis of γH2AX has potential to provide useful information on tumor and normal cell response to ionizing radiation after exposure to clinically relevant doses of radiation [7]. It was reported that radiation sensitivity, measured as clonogenic-survival fraction after 2 Gy, was correlated with the fraction of γH2AX remaining 24 hours after irradiation [8]. There are two techniques to detect γH2AX: image analysis of γH2AX foci and immunocytochemistry with flow cytometry. Although image analysis of γH2AX foci containing thousands of molecules of γH2AX could make it possible to detect a single break within a nucleus, flow cytometry provides an accurate way of measuring the rate of formation and loss of γH2AX in heterogeneous populations of cells [9]. This study chose the immunocytochemistry with flow cytometry method to analyze the variation of H2AX phosphorylation after carbon ion irradiations.

Different researchers came from various study groups reported different conclusions about the relationship between surviving fraction and histone H2AX phosphorylation. Olive PL research group reported that analysis of γH2AX had the potential to provide useful information on tumor and normal cell response to ionizing radiation after exposure to clinically relevant doses of radiation [7]. Other researchers suggested that there was not a close correlation between residual γH2AX foci and radiosensitivity in some tumor cell lines, which showed high expression of endogenous phosphorylated H2AX foci [10]. However, in this study, we concluded that there was significant linear correlation between surviving fraction and residual γH2AX level in human melanoma OCM-1 cells 8 hours after carbon ion irradiations.

References

[1] Ivanov VN, Zhou H, Hei TK. Sequential treatment by ionizing radiation and sodium arsenite dramatically accelerates TRAIL mediated apoptosis of human melanoma cells. Cancer Res. 2007; 67: 5397–5407.

[2] Schulz-Ertner D, Jakel O, Schlegel W. Radiation therapy with charged particles. Semin Radiat Oncol. 2006;16: 249–259.

[3] Olive PL, Banath JP, Keyes M. Residual gammaH2AX after irradiation of human lymphocytes and monocytes in vitro and its relation to late effects after prostate brachytherapy. Radiother Oncol. 2008; 86:336-346.

[4] Klokov D, Macphail SM, Banath JP, Byrne JP, Olive PL: Phosphorylated histone H2AX in relation to cell survival in tumor cells and xenografts exposed to single and fractionated doses of X-rays. Radiother Oncol 2006; 80:223-229.

[5] Banath JP, MacPhail SH, Olive PL. Radiation sensitivity, H2AX phosphorylation, and kinetics of repair of DNA strand breaks in irradiated cervical cancer cell lines. Cancer Res. 2004, 64:7144-7149.

[6] Sedelnikova OA. Histone H2AX in DNA damage and repair. Cancer Biol. Ther. 2003; 2: 233-235.

[7] Olive PL. and Banath JP. Phosphorylation of histone H2AX as a measure of radiosensitivity. Int J Radiat Oncol Biol Phys. 2004; 58: 331-335.

[8] Banath JP, MacPhail SH, et al. Radiation Sensitivity, H2AX Phosphorylation, and Kinetics of Repair of DNA Strand Breaks in Irradiated Cervical Cancer Cell Lines. Cancer Res; 2004, 64: 7144-7149.

[9] Ismail IH, Wadhra TI, et al. An optimized method for detecting gamma-H2AX in blood cells reveals a significant interindividual variation in the gamma-H2AX response among humans. Nucleic Acids Res. 2007; 35: e36.

[10] Yoshikawa T, Kashino G, ONO K, et al. Phosphorylated H2AX Foci in Tumor Cells Have No Correlation with Their Radiation Sensitivities. Journal of Radiation Research. 2009; 50: 151-160

15 years experience of the carbon-ion production; stability and reliability of HIMAC

Atsushi Kitagawa, Takashi Fujita, Shigekazu Fukuda, Akifumi Fukumura, Takuji Furukawa, Taku Inaniwa, Yoshiyuki Iwata, Mitsutaka Kanazawa, Nobuyuki Kanematsu, Tadafusa Kumagae, Naruhiro Matsufuji, Shinichi Minohara, Hideyuki Mizuno, Shinichiro Mori, Takeshi Murakami, Masayuki Muramatsu, Koji Noda, Yukio Sakamoto, Shinji Sato, Toshiyuki Shirai, Eiichi Takada, Yuka Takei

Research Center for Charged Particle Therapy, National Institute of Radiological Sciences, Chiba, Japan
Corresponding Author: Atsushi Kitagawa, e-mail address: kitagawa@nirs.go.jp

Abstract

Over 4000 cancer patients have already been treated by the heavy-ion medical accelerator in Chiba (HIMAC) at the National Institute of Radiological Sciences (NIRS) since 1994. HIMAC has been required to realize a stable beam with the same conditions for daily operation, and has completely satisfied over 15 years. We report the status of the recent operation of HIMAC. The production of carbon ions is harder effort than other ion species for ion sources, especially. We summarize 15 years experiences of the carbon-ion production too.

Outline of the HIMAC facility

1. Origin of requirement

In early 1980's, the mortality from cancer became the first cause, and the number of cancer deaths in 1990's was estimated to be approximately 300 thousands in Japan. Because the weight of the advanced aged people was expected to become heavier in the composition of the population. Japanese government required development of new treatment methods for the cure of cancer patients to hold good for the "Quality of Life" of the patients after the treatment. The heavy ion radiotherapy was studied at Lawrence Berkeley Laboratory since 1950's, and it was promising expected to realize a new radiotherapy.[1] The heavy-ion medical accelerator in Chiba (HIMAC) project had been promoted by the Government as one of the projects of "Comprehensive 10 year Strategy for Cancer Control" which came into operation in 1984.

Since HIMAC was designed as the first medical dedicated heavy-ion accelerator complex in the world, the requirement for the medical use of heavy ion beam was not well-known. In addition, all of researchers, i.e., medical doctors, biologists, and physicists expected enough high potential for the future research. For ion species, Si or Ar ions were considered giving the highest oxygen gain factor. The maximum range of 25 cm and irradiation field of 15 x 15 cm were required, respectively. The maximum dose rate was 5 Gy/min effectively. An accelerator and a treatment delivery system had to satisfy enough stability and reproducibility. As a result, established principle, structure, and devices were chosen. New challenging technology was avoided as possible as we could.

2. Design concept and original specification

Although the 3D spot scanning method had been realized for the proton therapy at NIRS, the wobbler method was chosen as the beam delivery to obtain a good uniformity for trunk organs.[2] The beam irradiation system is comprised of a pair of scanning magnets (so called 'wobbler magnets'), a beam scatterer, a range shifter, a ridge filter, a multileaf collimator and several beam monitoring devices.[3] A pair of scanning magnets is orthogonal bending magnets and is used in association with a beam scatterer to form a uniform dose in the lateral distribution. A range shifter is a device which uses absorbers for the fine tuning of the ion range to conform the depth of the tumor. A multileaf collimator is a field-shaping device which tailors the beam according to the perpendicular cross section of the tumor. The beam compensator, so called 'bolus collimator', and the patient collimator in certain cases

are to be set just in front of a patient. In order to obtain a better dose distribution by the multi-direction irradiation, a treatment room has a horizontal and a vertical beam lines. In order to measure and count the irradiated dose, the principal and subordinate ionization chambers are placed separately as dose monitors. These are prepared to protect against overdose irradiation in case of either counter disabled. Flatness monitor comprises are to be monitored continuously to keep the uniform distribution of the beam intensity in the irradiated area. This method gives a simple way for control the irradiation dose. It's easy to stop, continue, and abort the treatment due to the unexpected failures. In addition, it's also suitable for any gated irradiation techniques.

The maximum beam energy of 800 MeV/u is supplied for the treatment. It gives a range of 30 cm in water for Si ions and was enough for making the above required irradiation field by the wobbler method. The synchrotron consists of two rings, which are installed in the upper and lower underground floors and are operated independently of each other except the alternate injection and excitation of magnets. The storage of radioactive isotope beams or the forming of quasi-continuous beam were the scope of future developments. The diameter and the circumference are 41 and 130 m, respectively. The maximum magnetic rigidity is 9.75 Tm. The bending magnets are of sector type and have the maximum field of 1.5 T. A multi-turn beam injection scheme is adopted to increase the beam current.[4] Although these parameters of synchrotron were orthodox without risks, later developments were still necessary. For irradiation treatment gated by respiration of a patient in order to minimize an unwanted irradiation to normal tissues around tumor, a special beam extraction system has been developed too.[5]

The beam is accelerated up to 6 MeV/u for injection into the synchrotron. This energy gives enough charge stripping efficiency for fully stripped Si ions by a thin carbon foil which is located just after the injector linac. An Alvarez linac was chosen as the final injector accelerator. The Alvarez linac is operated at a frequency of 100 MHz with the maximum repetition rate of 3 Hz and the maximum duty of 0.3 %. It is comprised of three independent RF cavities. Each cavity is operated at the same frequency with the RFQ linac with a peak rf power of 1.4 MW. The diameter of the cavity is about 2 m and the total length of the linac is 24 m. A 100 MHz debuncher cavity is installed in the beam transport line and the energy spread can be reduced within 0.2 %. An RFQ linac was installed before the Alvarez linac and accelerate the beam up to 800 keV/u for injection into the Alvarez linac. The RFQ linac is operated at the same frequency, repetition rate and duty.[6] This structure was expected low risk to manufacture.

The linacs accept ions with an energy of 8 keV/u and a charge-to-mass ratio 1/7 or larger. Two ion sources, one is a PIG ion source and the other is an ECR ion source, were originally installed for production of various ions. A PIG ion source is a hot cathode type. A typical magnetic field strength, a pole gap and a typical extraction voltage are 7 kG, 20 cm and 35 kV, respectively. The source is operated by the typical pulsed arc with a width of 400 ms. The peak discharge power is of 2 A. A 10 GHz NIRS-ECR ion source has a simple minimum B structure for the magnetic confinement of the plasma, which is attained by two mirror magnets and a permanent sextupole magnet. The maximum axial mirror field and radial sextupole field on the magnet surface are 9.3 kG and 9.0 kG, respectively. The maximum extraction voltage is 25 kV. Since the lifetime of PIG source is shorter than the ECR ion source, the 10 GHz NIRS-ECR is utilized to produce carbon ions for the clinical treatment.[7] The PIG ion source is mainly utilized to produce lighter ions or ions by spattering a solid material.

A patient's positioning system, and a treatment planning system are also important for the treatment system. The details of such systems have been described in references 8 and 9.

3. Control system

One of the most important aims of the control of HIMAC facility was to obtain enough stable beams with good reproducibility. The control system was designed under the policy of the passive and static ways. The active feedback system is not used as possible. All of the devices of the accelerator components are made controllable through a computer system. All of the parameters and measured values are digitalized and can be saved as a parameter file after beam tuning. Under the well-known condition, since the parameter set up can be obtained automatically, it is only needed for an operator to select the parameter file and to turn on the start-up button. In

order to realize the same beam trajectory with the same magnetic field, all transport magnets are set towards the well-established excitation pattern. Although this procedure takes several minutes, the merit to obtain a good reproducibility. This policy is also effective for the quality assurance and control.

Status of the operation of HIMAC

In a typical weekly schedule of beam time, the beam tuning starts up on Monday. Patients are treated during the daytime of weekdays. Every night and on weekend, beam time is available for general experiments. The accelerator facility is shut down in the night of Saturday or in the morning of Sunday. The maintenance and the research development without the beam are carried out in the daytime of every other Monday. The combination of two synchrotrons to form the quasi-continuous beam was developed, but it's not necessary for the daily treatment. Almost experimental users also preferred to use longer machine time or more various ion species instead of the continuous beam. Therefore, in order to use the two synchrotrons more effectively, the time-sharing acceleration system of the injector was developed to supply different ion beams to the two synchrotrons simultaneously. All magnets in the beam transport line were replaced for the pulse operation. Another ECR ion source was installed to produce intensive highly charged heavier ions like Fe, Kr, and Xe. The 18 GHz NIRS-HEC ion source has the similar structure as the 10 GHz NIRS-ECR, however the magnetic field and the extraction voltage are improved. As a result, three independent users can use different beams after the lower, upper synchrotrons and the linac.

HIMAC is stopped in two long research and maintenance periods per year. Large modifications or installations were done in these periods. The number of operation days is normally 250 days. About 180 days are occupied by the treatment. Fig. 1 shows the statistics of HIMAC operation in the financial year 2008. The injector linac (INJ) was operated for 5774 hours. This operation time includes the beam providing to the synchrotrons and individual experiments with the injector's energy beam. The operation time for the experiment was 884 hours. The upper synchrotron and the lower one (USY & LSY) were also operated for 5713 and 5724 hours, respectively. The operation time for the treatment was 3174 hours by the upper beam transport line and the lower one (UBT & LBT). The operation time for the experiment was 4582 hours too. The users including the treatment received the beam for 8640 hours per year, successfully. The ratio of failure to operation for INJ, USY, and LSY were 0.3 %, 0.2%, and 0.1%, respectively.

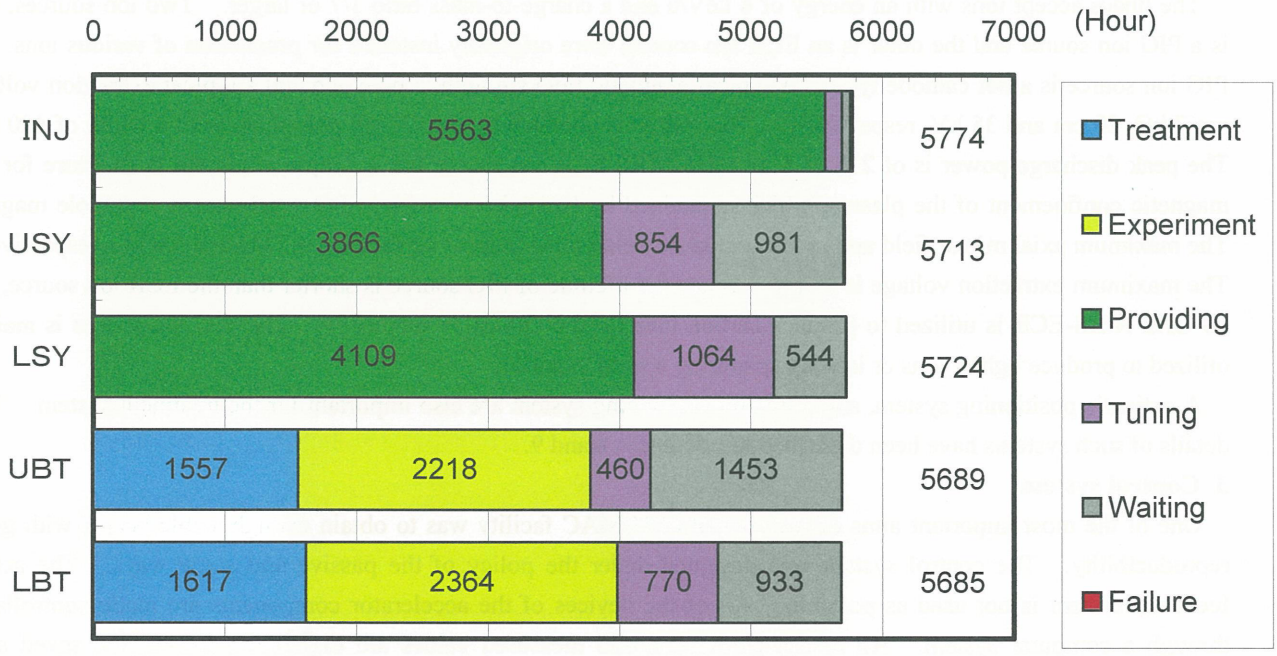

Fig. 1 Statistics of HIMAC operation (FY2008)

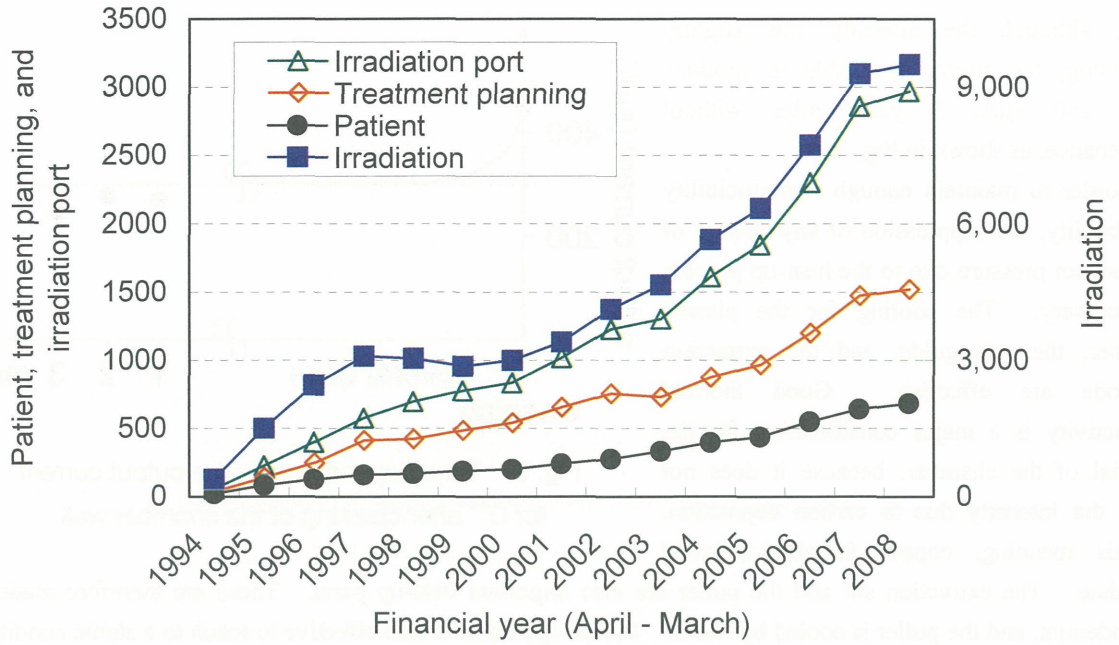

Fig. 2 Increasings of patients, treatment plannings, and irradiations

Fig. 2 shows the numbers of patient, treatment planning, and irradiation per year. At first, about 1000 irradiations per year were carried out in 1995. But now the total number of irradiation exceeded 9000. Although the capacity of irradiation mainly depends on the patient positioning time rather than the irradiation time, this increasing of irradiations clearly shows the evidence of the stable operation of the facility. On the other hand, the number of troubles of the irradiation system are increased as the number of patients.

Experience of producing carbon ions at HIMAC

1. Improvement of ion source

Although the best ion species principally depends on the tumor type and location and condition of the patient, the present facilities and almost all of the plans for heavy ion radiotherapy require a carbon beam due to its better biological dose distributions than helium or neon when the depth of a tumor and its thickness are 15 and 6 cm, respectively (typical conditions usually encountered). For almost components of the facility, it's not so different that the accelerated beam is carbon or not. However, for ion sources, the production of carbon ions is harder effort than other ion species. The performance of the 10 GHz ECR ion source is degraded due to carbon deposition on 1) an electric insulator, 2) the waveguide, 3) the plasma-chamber wall, and most of the other parts. This easy to prevent 1) since the insulator does not directly face the plasma or the beam. For the prevention of 2), it is effective that a simple rectangular waveguide is connected to the plasma chamber at the far position from the plasma. Microwaves are propagated in free space, and their transmission efficiency is worse in this way. Therefore, the chamber size must be sufficiently larger than the wavelength, and the power of the microwave amplifier must be sufficiently high. The deposition on 3) is normally unavoidable. This causes an 'anti-wall-coating effect', i.e. a decreasing of the beam, especially for the higher charge-state ions due to the surface material of the plasma-chamber wall. The ion source must be required to produce a sufficiently intense beam under the bad condition in which the wall is completely covered by carbon deposition. In order to supply carbon ions for clinical treatments at HIMAC, C^{2+} or C^{4+} ions are produced for daily clinical treatments, mainly by a 10GHz NIRS-ECR ion source. The record intensity has reached 430 eμA for C^{4+} under good conditions, just after a cleaning; however, the beam intensity decreases to about 300 eμA caused by rapid carbon deposition after several days. We performed the last cleaning on March 2004, and checked the intensity yearly. As a

result, although the intensity was slightly decreasing, the source was able to produce about 240 eμA, 3 years after without maintenance, as shown in Fig. 3.

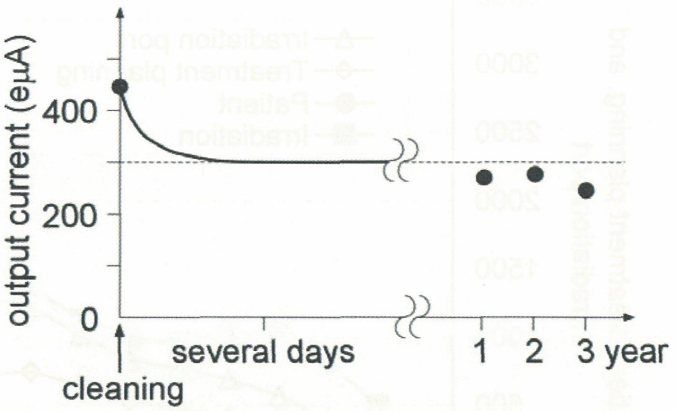

Fig. 3. Time dependence of the output current for C^{4+} after cleaning of the chamber wall.

In order to maintain enough reproducibility and stability, the suppression of any change of the vacuum pressure due to the heat-up process is necessary. The cooling for the plasma chamber, the waveguide, and the extraction electrode are effective. Good thermal conductivity is a major consideration for the material of the chamber, because it does not affect the intensity due to carbon deposition. In this meaning, copper is also a good candidate. The extraction slit and the puller are also important heat-up parts. These are therefore made of molybdenum, and the puller is cooled by water. Pulsed operation is also effective to reach to a stable condition as soon as possible. Although the beam intensity varies during the first few tens of minutes, it becomes fairly stable within 1 hour.

2. Effort to decrease failures

There are two types of the tendencies of the long-term variation of failures. One example is the case of the 10 GHz ECR ion source. This device's development was not completed at the design stage and it was necessary to improve by the commissioning. Fig. 4 shows the long-term variation on failures that have stopped beam production, or caused an instability. "Serious failures", which stopped the source operation for more than one day, and "Heavy failures", which required more than one hour for recovery, occurred during the early stage of operation. These were mainly due to bags of components, which have been improved. It was possible to recover from "Light failures" by resetting the parameters, or making small corrections, which also increased several years after. Since these are mainly due to aging deterioration, it can be managed by replacing any weak parts before their lifetime. It is also important to consider a reduction in the number of parts in the design. Failures of the klystron-based microwave amplifier account for one third of all the failures. It seems that the

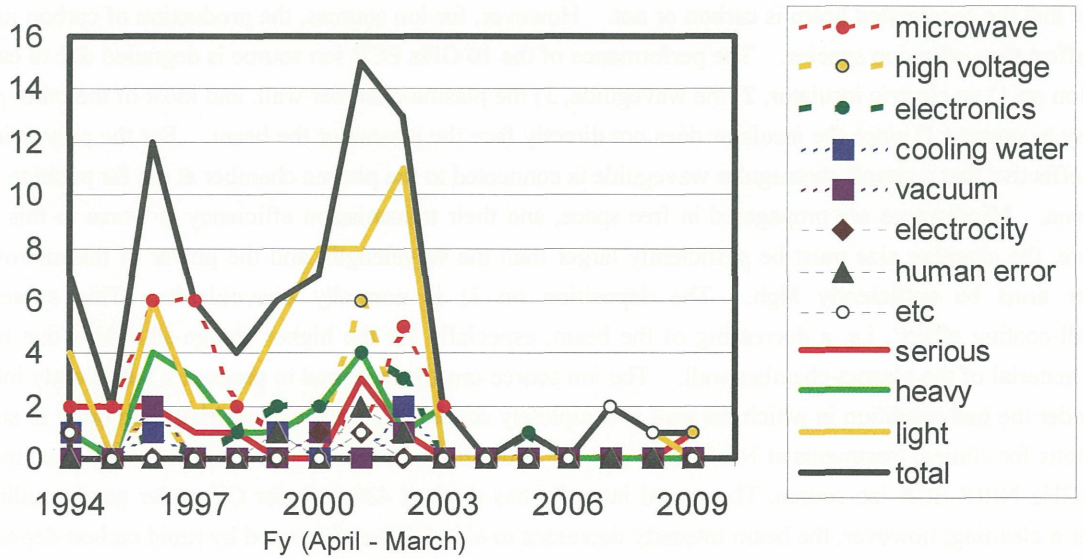

Fig. 4 Failure of 10 GHz ECR ion source

frequency of these failures is over the usual average. Finally, we aborted to use the old amplifier, and developed a new traveling-waveguide tube (TWT) amplifier with NEC microwave Co. Ltd. TWT has a smaller maximum power than that of the klystron. In the case of our microwave guide system, over 1 kW of microwave power is necessary to produce C^{4+} ions, due to the low transmission efficiency. We combined two 700 W TWT for the amplifier. Since the lifetime of TWT is expected to be over 15000 hours, the operational cost becomes cheaper. After we replaced the amplifier on August 2004, no failure has occurred at the microwave. So that, another medical facility, Hyogo, has also been replaced instead of old one. Gunma Univ. has adopted the same device too. Due to these improvements and maintenance, no serious or heavy failure had occurred for 4 years.

An example of another type of the tendencies of the long-term variation of failures is the failures at the irradiation system. If the probability of failures at each device does not change, these failures are proportional to the number of irradiations. In order to decrease such failures, the quality assurance (QA) and control in the daily operation are very important. The QA activity of the irradiation system was described minutely in Reference [11].

In July 2009, there was a serious failure on high-voltage after a long time. Although the precise analysis of the failure has not been completed, the cause is guessed as follows. The small leakage current was occurred due to the deterioration of electric isolation between the plasma chamber on the high-voltage and the yoke of mirror magnet and other parts on the ground potential. The current intensified the corrosion of cupper chamber and alumina insulator. It finally caused a large high-voltage breakdown. It seems such failure is categorized a long-term steady deterioration in the quality of parts 15 years after. We are afraid many parts will have more serious situations after 20 years since the construction.

References

[1] Biological and Medical Research with Accelerated Heavy Ions at the Bevalac, LBL-11220, UC-48, 1980.

[2] Chu WT, Ludewigt BA, Renner TR, Rev. Sci. Instrum. 64, 1993, 2055.

[3] Kanai T, Endo M, Minohara S, *et al.*, Biophysical Characteristics of HIMAC Clinical Irradiation System for Heavy-Ion Radiation Therapy. Int. J. Radiation Oncology Bio. Phys. 44, 1999, 201-210.

[4] Sato K, Yamada S, Ogawa H, *et al.*, Performance of HIMAC. Nuclear Physics A588, 1995, 229c-234c.

[5] Noda K, Kanazawa M, Itano A, *et al.*, Slow beam extraction by a transverse RF field with AM and FM. Nucl. Instrum. Meth. A374, 1996, 269-277.

[6] Murakami T, *et al.*, Proc. of 18th Intrnl. Linac Conf., Geneva, 1996, 830.

[7] Kitagawa A, Yamada S, Muramatsu M, *et al.*, Status of Ion Sources for the Heavy Iom Medical Accelerator HIMAC. Rev. Sci. Instrum., 1996, 67, 962-964.

[8] Minohara S, Kanai T, Endo M, *et al.*, Respiration gated irradiation system for heavy-ion radiotherapy. Int. J. Rad. Oncol. Bio. Phys. 47, 2000, 1097-1103.

[9] Endo M, Koyama-Ito H, Minohara S, *et al.*, HIPLAN – a treatment planning system at HIMAC. J. Jpn. Ther. Radiol. Oncol. 8, 1996, 231-238.

[10] Kitagawa A, Muramatsu M, Sekiguchi M, *et al.*, Status report on electron cyclotron resonance ion sources at the Heavy Ion Medical Accelerator in Chiba. Rev. Sci. Instrum., 2000, 71, 1061-1063.

[11] Torikoshi M, Minohara S, Kanematsu N, *et al.*, The current status of the treatment delivery at HIMAC. Proceedings of NIRS-ETOILE Joint Symposium 2009 on Carbon Ion Radiotherapy, Lyon, France, 136-144.

New Treatment Facility Project at HIMAC

Koji Noda, Takuji Furukawa, Taku Inaniwa, Yoshiyuki Iwata, Tatsuaki Kanai, Mitsutaka Kanazawa, Nobuyuki Kanematsu, Atsushi Kitagawa, Shinichi Minohara, Shinichiro Mori, Takeshi Murakami, Masayuki Muramatsu, Shinji Sato, Toshiyuki Shirai, Eiichi Takada, Yuka Takei, Masami Torikoshi

Research Center for Charged Particle Therapy, National Institute of Radiological Sciences, Chiba, Japan
e-mail address:noda_k@nirs.go.jp

Abstract

The first clinical trial with carbon beams generated from HIMAC was conducted in June 1994. The total number of patients treated was in excess of 4,000 as of June 2008. The impressive advance of carbon-ion therapy using HIMAC has been supported by high-reliability operation and by the development of accelerator technology. Based on more than ten years of experience with HIMAC, we have proposed a new treatment facility for the further development of therapy with HIMAC. The new facility, as an extension of the existing one, has been designed, and the related R&D work has been carried out. The following descriptions give a summary account of the design study and the related R&D work for this new treatment facility at HIMAC.

1. Introduction

Heavy-ion beams are very suitable for the treatment of deeply seated cancer because of an excellent physical-dose distribution and high-LET characteristics around the Bragg peak. Therefore, NIRS decided to carry out heavy-ion cancer therapy with HIMAC [1]. The first clinical trial of cancer treatment with carbon beams was conducted in June 1994. The total number of patients treated until June 2008 was more than 4,000. Based on more than ten years of experience with HIMAC, we have proposed a new treatment facility toward adaptive cancer therapy [2] with heavy ions, making the one-day treatment of lung cancer possible. Further, the new treatment facility should accurately treat a fixed target, a moving target with breathing and/or a target near a critical organ. For these purposes, a 3D-scanning method with a pencil beam is employed in the new treatment facility. A phase-controlled rescanning (PCR) method [3] has been proposed and studied, especially for treating a moving target. A rotating gantry with the PCR method [4] is also employed in order to reduce the patient's load, such as face-downward position during patient positioning, and to increase treatment accuracy for a tumor near a critical organ through multi-field optimization [5]. In addition, we have designed the beam-delivery system, the rotating gantry system, the treatment flow including patient positioning and the facility planning. The related R&D work has also been carried out with HIMAC since 2006. We review the design study and the related R&D work for the new treatment facility at HIMAC.

2. Design consideration

In HIMAC treatments, we have observed shrinkage of the target size as well as a change in its shape during the entire treatment. In order to keep the sophisticated conformations of the dose distributions even in such cases, it has been required that treatment planning is carried out just before each fractional irradiation, which we

call adaptive therapy. For this purpose, 3D scanning with a pencil beam should be employed, because it does not use any bolus and patient collimators, which take a long time to be manufactured. It is also well-known that 3D scanning has brought about a high treatment accuracy in the case of a fixed target [6]. However, this method has not yet been applied to treating a moving target with breathing in practical use. Therefore, we have developed the PCR method to treat a moving target, as mentioned in 3.1.

A ^{12}C beam is mainly used for treatments that have been carried out in the existing HIMAC treatment. Different ion species will also be employed for the further development of HIMAC therapy. Thus, the maximum ion energy is designed to be 430 MeV/n in both the horizontal and vertical beam-delivery systems, in order to obtain more than the residual range of 30 cm in a ^{12}C beam and more than that of 22 cm in an ^{16}O beam. The maximum lateral field and SOBP sizes are 25 cm × 25 cm and 15 cm, respectively, in order to cover almost all treatments with HIMAC [7]. On the other hand, the rotating gantry system employs a maximum energy of 400 MeV/n, a maximum lateral field of 15 cm × 15 cm, and a maximum SOBP size of 15 cm in order to downsize the gantry. Further, positron-emission beams, such as ^{11}C and ^{15}O, will be used to verify the irradiation area and their ranges in a patient's body. At HIMAC, R&D work has been carried out in order to obtain positron-emission beams accelerated directly through the HIMAC accelerator [8], instead of using the projectile-fragmentation method.

The new treatment facility is connected with the upper synchrotron at HIMAC. In the treatment hall, placed underground of the facility, three treatment rooms are prepared in order to treat more than the present number of patients with the HIMAC treatment. Two of the treatment rooms are equipped with both horizontal and vertical beam-delivery systems, and the other one is equipped with a rotating gantry. Two treatment-simulation rooms are also equipped for patient positioning as a rehearsal, and for observing any change in the target size and shape during the entire treatment period with an X-ray CT. Furthermore, there are six rooms devoted to patient preparation before irradiation. A schematic view of the new treatment facility is shown in Fig. 1.

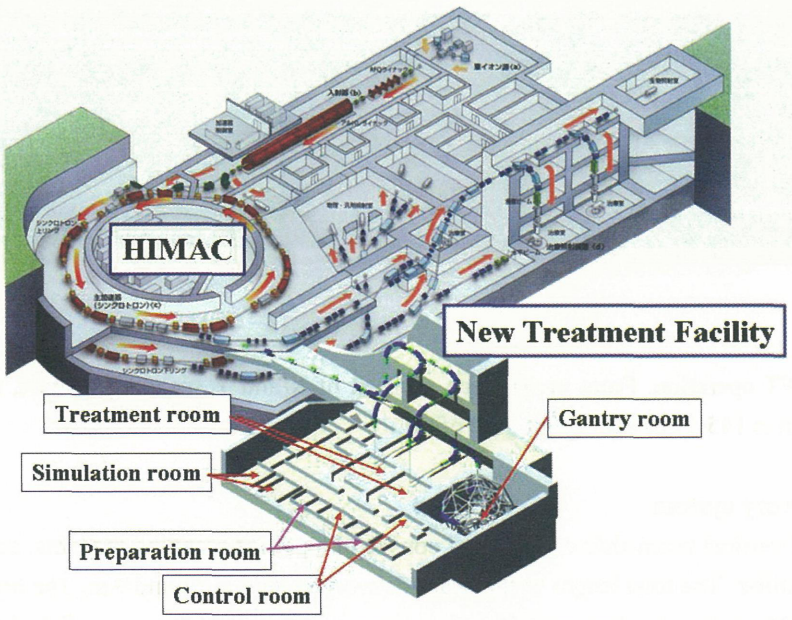

Fig. 1. Schematic view of the new treatment facility and the present HIMAC.

3. Design study and R&D work

3.1 Development of the HIMAC accelerator

The beam intensity from the HIMAC synchrotron has been increased in order to complete one fractional irradiation with one cycle of synchrotron operation. In this case, the efficiency of the gated irradiation will be increased by extending the flattop duration, which will save considerable irradiation time. In order to increase the beam intensity, we have thus carried out a tune survey during beam injection. As a result, it was found that the 3rd-order coupling resonance caused beam loss. This resonance was corrected by four sextupole magnets, and the beam lifetime was increased by more than 5 times. Further, we tried multi-harmonics operation of the RF acceleration system in order to suppress the space-charge effect after bunching. This operation increased the acceleration efficiency by around 40% [9]. Consequently, around 2×10^{10} carbon ions can be accelerated to the final energy. This intensity is sufficiently high to irradiate almost all tumors treated with HIMAC when using the 3D-scanning method with a beam-utilization efficiency of more than 90%. The extended flattop operation was successfully tested at the HIMAC synchrotron. In the scanning experiment described in 3.4, the flattop duration was successfully extended to around 25 s from 2 s used in routine operation, as shown in Fig. 2. Further, the beam profiles during an extraction duration of 100 s were measured by a multi-wire proportional counter in the high-energy beam-transport line. From the results of an analysis of the measurement, it was estimated that both the position and the size for the extraction duration of 100 s were stabilized within ±0.5 mm at the iso-center.

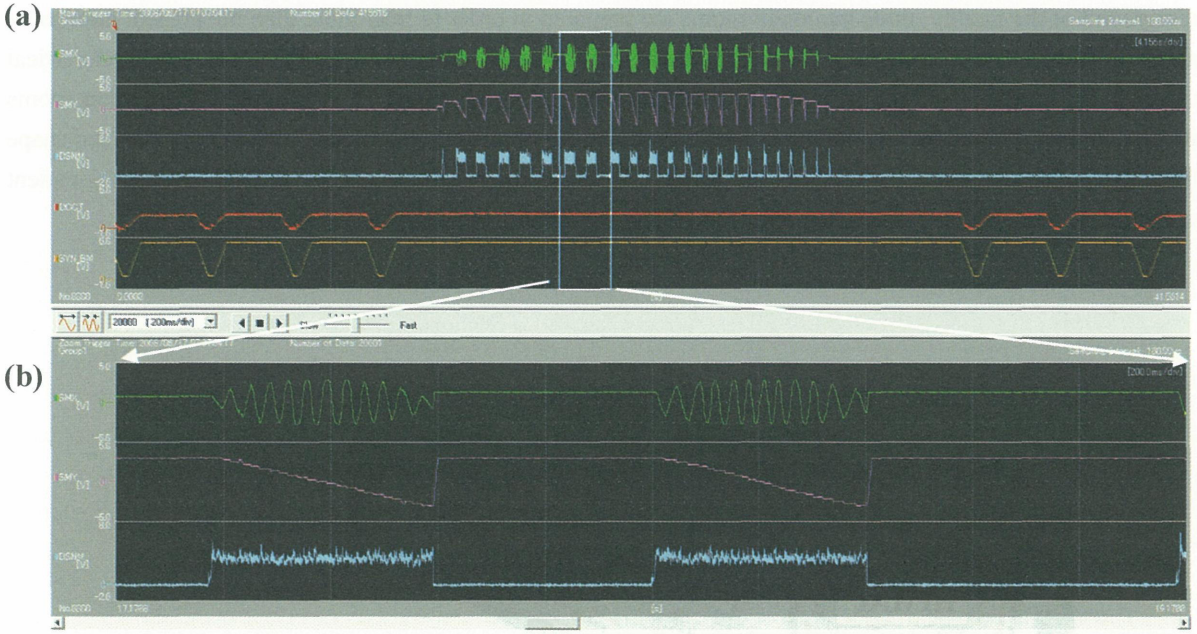

Fig. 2. (a) The extended FT operation. From upper trace, Current of X and Y scanning magnet, the extracted beam current. The full span is 145 s. (b) Enlarged figure of (a).

3.2 Design of beam-delivery system

Both the horizontal and vertical beam-delivery systems consist of a pair of scanning magnets, dose monitors, a ridge filter and a range shifter. The total length of the beam-delivery system is around 9 m. The beam-scanning speed is designed to be 100 mm/ms for fast scanning. Two dose monitors, which are parallel-plate ionization chambers with an effective area of 250 mm^2, are used for dose management. The beam position and size are monitored by multi-wire proportional counters. Considering the slice thickness, the Bragg peak is slightly

spread out by a mini ridge filter. The range shifter is utilized to change the slice in the target. Thus, the range shifter should be as close as possible to the iso-center in order to avoid any change of the beam size by multiple scattering through the range shifter. Ref. [3] describes its design in detail and the beam-delivery system is shown in Fig. 3. In order to verify the proposed 3D-scanning method, a test bench of the beam delivery system with 3D-scanning method has been constructed in the physics experimental hall at HIMAC.

In the present design, the rotating gantry employs a pencil-beam raster scanning, which is identical to the one used for the horizontal and vertical beam-delivery systems. It is important for the gantry design to avoid any change in beam size in accordance with the rotation angle. Thus, we will adapt a compensation method of asymmetric phase-space distribution [10]. This method is based on multiple scattering by a thin foil placed at the position with optimum beam-optical parameters in the beam-transport line. Further, the final dipole magnet is divided into 30-degree and 60-degree magnets, and two scanners are placed between the two magnets in order to extend the effective length from the scanners to the iso-center. The total weight of the gantry system is around 350 tons.

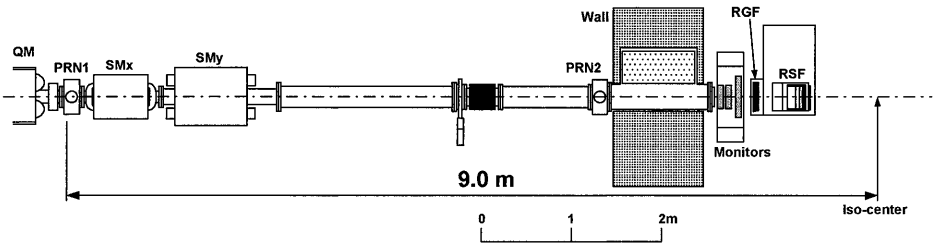

Fig. 3. Test bench of beam-delivery system

3.3 Verification of PCR method

In 3D pencil-beam scanning, an interplay effect between the scanning motion and the target motion brings about hot and/or cold spots in the target volume, even when using the gated irradiation method [11], because the sizes of the distal and lateral dose profiles of the pencil beam are comparable to the residual motion range. The PCR method, therefore, which is combined with the rescanning technique and gated irradiation, is employed in order to avoid producing hot/cold spots. In the PCR method, rescanning on a slice is completed during one gate generated in the respiration period of the patient's breathing. Since the moving target position is averaged in both the lateral and distal directions, the hot and/or cold spots are not produced. The rescanning method requires a relatively large number of scans, which cause a relatively long irradiation time. Based on the uniform time structure of a beam extracted from the HIMAC synchrotron, we have thus developed a novel optimization technique for fast scanning in order to shorten the irradiation time, in which extra exposure during the transition of each spot is taken into account [12]. The result of a simulation study showed that the PCR method provided a feasible solution in which a dynamic beam-intensity control technique [13] based on the RF-KO slow extraction method [14] plays an important role for adequately controlling the phase correlation under a relatively small number of rescanning procedures. In the PCR method, it is noted that the irradiation time for each depth slice should be adjusted to be within 1-2 s of the respiration gate duration. Consequently, we obtained a feasible solution for a moving target irradiation by fast raster-scanning method with rescanning and gating functions.

3.4 Scanning experiment

Since 3D-scanning is one of the key technologies for the PCR method, we carried out a fast raster-scanning experiment by using the HIMAC spot-scanning test line [15]. The irradiation control system was slightly

modified so as to be capable of raster scanning irradiation instead of spot scanning irradiation. At the present stage, we have adapted the measured dose response of the pencil beam with an energy of 350 MeV/n, corresponding to a 22-cm range in water. The beam size at the entrance and the width of the Gaussian-shaped mini-peak were 3.5 and 4 mm at one standard deviation, respectively. The validity of the beam model and the optimization calculation had already been verified experimentally [12]. Using the dynamic intensity control system, the beam intensity was kept almost constant during irradiation. In the experiment, a spherical target of 4 cm in diameter was irradiated so as to produce a uniform physical dose field. The measured dose distributions were in good agreement with the calculation result at different penetration depths.

4. Summary

At the HIMAC accelerator complex, beam studies were carried out especially for increasing the irradiation accuracy and treatment efficiency. As a result, we were able to upgrade the performance of the HIMAC accelerator complex. Based on this upgrade, we have proposed a new project for further development of heavy-ion therapy with HIMAC, entailing the construction of a new treatment facility. The new treatment facility has three treatment rooms: two rooms are equipped with horizontal and vertical beam-delivery systems equipped with a 3D pencil-beam scanning capability, and the other with a rotating gantry with a 3D pencil-beam scanning capability. The beam-scanning irradiation method uses the PCR method with a fast scanning performance. These developments have made continuous successful progress since 2006.

References

[1] Y. Hirao et al., Nucl. Phys. A 538, 541c–550c (1992).

[2] K. J. Halverson et al., Int. J. Radiat. Oncol. Bio. Phys. 21:1327-1336 (1991).

[3] T. Furukawa, T. Inaniwa, S. Sato, T. Tomitani, T. Minohara, K. Noda, T. Kanai, Med. Phys. 34 (3), 1085-1097 (2007).

[4] T. Furukawa, T. Inaniwa, S. Sato, Y. Iwata, S. Minohara, K. Noda, T. Kanai, in these proceedings.

[5] A. Lomax, Phys. Med. Biol. 44:1219-1226 (1999).

[6] Th. Haberer, W. Becher, D. Schardt, G. Kraft, Nucl. Instrum. Meth. A 330, (1993) 296-305.

[7] K. Noda et al., J. Rad. Res., 48 (2007) A43-A54.

[8] S. Hojo, T. Honma, Y. Sakamoto, S. Yamada, Nucl. Instrum. Meth. B 240 (2005) 75.

[9] C. Ohomori et al., Nucl. Instrum. Meth. A 547 (2005) 251.

[10] T. Furukawa and K. Noda, Nucl. Instrum. Meth. A 565 (2006) 430.

[11] S. Minohara, T. Kanai, M. Endo, K. Noda and M. Kanazawa: Int. J. Rad. Oncol. Bio. Phys. 2000;47:1097-1103.

[12] T. Inaniwa, T. Furukawa, T. Tomitani, S. Sato, K. Noda, T. Kanai, Med. Phys. 34 (8) 3302-3311 (2007).

[13] S. Sato, T. Furukawa, K. Noda, Nucl. Instrum. Meth. A 574, (2007) 226-231.

[14] K. Noda et al., Nucl. Instrum. Meth. A 374 (1996) 269.

[15] E. Urakabe et al., Jpn. J. Appl. Phys. 40 (2001) 254.

Treatment Planning for Scanned Carbon Ion Beams

Nobuyuki Kanematsu, Taku Inaniwa, Takuji Furukawa, Shinji Sato, Shinichiro Mori,
Takehiro Tomitani, Shinichi Minohara, Koji Noda, Tatsuaki Kanai

Research Center for Charged Particle Therapy, National Institute of Radiological Sciences, Chiba, Japan
Corresponding Author: Nobuyuki Kanematsu, e-mail address: nkanemat@nirs.go.jp

Abstract

In order to use an intensity-controlled raster scan method at the new treatment facility in HIMAC, we have developed a novel code system dedicated to the planning of radiotherapy with the scanned ^{12}C beam. The variation of beam-spread in the direction lateral to the beam axis and non-collinearity of the beam by scanning magnets in the horizontal and vertical directions are considered in the beam model. Inverse planning techniques are implemented in the software in order to obtain the uniform biological dose distribution within the planned target volume (PTV) as well as reduce the dose delivered to the organ at risks (OARs) delineated on clinical CT images. The scan trajectory is determined so that the path length will be minimized by applying a fast simulated annealing algorithm for scan trajectory optimisation. Furthermore, the extra dose inevitably delivered to the irradiated site is integrated into the inverse planning process to shorten the treatment time. The code also copes with the planning for intensity modulated ion therapy (IMIT). Treatment plans were produced for several CT images of the patients treated at HIMAC. The beam steering file is produced with the software in which the position and particle fluence for each raster point is written following the optimised scan trajectory. The reliability of the developed code has been confirmed through the irradiation experiments according to the beam steering file at the secondary beam line in HIMAC.

1. Introduction

A project to construct a new treatment facility as an extension of the existing Heavy-Ion Medical Accelerator in Chiba (HIMAC) facility has been initiated for further development of carbon-ion therapy at the National Institute of Radiological Sciences (NIRS) [1][2]. The new treatment facility will be equipped with three treatment rooms, two of them will provide the horizontal and vertical fixed beam ports, and another one a rotating gantry [3][4]. In all rooms, three-dimensional (3D) irradiation with pencil beam scanning [5] will be utilized in order to make full use of the advantages of heavy-ion therapy such as high dose concentration and high relative biological effectiveness (RBE) around the Bragg peak. This method has already been implemented for clinical use at the Paul Scherrer Institute (PSI) with protons [6] and the Gesellschaft für Schwerionenforschung mbH (GSI) with carbon ions [7]. In the method, a pencil beam is scanned in both the transverse (x and y) and longitudinal (z) directions within the target volume. The former can be achieved by a pair of deflection magnets while the latter can be achieved either by the insertion of range shifter plates, as used at the PSI, or active energy variation of a synchrotron as developed by the GSI. The range shifter plates will be used in the new treatment facility because of its capability to change the beam-stopping position within a few hundred milliseconds. The effect of the additional beam spread and the increase of the projectile fragments due to the insertion of the range shifter plates has to be included in the dose response function of the scanned beam. In addition, we will continue to use the RBE model for therapeutic carbon beams developed and verified by the clinical results obtained over the last 10 years in HIMAC [8][9]. Furthermore, in the facility, we intend to treat

not only static tumors but also moving tumors with the scanned carbon beam by using gated irradiation [10] and re-scanning methods in the run-up to establishment of other facilities [2][11]. In order to fulfill all of these requirements and produce a beam steering file, we have to develop an inverse planning code dedicated to radiotherapy with the scanned ^{12}C beam which suits for the unique scanning system designed at the new treatment facility in HIMAC. This paper describes the basic principles of the code.

This paper is structed as follows. The physical beam model employed in the treatment planning is described in section 2.1. The principle of the biological dose calculation and its incorporation into the software is shown in section 2.2. The dose optimization method is briefly described in section 2.3 and the flow of the treatment planning is shown in section 2.4. Some typical planning results are shown in section 3 both for single field planning and the intensity modulated ion therapy (IMIT) planning. The strategies for planning quality assurance (QA) and beam monitor unit (MU) calibration will be presented in section 4, and finally the study findings are summarized in section 5.

2. Methods and Materials

2.1. Beam Model

In 3D irradiation with pencil beam scanning, the prescribed dose distribution can be achieved by superimposing the dose of the individual pencil beams d with different stopping positions according to the optimized weights w for these beams. The beam model employed in the developed tool is described here.

The Bragg peak of the pristine beam is slightly broadened to produce a "mini peak" by the ridge filter, and is used as a pencil beam. In the new treatment facility, pristine beams with about 10 individual energies will be prepared between 140 MeV/u to 430 MeV/u. We assume that the x and y coordinates denote the horizontal and vertical directions and the z coordinate the direction parallel to the beam axis. Then, the 3D dose response $d(x_i,y_i,z_i;x_0,y_0,z_0)$ at a point (x_i,y_i,z_i) delivered by the pencil beam centered at (x_0,y_0,z_0) can be split into three components, two components in lateral directions, $d_x(x_i;x_0,\sigma_x(z_i;z_0))$ and $d_y(y_i;y_0,\sigma_y(z_i;z_0))$ and one, $d_z(z_i;z_0)$, in parallel to the beam direction, and represented as follows:

$$d(x_i,y_i,z_i;x_0,y_0,z_0)=d_x(x_i;x_0,\sigma_x(z_i;z_0))d_y(y_i;y_0,\sigma_y(z_i;z_0))d_z(z_i;z_0) \quad (1)$$

Here, $d_x(x_i,x_0,\sigma_x(z_i;z_0))$ and $d_y(y_i,y_0,\sigma_y(z_i;z_0))$ are the normalized Gaussian functions with standard deviations $\sigma_x(z_i;z_0)$ and $\sigma_y(z_i;z_0)$ representing the beam spread at a depth z_i described by

$$d_x(x_i,x_0,\sigma_x(z_i;z_0))=\frac{1}{\sqrt{2\pi}\sigma_x(z_i;z_0)}\exp\left(-\frac{(x_i-x_0)^2}{2\sigma_x(z_i;z_0)^2}\right) \quad (2)$$

and

$$d_y(y_i,y_0,\sigma_y(z_i;z_0))=\frac{1}{\sqrt{2\pi}\sigma_y(z_i;z_0)}\exp\left(-\frac{(y_i-y_0)^2}{2\sigma_y(z_i;z_0)^2}\right) \quad (3)$$

, respectively. On the other hand, $d_z(z_i;z_0)$ is the integerated dose at a depth of z_i derived by integrating the dose response over the plane perpendicular to the beam axis (x-y plane) as

$$\iint d(x_i,y_i,z_i;x_0,y_0,z_0)dxdy=d_z(z_i;z_0) \quad (4)$$

In 3D irradiation with pencil beam scanning, a pencil beam is scanned in both the transverse (x and y) and longitudinal (z) directions within the target volume. The beam scan in the transverse direction can be achieved using horizontal and vertical deflection magnets. The non-collinearity of the beam transport axis passing through the position (x_0, y_0) on the isocenter plane from the deflection magnet is represented by substituting x_0 and y_0 with $x_0'(z_i)=\left(1+\frac{z_i-z_{isocenter}}{L_x}\right)x_0$ and $y_0'(z_i)=\left(1+\frac{z_i-z_{isocenter}}{L_y}\right)y_0$ in equations (2) and (3), where $z_{isocenter}$, L_x and L_y are the position of the isocenter in z coordinate, the distance from the horizontal and vertical deflection magnets to the isocenter. On the other hand, the beam scan in the longitudinal direction can be achieved either by the insertion of range shifter plates or by active energy variation of the synchrotron.

In order to change the beam stopping position within a few hundred milliseconds, range shifter plates made of PMMA will be used in the new treatment facility. In this case, the integrated dose distribution, $d_z(z_i;z_0)$, is almost shift-invariant, i.e. the beam flux as well as the production of the fragment particles are almost constant, since water-equivalent thickness of the intervening material is constant. In the software, $d_z(z_i;z_0)$ measured with a large-area parallel plate ionization chamber (PPIC) at several depths are interpolated and used to obtain the value for a given depth z_i, as shown in Figure 1 for the ^{12}C pencil beam of 350 MeV/u. The PPIC has a sensitive area of 120 mm diameter, which was large enough to cover the whole beam diameter. The slight deviation of the bean flux due to the difference between total reaction cross-section of PMMA and that of water is corrected according to the thickness of the inserted range shifter plate. With regard the lateral distribution of the beam, it was found that the additional beam spread resulted from the insertion of range shifter plates due to the multiple scattering of the beam inside the plates. This effect may be negligible if the range shifter is positioned close to the isocenter, while it is pronounced as the distance between them increases. The variation of the lateral beam spread, i.e., $\sigma_x(z_i;z_0)$ and $\sigma_y(z_i;z_0)$, were determined from the measured beam spread as a function of the depth z for various thicknesses of the range shifter plates as shown in Figure 2 for the horizontal direction. They were fitted to a simple formula as a function of depth z and the maximum range z_0 determined from the thickness of the range shifter plate, and incorporated into the planning tool. With this algorithm, the effect of the beam spread due to multiple scattering in range shifter can be incorporated, at least for the primary particles. When the range shifter was set far from the isocenter, the additional spread of the fragment particles generated in the plate has the potential to cause the field-size dependence of the physical doses as reported by Kusano *et al.* [12]. However, the RBE for lighter fragments is relatively small comparing to that for primary particles, hence, we expect that the effect is negligible concerning to the biological dose distribution. The assessment of the effect is still remained in the future work.

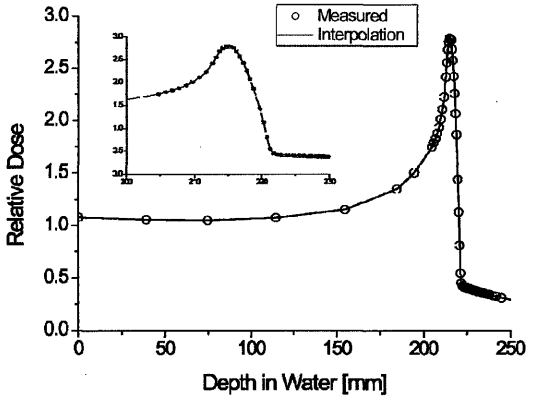

Figure 1: Dose distribution of a pencil beam measured with the PPIC (circles) as a function of depth z_i in water. The measured data were interpolated and used as the integrated dose $d_z(z_i;z_0)$.

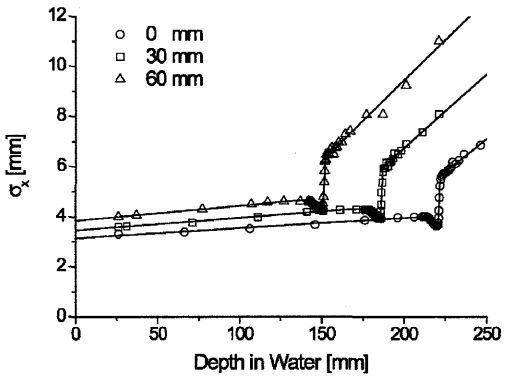

Figure 2: The lateral beam-spread $\sigma_x(z_i;z_0)$ of the pencil beam as a function of depth in water z_i in the x direction. Circles, squares and triangles represent the measured beam spread for the range shifter thickness of 0, 30 and 60 mm, respectively.

2.2. Biological Dose Calculation

When a biological system is irradiated with scanned pencil beams within a sufficiently short period of time, the survival at point (x_i, y_i, z_i) is derived by

$$S_{mix,i} = \exp\left[-\alpha_{mix,i} D_{phys,i} - \beta_{mix,i} D_{phys,i}^{2}\right] \quad (5)$$

In the above equation, $D_{phys,i}$ is the physical dose at the point i delivered by the scanned pencil beams with their weights w. α_{mix} and β_{mix} are the coefficients α and β in the LQ model at (x_i, y_i, z_i) given by

$$\alpha_{mix,i} = \sum_{j=1}^{N} w_j d_{i,j} \alpha_{i,j} \Big/ \sum_{j=1}^{N} w_j d_{i,j} \quad (6)$$

$$\sqrt{\beta_{mix,i}} = \sum_{j=1}^{N} w_j d_{i,j} \sqrt{\beta_{i,j}} \Big/ \sum_{j=1}^{N} w_j d_{i,j} \quad (7)$$

where $\alpha_{i,j}$ and $\beta_{i,j}$ are the α and β coefficients of beam j with the maximum range z_0 at a depth of z_i [13]. The formalism of survival fraction for mixed beam irradiation has been developed by Zeider and Rossi [14], and its reliability has been experimentally verified [13] and successfully utilized for treatment planning for carbon ions at HIMAC, NIRS [8][15]. Then the RBE at (x_i, y_i, z_i) can be obtained from the ratio between the doses required to obtain a desired level of cell killing, i.e. survival level S, by a reference radiation quality (Co-60) and by the carbon beam as

$$\mathrm{RBE}_i(S) = \frac{D_{Co-60}(\alpha_{Co-60}, \beta_{Co-60}, S)}{D_{phys}(\alpha_{mix,i}, \beta_{mix,i}, S)} \quad (8)$$

The survival level of 10% for HSG cells is used in the RBE calculation independent of the dose levels. Finally, the biological dose at the point, $D_{biol,i}$, can be calculated by

$$D_{biol,i} = D_{phys,i} \times \mathrm{RBE}_i(S) \quad (9)$$

The α and β coefficients for a pencil beam are defined as a function of depth z_i and its maximum range z_0, $\alpha(z_i; z_0)$ and $\beta(z_i; z_0)$, as the integrated dose distribution $d_z(z_i; z_0)$ for the beam. These coefficients appeared in the biological dose calculation in the form of the product with $d_z(z_i; z_0)$ as shown in equations (6) and (7). Therefore, we tabulated the products $d_z(z_i; z_0)\alpha(z_i; z_0)$ and $d_z(z_i; z_0)\sqrt{\beta(z_i; z_0)}$ to the input data file along with $d_z(z_i; z_0)$ and the formulae representing the lateral beam spread $\sigma_x(z_i; z_0)$ and $\sigma_y(z_i; z_0)$ for each energetic pencil beam.

2.3. Dose Optimization

In dose optimization for 3D irradiation with pencil beam scanning, the best particle numbers (weight) and positions of each pencil beam, i.e. the best 3D matrix of the pencil beams w, must be determined so that the resulting dose distribution is as close as possible to the prescribed dose distribution within the target and does not exceed dose restriction within the OARs. In determining the weighting matrix, the dose-based objective function $f(w)$ is minimized by an iterative process. The objective function can be calculated as

$$f(w) = \sum_{i \in \mathrm{T}} \left(Q_{\mathrm{P}}^{\mathrm{o}} \left[D_{biol,i}(w) - D_{\mathrm{P}}^{\max} \right]_+ + Q_{\mathrm{P}}^{\mathrm{u}} \left[D_{\mathrm{P}}^{\min} - D_{biol,i}(w) \right]_+ \right) + \sum_{i \in \mathrm{O}} Q_{\mathrm{O}} \left[D_{biol,i}(w) - D_{\mathrm{O}}^{\max} \right]_+ \quad (10)$$

where $D_{biol,i}(w)$, $D_{\mathrm{P}}^{\max}$, $D_{\mathrm{P}}^{\min}$, $Q_{\mathrm{P}}^{\mathrm{o}}$, $Q_{\mathrm{P}}^{\mathrm{u}}$, $D_{\mathrm{O}}^{\max}$, Q_{O} is the biological dose at a point i obtained with the matrix w, the maximum and minimum doses applied to the target T, the penalties for over- and underdosage specified for the target, the maximum dose allowed for the OAR and the penalty for overdosage in OAR, respectively. $[r]_+$ is the positive operator defined so as to take the value of r only if r is greater than zero. When the objective function $f(w)$ takes the minimum value, the corresponding matrix w is adopted as the optimized spot beam distribution. Our optimization calculation is based on the quasi-Newton method using the L-BFGS-B algorithm [16].

In raster scanning irradiation, the beam delivery is not switched off during the transition time from one spot to the next. Therefore, in this scheme, the extra dose is inevitably delivered to the sites between two successive spots during the beam spot transition, along the scan trajectory. The amount of the extra dose is proportional to the beam intensity. Therefore, in the fast scanning irradiation using the beam with high intensity, the contribution of the extra dose to the total dose has to be taken into account in the optimization calculation. We added an additional term U_i representing the contribution of the extra dose to a voxel i to the objective function as:

$$f(w)=\sum_{i\in T}\left(Q_P^o\left[D_{bio,i}(w)+U_i-D_P^{max}\right]+Q_P^u\left[D_P^{min}+U_i-D_{bio,i}(w)\right]\right)+\sum_{i\in O}Q_O\left[D_{bio,i}(w)+U_i-D_O^{max}\right] \quad (11)$$

The RF-knockout technique developed at the HIMAC synchrotron provides a beam with the desired intensity and suppressed spill structure [17]. Therefore, the amount of U_i can be predicted and treated as a constant offset in the optimization calculation. With this method, we can find the best weighting matrix suitable for the fast scanning irradiation [11].

In order to reduce the computation time required for dose optimization, the calculation of dose distribution is limited within the target and OARs, and that of the gradient is limited within the region of raster-point in iteration phase.

2.4. Flow of treatment planning

By using the developed software, the treatment plans are produced in the following procedure.

(a) Radio-oncologists delineate the PTV and OARs on the clinical CT images using an external platform, and determine the primary treatment parameters, e.g. isocenter, desired dose level, irradiation method (single field or IMIT), number of ports, and beam directions, based on the information about the position and type of tumor as well as critical structures. The isocenter in CT coordinates coincides with the origin of the raster scanner system. The scanner step size in the horizontal and vertical directions, Δx and Δy, and step size of range shifter plate, Δz, are also determined at this stage. The CT images, geometrical information determined by the radio-oncologists and the primary treatment parameters are imported from the platform to the software.

(b) The CT images are stored into the segmented region for dose calculation by using the tri-linear interpolation. The voxel size is determined taking both the precision and time required for the dose optimization into account. The voxels within the PTV and OARs are identified with different flags.

(c) The x-ray CT numbers stored into each voxel is converted to the stopping powers relative to the stopping power of water using a conversion table created based on the polybinary tissue model [18].

(d) The selection of raster-points is done automatically by the software from the PTV so as to account for the dose fall-off at the longitudinal and lateral edges of the PTV due to the finite size of the mini peak and beam width. At first, the PTV is extended laterally toward the outside by ΔS_x and ΔS_y. Then the extended PTV is back projected onto the isocenter plane in beam's eye view. The raster grids in the horizontal and vertical directions, x_0 and y_0, are determined within the contour of the projected PTV. Then, the water-equivalent depth is analyzed for every voxel along the beam transport axis passing through each raster grid (x_0, y_0) defined on the isocenter plane from the deflection magnets. From this information the extent of the extended PTV by ΔS_z in the beam direction and hence the maximum and minimum ranges of the pencil beam is determined. With a knowledge of the maximum and minimum ranges, the new raster-points are placed in between them along the axis according to the step size of range shifter plate Δz.

(e) From the information about the maximum range found in (d), the optimum beam energy is selected among 10 individual energies prepared in the HIMAC synchrotron.

(f) In the raster-scan method, the region of raster-point was divided into slices of equal ion ranges. The beam scanning begins at the distal slice (highest energy) and laterally covers each slice on a discrete *x*-*y* grid, until the most proximal slice (lowest energy) is reached. In order to minimize the extra dose in raster scanning [11] and shorten the treatment time, we determined the scan trajectory on each slice so that the path length would be

minimized by applying a fast simulated annealing algorithm to scan trajectory optimization [19][20]. In figure 3, the result of the scan trajectory optimization is shown for a single energy slice of a given plan.

(g) The particle numbers (weight) for each raster-point are determined by the dose optimization method described in 2.3.

(h) Finally, the beam steering file is produced in which the position of the raster-point x_0, y_0, z_0, corresponding thickness of the range shifter plates, and the particle numbers (weights) of all pencil beams are written in following the order of the optimized scan trajectory.

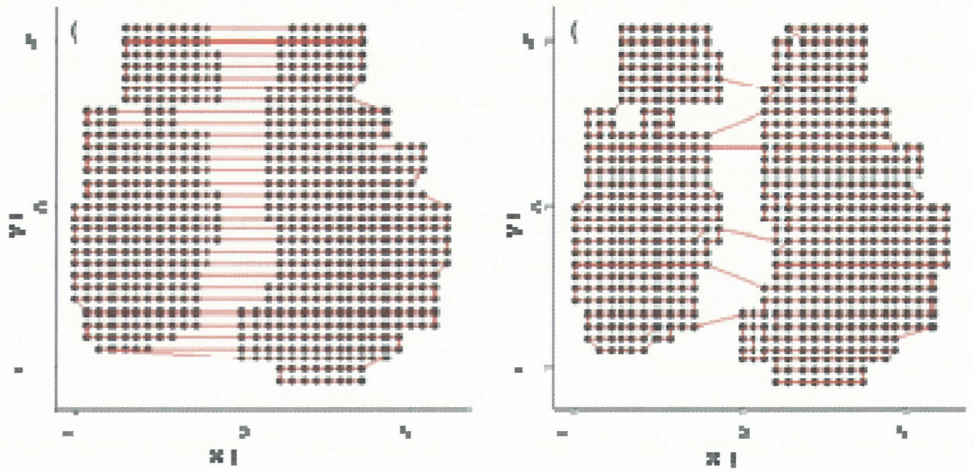

Figure 3: The example of scan trajectory optimization on a single energy slice. (a) Initial zigzag trajectory. (b) Optimized scan trajectory.

3. Results and Discussions

In order to investigate the clinical applicability of the developed software, treatment plans are produced for data of patients treated at HIMAC. We can produce both a single field plan and an IMIT plan with the software.

3.1 Single field planning

As an example of single field planning, a patient having bone and soft tissue sarcoma was selected (Figure 4). The biological dose of 1.0 GyE is delivered from a single port in the anterior to posterior direction. In this plan, only the target volume is specified on the CT images and implemented for dose optimization. The maximum and minimum doses applied to the PTV is 1.0 GyE and the penalties for over- and underdosage are 6 and 8, respectively. The voxel resolution as well as the scanner step sizes , Δx and Δy, and step size of range shifter plate, Δz, was set to 2.0 mm. The beam energy determined for the plan was 350 MeV/u, and the total of 36351 raster points were located within the raster-point region. In figure 4, the planned distribution of the physical dose, RBE and biological dose are shown with color-wash display on axial, sagittal and frontal CT images. We can see that highly conformal biological dose distribution can be achieved within the PTV.

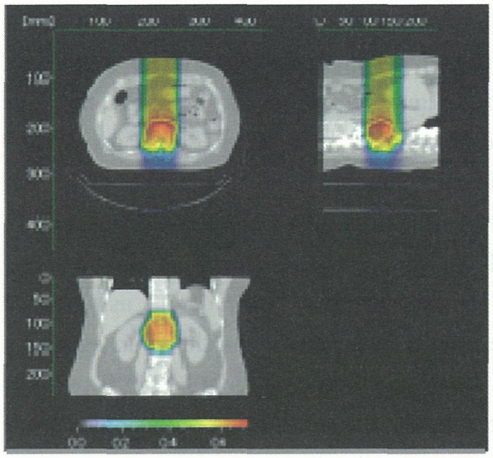

(a) Physical Dose

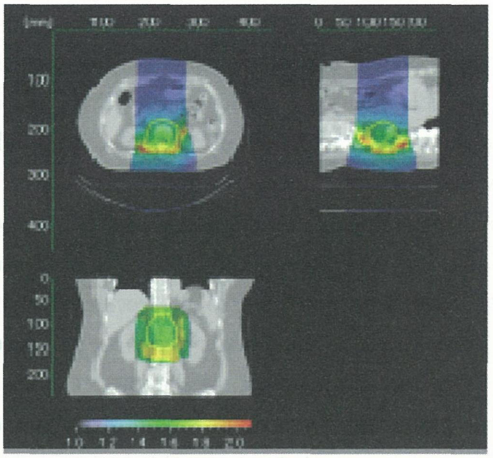

(b) RBE

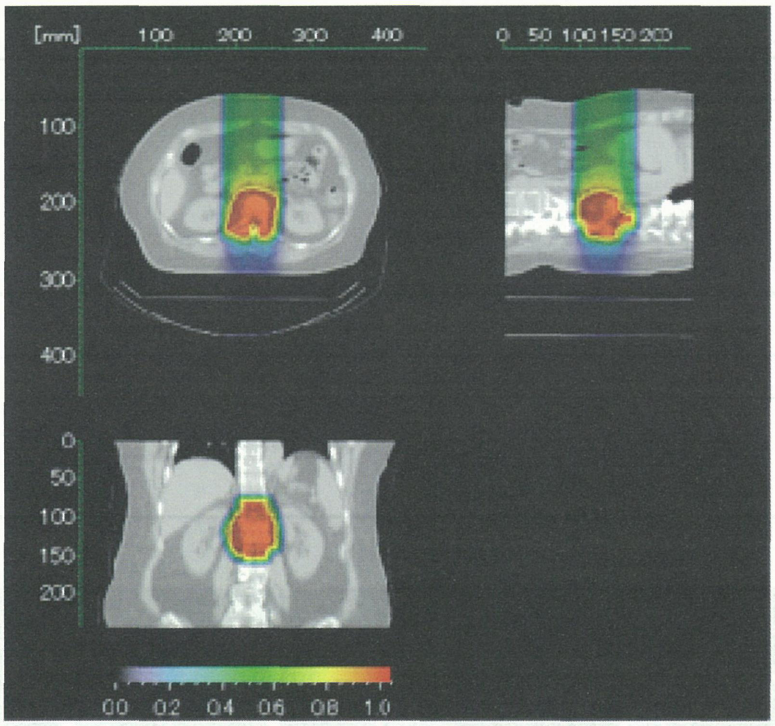

(c) Biological Dose

Figure 4: CT images with color-wash display of (a) physical dose, (b) RBE and (c) biological dose distribution. The PTV is identified with yellow curve on each CT image.

3.2 IMIT planning

As examples of the intensity modulated ion therapy (IMIT) planning, two representative patients were selected. The first patient had horseshoe-shaped cervical chordoma surrounding the spinal cord. The second patient was a prostate patient. The problem for the treatment of prostate patients is the proximity of two critical structures (rectum and bladder) adjacent to the target volume. A five equidistant, coplanar beam setup was chosen for the treatment plan of both patients. The voxel resolution was set to 2.0 mm in all directions, while the scanner step size as well as the step size of the range shifter was set to 2.0 mm for the chordoma patient and 3.0 mm for the prostate patient. Two types of plans were generated for each patient, a plan that considers each of the five fields separately and an IMIT plan, in order to investigate the effectiveness of IMIT planning. For the optimization of the chordoma and prostate patient the organ parameters listed in tables 1(a) and (b) were used.

In figure 5, the biological dose distributions by a single-field plan and an IMIT plan are shown with color-wash display for the cervical chordoma patient. Corresponding dose-volume histograms are shown with dashed-curves (single-field plan) and solid curves (IMIT plan) in figure 6. It can be seen that the effective dose delivered to the critical structure, i.e. spinal cord, could be reduced by a factor of 2.0 using the IMIT plan without any deterioration in dose conformation to the PTV as compared to the single-field plan. On the other hand, the biological dose distributions planned for the prostate patient with a single-field and an IMIT plan are shown in figure 7(a) and (b), respectively. The dose-volume histograms corresponding to both plans are shown in figure 8. The dose delivered to the rectum could be reduced by a factor of 1.2 using the IMIT plan. However, that delivered to the bladder is almost the same among these plans. As shown in figure 7, the critical structures, i.e. rectum and bladder, overlap the PTV, and hence a high dose of about 5 GyE is partially delivered to the critical structures. In a future study, reasonable criteria for the selection of the planning strategy, single field or IMIT planning, needed to be established according to each patient.

Table 1: The organ parameters specified for the PTV and the critical structures implemented into dose optimization.
(a): Cervical Chordoma

Organ/Tissue	max dose [GyE]	penalty	min dose [GyE]	penalty	volume [cc]
PTV	5.10	50	4.90	99	79.5
Spinal Cord	1.50	120	-	-	7.0
Brainstem	1.50	120	-	-	24.8
Right Eye	2.15	3	-	-	6.6
Left Eye	2.15	3	-	-	6.0

(b): Prostate

Organ/Tissue	max dose [GyE]	penalty	min dose [GyE]	penalty	volume [cc]
PTV	5	6	5	8	177.6
Bladder	3.4	4	-	-	159.2
Rectum	3.4	4	-	-	68.8

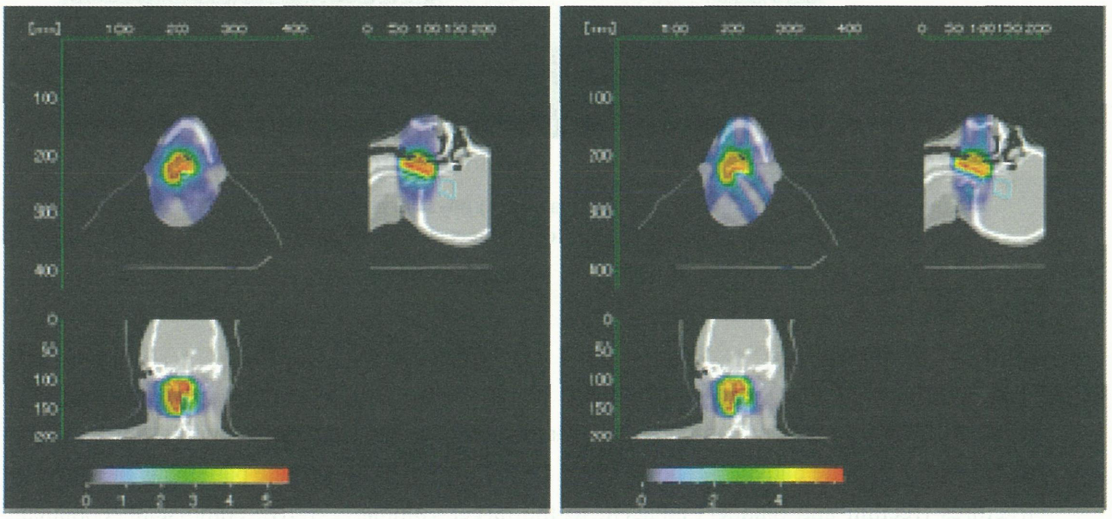

(a) Separate plan (b) IMIT plan

Figure 5: CT images of the cervical chordoma patient with color-wash biological dose display . The yellow line outlines the PTV and the watery lines delineate the OARs (spinal cord and brain stem). A five equidistant, coplanar beam setup was chosen during planning.

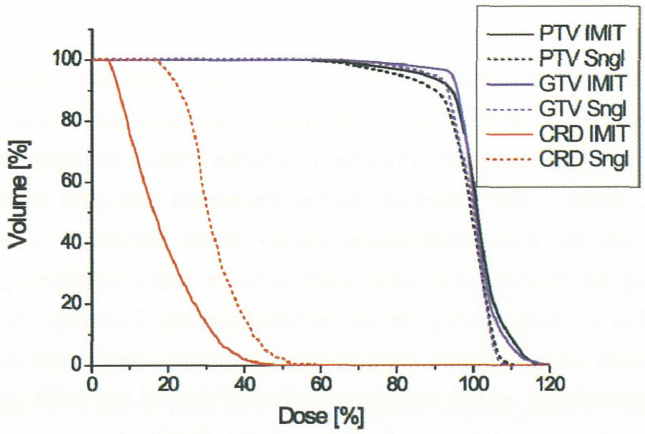

Figure 6: Dose-volume histogram of a five separate-beams plan (dashed curves) and a five-beam IMIT plan (solid curves) for the cervical chordoma patient.

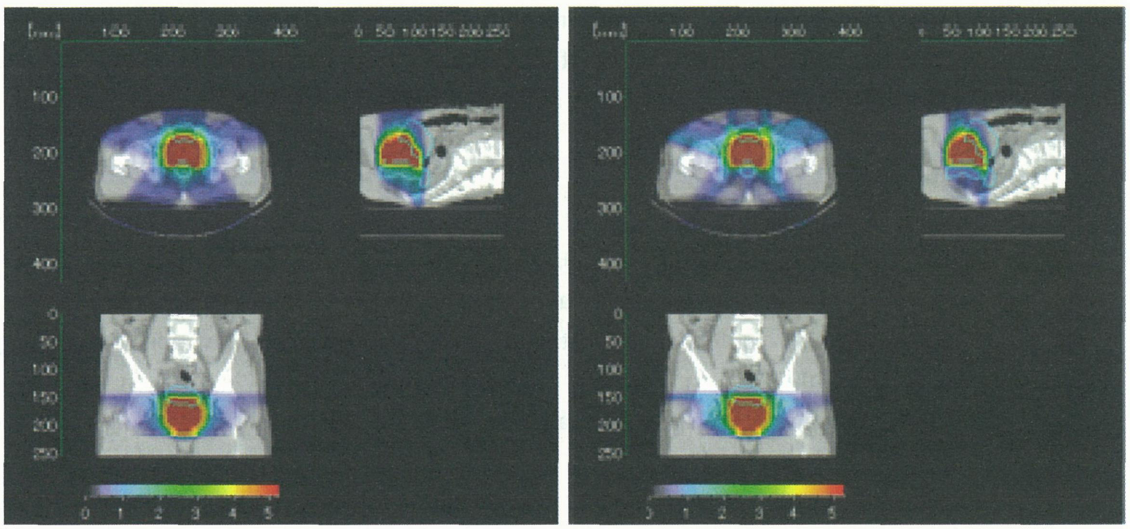

(a) Separate plan (b) IMIT plan

Figure 7: CT images of the prostate patient with color-wash biological dose display.
The yellow line outlines the PTV and the watery lines delineate the OARs (rectum and bladder).
A five equidistant, coplanar beam setup was chosen during planning.

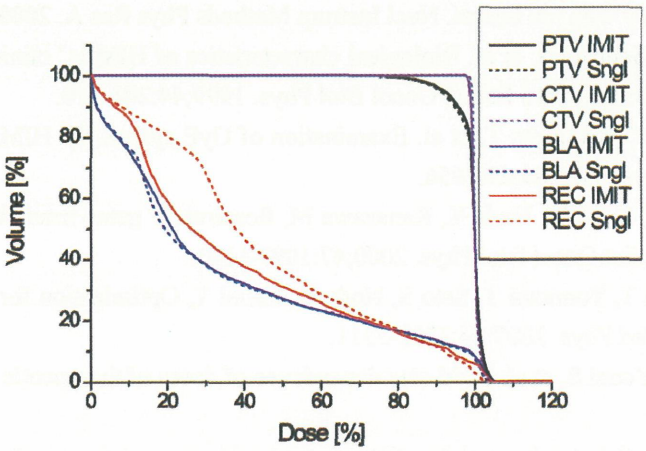

Figure 8: Dose-volume histogram of a five separate-beams plan (dashed curves) and a five-beam IMIT plan (solid curves) for the prostate patient.

5. Conclusions

We have developed the inverse planning software for an intensity-controlled raster scan method, which is to be used at the new treatment facility in HIMAC. The effect of the additional beam-spread due to the insertion of range shifter plates and the production of projectile fragments within the plates are included into the beam model of the scanned ^{12}C beam. The biological model developed and used in HIMAC clinical trials was successfully incorporated into the dose optimization engine of the software. The software was capable of producing the beam steering file in which the raster position (x-, y- and z-coordinate), thickness of range shifter plate and the particle number for each raster point are written in a way following the optimized scan trajectory. The reliability of the software was confirmed through the irradiation experiments at the SBL in HIMAC. In order to investigate the applicability of the developed software also to the IMIT planning, two patients with cervical chordoma and prostate tumor were selected, and the IMIT plans were produced for them. The effectiveness of the IMIT was clearly demonstrated in the cervical chordoma patient but no remarkable benefit of IMIT was observed in the prostate patient. We plan to make a criteria which planning method (single field or IMIT planning) should be used for respective treatment.

Currently, we are applying our software only for the CT images without a time axis. However, the assessment of the effect of inter- and intrafractional motions on dose distribution with the intensity-controlled raster scan method has already been started, and details will be presented in the separate paper.

References

[1] Hirao Y, Ogawa H, Yamada S, et al. Heavy ion synchrotron for medical use HIMAC project at NIRS-Japan. Nucl Phys A. 1992;538:541-550.

[2] Furukawa T, Inaniwa T, Sato S, et al. Design study ifa raster scanning system with phase-controled escanning toward conformal irradiation of moving target in heavy-ion radiotherapy. Med Phys. 2007;34:1085-1097.

[3] Noda K, Furukawa T, Fujisawa T, et al. New accelerator facility for carbon-ion cancer-therapy. J Radiat Res. 2007; 48: Suppl. A43-A54.

[4] Furukawa T, Inaniwa T, Sato S, et al. Design study of scanning system and rotating gantry for HIMAC new treatment facility. Proc of NIRS-CNAO joint symposium on carbon ion radiotherapy. 2006;142-153.

[5] Haberer T, Becher W, Schardt D, Kraft G. Magnetic scanning system for heavy ion therapy.NuclInstrumMethods Phys Res A. 1993;330:296-305.

[6] Pedroni E, Bacher R, Blattmann H, et al. The 200 MeV proton therapy project at PSI: Conceptual design and practical realization. Med Phys. 1995;22:37-53.

[7] Kraft G. Tumortherapy with ion beams. Nucl Instrum Methods Phys Res A. 2000;454:1-10.

[8] Kanai T, Endo M, Minohara S, et al. Biological characteristics of HIMAC clinical irradiation system for heavy-ion radiation therapy. Int J Radiat Oncol Biol Phys. 1999;44:201-210.

[9] Kanai T, Matsufuji N, Miyamoto T, et al. Examination of GyE system for HIMAC carbon therapy. Int J Radiat Oncol Biol Phys. 2006;64:650-656.

[10] Minohara S, Kanai T, Endo M, Noda K, Kanazawa M, Respiratory gated irradiation system for heavy-ion radiotherapy. Int J Radiat Oncol Biol Phys. 2000;47:1097-1103.

[11] Inaniwa T, Furukawa T, Tomitani T, Sato S, Noda K, Kanai T, Optimization for fast-scanning irradiation in particle therapy. Med Phys. 2007;34:3302-3311.

[12] Kusano Y, Kanai T, Yonai S, et al. Field-size dependence of doses of therapeutic carbon beam. Med Phys. 2007;34:4016-4022.

[13] Kanai T, Furusawa Y, Fukutsu K, et al. Irradiation of mixed beam and design of spread-out Bragg peak for heavy-ion radiotherapy. Radiat Res. 1997;147:78-85.

[14] Zaider M, Rossi H H. The synergistic effects of different radiations. Radiat Res. 1980;83:732-739.
[15] Kanematsu N, Endo M, Futami Y, et al. Treatment planning for the layer-stacking irradiation system for three-dimensional conformal heavy-ion radiotherapy. Med Phys. 2002;29:2823-2829.
[16] Nocedal J, Wright S J, *Numerical Optimization (Springer Series in Operations Research)* (New York: Springer) 1996.
[17] Furukawa T, Noda K, Muramatsu M, et al. Global Spill Control in RF-knockout Slow-Extraction. Nucl Instrum Methods Phys Res A. 2004;522:196-204
[18] Kanematsu N, Matsufuji N, Kohno R, Minohara S, Kanai T. A CT calibration method based on the polybinary tissue model for radiotherapy treatment planning. Phys Med Biol. 2003;48:1053-1064.
[19] Furukawa T, Inaniwa T, Sato S, et al. HIMAC-124. 2007 (in Japanese).
[20] Kang J H, Wilkens J J, Oelfke U, Demonstration of scan path optimization in proton therapy. Med Phys. 2007;34:3457-3464.

Status of New Carbon Therapy Facility at Gunma University

S. Yamada, T. Kanai, M. Sakama, H. Shimada, M. Tashiro, K. Torikai and K. Yusa

Heavy-ion Medical Center, Gunma University, Maebashi, Japan

Corresponding Author: Satoru Yamada, e-mail address: satoru@showa.gunma-u.ac.jp

Abstract

A new carbon therapy facility is under construction at Gunma-University Heavy-Ion Medial Center, GHMC. The main accelerator is a slow-cycling synchrotron with an average diameter of around 20 m, and it accelerates carbon ions up to an energy range from 140 to 400 MeV per nucleon. We have four treatment rooms in the new facility, three of which will have a fixed horizontal beam line, both fixed horizontal and fixed vertical beam lines, and a fixed vertical beam line, respectively. The fourth room will be used for developmental studies for advanced irradiation techniques. The number of patients treated in the facility is expected to be around 800 per year. The design details of the facility are based on design and R&D studies performed at the National Institute of Radiological Sciences. Construction will be completed by the end of FY2008, and beam tests are now underway.

Introduction

In Japan, more than 300,000 patients succumb to cancer every year, with the number increasing rapidly year by year. Protecting the public against the spread of cancer is of the highest priority. The National Institute of Radiological Sciences (NIRS) decided to construct a high-energy heavy ion therapy facility, HIMAC [1], for this purpose. Clinical trials were initiated with carbon beams in 1994. Accumulating the clinical results of more than 4,000 patients, it has been made clear that carbon therapy is greatly effective in the fight against human cancers [2]. High construction and operation costs of a therapy facility, however, are the big obstacles in the growth of carbon therapy. Design and R&D studies have been carried out at NIRS to obtain a cost-effective design for such a therapy facility. Gunma University has been collaborating with these studies since 2004. A new facility under construction at Maebashi will be the first demonstration facility of these developmental studies.

In the design process, the following are considered to be important. Only high-energy carbon ions will be used in the facility to reduce the size and cost of the apparatus. Beam characteristics should cover the clinical beam characteristics of HIMAC. Our final goal is to establish a cost-effective design of a carbon therapy facility in a hospital environment.

Our project is financially supported by the Japanese Government and local governments of Gunma Prefecture, Maebashi City, Takasaki City, and many other cities in Gunma Prefecture.

2. Major specifications of the facility

Major specifications of the facility were determined on the basis of the statistics of clinical treatments at HIMAC. It was decided to accelerate only carbon ions in the new therapy facility, with a maximum energy established at 400 MeV/u. This energy ensures a 25-cm residual range in water and, for example, carbon ions can penetrate a human body and reach the prostate through a patient's pelvis. Another important requirement of the new facility is to have two orthogonal beam lines directed toward the same isocenter. This beam line configuration is required in order to realize sequential beam irradiation from different directions with single positioning of a patient. A fast beam course and energy switching are also required for the same purpose. The

major specifications of the facility are summarized in Table 1. The layout of the new facility is shown in Fig.1. The main building of the facility is about 65 m × 45 m, completed at the end of October 2008. An outside view of the new building is shown in Fig. 2.

Table 1. Major specifications of the therapy facility

Items	Contents
Ion Species	Carbon ions only
Range	25 cm max. in water (400 MeV/u)
Field Size	15 cm × 15 cm max.
Dose Rate	5 GyE/min. (1.2×10^9 pps)
Treatment Rooms	3 (H, V, H&V)
	No rotational gantries
Fourth Room	Prepared for future developments
Irradiation Techniques	Respiration Gated
	Single & Spiral Wobbling Methods
	Layer-Stacking Method

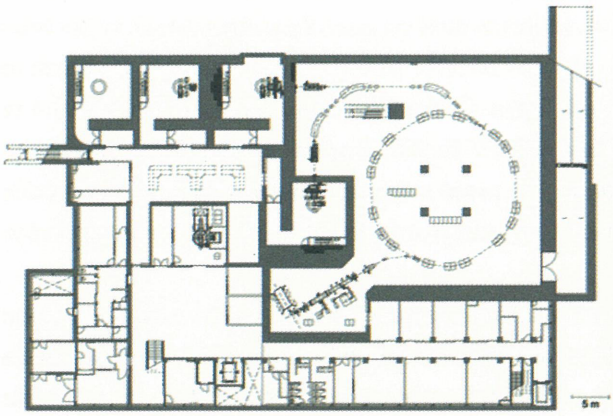

Fig.1 Plan view of the facility.

Fig. 2. Outside view of the facility

3. Accelerator system

The accelerator of the facility consists of an Electron Cyclotron Resonance (ECR) type ion source, a Radio-Frequency Quadrupole (RFQ) linac, an Interdigital-H (IH) linac with Alternating Phase Focusing (APF) structure and a synchrotron ring followed by a high-energy beam transport system. C^{4+} ions will be produced by the ECR source and pass through a thin carbon foil installed downstream of the IH linac. An output energy of the linac is determined at 4 MeV/u so that more than 90% of C^{4+} ions are converted to fully stripped ions. An averaged diameter of the synchrotron is about 20 m and will accelerate C^{6+} ions up to 400 MeV/u.

3.1. Ion source

In the ECR source, permanent magnets are adopted to generate magnetic fields both for sexta-pole and mirror fields [3], [4]. Based on experimental studies with a conventional 10 GHz ECR source at HIMAC, the field distribution of the mirror magnet is designed so that a charge distribution of carbon ions is optimized at 4+. A microwave source with traveling wave-type power tube was adopted, with a frequency range and maximum power of 9.75 – 10.25 GHz and 650 W, respectively. By tuning the microwave frequency, power level and bias disc potential, we obtained more than 300 e μ A C^{4+} ions stably at an extraction voltage of 30 kV. The normalized

beam emittance was about 1 π mm·mrad as expected. An example of charge spectra is shown in Fig. 3. A photograph of the ECR source in the new facility is shown in Fig. 4.

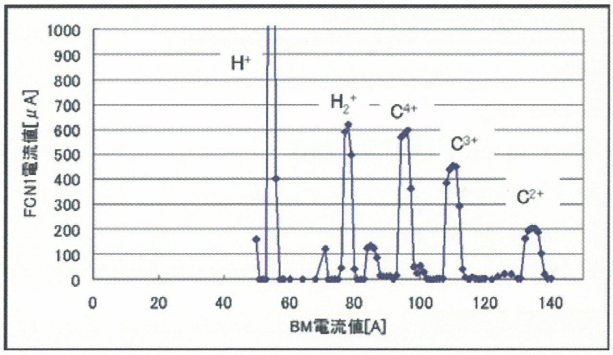

Fig.3. An example of charge spectra

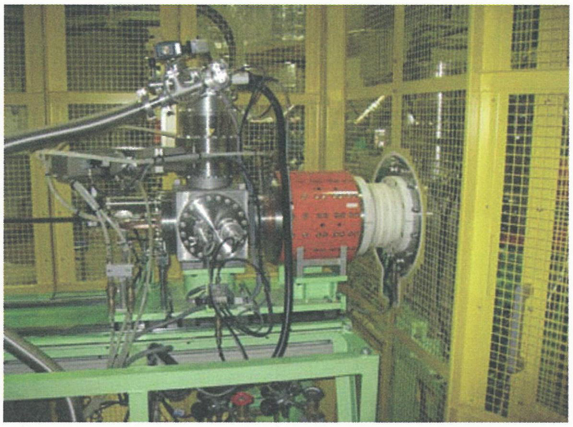

Fig. 4. ECR source installed at the new facility

3.2. Linac system

A linac system is composed of a conventional four-vane type RFQ linac and an interdigital-H type linac with alternating-phase focusing (APF) structure [5], [6]. The RFQ accelerates carbon ions from 10 to 600 keV/u, and the output energy of the APF-IH linac is 4 MeV/u. Since both linacs need no extra focusing element in the linac cavities, the tuning procedure of the linac system is very simple and easy. The operation frequency is chosen to be 200 MHz, and the cavity diameter is about 35 cm for both linacs. Cavity lengths are 2.4 m for RFQ and 3.4 m for IH. The estimated rf power is about 100 kW for RFQ and 400 kW for IH. The peak surface field in the cavity is kept at a rather low value of 23.6 MV/m (1.6 Kilpatrick) to avoid sparking problems. A 50 μg/cm^2 thick carbon foil stripper is installed at the output of the IH linac. A stripping efficiency of C^{4+} to C^{6+} was estimated to be better than 90% [7].

In the design process of the APF-IH linac, a three-dimensional field calculation code, Microwave Studio, was very powerful for obtaining resonant frequency, gap voltage distribution, etc. Only one model cavity was made to check the validity of the computer code before constructing a full-scale model at NIRS. With the full-scale model, beam tests have been performed at NIRS, and the measured values of energy, energy spread, and beam emittance of the accelerated beam reproduced the design values quite accurately. The transmission efficiency through the linac system was also good, as expected.

The injector linac in the new building is shown in Fig. 5, together with the ECR source on the right. Major specifications of the linacs are listed in Table 2.

Table 2. Specifications of the linac system

Items	RFQ	APF-IH
q/A	1/3	1/3
Frequency, MHz	200	200
Input/Output Energy, MeV/u	0.01/0.6	0.6/4.0
Inside Diameter of Tank, cm	~ 35	~ 35
Tank Length, m	2.4	3.4
Max. Surface Field, MV/m	23.6 (1.6 Kilp.)	23.6 (1.6 Kilp.)
RF Power	~ 100	~ 400

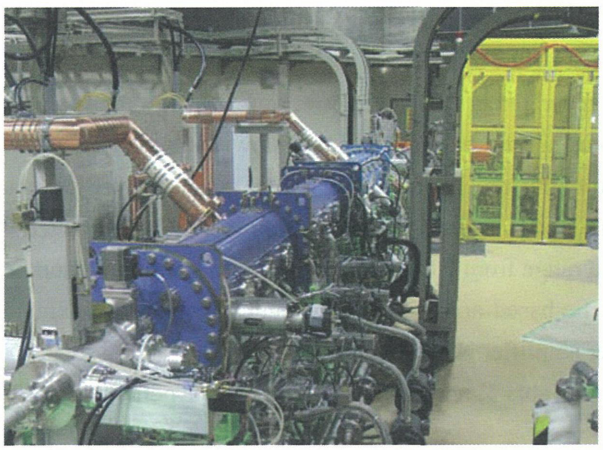

Fig. 5. Injector in the new facility

Fig. 6. Synchrotron ring under construction

3.3. Synchrotron

The synchrotron has a conventional FODO type lattice structure and accelerates fully stripped carbon ions from 4 up to 400 MeV/u [8], [9]. The circumference of the ring is 63.3 m and the average diameter is about 20 m. The bending field changes from 0.13 to 1.48 T. There are 18 bending magnets in the ring, each of which is about 6 t, making the total weight over 100 t.

Horizontal and vertical tunes are designed to vary from (1.775, 1.198) to (1.73, 1.218) and (1.68, 1.235) at injection, acceleration and extraction stages, respectively. The momentum compaction factor is around 0.33, and errors in the bending field may affect rather strongly the beam orbit in the ring. The drift of the bending field should be less than 5×10^{-4} at the flat top. The tune spread due to space charge effects is estimated to be around -0.07 in the vertical direction at injection.

Table 3. Major specifications of the synchrotron

Items	Contents
Ion Species	C^{6+}
Injection Energy	4 MeV/u
Extraction Energy	140 ~ 400 MeV/u
Beam Current	1.3×10^9 pps max.
Repetition	1/3 Hz, typical
Circumference	63.3 m
Bending Field	0.13 ~ 1.48 T
Acceptance	
Momentum	± 0.3%
Horizontal/Vertical	250/26 π mm·mrad
Injection Method	Multiturn
Extraction Method	Slow, 1/3 resonance
RF System	
Frequency Range	0.87 ~ 6.77 MHz
Harmonic Number	2
Acceleration Voltage	2 kV max.
Estimated Power	~ 7 kW

A typical excitation pattern of the synchrotron field is the flat base, smoothing, flat top and total period of 0.05, 0.05, 1.6 and 3.0 sec., respectively. The value of dB/dt is designed to be 2.148 T/s. Ions not extracted during the flat top will be decelerated to reduce unwanted radiation generated in the synchrotron ring.

The injection and extraction methods are conventional multiturn injection and slow extraction using 1/3 resonance, respectively. Acceptances of the synchrotron ring are 26 and 250 π mm·mrad for vertical and horizontal directions. During 25 turns of multiturn injection of 57.1 μs, 5.1×10^9 carbon ions will be injected in the synchrotron ring. Acceleration rf frequency varies in a range from 0.88 to 6.77 MHz with a harmonic number of two. A single-gap acceleration cavity is loaded with Fe-based amorphous cores and generates a maximum voltage of 2 kV. The maximum output power of the power amplifier is 8 kW.

The major specifications of the synchrotron are listed in Table 3, and a photograph of the synchrotron ring is shown in Fig. 6.

4. Beam delivery system

The wobbler method was adopted for our beam delivery system based on more than 10 years experience at HIMAC. In order to improve the beam efficiency in a large irradiation field size, we adopted a spiral wobbler technique [10]. By single wobbler technique, the beam size is required to satisfy a definite relation with the radius of the circular wobbling orbit at an isocenter. In the spiral wobbling scheme, however, the amplitude of AC currents of the wobbler magnets is modulated properly, and the beam spot size can be much smaller than that of a simple wobbling scheme. It takes less than 1 sec. to form uniform dose distribution when the frequency of the wobbler field and amplitude modulation are 80 and 30 Hz, respectively. In Fig. 7, the principle of the spiral wobbler method is shown schematically in comparison with the single wobbler method.

The distance between the iso-center and the final beam transport element of the bending magnet was chosen to be 9 m. We can make a maximum 15 cm × 15 cm irradiation field with a dose distribution error better than ±2.5%.

The layer-stacking irradiation technique developed at NIRS [11] will be adopted. This technique is considered to be effective for reducing an unwanted high-dose area in front of the target by controlling precisely the multilieaf collimator during stacking irradiation.

A horizontal beam delivery system is installed in treatment rooms A and B, whereas a vertical system is installed in rooms B and C. Treatment room D is empty at the beginning stage, and a scanning irradiation technique with a sharp pencil beam will be developed in this room.

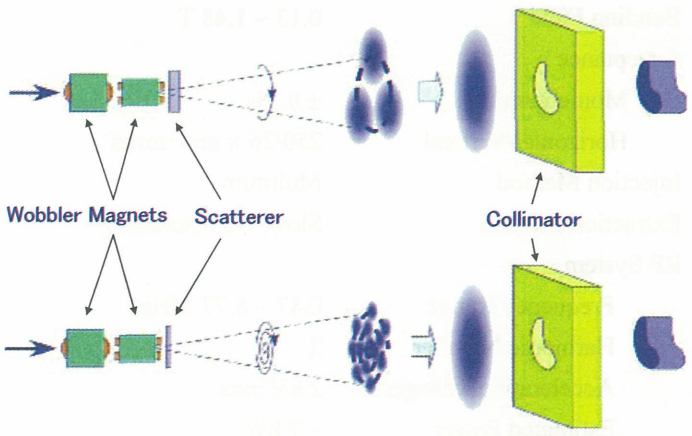

Fig. 7. Single wobbler method (top), and spiral wobbler method (bottom)

5. Construction schedule

Construction of our facility started in February 2007. After completion of the new building in October 2008, major apparatuses have been installed in the building until the end of 2008. Beam tests started with the ECR source, and high power tests of the injector linacs have also been successfully completed. Beam tests of the whole accelerator system will be carried out during the summer. The first treatment of a patient is scheduled in March 2010. By 2017, we expect the total number of treatments to reach its final level of 800 per year.

6. Acknowledgements

Design and R&D studies have been performed under the strong initiative of the HIMAC group at NIRS. The authors give their sincere thanks to Dr. K. Noda and other members of the HIMAC group.

References

[1] Y. Hirao, et al. Heavy Ion Synchrotron for Medical Use – HIMAC project at NIRS, Japan, Nucl. Phys. A538, 541c, 1992.

[2] H. Tsujii, J. Mizoe, T. Kamada, et al. Clinical Results of Carbon Ion Radiotherapy at NIRS, J. Radiat. Res., 48, A1, 2007.

[3] M. Muramatsu, A. Kitagawa, Y. Sakamoto, et al. Compact ECR ion source with permanent magnets for carbon therapy. Rev. Sci. Instr., 75(5), 1925, 2004.

[4] M. Muramatsu, A. Kitagawa, S. Sato, et al., Development of a compact electron-cyclotron-resonance ion source for high-energy carbon-ion therapy, Rev. Sci. Instr. 76, 113304, 2005.

[5] Y. Iwata, S. Yamada, T. Murakami, et al., Alternating-phase-focused IH-DTL for an injector of heavy-ion medical accelerators, Nucl. Instr. & Meth. in Phys. Res., A569, 685, 2006.

[6] Y. Iwata, S. Yamada, T. Murakami, et al. Performance of a compact injector for heavy ion medical accelerator, Nucl. Instr. & Meth. in Phys. Res., A572, 1007, 2007.

[7] Y. Sato, T. Miyoshi, T. Muramatsu, et al., Penetration of 4.3 and 6.0 MeV/u highly charged heavy ions through carbon foils, Nucl. Instr. & Meth. in Phys. Res., B225, 439, 2004.

[8] K. Noda, K., T. Furukawa, Y. Iwata, et al. Design of carbon therapy facility based on 10 years experience at HIMAC, Nucl. Instr. & Meth. in Phys. Res., A562, 1038, 2006.

[9] K. Noda, T. Furukawa, T. Fujisawa, et al. New Accelerator Facility for Carbon-Ion Cancer-Therapy, J. Rad. Res., 48, Suppl. A, A43, 2007.

[10] M. Komori, T. Furukawa, T. Kanai and K. Noda, Optimization of Spiral-Wobbler System for Heavy-Ion Radiotherapy, Jpn. J. Appl. Phys. 43, 6463, 2004.

[11] T. Kanai, et al. Commissioning of a conformal irradiation system for heavy-ion radiotherapy using a layer-stacking method, Med. Phys. 33, 2989, 2006.

Evaluation of Absolute Doses for Therapeutic Carbon Ion Beams

Makoto Sakama[1)], Tatsuaki Kanai[1)], Akifumi Fukumura[2)] and Yuki Kase[2)]

[1)]*Heavy Ion Medical Research Center, Gunma University, Maebashi, Japan*
[2)]*Research Center for Charged Particle Therapy, National Institute of Radiological Sciences, Chiba, Japan*
Corresponding Author: Makoto Sakama, e-mail address: m-sakama@showa.gunma-u.ac.jp

Abstract

In order to sophisticate the radiotherapy, high accuracy knowledge of the absorbed dose delivered to the patient is essential. Despite recent progress in carbon ion therapy, accurate values for physical data such as the *w* value in air or stopping power ratios for ionization chamber dosimetry have not been obtained. Therefore, that causes the uncertainty in determination of the absolute doses for the carbon ion beams. For this reason, we developed and performance-tested a portable graphite calorimeter designed to measure the absolute dosimetry of various beams including heavy-ion beams, using a flexible and convenient means of measurement. The absorbed dose obtained with the calorimeter was compared with that obtained using the ionization chambers following the IAEA protocol in order to evaluate the *w* values in air for mono-energetic carbon ion beams of 135, 290, 400, and 430 MeV/n. The comparisons to our calorimeter measurements revealed that, using the ionization chambers, the absorbed dose comes out low by 2 to 6 % in this experimental energy range and with the chamber types and calibration methods. The *w* values in air of the carbon ion beams were evaluated to be 35.72 J/C ± 1.5% in the energy range used in this study. This value is 3.5% larger than that recommended by the IAEA TRS 398 for heavy-ion beams. Using this evaluated result, the absorbed dose to water in the carbon ion beams would be increased by the same amount.

Introduction

Carbon radiotherapy is now one of the most effective methods for cancer therapy. The increased interest in light ion therapy in the last few years has led to considerable efforts to improve the accuracy of light ion dosimetry [4),7),11),12)]. In comparison to electron, photon, or proton dosimetry, light ion dosimetry is still at an early stage of development and has significantly larger levels of uncertainty. There is no established standards laboratory supplying a dose calibration factor for light ion therapy. The comparability of tumor treatment with different types of radiation requires measurement devices that allow an absolute and direct dose determination with high accuracy. In radiotherapy, the relative standard uncertainty of the dose determination delivered to tissue should be less than 5 %[2),3),8)].

For radiation fields in radiotherapy, dose determination generally relies on ionization chamber dosimetry because of its good reproducibility, reliability, and its convenience in measurements. This dosimetry is based on calibration in terms of air kerma or absorbed dose to water of ionization chambers in a well-known photon reference field and is traced back to a national standard laboratory. A formalism of ionization chamber dosimetry for clinical light ion therapy was presented in the TRS-398 Code of Practice issued by the International Atomic Energy Agency[8)]. In this protocol, constant values of 1.13 and 34.5 J/C for the stopping power ratio of water to air and the *w*-value of air for heavy-ion beams are recommended to be used for the dosimetry. The relative standard uncertainty in the determination of the absorbed dose to water in the case of an ion beam is listed as 3.0% for cylindrical chambers and 3.4% for plane-parallel chambers. This uncertainty comes primarily from the stopping power ratio of water to air and the *w*-value, which are estimated to be 2.0% and 1.5%, respectively.

The most direct approach to determine the absorbed dose, D, is calorimetry[5),6),13)], as it directly measures the temperature rise of the irradiated material, that is, the absorbed energy. The dose is obtained by dividing the measured absorbed energy dE by the mass of the material dm. Standardization of the clinical dosimetry procedures, however, is achieved by the use of ionization chamber dosimetry and of commonly agreed-upon dosimetry protocols[1),8),9),15),16)]. These protocols recommend the use of water as a reference material. For heavy-ion beams, the only report concerns the absolute dose by calorimetric measurements[4)]; therefore, it is necessary to compare ionization chamber dosimetry and calorimetry for various beams.

We developed a portable graphite calorimeter and a fully remote-controlled measuring system for flexible operations using a LabVIEW program on a notebook PC in order to investigate the absolute dosimetry of various beams including heavy-ion beams. The absorbed doses of carbon beams were measured by the developed graphite calorimeter and also by ionization chambers following the IAEA protocol. Comparisons of absorbed dose obtained by the graphite calorimeter and the ionization chambers are discussed in order to evaluate the w values in air in the therapeutic carbon beams.

Methods and Materials

A schematic diagram of the developed graphite calorimeter is shown in figure 1[14)]. Irradiations were performed using the ^{60}Co gamma ray, 155 MeV proton beam at PMRC, the following mono energetic beams: 135, 290, 400 and 430 MeV/n ^{12}C which were accelerated by Heavy Ion Medical Accelerator in Chiba (HIMAC) at National Institute Radiological Sciences (NIRS). The ^{60}Co photon field and proton beam were used for verification of the graphite calorimeter. The ion beams were irradiated with a uniform field of 10 cm in diameter[10)]. Depth dose distributions and lateral profiles measured with a parallel plate ionization chamber are shown in figure 2. The water equivalent depth of the measurements was 16.4 mm in the plateau region.

In order to estimate the w value for ionization chamber dosimetry in the energy region used in carbon ion therapy, the calorimetric method was utilized to determine the differential w value for carbon ions in air. The w value can be estimated by the comparisons between absorbed doses obtained using the ionization chamber dosimetry and those obtained using the calorimetry. The absorbed dose to graphite in the carbon beams by the ionization chamber dosimetry was calculated by following equation.

$$D_{graphite,carbon} = M_{IC,carbon} \cdot N_{D,graphite,60Co} \cdot \frac{(\bar{S}_{g,air})_{carbon} (\bar{W}_{air})_{carbon} P_{g,carbon}}{(\bar{S}_{g,air})_{60Co} (\bar{W}_{air})_{60Co} P_{g,60Co}}$$

where $M_{IC,carbon}$ is the ionization chamber output in the carbon beams, $N_{D,graphite,60Co}$ is absorbed dose to graphite calibration factor for ^{60}Co gamma ray, $S_{g,air}$ is the stopping power ratio of graphite to air for the carbon beams, W_{air} is the w value in air for the carbon beam and $P_{g,carbon}$ is the all perturbation factor in graphite for the carbon beam. Therefore w values in air for carbon beam are estimated by

$$\left(\frac{\bar{W}_{air}}{e}\right)_{carbon} = \frac{D^{calorimetry}_{graphite,carbon} \cdot (\bar{S}_{g,air})_{60Co} \cdot P_{g,60Co} \cdot \left(\frac{\bar{W}_{air}}{e}\right)_{60Co}}{M_{IC,carbon} \cdot N_{D,graphite,60Co} \cdot (\bar{S}_{g,air})_{carbon} \cdot P_{g,carbon}}$$

where $D^{calorimetry}_{graphite,carbon}$ is the absorbed dose to graphite obtained by the calorimetry in the carbon beams.

The typical measured voltage change of a Wheatstone bridge corresponding to core temperature in the calorimeter is shown in figure 3. Figure 3a shows the process of electrical calibration for the calorimeter measurements. The electrical power was added continuously to the core for the calibration in Fig. 3a. Figure 3b shows the measurement of core temperature rise by carbon ion irradiation. Beam spill patterns with a period of 3.3 seconds are clearly observed in Fig. 3b.

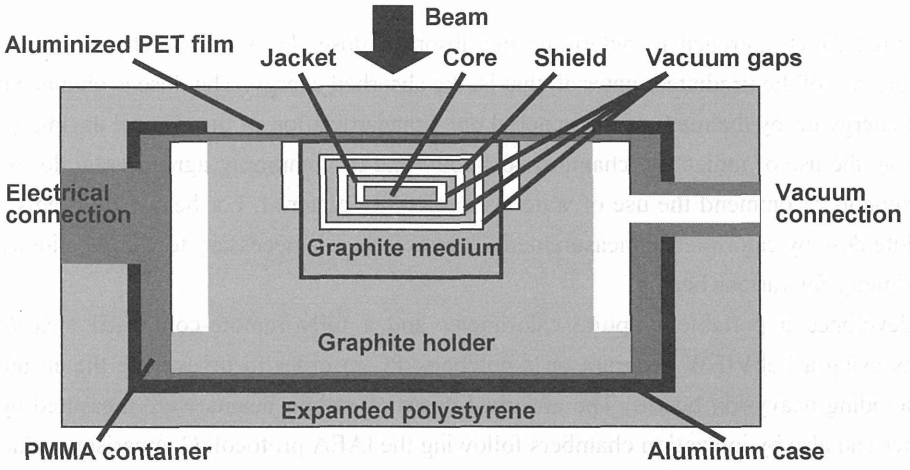

Figure 1. A schematic diagram of the graphite calorimeter used in this study[14].

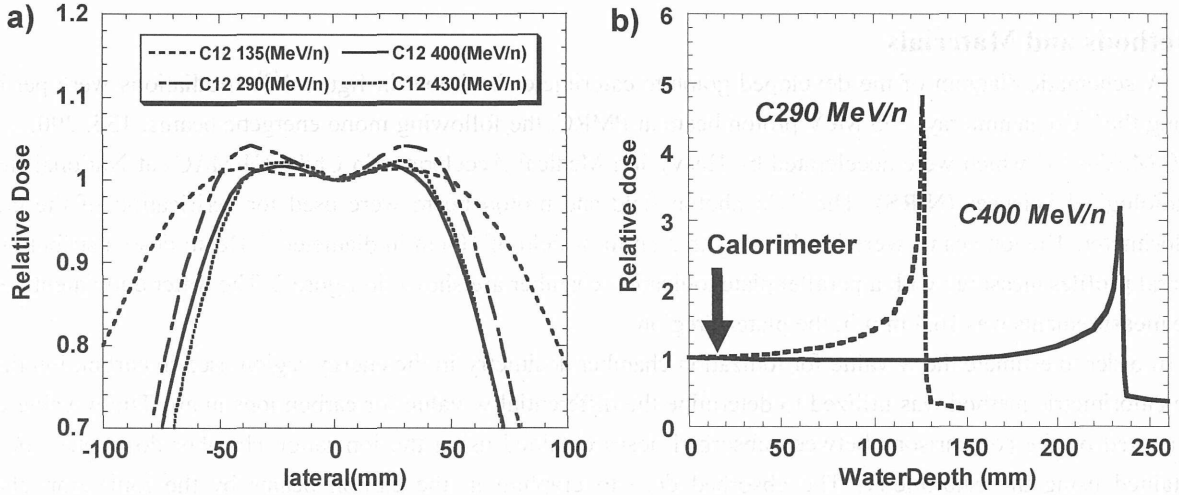

Figure 2. a): lateral profiles measured with a parallel plate ionization chamber in 135, 290, 400 and 430 MeV/n ^{12}C beams normalized at the center. b): Relative depth dose distributions of 290 and 400 MeV/n ^{12}C beams in water.

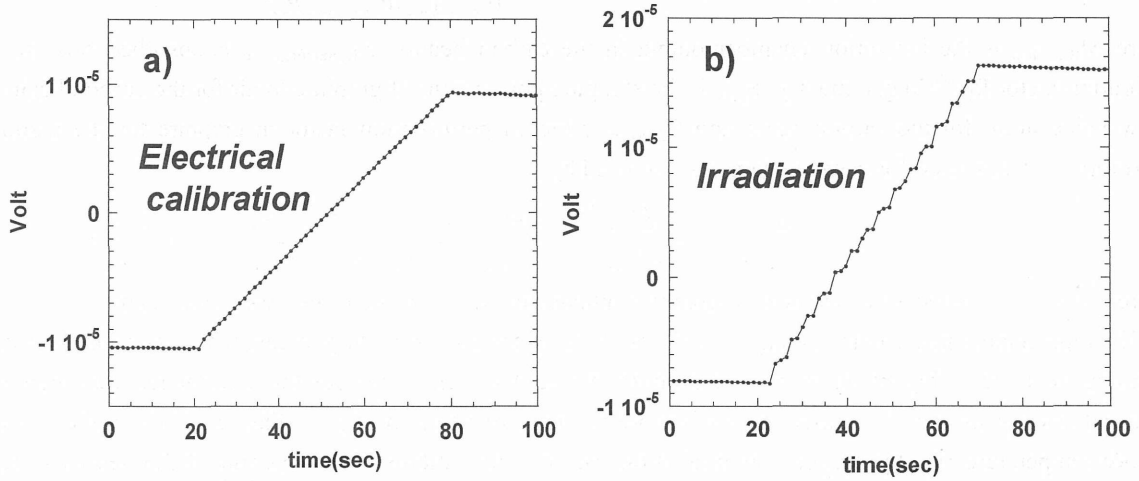

Figure 3. The typical measured voltage change of a Wheatstone bridge corresponding to core temperature. Figure 3a shows the process of electrical calibration and Figure 3b shows the measurement of core temperature rise by carbon irradiation. The electrical power was added continuously to the core for the calibration in Fig. 3a and beam spill patterns with a period of 3.3 seconds are clearly observed in Fig. 3b.

Results and Discussion

The ratio of the absorbed dose obtained by the graphite calorimeter measurements and by the ionization chambers measurements in a ^{60}Co photon beam and 155 MeV proton beam are shown in figure 4. The left side of the graph indicates the ratio of the absorbed dose by the calorimeter to those of the cylindrical and plane-parallel chambers in a ^{60}Co photon beam, and the right side of the graph shows the same ratio for the absorbed dose in 155 MeV proton beam. The relative standard deviation of the graphite calorimeter measurements in a ^{60}Co photon beam at a dose rate of 0.8 Gy/min was 0.79 % for seventeen calorimeter runs. The horizontal dashed line represents the mean values for all ionization chamber types of the absorbed dose. The average of the ratio of the absorbed dose by calorimeter to that by ionization chamber measurements in a ^{60}Co photon beam was 1.0025; in 155 MeV proton beam, the ratio was 0.9957.

The ratios of the absorbed dose to graphite obtained by the graphite calorimeter to that obtained by the ionization chambers are shown in figure 5. The constant w_{air} value of 34.50 J/C in the IAEA TRS 398[8] was used for the ionization chamber dosimetry. The combined uncertainty of these ratios was 2.3% at all energies and in all chambers used in this study. The absorbed doses obtained using the ionization chambers were underestimated by approximately 2 to 6% compared with those evaluated by the graphite calorimeter in this energy range and with these chamber types and calibration methods. The large deviation of the absorbed doses obtained by the cylindrical chambers for the 135 MeV/n carbon beam may be due to the uncertainty of the displacement effect. It was found that these ratios have a slight energy dependence in the energy range studied.

The w_{air} values for the carbon ion beams obtained in this study are shown in figure 6. The mean values of w_{air} for the carbon ion beams by the N_x calibration method and the $N_{D,graphite,\ ^{60}Co}$ calibration method were 35.74 J/C with a standard uncertainty of 1.4% and 35.68 J/C with uncertainty of 1.8%, respectively. The mean values by the two calibration methods agree well within 0.2%. The mean value of the w_{air} for the carbon beams in the both calibration methods was 35.72 J/C with a standard uncertainty of 1.5%. The w_{air} value obtained is 3.5% larger than that evaluated by the IAEA TRS 398 for heavy-ion beams. In the therapeutic energy range, the w_{air} values for the carbon beams should be adopted as the constant value for practical use because of the large uncertainty and unknown perturbation factors of the ionization chambers.

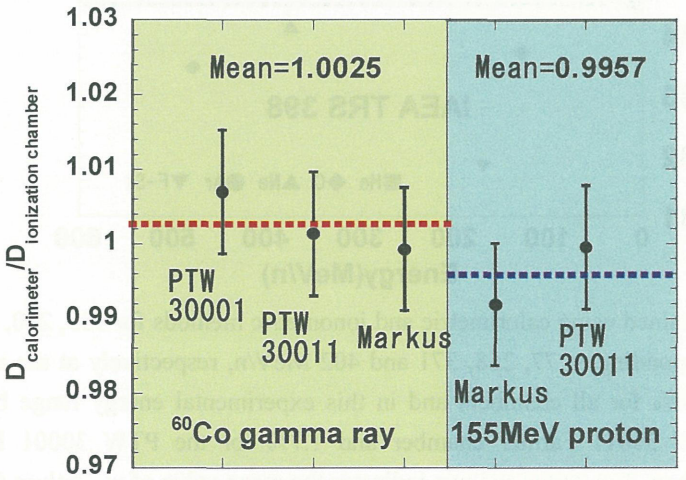

Figure 4. Comparison between absorbed doses obtained by the graphite calorimeter and the ionization chambers. The left side of the graph indicates the ratio of the absorbed dose by the calorimeter to those of the cylindrical and plane-parallel chambers in a ^{60}Co photon beam, and the right side of the graph shows the same ratio for the absorbed dose in 155 MeV proton beam.

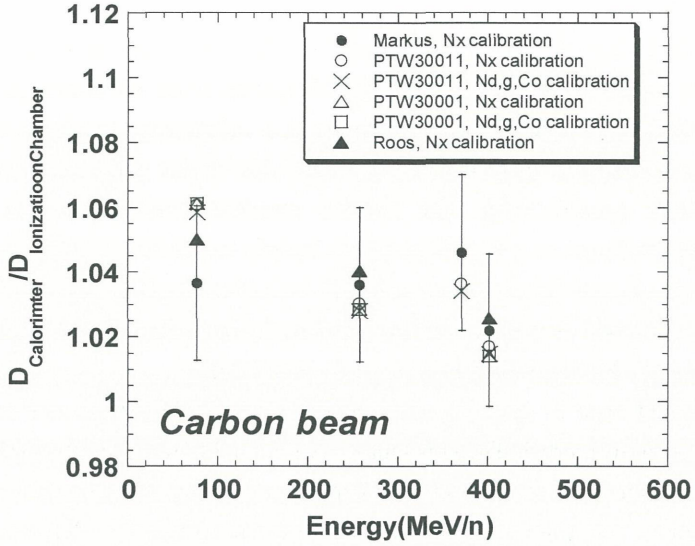

Figure 5. The ratio of the absorbed dose obtained by the graphite calorimeter to that obtained by the ionization chambers following the IAEA protocol in two calibration methods for 135, 290, 400 and 430 MeV/n of the carbon beams (corresponding to 77, 258, 371 and 402 MeV/n, respectively at the measurement depth). Combined uncertainty of these ratios was 2.3% in this study using the constant w_{air} value for the heavy-ion beams recommended by IAEA TRS 398[8]. The error bar indicates the uncertainty for the Markus chamber.

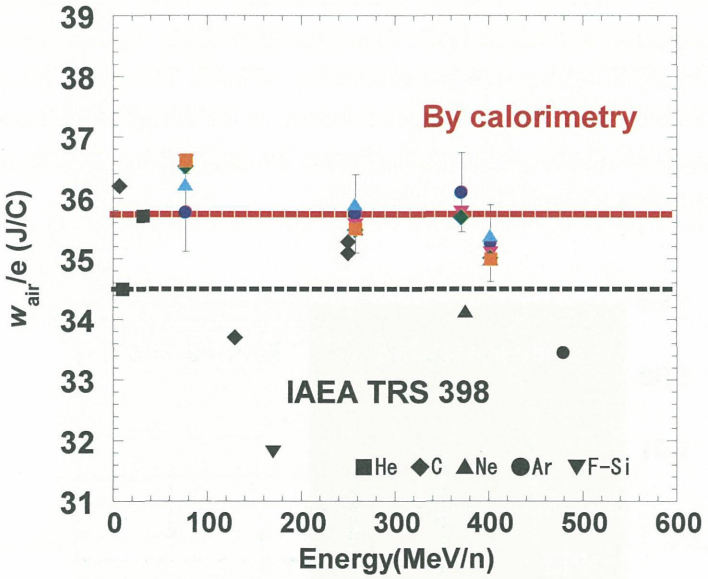

Figure 6. The w_{air} values obtained using calorimetric and ionometric methods for 135, 290, 400 and 430 MeV/n of the carbon beams (corresponding to 77, 258, 371 and 402 MeV/n, respectively at the measurement depth). These uncertainties were 1.8% for all chambers and in this experimental energy range by the N_x calibration method, 1.6% for the PTW 30011 Farmer chamber and 1.7% for the PTW 30001 Farmer chamber by $N_{D,graphite,}{}^{60}{}_{Co}$ calibration method. The dotted red line indicates the mean value of w_{air} values for the carbon beams (35.72 J/C with a standard uncertainty of 1.5%). The error bar indicates the uncertainty for the Markus chamber. The black symbols indicate the w_{air} values for heavy-ion beams adopted by the IAEA TRS 398[8]. The dotted black line indicates the w_{air} values for heavy-ion beam dosimetry recommended by the IAEA protocol.

Conclusions

In this study, the absorbed dose was measured with the developed graphite calorimeter and also with ionization chambers following the IAEA protocol in order to evaluate the w values in air for mono-energetic carbon beams of 135, 290, 400, and 430 MeV/n. The combined uncertainties of the absorbed dose to graphite obtained by the calorimeter were approximately 0.4%. The comparisons to our calorimeter measurements revealed that, using the ionization chambers and the IAEA protocol, the absorbed dose to graphite comes out too low by 2 to 6 % in the energy range of this study.

The w_{air} values were obtained using calorimetric and ionometric methods for the carbon beams. The uncertainties were 1.8% for all chambers and in this experimental energy range by the N_x calibration method, 1.6% for the PTW 30011 Farmer chamber, and 1.7% for the PTW 30001 Farmer chamber by the $N_{D,graphite,}{}^{60}{}_{Co}$ calibration method. The mean value of the w_{air} for the carbon beams in the both calibration methods was 35.72 J/C with a standard uncertainty of 1.5%. This value is 3.5% larger than that estimated by the IAEA TRS 398 for heavy-ion beams. In the therapeutic energy range, the w values in air for carbon beams indicated a slight energy dependence, but these should be applied as a constant value for practical use because of the large uncertainty and unknown perturbation factors of the ionization chambers. Using this evaluated result, the absorbed dose to water in the carbon beams would be increased by the same amount.

References

[1] AAPM (American Association of Physicists in Medicine): A protocol for the determination of absorbed dose from high-energy proton and electron beams. Radiation therapy committee, AAPM, Task Group 21 *Med. Phys.* 10: 741–771, 1983

[2] Brahme A: Dosimetric precision requirements in radiation therapy. *Acta Radiol. Oncol.* 23: 379–391, 1984

[3] Brahme A, Chavaudra J, Landsberg T, et al.: Accuracy requirements and quality assurance of external beam therapy with photons and electrons *Acta Oncol. Suppl.* 1, 1988

[4] Brede H J, Greif K-D, Hecker O, et al.: Absorbed dose to water determination with ionization chamber dosimetry and calorimetry in restricted neutron, photon, proton and heavy-ion radiation fields. *Phys. Med. Biol.* 51: 3667-3682, 2006

[5] Caumes J and Simeon J P: A TE-calorimeter as a primary standard for neutron absorbed dose calibrations. *J. Eur. Radiother.* 5: 235–239, 1984

[6] DuSautoy A R: The UK primary standard calorimeter for photon-beam absorbed dose measurement. *Phys. Med. Biol.* 41: 137–151, 1996

[7] Geithner O, Andreo P, Sobolevsky N, et al.: Calculation of stopping power ratios for carbon ion dosimetry. *Phys. Med. Biol.* 51: 2279–2292, 2006

[8] IAEA (International Atomic Energy Agency): Absorbed Dose Determination in External Beam Radiotherapy: An International Code of Practice for Dosimetry based on Standards of Absorbed Dose to Water. *IAEA TRS No. 398*, Vienna 2000

[9] ICRU (Bethesda, MD: International Commission on Radiation Units and Measurements): Photon, electron, proton and neutron interaction data for body tissues *ICRU Report* 46, 1992

[10] Kanai T, Endo M, Minohara S, et al.: Biophysical characteristics of HIMAC clinical irradiation system for heavy-ion radiation therapy. *Int. J. Radiat. Oncol. Biol. Phys.* 44: 201-210, 1999

[11] Kanai T, Fukumura A, Kusano Y, et al.: Cross-calibration of ionization chambers in proton and carbon beams. *Phys. Med. Biol.* 49: 771–781, 2004

[12] Paul H, Geithner O, Jäkel O: The ratio of stopping powers of water and air for dosimetry applications in tumor therapy. *Nucl. Instr. And Meth. in Phys. Res. B* 256: 561-564, 2007

[13] Ross C K and Klassen N V: Water calorimetry for radiation dosimetry *Phys. Med. Biol.* 41: 1–29, 1996

[14] Sakama M, Kanai T and Fukumura A: Development of a portable graphite calorimeter for radiation dosimetry. *Jpn. J. Med. Phys.* Vol. 28 No. 1: 1-14, 2008

[15] Vynckier S, Bonnett D E and Jones D T L: European code of practice for clinical proton dosimetry. *Radiother. Oncol.* 20: 53–63, 1991

[16] Vynckier S, Bonnett D E and Jones D T L: Supplement to the code of practice for clinical proton dosimetry. *Radiother. Oncol.* 32: 174–179, 1994

Research for the RI Beam Medical Application at HIMAC and RI Production Technique

Mitsutaka Kanazawa

Research Center for Charged Particle Therapy, National Institute of Radiological Sciences, Chiba, Japan
e-mail address: kanazawa@nirs.go.jp

Abstract

Short-lived radio-pharmaceuticals are extensively used in NIRS (National Institute of Radiological Sciences). One of most important field is diagnosis for cancer treatment by PET (Positron Emission Tomography) before and after radio-therapy, and the accumulated number of these PET diagnoses was more than 1000 times in 2008 financial year. To produce RI's for these radio-pharmaceuticals, three cyclotrons of NIRS-930, HM18, and BC2010N are operated. In the field of RI is as the beam, which is produced in projectile fragment. In the HIMAC facility, fragment separator was constructed to use RI beam and several R&D's were performed with this beam course. In this experiment, effectiveness of positron emitter like ^{11}C beam was used to verify an irradiated volume.

1. Introduction

Since 1994, a clinical trial of cancer therapy with carbon ions has been successfully carried out at HIMAC (Heavy Ion Medical Accelerator in Chiba) in NIRS, and more than 4500 patients were treated by this spring (2009). Now, carbon beam is expected important treatment method with high local control and less damage on normal tissue. To perform good treatment with the carbon ion therapy, information on metastasis in the patient is important. The treatment with carbon ion beam will be applied in the case of no metastasis in general. To make clinical choice in the cancer therapy, medical diagnosis with X-ray CT, MRI, and PET will be used properly. Especially, PET shows biological activities of cancer cell and this information is important to judge the carbon ion therapy is suitable or not for the patient. The PET information is also important to determine the irradiation volume, which will be used in the treatment planning. After irradiation, PET measurement is also required to know a local control of the treatment is good or not. This measurement is important to know the irradiation results in the early time. With these extensive usages of PET measurements, there is no period for stop of PET measurements, though there are stop periods of HIMAC operation in March and August. To supply RI's for PET measurements without long stop-period, operation schedule of three cyclotrons must be arranged with shifted maintenance periods between two compact cyclotrons.

As another field of application with RI, there are researches with radioactive nuclear beams (RNB). In the current irradiation planning, beam range is calculated with x-ray attenuation strength that is measured with x-ray CT as CT number. Though an empirical formula of relation between measured CT number and electron density

is measured on each x-ray CT, there will be some ambiguity of few percent in its measured relation. By use of a radioactive nuclear beam, there is possibility to measure a stopped region of the beam directly. The application of an RNB beam was originally studied at BEVALAC of Lawrence Berkeley Laboratory [1]. Although their early results showed useful data on the error of the stopping power in treatment planning with pencil beam, which arises from the difference between the X-ray CT number and the actual stopping power [2]. Recently, the PET (Positron Emission Tomography) has good efficiency and high efficiency with 3D data acquisition. With the clinical dose of one fraction is possible to have a good activity image of injected ^{11}C beam. To obtain a clinical dose with an ^{11}C beam whose intensity is lower than 1% of the primary beam in a fragment separator [3], we must use an irradiation method with high beam-utilization efficiency. For this purpose, a spot scanning irradiation system with ^{11}C beam [4] was developed.

2. Cyclotron Operation and RI Production in NIRS

RI production for the use of diagnosis of cancer has started in 1975 by use of a NIRS 930 cyclotron, which was constructed for the fast neutron therapy of cancer. Figure 1 shows a floor plan of the cyclotron building, where beam lines of c1 and c2 are for RI production. When the treatment with carbon ion beam has started, a compact cyclotron HM18 was installed in the same building as shown in Figure 1. From the beginning of the treatment with carbon ion therapy, PET diagnoses have been used before and after treatment in many cases except for prostate cancer. Since 1994 when the clinical trials have started with carbon beam, treated patient number have increased rapidly. In 1999, another compact cyclotron of BC2010N has been installed in a medical imaging building. With these two compact cyclotrons, short life RI can be supplied without stop period. To realize this requirement with these two cyclotrons, machine maintenance periods are shifted between these compact cyclotrons. In the PET diagnoses for carbon ion therapy, radio-pharmaceuticals of [^{11}C]methionine and [^{18}F] Fluoro-deoxy-glucose ([^{18}F]FDG) are commonly used. These RI's of ^{11}C and ^{18}F will be produced at the beam ports of c1 or c2, and also at the directly attached targets in compact cyclotrons of HM18 and BC2010N. Other radio-pharmaceuticals of [^{18}F]3'-deoxy-3'-F-fluorothymidine([^{18}F]FLT) and [^{62}Cu]Copper-diacetyl-bis(N^4-methylthiosemicarbazone) ([^{62}Cu]Cu-ATSM) are used as a research of PET diagnoses in the carbon ion therapy. We can obtain the ^{62}Cu as a decay product of ^{62}Zn, whose half-life is 9.26 hours. To produce ^{62}Zn, copper metal target is irradiated with 30 MeV proton in the beam port of c4 (see Figure 3) in the Figure1. Annual frequencies of PET measurements with these radio-pharmaceuticals in 2008 financial year are shown in Figure 4. Frequencies classified with each RI and its applied fields are shown in Figure 5.

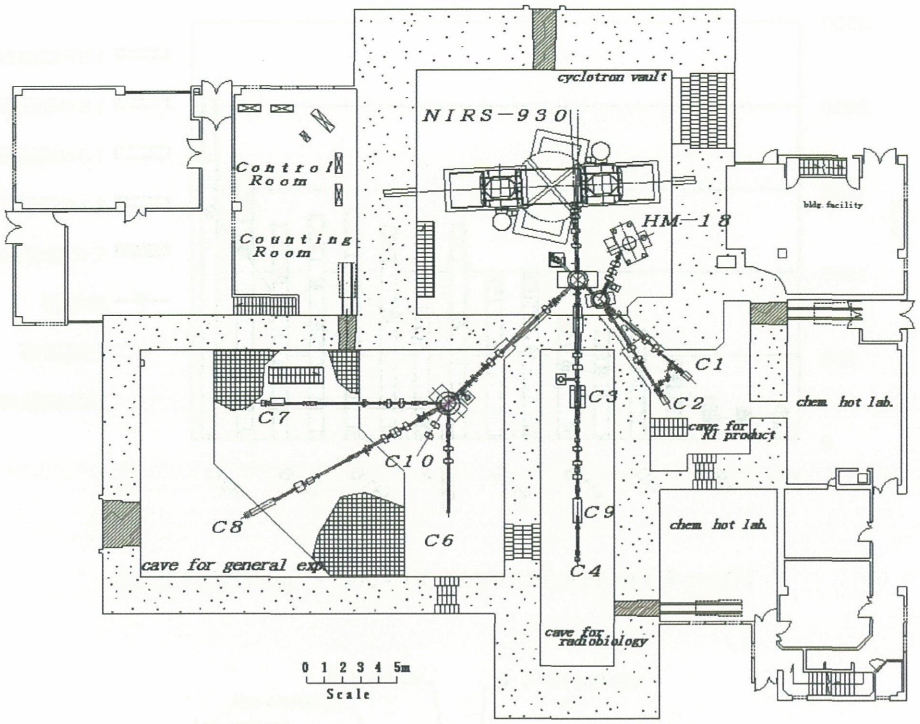

Figure 1: Floor plan of the cyclotron building with NIRS-930 and HM-18 cyclotron. Beam lines of c1, c2, c4, c9 are used for RI production

Figure 2: Beam lines of c2 and c2

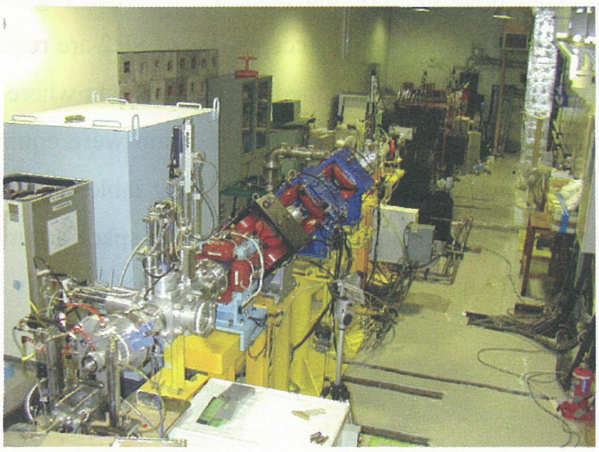

Figure 3: Beam line of c4

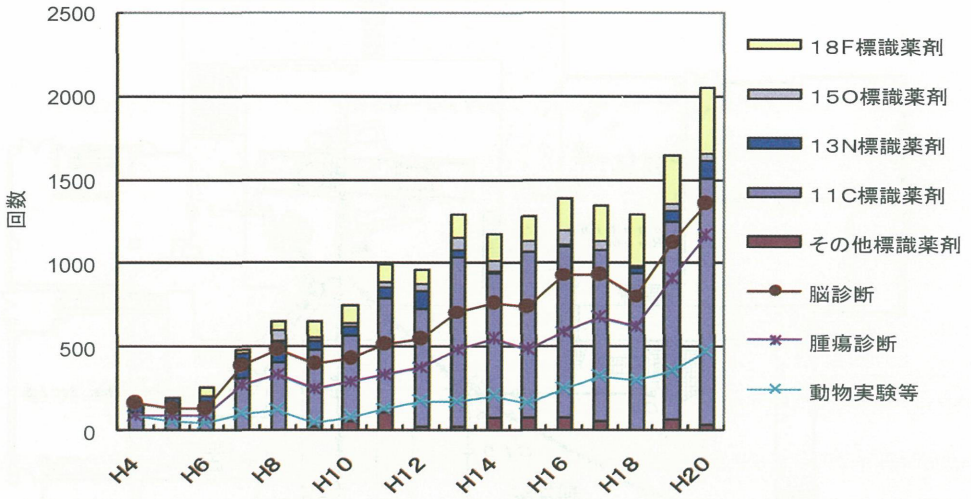

Figure 4: Frequencies of each RI's and its application fields

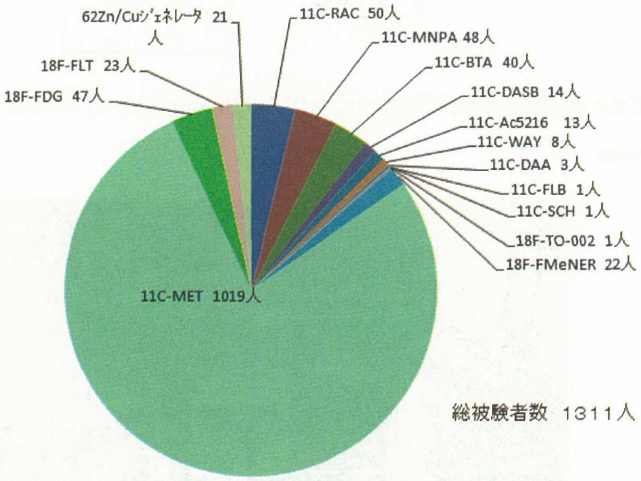

Figure 5: Diagnosis frequencies of each radio-pharmaceutical for cancer patients and other medical studies

3. Secondary Beam Lines in HIMAC

There are two secondary beam lines of SB1 and SB2, as shown in Figure 1. In table 1-1, the basic requirements for these courses are listed, where the acceptances of SB2 are required same values as in SB1 course. The first course (SB1) is mainly used for medical experiments where an irradiation system with spot scanning and a positron camera system for range verification were equipped. Also, there is patient positioning system around the final focus point, where a rotating table was installed. The second course (SB2) is used for general physical experiments, which require free space around the target point. Distance between the final focus point of SB2 and the wall of this experimental hall is limited to about 2m, which may limit the possible experiment.

Table 1-1. Specifications of the secondary beam courses.

Maximum magnetic rigidity	8.13 Tm
Momentum acceptance	±2.5%
Angular acceptance (H/V)	±13 mrad
Momentum dispersion at F1	2.0 m

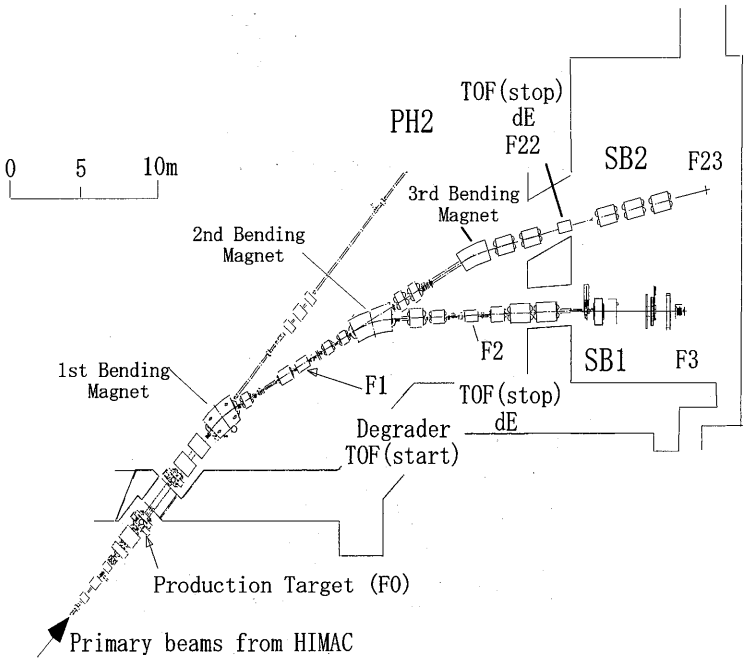

Figure 1: Layout of the secondary beam courses of SB1 and SB2

4. Activity Measurements with PET

To see activity image of the irradiated ^{11}C beam, a commercial PET-CT system was used to measure a 3D image of the activities. The spot scanning irradiation was used, and the irradiated dose distribution was checked in the water. Sa shown in Figure 7, good agreement could be obtained between calculated and measured dose distribution. In Figure 8, measured PET-CT data are shown, and we can see clear ^{11}C activity image in the irradiated head phantom.

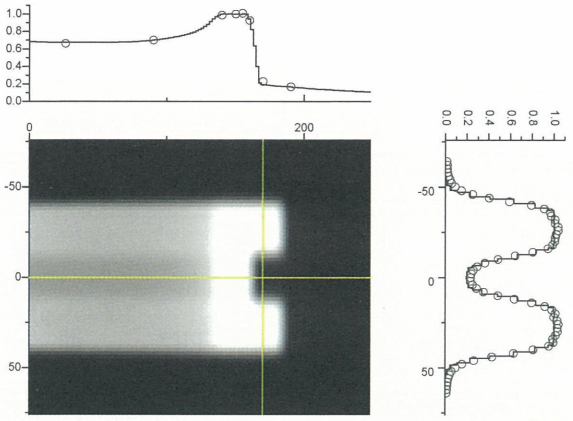

Figure 7: Measured dose distribution of ^{11}C beam and calculated dose distribution

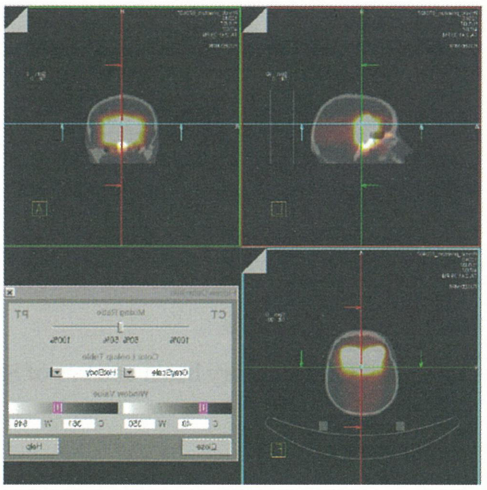

Figure 8: Measured PET-CT image with irradiated ^{11}C beam on the head phantom

5. Metabolic Effects in Rabbits

The injected activity of ^{11}C will be affected by a metabolic effect in the patient's body, and the measuring accuracy of beam range will depends on the strength of the effect. For this reason, it is important to know this effect for an actual measurement of the irradiated activities. To investigate this effect, rabbit experiments were performed with a developed positron camera[5]. Selected organs were brain and thigh muscle, where the positron emitter beam was injected. In the case of a brain, the measured time-activity curves of ROI (region of interest) are shown (see Fig.7) for the case of the live and dead cases with red (lower) and blue (upper) colors, respectively[6]. In this figure, one can see a strong metabolic effect in the volume where the ^{11}C beam is injected. The obtained activity data were fitted with three exponential decay components, and the results of fitted curves are also shown in the figure. In these fittings, a fast component was determined in the experiments with ^{10}C injection. Though there are large and fast decay components, whose activities cannot be measured with an off-line PET, there exist 1/3 fraction of the slow decay component that can be measured with it.

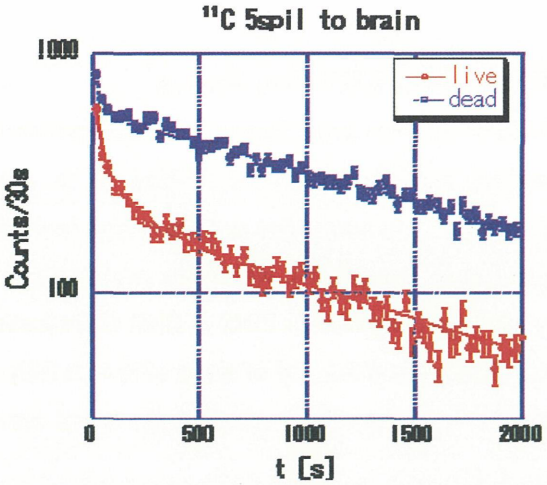

Figure 9: Activity decay curve in live and dead rabbit

6. Biological Effects of Radioactive Ion Beam

We have tested biological effects of the ^{9}C beam around Bragg peak, where ^{9}C will decay to 2α and proton. In comparison with a therapeutic ^{12}C beam that have similar depth dose distribution to the ^{9}C beam, the HSG cell experiment has been conducted using the ^{12}C beam. The ^{9}C beam came out more efficient in cell killing at the depths around its Bragg peak than its counterpart, *i.e.* the ^{12}C beam, especially at the distal side of the Bragg peak, corresponding to the stopping region of the incident ^{9}C ions and where delayed low-energy alpha particles and protons were emitted isotropically. Compared to the ^{12}C beam, the RBE values for the ^{9}C beam were always higher, and an increase in RBE by a factor of up to 1.87 has been observed[7] at the depths distal to the Bragg peak as seen in Fig.10. At the proximal side of the Bragg peak and the tail of the Bragg curves, the RBE values of both the beams tended to merge into each other. Based on an elaborate biophysical analysis, the stopping ^{9}C ions in cells are responsible for the enhanced cell lethality at the depths around the Bragg peak of the ^{9}C ion beam.

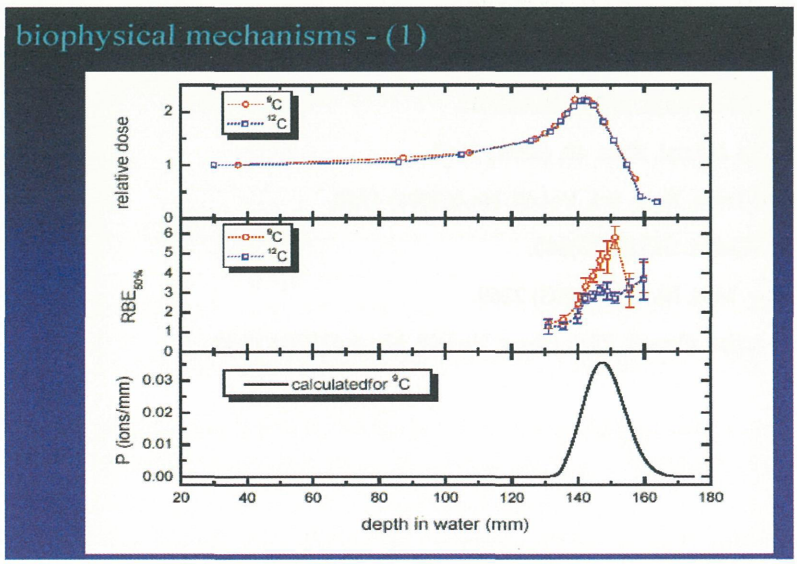

Figure 10: Comparison of biological effects between ^{9}C and ^{12}C beams

7. Feasibility Study to get RI Beam in EBIS Ion Source

Another method to obtain the RI beam is to use target fragment nuclear reaction instead of projectile fragment reaction as in the above secondary beam course. This method is to use technology of short life radio-pharmaceuticals in conjunction with an ion source that must have high ionization efficiency. One candidate of the ion source is Electron Beam Ion Source (EBIS), which can produce high charge ions efficiently with pulsed operation. Feasibility study has been done with an EBIS at JINR (Joint Institute for Nuclear Research) in Russia (see Figure 11). In this test, ionization efficiency of about 10% with fully stripped ion was obtained in an optimized condition for efficiency. To realize this method in the actual condition, further R&D will be required.

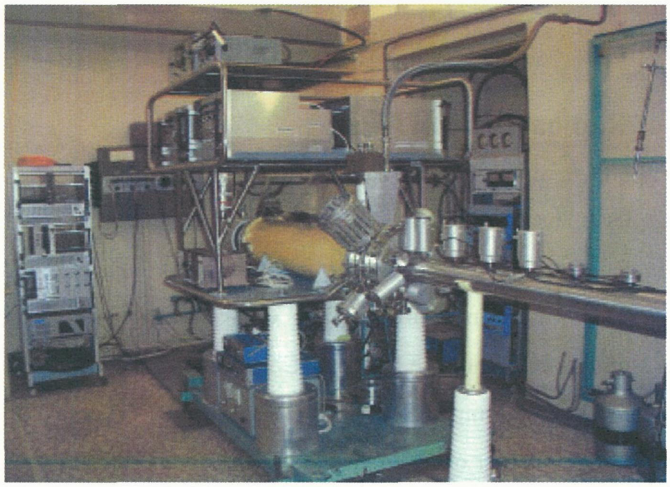

Figure 11: EBIS ion source in JINR (Russia) that was used in the test

References

[1] A. Chatterjee *et al.*, Nucl. Phys. A **616**(1997)478c.

[2] N. Matsufuji et al., Phys. Med. Biol. **43** (1998)3261

[3] M. Kanazawa *et al.*, Nucl. Phys. A **701**(2002)244c.

[4] E. Urakabe *et al.*, Jpn. J. Appl. Phys. **40**, (2001) 2540

[5] Y. Iseki *et al.*, IEEE Trans. Nucl. Sci. Vol.**48**, No.4(2001) 1550,
Y. Iseki *et al.*, NIM-A. **515** (2003)840.

[6] H. Mizuno et al., Phy. Med. Biol. **48** (2003) 2269.

[7] Q.Li et al., Int. J. Radiat. Oncol. Biol. Phys. Vol.**63**, No.4 (2005) 1237.

Therapeutic Techniques Used in the Heavy Ion Therapy Project at IMP

Qiang Li, Zhongying Dai, Xinguo Liu, Xiaodong Jin, Qingfeng Wu, Ping Li, Fei Ye, Guoqing Xiao

Institute of Modern Physics, Chinese Academy of Sciences, Lanzhou, China
Corresponding Author: Qiang Li, e-mail address: liqiang@impcas.ac.cn

Abstract

Basic research related to heavy ion cancer therapy has been conducted at the Institute of Modern Physics (IMP), Chinese Academy of Sciences since 1995. A project of patient treatment with carbon ions has been started at IMP. Heavy ion therapy becomes reality in manner of two steps, that is the treatment for superficially-placed tumors at the Heavy Ion Research Facility in Lanzhou (HIRFL) first and then for deep-seated tumors at the Cooling Storage Ring (HIRFL-CSR). Two therapy terminals equipped with passive beam delivery systems had been built at HIRFL and HIRFL-CSR. Up to now, 103 superficially-placed and 6 deep-seated tumor patients have been irradiated with intermediate and high energy carbon-ion beams in the two therapy terminals, respectively. In this paper, the therapeutic techniques in terms of beam delivery, conformal irradiation and treatment planning used at IMP are introduced.

Introduction

Due to the favorite characteristics of heavy ion beam such as inverted depth-dose distribution as well as high relative biological effectiveness (RBE), heavy-ion cancer therapy is attracting growing interest all over the world [1]. Based on the accelerators available, the Institute of Modern Physics (IMP), Chinese Academy of Sciences (CAS) plans to realize heavy-ion cancer therapy in a manner of two steps, that is the treatment for superficially-placed tumors with intermediate energy (≤100MeV/u) carbon-ion beam at the existing Heavy Ion Research Facility in Lanzhou (HIRFL) at first and then for deep-seated tumors with high-energy carbon ions at the newly-built Cooling Storage Ring (CSR) synchrotron, where the HIRFL is the injector for the CSR. In fact, basic research related to heavy-ion cancer therapy has been carried out at IMP since 1995. Fruitful achievements have been obtained in the aspects of radiation physics, radiobiology and therapeutic technique [2]. For the first step, a therapy terminal had been constructed underground the experimental hall of the HIRFL cyclotron complex, where a vertical beam line is equipped [3]. Superficially-placed tumor treatment with intermediate-energy carbon ions has been conducted in the earlier therapy terminal at HIRFL since November 2006. Up to now, 103 patients with shallow-seated tumors have been irradiated successfully and lots of therapeutic and clinical experiences have been acquired at IMP. To extend the heavy-ion therapy project to deep-seated tumor treatment at IMP, another therapy terminal dedicated to deep-seated tumor treatment with high-energy heavy ions has been built at HIRFL-CSR. Therapeutic high-energy carbon ion beams extracted from the HIRFL-CSR have been supplied in the deep-seated tumor therapy terminal and the beam delivery and shaping devices installed there have been validated through therapeutic beam tests. From March to April 2009, first 6 deep-seated tumor patients had been treated with high-energy carbon ions at HIRFL-CSR. In this paper, the beam delivery system, conformal irradiation method and treatment planning at IMP are described and a summary is presented in the end.

Beam delivery system

Shown in Fig.1 (a) and (b) are the vertical and horizontal beam lines in the therapy terminals for superficially-placed and deep-seated tumor treatments with intermediate- and high-energy carbon ions at HIRFL and

HIRFL-CSR, respectively. Passive beam delivery and shaping techniques are preferred at IMP due to their simplicity and good applicability to moving targets. The passive beam delivery system developed in the therapy terminal at HIRFL consists of a pair of orthogonal dipole magnets (fast and slow scanning magnets), a range shifter (different degraders with stepping thickness), a range modulator (ridge filter), and a manual multi-leaf collimator. Because constant beam intensities can be supplied by the HIRFL cyclotron, the scanning magnets driven by zigzag periodic currents with high (50~150Hz) and low (15~50Hz) frequencies deflect pencil beams fast and continuously in a zigzag-scanning manner for lateral beam spreading. Due to the limited space of the basement where the therapy terminal situated, only 5cm×5cm square uniform fields at the isocenter can be generated by the beam scanning system when the fast magnet is driven by a current with the maximum amplitude of 160A. The beam delivery system developed in the therapy terminal at HIRFL-CSR includes a pair of orthogonal scanning magnets, a range shifter (binary filter), a ridge filter, and a commercial dynamic multi-leaf collimator. It should be stated that the magnetic scanning system in the deep-seated tumor treatment terminal can be operated in two patterns such as continuous zigzag [3] and hybrid raster [4] scanning. Therefore, passive beam shaping using multi-leaf collimator and range shifter and active beam delivery with raster scanning and energy variation by the CSR synchrotron itself can be realized in the latest therapy terminal. In addition, mini ridge filters like the ripple filter used at GSI [5] were installed downstream the range shifter in order to spread out the Bragg peak of a mono-energetic beam slightly in a manner of Gaussian profile.

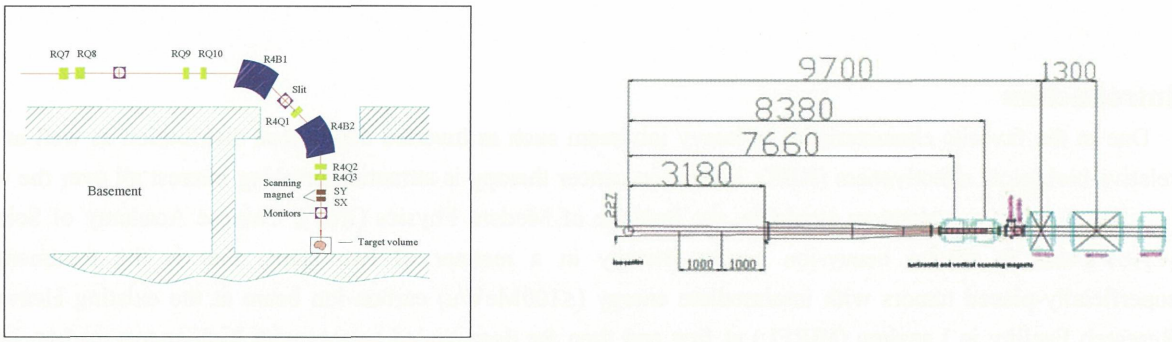

(a) (b)

Fig.1 The vertical (a) and horizontal (b) beam lines in the therapy terminals for superficially-placed and deep-seated tumor treatments with carbon ions at HIRFL and HIRFL-CSR, respectively.

Conformal irradiation method

Up to now 2D and 3D conformal irradiations dedicated to particle therapy have been explored on the basis of passive beam delivery system [6, 7, 8, 9], and even have been applied to clinical trials [7, 10]. Because the passive beam delivery system mentioned above has been developed at IMP, 2D and 3D conformal irradiations to target volumes can be readily performed under the condition of broad and uniform irradiation field generated by the beam scanning system.

A strategy of 2D conformal irradiation in conjunction with layer stacking is adopted at IMP. A mini ridge filter is employed to extend a pristine sharp Bragg peak slightly so as to form a Gaussian shaped mini spread-out Bragg peak (mini-SOBP) like those used in the active scanning system at GSI [5] and the 3D layer-stacking conformal method at NIRS [8, 11, 12]. So the range shifter made of PPMA plates shifts the mini-SOBP peak forwards layer by layer to yield a desired dose distribution in depth together with weighting parameters coming from the dose optimization. Laterally, the multi-leaf collimator is used to tailor the irradiation field according to the maximum contour of a target

volume projected on a plane perpendicular to the beam direction. In this way, variably uniform biological effective dose or uniform physical dose can be delivered to the target volume using the present irradiation system.

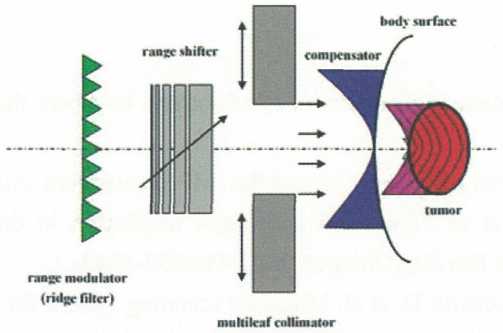

Fig.2 Schematic diagram of the 2D layer-stacking conformal irradiation method applied at IMP.

Treatment planning

A preliminary treatment planning system (TPS), which is anticipated to serve the heavy ion therapy project at IMP, has been developed. 3D reconstruction of CT slice images and dose calculation based on CT images with the code of HIBRAC [13] can be done with the preliminary TPS. The mini-SOBPs of different therapeutic beams are stacked according to the thickness of a tumor along the direction of beam penetration. At present, constant RBE values (2.5 or 3, depending on tumor types) across a SOBP are assumed for patient treatment at IMP. Uniform physical doses across the SOBP, therefore, are created using the mini-SOBP peak stacking method. Nevertheless, more developments of the TPS, for example, dose calculation based on more accurate beam and RBE models, are needed. Fig.3 illustrates the result of a dose verification measurement for an emulation phantom exposed to high-energy therapeutic carbon ions. The measured dose at the point of interest was in good agreement with the one planned by the TPS.

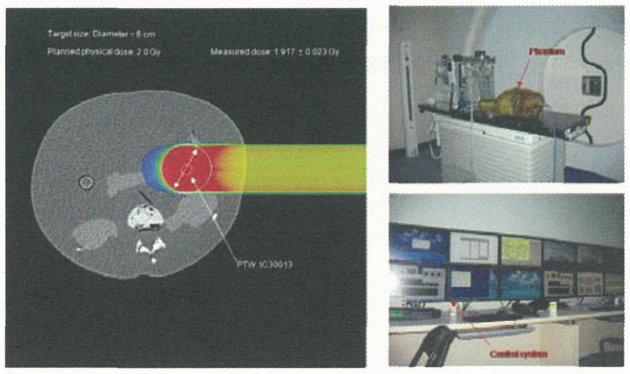

Fig.3 The result of a treatment planning verification for an emulation phantom.

Summary

Passive beam delivery system and 2D layer-stacking conformal irradiation have been developed at IMP, and the beam delivery system in the therapy terminal at HIRFL-CSR remains the possibility of upgrade to an active

one in the near future. These therapeutic techniques have been tested experimentally in the therapy terminals at HIRFL and HIRFL-CSR and have been applied to the patient treatment with intermediate- and high-energy carbon ions at IMP successfully. We believe the experience acquired up to now in the project of heavy ion therapy in terms of therapeutic technique is very useful for us to improve our clinical trial at IMP.

References

[1] Amaldi U, Kraft G. Recent applications of synchrotrons in cancer therapy with carbon ions. Europhys News. 2005;4:114-118.

[2] Li Q. Biomedical research with heavy ions at the IMP accelerators. Adv Space Res. 2007;40:455-460.

[3] Li Q, Dai Z, Yan Z, et al. Heavy-ion conformal irradiation in the shallow-seated tumor therapy terminal at HIRFL. Med Bio Eng Comput. 2007;45:1037-1043.

[4] Haberer T, Becher W, Schardt D, et al. Magnetic scanning system for heavy ion therapy. Nucl Instrum Meth A. 1993;330:296-305.

[5] Weber U, Kraft G. Design and construction of a ripple filter for smoothed depth dose distribution in conformal particle therapy. Phys Med Biol. 1999;44:2765-2775.

[6] Chu W T, Ludewigt B A, Renner T R. Instrumentation for treatment of cancer using proton and light-ion. Rev Sci Instrum. 1993;64:2055-2122.

[7] Kanai T, Endo M, Minohara S, et al. Biophysical characteristics of HIMAC clinical irradiation system for heavy-ion radiation therapy. Int J Radiat Oncol Biol Phys. 1999;44:201-210.

[8] Futami Y, Kanai T, Fujita M, et al. Broad-beam three-dimensional irradiation system for heavy-ion radiotherapy at HIMAC. Nucl Instrum Meth A. 1999;430:143-153.

[9] Kanai T, Kawachi K, Matsuzawa H, et al. Broad beam three-dimensional irradiation for proton radiotherapy. Med Phys. 1983;10:344-346.

[10] Kanai T, Kanematsu N, Minohara S, et al. Commissioning of a conformal irradiation system for heavy-ion radiotherapy using a layer-stacking method. Med Phys. 2006;33:2989-2997.

[11] Schaffner B, Kanai T, Futami Y, et al. Ridge filter design and optimization for the broad-beam three-dimensional irradiation system for heavy-ion radiotherapy. Med Phys. 2000;27:716-724.

[12] Kanematsu N, Endo M, Futami Y, et al. Treatment planning for the layer-stacking irradiation system for three dimensional conformal heavy-ion radiotherapy. Med Phys. 2002;29:2823-2829.

[13] Sihver L, Schardt D, Kanai T. Depth-dose distributions of high-energy carbon, oxygen and neon beams in water. Jpn J Med Phys. 1998;18:1-21.

The Beam Monitoring Detectors for the Heavy-Ion Therapy at IMP

Zhengguo Hu, Bin Tang, Zhiguo Xu, Hushan Xu, Ruishi Mao, Tiecheng Zhao, Jinda Chen, Limin Duan, Jiansong Wang, Zhiyu Sun, Qiang Li, Youjin Yuan, Xiao Guoqing

Institute of Modern Physics, Chinese Academy of Sciences, Lanzhou 730000, China

Corresponding Author: Zhengguo Hu, e-mail address: huzg@impcasac.cn

Heavy ion beams have been used for medical purposes since early 1950s [1]. Because of the Bragg peak in dose distributions of the ions, the healthy tissues received much lower doses than the region defined by spread-out Bragg peaks (SOBPs). Particle therapy (PT) facilities in operation include HIMAC (Japan) and GSI (Germany) [2]. Other facilities are in construction in Italy (TERA) [3], Germany (Heidelberg) [4], Japan (several facilities), and so on . Referring to the clinical cases of PT [5], it is evident that good localized tumor control and high patient survival rates have been achieved by heavy ion treatment without side effect or with tolerably acute toxicity. Accordingly, carbon ion therapy has been recognized as a promising modality against tumors in the community of radiation therapy.

A facility for treatment of localized skin-seated tumors has been installed at Institute of Modern Physics (IMP) in Lanzhou [6]. 103 patients have been treated with 100 MeV/u ^{12}C beam in the PT terminal since November 2006. At the beginning of 2008, a new terminal for deep-tumor therapy has being installed. The greatest difference between shallow-tumor therapy and deep-tumor therapy is the beam scan mode which requests the different beam monitor system to achieve the precise radiotherapy. With the high energy ^{12}C beam in active pencil beam scanning mode in deep-tumor therapy, the beam intensity is about two orders of magnitude higher than that of passive shaping mode used in shallow-tumor therapy and the energy increased from 100 MeV/u to 430 MeV/u . On other words, we have to develop a new beam monitor system to check the ^{12}C energy and irradiation dose during the treatment.

The new beam monitor system consists of an ionization chamber(IC) as an online beam intensity monitor, and an IC-stack as Bragg-Peak detector used before irradiation treatment. The online IC contains of two windows and three poles. The anode inside the two cathodes is made by 1.5μm gold-filled Mylar foils with 200×200 mm^2 active area. The working gas is N_2 (99.9%) under one atmosphere. The IC-stack consists of thirty ICs with 5mm polymethyl methacrylate (PMMA) plates inserted as the tissue-equivalent materials. For each IC of the IC-stack, there is an active area of 100× 100 mm^2 and a thickness of 10mm with three poles structure as the online beam density monitor IC.

The NI-PXI-6133 (PC based DAQ system) is chosen as the read-out electronics for the detectors to delivering simultaneous sampling with an adjustable 20MHz clock. The signal of the detector is output in the integral mode and varies from several nC/s to tens of μC/s. With the E/F (electric charge to frequency) shift board, the output of online monitor IC became TTL signal. While going through 66MΩ resistances the output signal of IC-stack converts from electric charge to voltage (0~10V). The LabVIEW program is used to analyze and display the acquired data from the detector, as well as giving the trigger signal to the control catenation devices according to the beam condition and the therapy plan [7].

For the online monitor IC, the recombination of the ions and electrons produced by the ionizing

radiation will increase with the increasing of the beam intensity. This will reduce the collected charge in the detector and hence affect directly the dose measurement. To ensure the measurement results reliable, we have to test whether the output of the detector is linear to the beam intensity in the range from 0~10^8 particles/pulse. The scintillator counter and SEM (scanning electron microscope) are used as the cross-check detector to test the linearity of the online monitor IC (Fig.1). When the beam intensity is less than 1.0×10^4 particles/pulse, the output of online IC is proportional to that of the scintillator as shows in Fig.1 (a), the last measurement point with red color is out of the fit line, which indicates that the counts from the scintillator detector is somewhat saturated in the high beam intensity. Fig.1 (b) shows the online IC counts increase with the increasing of the beam intensity, the SEM, which works in vacumm without the effects of recombination, can measure the real beam intensity even it reaches to 1.0×10^8 particles/pulse. The linear fit of IC output in the all range of beam intensity shows that it can work well in the condition of active pencil beam scanning mode.

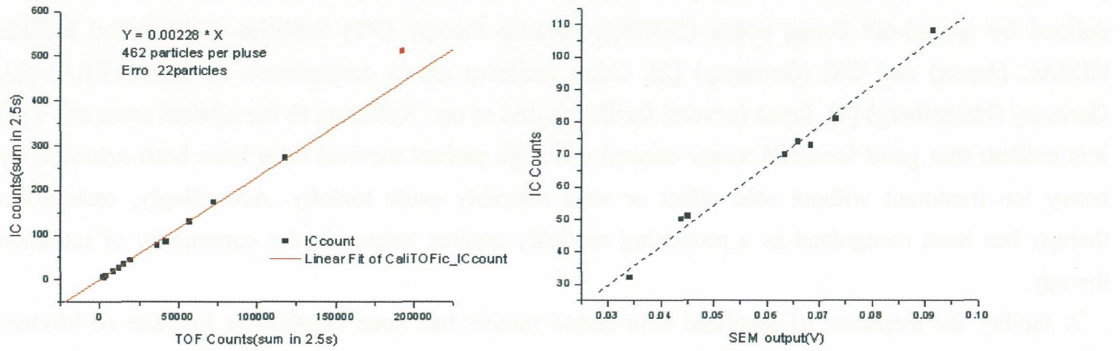

a b

Fig.1 The Linearity of online integral IC

Fig.2 shows the measurements of IC-stack for different beam energies. The comparison between HIMAC Beam calculations [8] (solid line) and the measurements reveals the well agreement. Nevertheless, the granularity of each IC decides by the depth of PMMA is not best suited to resolve the peaks for all energies. In the next measurement, we will improve the precision of measurement by adding thinner PMMA in the front of the detector as a subset of the layers.

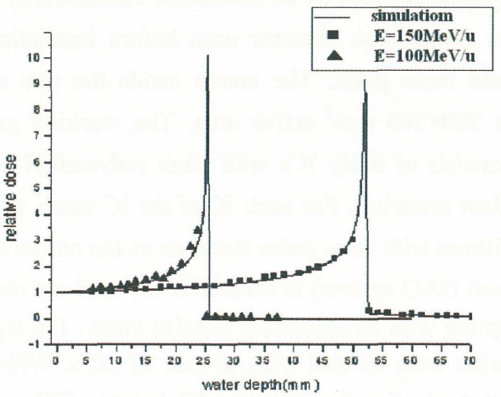

Fig.2 The Bragg peak curves measured by IC-stack

References

[1] Tobias C A, Anger H O, Lawrence J H. Am J Roentgenol Ther Nucl Med, 1952, **67**(1):1-27.

[2] Particle therapy facilities in operation (March 2009), available at http://ptcog.web.psi.ch/ptcentres.html.
[3] Amaldi U. Phys Med, 1998, **14**: 76-84.
[4] Eickhoff H, Böhne D, Debus J, *et al.* The proposed accelerator facility for light ion cancer therapy in Heidelberg Proc. 1999 Particle Accelerator Conf. New York, 1999, 2513-2515.
[5] Carstro J R. Radiate Environ Biophys, 1995, **34**: 45-48.
[6] TANG Bin, HU Zhengguo, XU Zhiguo, *et al.* Nucl Electron Detect Technol (in Chinese), 2008, **28**(4): 699-701.
[7] MAO Ruishi, XIAO Guoqing, ZHAO Tiecheng, *et al.* High Power laser and Particle Beams((in Chinese), 2008(09),1537-1540
[8] Lembit Sihver, Deter Schardt, Tatsuaki Kanai, Jpn. J. Med. Phys. 1998, Vol18, No.1, 1-21

Accelerator Aspects of the Proposed Tumor Therapy System

Mingtao Song

Institute of Modern Physics, Lanzhou, China
Corresponding Author: Mingtao Song, e-mail address: songmt@impcas.ac.cn

Abstract

Since 2006 about 100 patients have been successfully treated with carbon ion in the IMP experimental tumor treatment program. The developments and experiences of this program encourage a proposal for a hospital based tumor therapy system. Design of accelerator aspects of the system is based on the experiences at IMP. However, the hospital based facility requires compactness, 'turn-key' operation and large throughput of treating 2000 patients/year. Besides, proton beam is also demanded to meet the specific medical requirements. The designed accelerator system consists of a cyclotron injector and a compact synchrotron. The intensity for protons and carbon ions is sufficient for the needs of scanning beam applications. The beams can be slowly extracted over a period of up to 5 s and delivered to treatment ports. The details of the particular system of this kind with four treatment ports will be presented.

Introduction

Tumor therapy with light ions and protons has made great progress in the last decade. Several facilities have already been built or are under construction world-wide. The proposed accelerator system is designed in accordance with the lines of modern light-ion therapy accelerators on the whole. However, modification is made for the injector, considering the experiences of tumor treatment employing the IMP accelerator facilities in the past years. Fig. 1 shows the overall layout of the designed accelerator system. Its main parameters are given in Table 1.

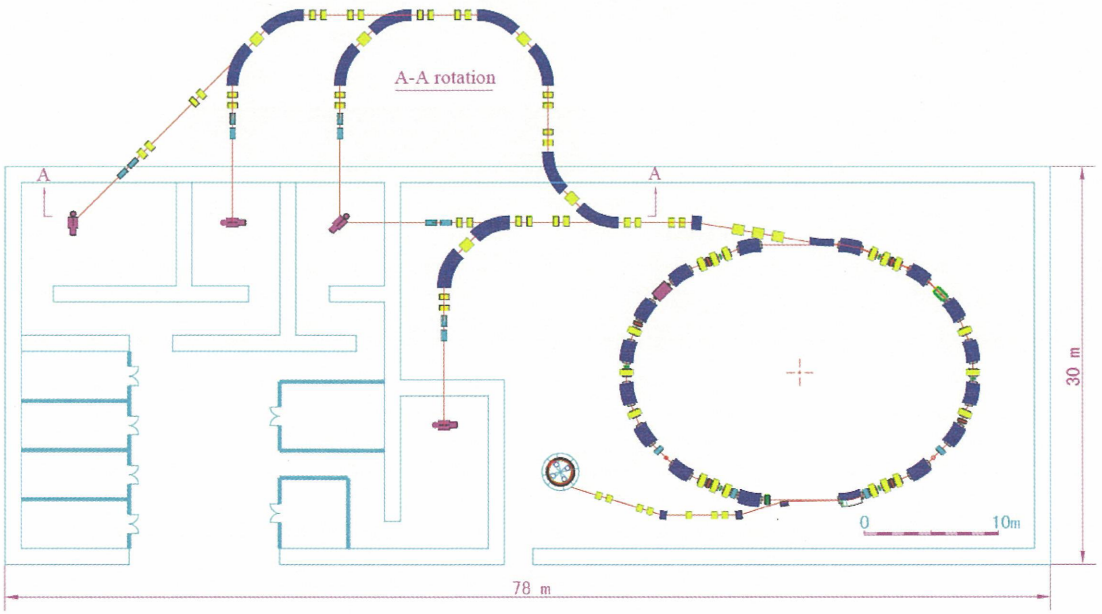

Fig. 1 The overall layout of the accelerator system.

Table 1: Basic specifications of the cancer therapy facility

Particles	$^{12}C^{+6}$, p
Max. bema energy	250 - 400 MeV/u
Spill duration	1~5 s
Beam range in water	27 - 30 cm
Range adjustment	2 mm
Max. dose rate	2 Gray/min
Field size	20×20 cm^2
Field size accuracy	±0.5 mm
Field uniformity	95%
Dose accuracy	± 2%
Beam size at iso-center	4 - 10 mm (FWHM)
Source to surface distance	>6 m
Beam intensity	4×10^8 - 10^9 pps
Beam dump time	<300 μs
Treatment mode	Active scanning (>1 cm/ms)
Ports	1 hor., 1 vert., 1 hor. + vert. and 1 45° port in vert. plane

Cyclotron injector

The unique feature of the medical accelerator complex is its injector of cyclotron in contrast to the wide used injector type of linac. Charge exchange injection (CEI) is employed in the main accelerator of synchrotron benefiting from the continuous beam of the cyclotron injector, since the stripping process is inevitable for the sake of efficient acceleration. The CEI method, regardless of the Liouville's theorem, has the merit of beam accumulation capacity superior to the conventional multiturn injection method. The combination of CEI and cyclotron injector is well proved in IMP and also in other laboratories. To further minimize the size and consequently the cost of injector, the carbon ion with a charge state of 5+ will be accelerated up to 7 MeV/u. Acceleration of ionized hydrogen to the same energy is foreseen.

The cyclotron features a deep valley design with a hill-gap of 50 mm and a valley gap of 360 mm, providing sufficient axial focusing. It has four straight-edged sectors of 56 degrees. The RF frequency is 31.02 MHz. The beam extraction radius is 75 mm so that the outer radius of magnet yoke is no more than 3 m. Hydrogen ions will be accelerated with the aids of four groups of trim coils. The low energy beam line for axial injection into cyclotron is equipped with a chopper system producing macro-pulse beam for the injection process of the synchrotron. The whole length of the beam line is so short that it could be put on the top of the cyclotron together with ion sources. Two all-permanent ECR sources will be prepared for hydrogen and carbon ion production with the extraction voltage of 16.6 kV and 20 kV, respectively.

The medium energy beam transport (MEBT) system accepts the extracted ion beam from the cyclotron and transfers to the synchrotron. The MEBT is relatively short owing to the absence of stripping section. Appropriate manipulation of the phase ellipse at the injection point, i.e., the stripping foil in the synchrotron, is helpful for CEI efficiency. In addition, an RF debuncher inserted in the middle of the MEBT reduces the momentum spread so as to maximize the injection efficiency.

Synchrotron

For the synchrotron with a circumference of about 72.3 meters, 16 bending magnets with a maximum flux density of 1.6 T are provided. These bending magnets excited in pairs by 8 power supplies also take the role of closed obit corrector in the horizontal plane. Six additional correctors will be used all for the correction in the vertical plane. The lattice consists of two super-periods, whose closed dispersion bump essentially stems from three bend achromatic structure. 18 quadrupoles are grouped into four families. Two 6-meters-long dispersion-free drift spaces are available for the installation of injection and extraction magnet elements, while four dispersive drift spaces of 2.2 m long accommodate RF-cavity, electrostatic deflector for extraction and other devices. The ion optical setting keeps constant throughout the entire cycle.

As mentioned earlier, the injection process utilizes the CEI method. At the very beginning, four bump magnets move the closed orbit 45 mm outwards to the stripping foil in order to accept the injecting ions losing one more electron. When the bump orbit collapses, fully striped ions gradually move inwards making room for newcomers. The phase space is painted while the phase density is increasing. After 100 turn injection or so, the carbon ion acceleration to the nominal energy of 400 MeV/u takes place within 1 second.

For the beam extraction the third order resonance extraction is chosen with variable extraction time up to 5 s. The hardt condition [1] is elaborately fulfilled for high extraction performance by 5 sextuples grouped into three families. The transverse RF knock-out method is employed to continuously drive the ions out. Quick response to beam on/off request is extremely favorable. Thus, multiple beam extraction is also possible in the same cycle.

Treatment ports

To meet the requirement for a throughput of 2000 patients/year four treatment ports are provided. The first port is served by a horizontal beam line, may be used mainly for treatment of ocular tumor. For the second port, the beam could be delivered from a horizontal beam line or a vertical beam line alternatively. For the third and fourth ports the beam is delivered vertically and semi-vertically (45 degree), respectively. All beam lines are equipped with identical two dimensional scanning magnets and beam diagnostic devices. With such an arrangement, it is hopeful to perform the function of amazing rotating gantry to some extent while keep the size of irradiation field unchanged.

Conclusions

We have proposed an accelerator system for tumor therapy, where the combination of CEI and cyclotron injector is employed.

References

[1] L. Badano, M. Benedikt, P. Bryant, et al., Synchrotrons for hadron therapy: Part I, Nucl. Instr. Meth., 1999, A**430**, 512-522.

Injection and Slow Extraction for Carbon Ion Therapy at IMP

Youjin Yuan

Institute of Modern Physics (IMP),CAS,730000, Lanzhou, China
Corresponding Author: Youjin Yuan, e-mail address: yuanyj@impcas.ac.cn

Abstract

The injection and slow extraction schemes chosen for carbon ion therapy machine in IMP are described in this paper, they were chosen with high performance to price ratio for a complex machine of cyclotron and synchrotron for carbon ion therapy. The charge stripping injection(CI) scheme is chosen for carbon ions as it can easily reach high beam intensity by one shot and the injection setting-up is simple and easy for commissioning. For slow extraction, the horizontal 1/3 integer resonant RF knock-out scheme is used, which is suitable for small synchrotron where the chromaticity is also small. It makes the control system of slow extraction easier too.

Preface

The cancer therapy study setting at IMP is based on the Heavy Ion Research Facility at Lanzhou(HIRFL) in China, which is a complicated research facility for fundamental science. The HIRFL consists of two cyclotrons (SFC, SSC) as injectors and two rings as synchrotron (CSRm) and storage ring (CSRe). For carbon therapy study, the machine setting is ECR+SFC+CSRm. The cyclotron SFC is chosen as injector by historical reason. Despite the intensity is 1pμA much weak than that from LINAC, properly designed injection scheme makes it possible to match the required particle number per spill.

An ideal therapy machine can discharge accurate dose at precise position of the tumor. It's not easy to be realized along beam direction, although for heavy ions the Bragg's peak reduces the energy deposition at healthy tissue. But for cross section, there are methods to realize good approach.

The time structure of slow extracted beam at therapy site is very important for people to reach required dose distribution uniformity. The scheme for slow extraction is the major but not the only aspect to get good time structure. The beam distribution in phase space after injection also plays an important role, as it's the main reason for irregular dose fluctuation.

For uniform scanning, to reach required ~90% uniformity, better time structure of beam and higher scanning frequency are required than that for raster scanning. We are expecting good performance from raster scanning scheme not only to reach better uniformity but also more precise dose distribution according to dosage for different tissues.

Charge Stripping Injection

The charge stripping injection (CI) scheme is designed for the synchrotron CSRm after the project started, It's based on the multi-turn injection (MI) scheme so as to use the same injection beam line. It's suitable for light heavy ions, where the cooling time of e-cooler is much longer than heavier ions, to reach high intensity in shorter time.

The layout of CI for CSRm is shown in Figure 1. It's a novel idea to put carbon stripper inside one of the main dipoles, which keeps the symmetry of racetrack layout of the ring and saves budget. The stripper system (see Figure 2) consists of motor driven probe and foil chamber. The carbon foil are chosen for CI, about 20 foils can be stored in the foil chamber and easily changed on need.

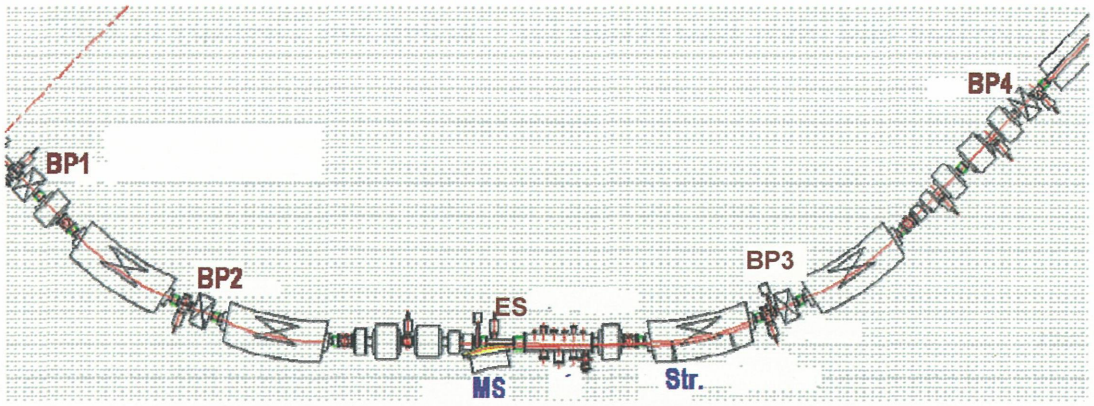

Figure 1. The layout of charge stripping injection

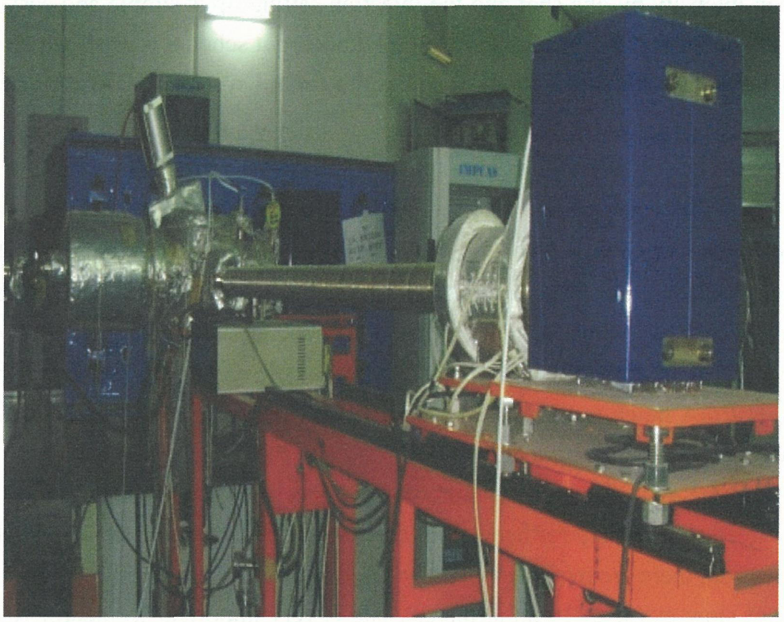

Figure 2. Stripper system for CI

The beam orbits calculation for CI of C, N and O are shown in Figure 3. For carbon beam with momentum spread of ±0.5%, the CI orbits are shown in Figure 4.

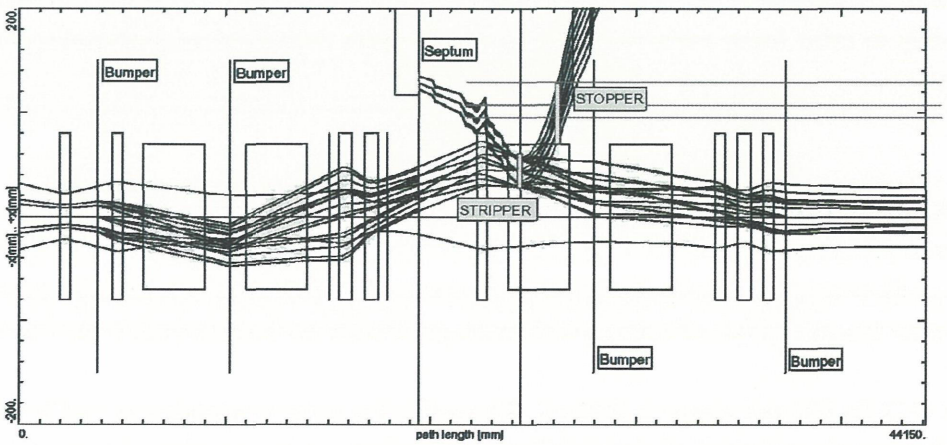

Figure 3. The orbits of charge stripping injection for C, N and O

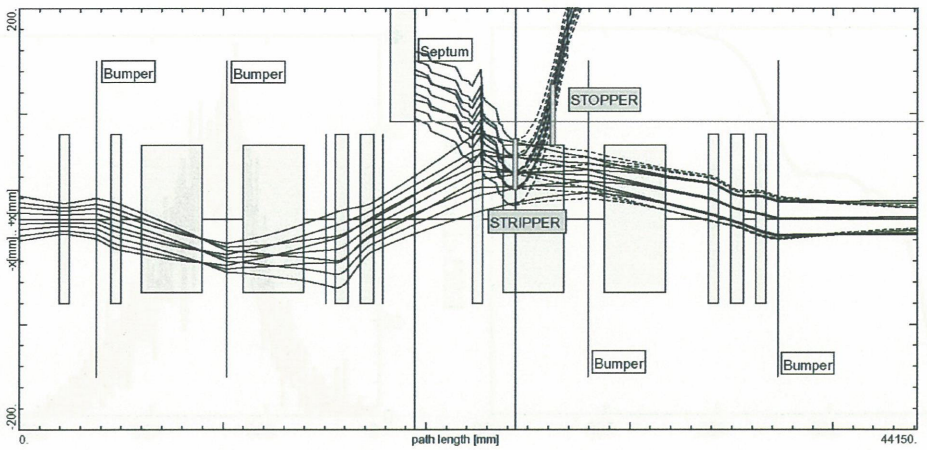

Figure 4. The orbits of charge stripping injection for carbon with momentum spread of ±0.5%

The simulation of CI is done to fit the parameters of injection beam for high intensity. The self developed program code is written in Visual Basic language. The program starts from parameters of injection beam, stripper setting, ring matching and bump orbit distortion (see Figure 5).

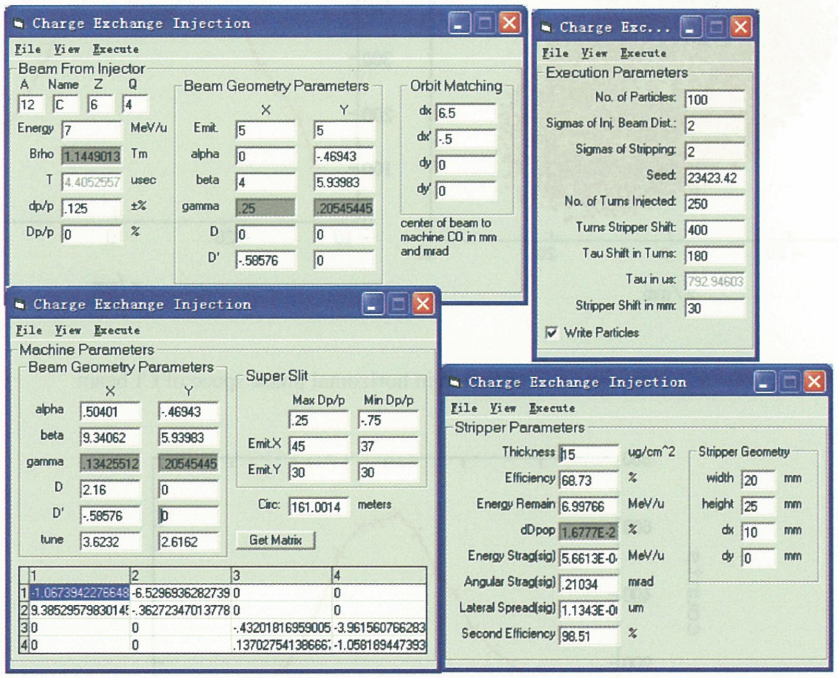

Figure 5. Parameters inputting interface for CI simulation

The simulation shows a gain of about 60 relative to single turn injection from parameters in Figure 5. The beam intensity during simulation and efficiency of each injected turn are show in Figure 6. The particle distribution in horizontal phase space is shown in Figure 7, it can be used to simulate the time structure of slow extracted beam. The CI result shows a central momentum shift of 0.2% relative to the injection beam (see Figure 8).

The DCCT measurement of beam intensity of single CI and acceleration is shown in Figure 9.

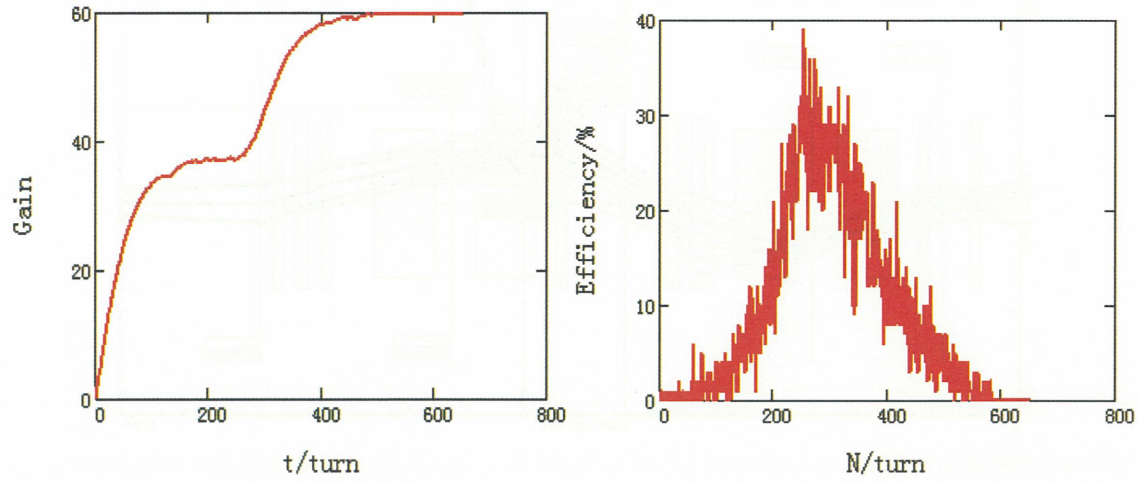

Figure 6. The beam intensity (left) during simulation and efficiency of each turn (right)

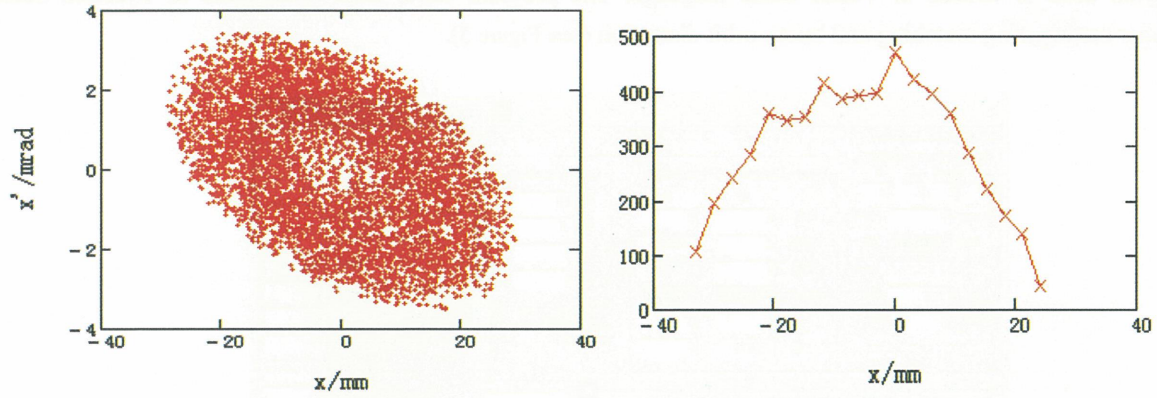

Figure 7. The particle distribution in horizontal phase space of CI beam

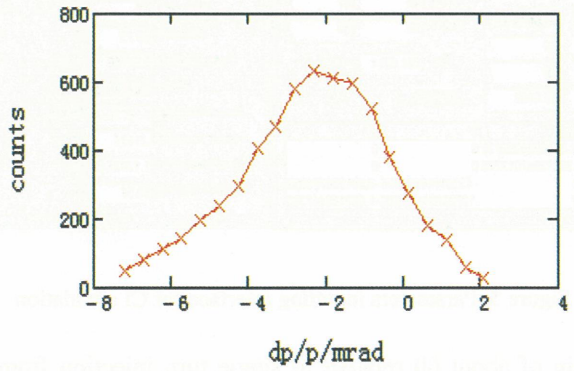

Figure 8. The momentum distribution of CI beam

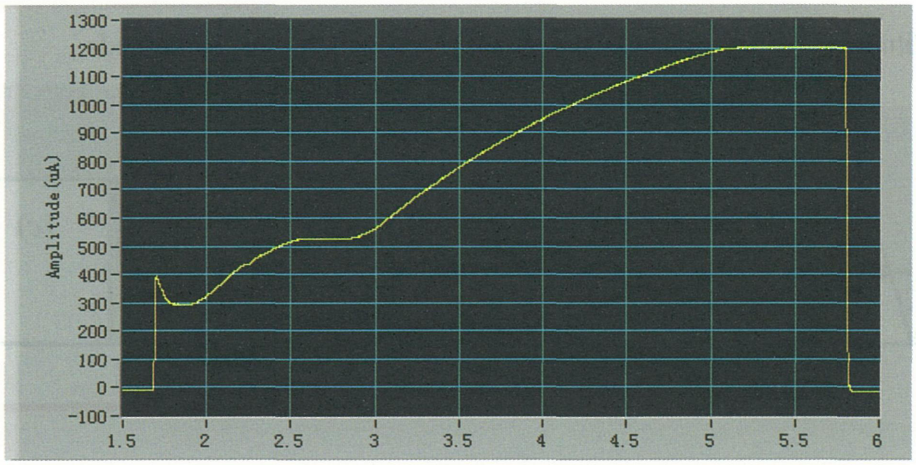

Figure 9. DCCT measurement of beam intensity of single CI and acceleration

Slow Extraction

The layout of slow extraction of CSRm is shown in Figure 10, the layout of injection are shown too. It's designed based on fast extraction tunnel of CSRm. The RF knock-out method[1] is chosen for CSRm (Figure 11) as the chromaticity can be corrected to zero with sextuples, it's convenient for construction and commissioning.

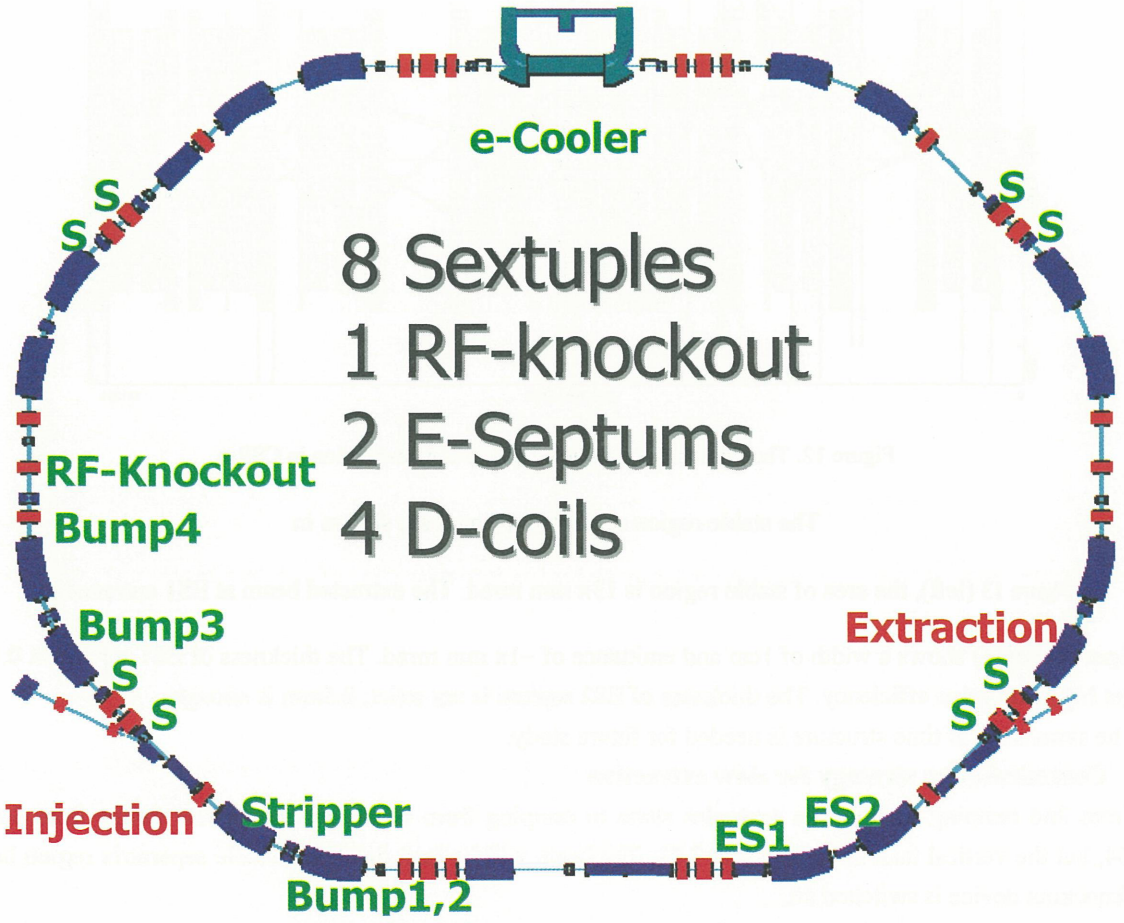

Figure 10. The layout of slow extraction of CSRm

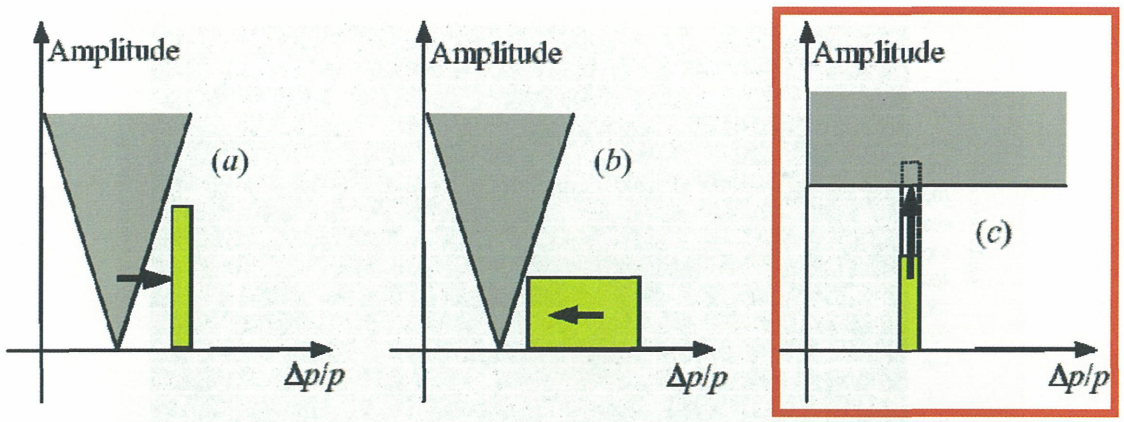

Figure 11. Comparison of the main extraction methods: (a) moving the resonance, (b) moving the beam, (c) increasing the particle amplitude. From Ref. [1]

- **Calculation and Simulation**

At first the transversal chromaticity is corrected to zero using the 8 sextuples in two groups, then the stable separatrix in horizontal phase space is form by 4 sextuples separately. The final turns of particles before slow extraction in CSRm are shown in Figure 12.

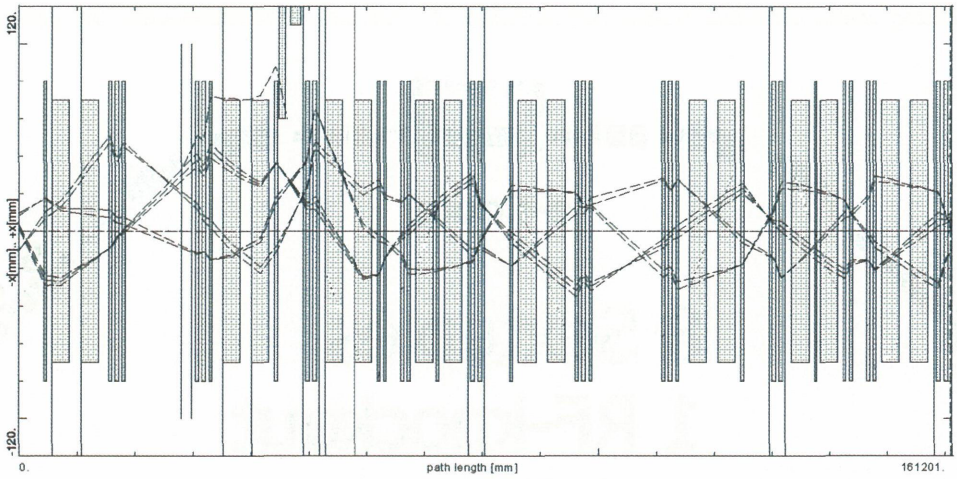

Figure 12. The final turns of particles before slow extraction in CSRm

The stable region separatrix formed are shown in

Figure 13 (left), the area of stable region is 13π mm mrad. The extracted beam at ES1 entrance in

Figure 13 (right) shows a width of 1cm and emittance of ~1π mm mrad. The thickness of ES1 septum is 0.1mm to get high extraction efficiency. The thickness of ES2 septum is not strict, 0.5mm is enough.

The simulation of time structure is needed for future study.

- **Commissioning strategy for slow extraction**

From 2nd ramping section, the sextuples starts to ramping from 0, the horizontal tune ramps from 3.63 to 3.664, but the vertical tune value keeps at 2.61. The beam will be kept inside the stable separatrix region before RF knockout device is switched on.

At the extraction flat-top, the RF knockout device is triggered to increase the oscillation amplitude of particles and beam is extracted. It's easy and fast to stop extraction when required by switching off the RF knockout device.

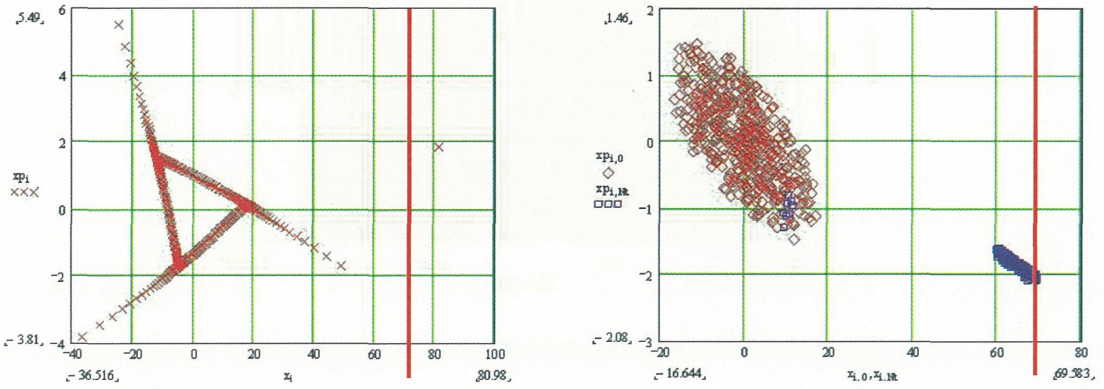

Figure 13. The stable region separatrix (left) and the extracted beam at ES1 (right)

- **Extracted beam**

We got the first slow extracted beam in Jan. 2008, it's detected by scintillator outside the flange of beamline, see Figure 14. It's over modulated by 50Hz ripple of power supply, the filling factor is about 20%.

In Nov. 2008, we got the first beam at cancer therapy terminal, see Figure 15. The time structure is better, but still modulated by power supply ripper of 100Hz. The filling factor reaches 60%, see Figure 16.

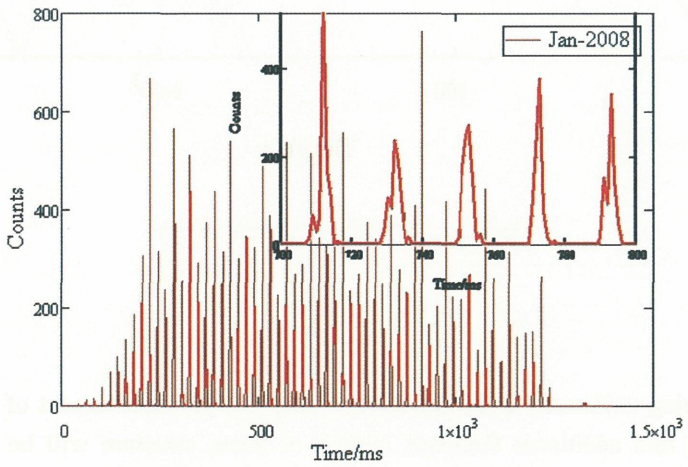

Figure 14. The first slow extracted beam

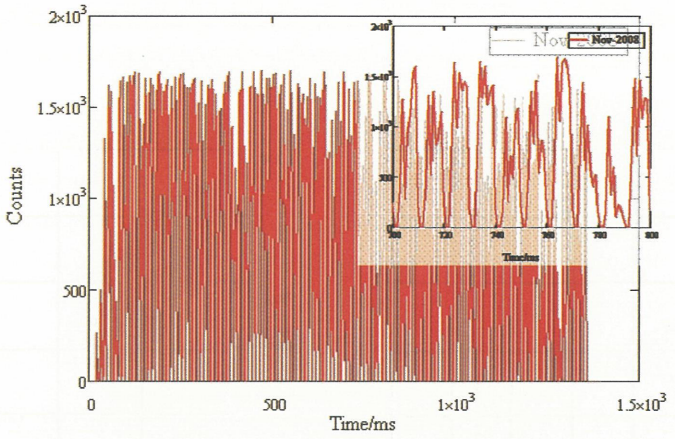

Figure 15. The first slow extracted beam at cancer therapy terminal

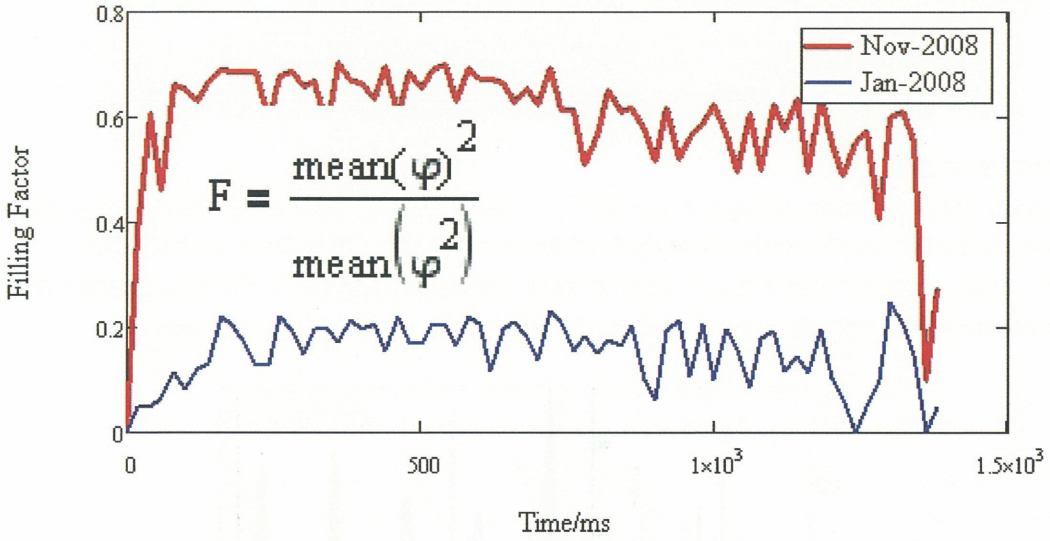

Figure 16. The filling factor improved

Conclusions

To improve the scanning uniformity at cancer therapy site, further improvement of power supply of CSRm and beam transfer line, and additional feedback system of beam structure will be developed. The further simulation of beam slow extraction based on injection beam distribution is important.

References

[1] Marco Pullia, Dynamique de l'éjection lente et son influence sur les lignes de transfert, N° d'ordre : 254-99 Année 1999.

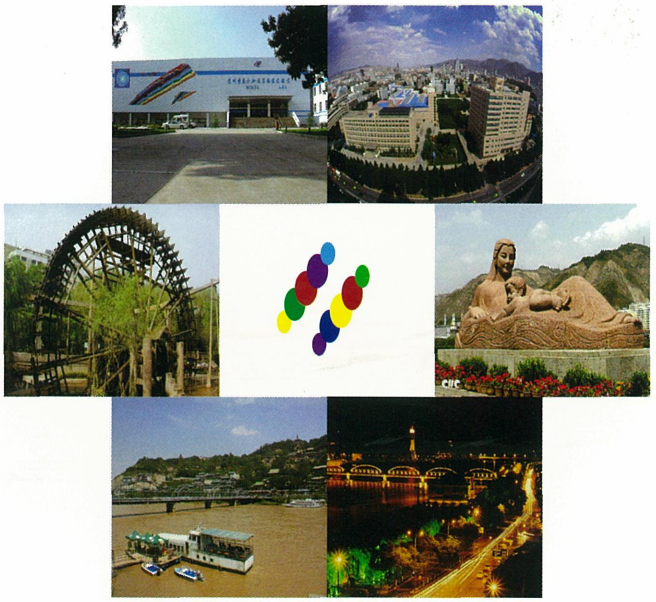

NIRS

National Institute of Radiological Sciences

Education and International Cooperation Section

4-9-1 Anagawa, Inage-ku, Chiba 263-8555, Japan

e-mail: kokusai@nirs.go.jp

Tel: +81-43-206-3025

Fax: +81-43-206-4061

IMP

Institute of Modern Physics

509 Nanchang Rd.,Lanzhou 730000,China

e-mail: webmaster@impcas.ac.cn

Tel : 86 - 931 - 4969221

Fax : 86 - 931 - 82721004

Scientific Secretariat